Universitè Pierre et Marie Curie

Laboratory of LOCEAN

Doctoral school ED129

Ph.D. thesis of

Alberto Baudena

How do marine mid trophic levels respond to fine scale processes?

Supervisors

Dr. Francesco d'Ovidio

Dr. Xavier Capet

Prof. Guido Boffetta

Candidate

Alberto Baudena

Declaration of Authorship

I, Alberto Baudena, declare that this thesis titled, 'How do marine mid trophic levels respond to fine scale processes?' and the work presented in it are my own. I confirm that:

- This work was done wholly or mainly while in candidature for a research degree at this University.

- Where any part of this thesis has previously been submitted for a degree or any other qualification at this University or any other institution, this has been clearly stated.

- Where I have consulted the published work of others, this is always clearly attributed.

- Where I have quoted from the work of others, the source is always given. With the exception of such quotations, this thesis is entirely my own work.

- I have acknowledged all main sources of help.

- Where the thesis is based on work done by myself jointly with others, I have made clear exactly what was done by others and what I have contributed myself.

Signed:

Date: 22/10/2018

Abstract

The comprehension of the coupling between physical and biological dynamics is a pivotal step to assess the health of the oceans, in order to protect the ecosystems therein from the effects of global change, human exploitation and pollution as well as for understanding the role of the ocean in the climate system. Indeed, in the oceans, physical phenomena and biological processes are intimately linked, since marine organisms live in a fluid environment, continuously under the effect of the currents. Thus, contrary to what happens on land, where the landscape topography changes over evolutionary timescales (periods in the order of hundreds to millions of year) in the ocean the landscape ("seascape") evolves on the same timescales of ecological processes. In the present thesis I analyse in particular the role of the fine scales, which present a peak in the ocean energy spectrum, and whose time scales (of days to weeks) overlap important marine ecological processes like the development of planktonic blooms and the duration of foraging trips for top predators. The fine scale features have been already shown to play a central role into conditioning primary production, lower trophic levels abundance and composition, and apex predators behaviors. However, less is known on their influence on intermediate trophic levels, i.e. swimming organisms (such as fish), which however constitute an essential part of the trophic chain, and which are under unprecedented pressure by human activities. This is mainly due to the scarce availability of data on them at large scales, and to problems of ship-based measurements. Two knowledge gaps are addressed in this thesis. The first is the fact that intermediate trophic levels distributions cannot be detected by remote sensing, and thus require the development of novel, ad hoc sampling strategies. The second open challenge addressed by this thesis is how the swimming ability of the nekton can interact with the fine scale physical dynamics.

In order to address the aforementioned questions, in this work I adopt a Lagrangian approach, therefore focusing on water parcel trajectories, and I integrate it with novel methodologies applied to acoustic data, complex system analysis and network theory. I focus on the Kerguelen region, because of its ecological importance and the large availability of informations, which permitted to characterize its relatively simple ecological dynamics, mainly based on iron limitation which is furnished by the plateau. I consider the myctophids as reference fish of the present study, for their worldwide abundance and for their importance for the ecology of the area, and because they may constitute a future target by commercial fishing.

In the first part of the work I analyze the relationship between satellite-derived fine scale processes and acoustic data of fish concentration, finding that high biomass levels are observed in correspondence of frontal systems identified through Lagrangian structures.

I then propose a possible mathematical mechanism of fish aggregation on frontal features based on gradient climbing strategy and reduction of fish hotspots by horizontal currents, finding that frontal features can couple with swimming behavior and enhance fish aggregation. I assess also that frontal system presence is a necessary but not sufficient condition to assure large fish concentrations, a result which is confirmed also by the analysis of the acoustic data.

In the second part of the thesis I analyze flow circulation properties through Lagrangian Flow Network methods in order to develop an efficient monitoring strategy of waters coming from, or going to, a target region. This methodology could be used to design an optimal sampling network to assess fish or larval abundance. I validate the method proposed with 43 real drifters released in Kerguelen region, and I find that the monitoring network built in this way has a performance two times greater than a regular grid, assessing furthermore its robustness even when sampling high turbulent regions.

The results provided open interesting perspectives, concerning applications in marine spatial planning, conservation issues and design and protection of marine protected areas. In particular, the extension of the aggregating mechanism to two and three dimensions is discussed and some preliminary results shown.

Acknowledgements

During the three years of my PhD, many people helped me. Here I would like to thanks them all, and I apologize if I will forget someone or I would not be able to thank them with the good words they deserve. This is a short and totally non exhaustive list.

First of all, I would like to thank my thesis director, Francesco d'Ovidio, for transmitting me his enthusiasm for the research, for his competence in such a vast discipline, for being a very good friend, for all the help he gave me during my thesis, including very nice dinners and hospitality at its place.

I would like to thank also my thesis co-director, Guido Boffetta and Xavier Capet, for their very useful support, for their preparation and competence which always emerged during our discussions, and for helping me with their review of my work.

I would like to thank the two thesis reviewer, Bettina Fach and Daniele Iudicone, for having accepted to correct the manuscript and their precious comments.

Voglio poi ringraziare i miei genitori, per i tanti insegnamenti e per avermi trasmesso valori di cui vado fiero, per avermi sempre consigliato bene, aiutato, e aver sempre rispettato le mie decisioni. Un grazie enorme anche a mia sorella, per avermi mostrato la strada della ricerca, per il suo aiuto in questo lavoro, per i suoi consigli al tempo stesso da sorella e da collega.

Un grazie gigante anche a Enrico Ser-Giacomi, collaboratore, collega d'ufficio e soprattutto amico. Grazie per il contributo che hai dato a tutta la tesi e per la tua serietà, passione, precisione, competenza che ho cercato di imparare da te.

Grazie anche a Alice Della Penna, per la pazienza e la precisione con cui mi ha sempre aiutato durante questi 3 anni. Grazie a Sara per le discussioni scientifiche e non avute insieme, e per essere stata pazienta correttrice dei miei tesi in francese.

Grazie a tutti i miei amici, in particolare a Orso Romano con cui ho trascorso 2 anni e mezzo fantastici a Parigi, a Marco, a Arrigo, a Lucas e a tutti gli altri.

Je voudrais faire un très grand remerciement à Eric Fourlon. Sans son aide, je n'aurais pas pu obtenir et remplir correctement tous les documents nécessaires pendant mon doctorat. Merci pour la disponibilité continue, et meme pour l'aide dans questions que souvant concernaient pas ses competences. Merci aussi à tout le secrétariat, à partir de Dany, qui a été super disponible et toujours souriante, à Nathalie, fondamentale pour tous les ordres de mission, très patiente, et à tous les autres.

Finalement, merci à toi, Inés, pour m'avoir toujours motivé dans le travail, pour la patience que t'as eu avec moi, et pour tout le temps fantastique qu'on a passé ensemble. J'espère qu'on en passera encore beaucoup ensemble.

Contents

List of Figures

List of Tables

Alla mia famiglia

Chapter 1

Introduction

1.1 The dynamical landscape of the open ocean

The understanding of the interactions between physical dynamics and biological processes is a fundamental step toward the comprehension of ocean ecosystems. This issue concerns a series of challenges, such as the protection of the oceans from human exploitation [Viikmäe et al., 2011, Delpeche-Ellmann and Soomere, 2013a, Ehler, 2018], the effect of global change on marine systems [Orr et al., 2005, Halpern et al., 2008, Domingues et al., 2008, Iudicone et al., 2016] and their reciprocal role on climate regulation [Ramanathan, 1981, Ducklow et al., 2001], the monitoring of ecosystems biodiversity and abundance [Noss, 1990, Agnew, 1997, Boyd and Murray, 2001, Wells et al., 2004], and several others questions (see for instance [Mann and Lazier, 2013]). Compared to the terrestrial environment, in the oceans the coupling of physical and biological processes is even more important, because of the dynamical nature of the landscape in which the organisms live, with water masses continuously transported, rearranged and mixed by the flux [Lévy et al., 2012, Woodson and Litvin, 2015, McGillicuddy Jr, 2016, Lehahn et al., 2017]. Hence, during their lifetime, marine organisms typically experiment several conditions which can be really different among them. This is why, among the wide range of spatial and temporal scales which characterize the physical processes in the ocean [Chelton et al., 2007], I am particularly interested to the submeso- and mesoscale processes (few to hundreds of kilometers, few days to several weeks) [Capet et al., 2008a], from now on (sub)mesoscale or fine scale processes, since their timescales overlap with the ecological ones. Fine scale processes are ubiquitous in the ocean [Chelton et al., 2007] and present highly energetic features [Ferrari and Wunsch, 2009]. The latter are important for the redistribution of ocean properties, that would otherwise result much more homogeneous. In term of heterogeneity, one of the main processes involving the

fine scales is the horizontal stirring, which modulates water masses, stretching them and creating long convoluted filaments. In this dynamic, the lack of fixed points of reference (at least for human sight) makes the study of fine scale variability very complex. The Lagrangian approach, consisting in the analysis of the trajectories of the water masses, provides a natural framework for the comprehension of the history and the properties of the water masses (see for instance [Abraham and Bowen, 2002, d'Ovidio et al., 2004, van Sebille et al., 2018]). The Lagrangian approach has seen an increasing use since the beginning of the 1990s, particularly because of the technological advancements in satellite data acquisition. These have permitted to obtain observations of the velocity currents, on the horizontal dimension, with the temporal continuity and the spatial resolutions required for its application. This allowed to shed some light on the interactions between physical mechanisms and biological activity [Lévy et al., 2012, McGillicuddy Jr, 2016]. In particular, it has been possible to show the structuring role of fine scale processes on lower trophic levels, demonstrating how a physical front can be also an ecological front (i.e., a transition between regions with contrasted ecological properties), showing for instance how currents modulate phytoplanktonic blooms and community composition [Abraham, 1998, Mahadevan and Campbell, 2002, Martin, 2003, Lehahn et al., 2007, d'Ovidio et al., 2010, d'Ovidio et al., 2015, Lehahn et al., 2017] or distribution of crustaceans such as krill [Fach et al., 2002, Fach and Klinck, 2006]. On the other hand of the trophic chain, it has been observed how fine scale structures are persistently targeted by top predators, in particular during their foraging activities [Scales et al., 2014b, Waluda et al., 2001, Polovina et al., 2006, Kai et al., 2009, Bailleul et al., 2010, De Monte et al., 2012, Della Penna et al., 2015]. However, while several studies shown the importance of these features for the "extreme" elements of the trophic chain, less is know on intermediate levels of the food web. Nonetheless, these occupy a strategical position in the trophic chain [Frederiksen et al., 2005, Smith et al., 2011], and their importance, due also to their huge biomass [Irigoien et al., 2014], is acknowledged for several reasons, such as their role in the biological pump [Parekh et al., 2006, St. John et al., 2016], in climate regulation [Hidaka et al., 2001a, Hudson et al., 2014], in preservation of biodiversity [Tittensor et al., 2010, Webb et al., 2010], and in societal issues, from an economic [St. John et al., 2016], dietary (FAO State of World Fisheries and Aquaculture, 2014), cultural [Bell et al., 2018], and healthcare [Lea et al., 2002, Koizumi et al., 2014] point of view. While global patterns of primary production can be assessed by satellite observations [Antoine et al., 1996], and several tagging programs allow now to target the behavior of apex predators in most of the oceanic regions [Boehlert et al., 2001, Ropert-Coudert and Wilson, 2005], global patterns of micronekton by direct observations are very coarse [Tittensor et al., 2010] or are determined indirectly through connectivity analysis of early stages of their development, such as larvae [Mariani et al., 2010], or sources of possible nutrients, such as chlorophyl blooms, that however are

transported by the currents and need a maturation time. In particular, direct information on mid-trophic organisms can only be obtained by ship-based observations, with the notorious difficulty of disentangling space from time variations, and with biases due to several reasons [Pakhomov and Yamamura, 2010a, Brodeur and Yamamura, 2005]. Efficient monitoring strategies are therefore needed to provide more informations about their ecology [Robison, 2009, Handegard et al., 2012, St. John et al., 2016].
Therefore, two main questions arise.

- How does the structuring role of Lagrangian structures, seen for the top and the bottom of the trophic chain, extend to the distribution of mid-trophic organisms?

- How do sampling strategies can be optimized for observing mid-trophic organisms?

The answers to these questions are complex, often depending on several factors, such as the region of study, for which it is thus important to choose a biogeographical partition of the domain considered, the species examined, for which biological considerations must be involved, the season, among other aspects. Furthermore, the integration of Lagrangian tools to intermediate trophic levels is an uncharted territory. This requires to cross multi satellite data with acoustic measurements, and to develop mathematical models to combine the effect of active swimming organisms and passive transport. Given these considerations, in my thesis I try to address the aforementioned questions in this way:

- I analyse the relationship between satellite derived Lagrangian diagnostics, such as Finite-Size Lyapunov Exponents, and acoustic measurements of fish concentration along several boat transects in the Southern Ocean. I then investigate the structuring role of fine scales on mid trophic webs by developing mathematical mechanisms of fish aggregation based on horizontal currents in proximity of a frontal structure and basic swimming behavior.

- I develop a new Lagrangian diagnostic which enables to build an optimal monitoring network of fixed stations. This could potentially be used to sample mid trophic levels in a more efficient way, and to estimate their spatial provenance.

In this thesis I analyse the Kerguelen region in the Southern Ocean. The area presents highly energetic fine scale processes, especially on its eastern part. In this region, the effects of the currents on primary production are well known, along with the interactions of top predators with the fine scale structures. Furthermore, the region presents high

concentrations of myctophids, a micronektonic organism fundamental for the ecology of that area. One of the major challenge of this study is the parameterization of their behavior: indeed, they present cruising swimming speeds comparable with those of the currents. This pose them in an intermediate position between planktonic organisms, passively advected by the currents, and apex predators, which can almost neglect the effect of the currents when swimming. Given therefore the order of magnitude of their swimming speed, we define them as "semi-passive" in the sense that we suppose that they can swim fast enough to locally follow some targets and eventually aggregate, but that they are unable to contrast the currents at large scales.

The thesis is organised in this way. Chapter 1 presents the background topics necessary for the comprehension of the problems analysed in this thesis, from a physical description of the oceanic dynamics, the illustration of the importance of mid trophic web elements, the characterisation of the physiology of the organisms considered in this study, to the description of the region analysed. In Chapter 2, I analyse acoustic data revealing fish concentration and I correlate them with satellite derived diagnostic. Indeed, part of my thesis work concerned the acquisition of acoustic data with the THEMISTO project during my participation at the at-sea campaign MD206 in January and February 2017. I then develop a simple model in order to analyse the aggregating role of fine scale structures on fish, which may explain the results obtained in the first part of the Chapter. In Chapter 3, I face the problem of the lack of informations on mid trophic levels, by developing a diagnostic which estimates the surface flow coming from or going to a target region. I show that this allows one to build an optimal network of fixed stations, which could be used to monitor and provide informations on mid trophic levels at large scales. In Chapter 4, I discuss the results obtained in Chapter 2 and 3 and I describe a first attempt of building an explicit physical-nekton circulation model, in which the interactions between fine scale dynamics and swimming are explicitly represented.

1.2 Fine scale processes

fine scale processes characterize the dynamics of all the oceans worldwide. They include so-called mesoscale features, typically oceanic eddies of ∼100 km representing the 50% of the total variability of the kinetic energy [Chelton et al., 2007], as well as smaller filamentary structures (1-10 km, [Capet et al., 2008b]). These features are highly energetic, and present a peak in the energy spectrum of the ocean turbulence [Ferrari and Wunsch, 2009]. In the present thesis, I will focus mainly on fine scale processes along the horizontal dimension. First, because at present, reliable estimation of oceanic currents over large scales are available only along this dimension. Then, because on the ecologically-relevant

temporal scales considered in the present study (from few days to 2∼3 months) the contribution of the vertical displacement is much smaller compared to the horizontal ones [d'Ovidio et al., 2004, Rossi et al., 2014]. Furthermore, important vertical structures, such as submesoscale upwellings in correspondence of fronts, are highly related to the presence of horizontal features, and their pattern are often in phase with those that can be obtained from horizontal information only [Holloway and Kristmannsson, 1984, Klein et al., 1998, Young et al., 1982, Capet et al., 2008b, Lapeyre and Klein, 2006, Smith and Ferrari, 2009]. One of the main dynamics responsible for the redistribution and transport of the water parcels and their contents at the (sub)mesoscale is the so-called "horizontal stirring". According to [Ottino, 1989], the stirring is the process of advection without the effect of diffusion, therefore a reversible process which enhances the formation of tracers gradients [Eckart, 1948, Okubo, 1978, Garrett, 1983, Sundermeyer and Price, 1998] and vertical currents [Holloway and Kristmannsson, 1984, d'Ovidio et al., 2004, Smith and Ferrari, 2009]. Alongside, the effect of stirring and diffusion together, irreversible, is referred to as "mixing", and reduces the gradients. Horizontal stirring dynamic, from one side, is responsible for the stretching of water masses, which are shaped in elongated and twisted filaments. On the other, it can provoke the retention of portions of the original water masses, close to their original position, by the so called transport barriers. In presence of eddies, water masses can thus be trapped in their cores for timescales comparable with their lifetime [Lehahn et al., 2011, d'Ovidio et al., 2013], while at their periphery the process of filament formation can make them intrude far away from their origin, making possible the contact of water masses with different properties and enhancing mixing. Horizontal stirring can furthermore improve submesoscale instabilities [Capet et al., 2008b], and is therefore a key process for merging together the effect of velocity currents variability on tracer dispersion. Indeed, at fine scales, distribution of water properties by horizontal stirring have important consequences on the whole marine biota. It is possible to speculate that, without these fine scale dynamics, resources would be pretty homogeneously allocated, with gradients present only over large scales, mainly due to latitudinal variations. In this scenario, favorable grounds for a determined species would be confined to regions with specific environmental conditions, and thus to a reduced areas. The development of efficient foraging strategies would not be favoured by selection, because any searching system would be equally profitable. The effect of fine scale processes on resource partitioning makes their patchiness increasing, helping the development of selection mechanisms and biodiversity increments. However, due to the chaotic nature of these processes, their study is complex and the development of appropriate tools of investigation, such as the Lagrangian methods, has become necessary.

1.3   The Lagrangian approach

In the investigation of fine scale structures, since their typical timescales overlap with those of several ecological processes and organism behaviors, it is important to untangle the biological from the physical dynamics. One example is given, for instance, by the classic problem of the "spatial vs temporal variability". Indeed, supposing of measuring the primary production in a fixed station, in which for instance the chlorophyll concentration arises during a period of some days to few weeks, it is difficult to determine if the effect is due to a bloom occurring in proximity of the measuring station, or if the peak occurs because some previously formed chlorophyll crosses the station, being transported there by the currents. Indeed, fine scale processes which modulates the primary production can travel distances comparable to their length (few tens of kilometers) in few weeks, or, in some cases, few days. These are also the typical timescales of phytoplanktonic blooms. The problem is even exacerbated by the fact that fine scale processes can modulate other processes (such as vertical fluxes) which in turn influence the primary production. For the case of chlorophyll observation, satellite measurements could be a solution to better comprehend these problems. However, even in that case other issues arise, such as the unavailability of satellite measurements due to cloud coverage: this forces to merge together observations on different days, and confuses again spatial and temporal variability. In order to untangle these problems, a useful approach is focusing on the water parcels trajectories: in a certain way, this is like converting the observation to the case of a fixed observational point, like in a terrestrial reference system [Lehahn et al., 2018]. This approach is developed naturally in the framework of the Lagrangian methods. Even if plotting all together the trajectories originating from a certain domain results in a composite of intricate and apparently senseless ensemble of curves —the so called "spaghetti diagram" —Lagrangian methods allow to compute statistical properties over them capable of identifying some important properties of the flow. The use of Lagrangian tools has seen a dramatic increase since the 1990s, when the availability of currents data from satellite observations provided the temporal and spatial resolution necessary for the computation of water parcels trajectories with the needed continuity (see also Subsec. 1.3.1). Thanks to the application of Dynamical System Theory [Ottino, 1989, Mancho et al., 2004, Shadden et al., 2005, Wiggins, 2005], Lagrangian approach allowed the identification of several transport features. Among them, one of the most important is the concept of Lagrangian Coherent Structures [Haller and Yuan, 2000, Beron-Vera et al., 2008, Haller, 2015], which help identifying barriers to transport [Boffetta et al., 2001, Abraham and Bowen, 2002, d'Ovidio et al., 2004, Beron-Vera et al., 2008, Prants et al., 2014a, Prants et al., 2014b] and retentive or coherent (i.e., long lasting) regions [Lehahn et al., 2007, Froyland et al., 2007, d'Ovidio et al., 2013, Berline

et al., 2014, Hadjighasem et al., 2016, Miron et al., 2017]. Other Lagrangian diagnostics provide informations on more dispersive structures [Carlson et al., 2010, Haza et al., 2012, Poje et al., 2014] or transport pathways [Sandulescu et al., 2006, Rossi et al., 2008, Griffa et al., 2013]. Recently, network theory, which in the framework of fluid motion has been applied to geophysics [Phillips et al., 2015], flow transport [Ser-Giacomi et al., 2015a, Lindner and Donner, 2017, Fujiwara et al., 2017, Molkenthin et al., 2017, Padberg-Gehle and Schneide, 2017, Ser-Giacomi et al., 2017, McAdam and van Sebille, 2018] and turbulence [Iacobello et al., 2018, Gopalakrishnan Meena et al., 2018], have been extended also to Lagrangian trajectories with the so called Lagrangian Flow Networks (LFNs, [Ser-Giacomi et al., 2015a]). The question addressed by LFN is somehow opposite to the classical questions of Lagrangian tools, which are more focused on the identification of frontal zones characterized by minimal exchanges toward the neighborhoods. Indeed, the aim of LFNs is to identify which zones in a given domain promote the exchange of water mass between the system. Properties borrowed from network theory, applied to LFNs, help addressing this issue. In this context, in a work with Enrico Ser-Giacomi et al., we demonstrated how it is possible to relate a classical network theory property, the *betweenness*, to Finite-Time Lyapunov Exponents (FTLEs), a classical Lagrangian diagnostic (Ser-Giacomi et al., in prep.). The betweenness allows one to identify the bottlenecks of a flow system, therefore regions that convey water from a large surface, and that spreads it over a vast area, which play therefore a key role for the connection of a given domain (Fig. 1.1). Finally, Lagrangian properties can be extracted also from drifters trajectories. These, compared to numerical trajectories, have the advantage of being more reliable ("ground truth"), but are more sparse in space and time, due to their cost and their logistic demands, as will be discussed in the next Subsection.

1.3.1   *In-situ* and remote sensing data

Satellite data are the main source of synoptic information used in the present thesis, and, as seen in the previous Section, are precious tools for the application of Lagrangian methods. Indeed, they permit one to survey a region several orders of magnitude larger than what is possible with *in-situ* samplings. Furthermore, the quality of their measure is not affected by the remoteness of the region, and can even improve in distant zones. Their outputs are nearly homogenous at basin or global scales, and with long recording series which can cover tens of year. Finally, their spatial and temporal resolutions are often well suited to sample meso- or submeso- scale processes.

However, as seen in Sec. 1.3, Lagrangian information can be derived also from drifters trajectories, which provide *in-situ* observations. These are effectively the only possible
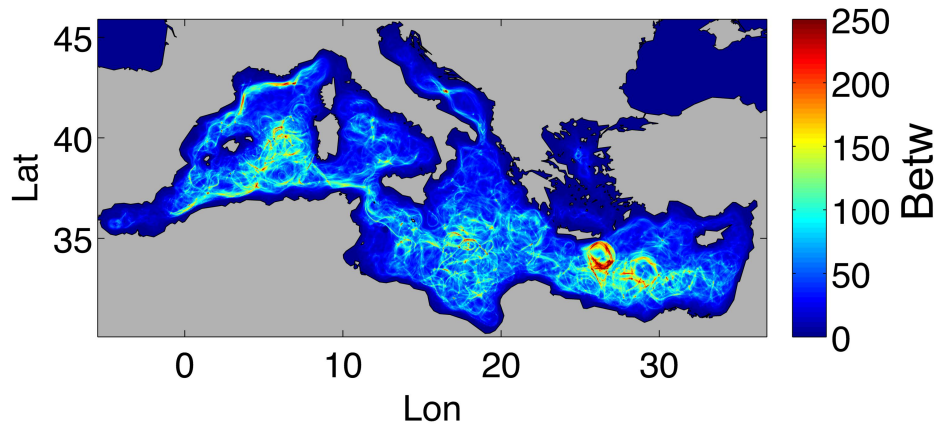
FIGURE 1.1: In collaboration with E. Ser-Giacomi et al. (in prep.). Climatology of Lagrangian betweenness, on the month of December, between 2002 and 2011. The Lagrangian approach has proved to be an efficient tool for the investigation of the complex biophysical dynamics of the ocean. In this work, borrowing some concepts from Lagrangian Flow Network theory, we applied the *central betweenness* property, a concept developed in network theory and particularly used in Lagrangian Flow Networks [Ser-Giacomi et al., 2015a], to the study of ocean transport, finding a correlation with a Lagrangian diagnostic, the Finite Time Lyapunov Exponents. The betweenness obtained in this way identifies"bottlenecks", of the circulation, i.e. structures that convey water from large regions and spread it over a vast surface, which thus play a major role in the connectivity of the domain considered.

ground truth for the computation of Lagrangian trajectories of water parcels containing biotic and abiotic parameters. Indeed, currents speed or other type of satellite measures are based on indirect measurements. For instance, satellite derived velocities are computed from the sea surface height (SSH), through the geostrophic approximation. They are, nowadays, limited to scales of ∼70-100 km (even if future missions such as SWOT will reduce this measure to 10∼20 km), and they neglect vertical processes like mixed-layer instabilities [Capet et al., 2008a] and all the ageostrophic components. Altimetry is also unreliable close to the coasts. Also the measure of the Absolute Dynamic Topography, necessary for the computation of the currents, depends on ancillary estimations of the geoid. Numerical trajectories computed from satellite-derived currents have been shown to be consistent with drifters trajectories (i.e., keeping distances in the order of ∼10 km on days to weeks, temporal horizons), only in proximity of attractive Lagrangian Coherent Structures [Poje et al., 2002, Resplandy et al., 2009, Nencioli et al., 2011, Schroeder et al., 2012, Olascoaga et al., 2013]. On the other hand, trajectories of real drifters have seen in the last years a dramatic increase. Nonetheless, the spatial and temporal resolutions needed in particular for the analysis of fine scale processes are far from being covered by the *in-situ* measurements actually available, even if recently, specific regional campaigns (such as the Grand Lagrangian Deployment, GLAD, or the Consortium for Advanced Research on Transport of Hydrocarbon in the Environment, CARTHE) provided interesting results [Olascoaga et al., 2013, Mariano et al., 2016].

Considered the advantages and lacks of both methods, drifter and altimetry-derived trajectories can be seen as complementary in Lagrangian studies, and it thus important to develop strategies in order to integrate and cross-validate them.

1.4   The influence of fine scale processes on pelagic ecosystems

The Lagrangian approach, illustrated in Sec. 1.3, has been used to shed some light on the effect of fine scale processes on biological processes, inferring how fine scale structures, even if constituting a relatively small portion of the total surface, play a huge role in ecosystems regulation [Lévy et al., 2012, McGillicuddy Jr, 2016], from primary production to top predators. Indeed, the structuring role of (sub)mesoscale currents on chlorophyll bloom has been assessed since the 1980s, when the first high resolution images of chlorophyll blooms from satellite permitted to analyze their spatial heterogeneity with different methods (spectral, semivariogram, autocorrelation and patchiness analysis [Platt and Denman, 1975, Gower et al., 1980, Yoder et al., 1994, Denman and Abbott, 1988, Piontkovski et al., 1997, Washburn et al., 1998, Mahadevan and Campbell, 2002]) and to relate them to horizontal stirring and mixing effect. Lagrangian methods, which started to be applied consistently in the following decade, are based on the comparison between different temporal snapshots of chlorophyll blooms (or other passive-like organisms, such as krill), characterized by patterns between ~ 100 and ~ 1000 km, and the spatial distribution of the numerical advection of virtual parcels from target regions advected by satellite or model derived velocity currents [Fach et al., 2002, Toner et al., 2003, Fach and Klinck, 2006, Lehahn et al., 2007, Olascoaga et al., 2008, Calil and Richards, 2010, Guidi et al., 2012, Huhn et al., 2012]. This is for instance the case reported in Fig. 1.2 and 1.3: in the study of Ozier et al. (in preparation), we studied the northward intrusion of an invasive phytoplankton, the *coccolithophorids*. These started to appear in the August-September bloom characterising the Barents Sea. Anomalous phytoplanktonic bloom are indeed more and more present in North Antlantic waters (see for instance [Lacour et al., 2017]). Through a Lagrangian analysis, we identified as co-causes of the coccolithophorids invasion the increased water temperature in the Norway Sea, and the strengthening of the currents speed. Both the effects are probably due to climate change.

Sometimes, in regions where mesoscale components are dominant or entrain finer ones, Lagrangian methods can predict phytoplanktonic patterns even on features at sizes of the submesoscale. This is possible because of the temporal variability of the velocity
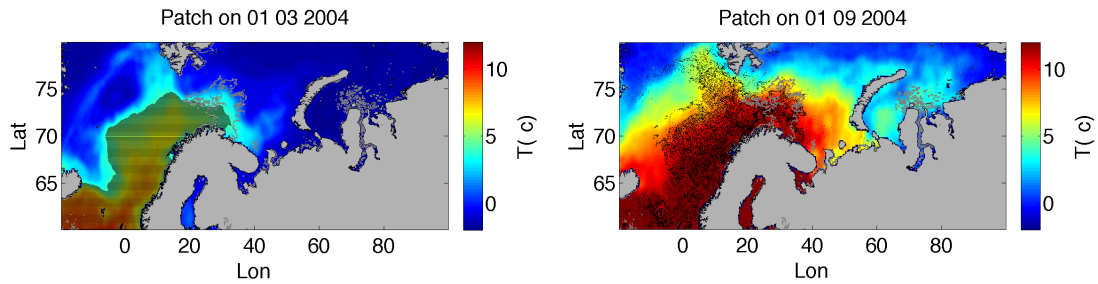
FIGURE 1.2: Understanding the role of transport on phytoplankton is essential for many aspects, and can help identifying the effects of climate change on primary production. In this collaboration with Ozier et al. (in prep,.), we analyse the northward intrusion of an invasive species, the *coccolithophorids*, in the Barent Sea. We find that the increase of temperature and currents may be responsible for this phenomenon. Left panel: average SST field of March. Black dots identify the points with SST< 4°C. They are separated by $\delta = 0.1°$. Right panel: final position of the black dots identified in the left panel, which are advected between the 1st of March and the 1st of September 2004. The gray line represent the contour of the PIC field of August 2004 at 3 mg/m^3.
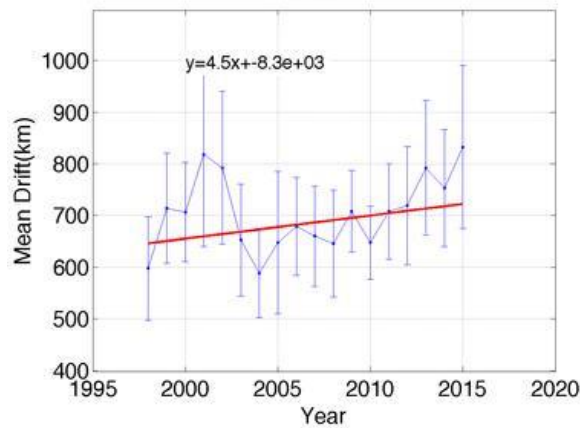
FIGURE 1.3: In collaboration with L. Ozier et al., (in prep.) Mean distance travelled by a reference patch along the year, with error bars representing the standard deviation. The reference patch was built selecting the points with SST< 4°C and longitude> 7°W. The SST field considered is the climatology of March between 1998-2016. For each year then, we considered only the particles whose final position has longitude > 32°E. The mean distances were fitted taking into account their standard deviation. The equation of the fit is reported in the plot.

fields used for the computation of the trajectories [Iudicone et al., 2002]. Indeed, without temporal variability, parcels advected follow current streamlines, and are thus trapped forever if these are closed. If the velocity field changes at each time step instead, once the parcel has completed its loop it will projected in a slightly different streamline, eventually forming a spiraling pattern. This mechanism gives raise to complex patterns of circulation at finer scales, described by dynamical system and chaos theory [Wiggins, 2005, Prants et al., 2017]. fine scale processes play also a fundamental role in the structuring of the microbial community. Indeed, thanks to the several new methods that

allowed to identify the main composition of the phytoplanktonic community from satellite, in the study of [d'Ovidio et al., 2010] it has been possible to show how ecological fronts, which separate communities dominated by different species, are well predicted by Lagrangian fronts identified by Finite Size Lyapunov Exponents. Indeed, waters dominated by different phytoplanktonic species, are advected and elongated by horizontal stirring, creating complex patterns. This can in turn favors also the intrusion of some species far from their origin, enhancing contact and mixing of different communities, and improving and regulating the biodiversity of the primary production [De Monte et al., 2013].

The Lagrangian approach has been applied successfully also to higher elements of the trophic chain, in particular to top predators which have strong swimming capabilities. The reason of this positive correlation originates by the fact that a time gap between the primary production and the appearance of favorable conditions for top predators is necessary for the maturation of the ecosystem: during this time gap, the waters are advected by the circulation features. This issue has been clearly shown in the study of [Cotté et al., 2015] concerning some individuals of elephant seals (*mirounga leonina*) of the Kerguelen basin, which, during their foraging behavior, were targeting waters with no presence of chlorophyll. However, advecting them backward, it has been possible to infer how those were the waters which were supporting the phytoplanktonic bloom at spring, and that in the meanwhile had been transported more than 1000 km away from the bloom zone. The relationship between top predators behavior and Lagrangian Coherent Structures has been shown also at finer scales by several studies which focused on sea turtles ([Eckert et al., 2006, Fossette et al., 2008, Polovina et al., 2006] and [Chambault et al., 2017], Fig. 1.4 and Appendix A), Mediterranean whales, fur and elephant seals [Della Penna et al., 2015, Dragon et al., 2010, Cotté et al., 2011b, Nordstrom et al., 2013, Cotté et al., 2015], penguins [Bon et al., 2015, Penna et al., 2017] and seabirds [Kai et al., 2009, De Monte et al., 2012, Scales et al., 2014a].

While "extremes" of the trophic chain are well studied and relationship with fine scale structures is well documented, less is known about intermediate trophic levels. These can not be easily instrumented as some of top predator species, neither observed directly via satellite as the chlorophyll, and present several sampling difficulties (see also Section 1.5). The study of [Sabarros et al., 2009] showed the importance of mesoscale eddies into influencing mid trophic levels distribution, focusing however on Eulerian quantities such as sea level anomalies and not on Lagrangian analysis, and only on broad scales. The works of [Prants, 2013, Prants et al., 2014a, Prants et al., 2014b] provide instead, to my knowledge, the first application of Lagrangian methodologies to the study of fish, notably the Pacific saury. These studies identified increased catches of this species by commercial fisheries in correspondence of Lagrangian structures. It is however difficult
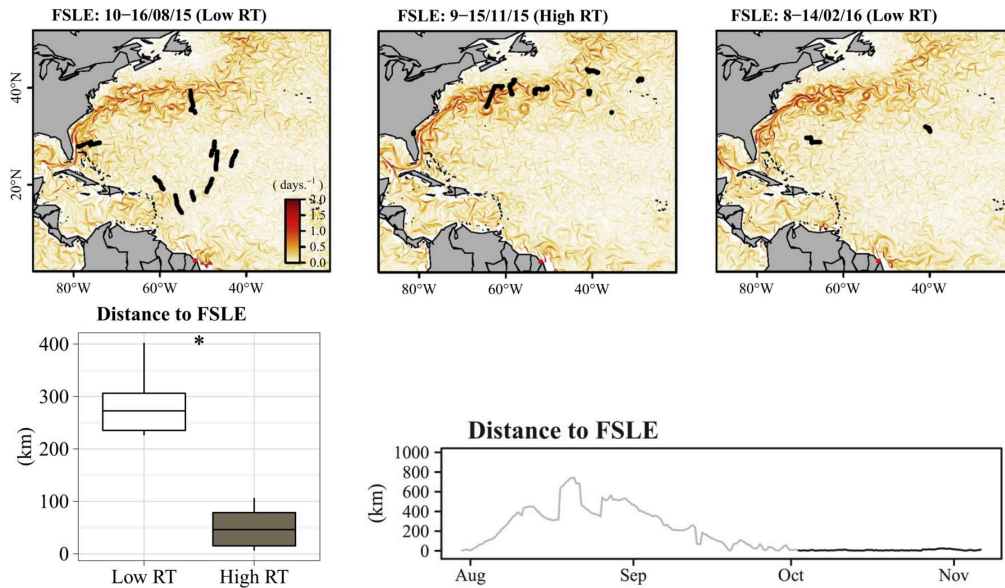
FIGURE 1.4: In collaboration with P. Chambault ([Chambault et al., 2017] , Appendix A). Study of the role of fine scale structures on leatherback turtles behavior. We computed Lyapunov exponents in the Northern Atlantic Ocean, in order to highlight the fine structures at the (sub-)mesoscale of the region. Lyapunov exponents were computed for three different weeks (three upper panels). This diagnostic was then compared to the trajectories of 11 adult females of leatherback turtles. For each upper panel, the black dots correspond to the trajectories of the turtles during that week. In particular, high residence times (HRT) were computed along each trajectory. These values account for the time spent in the neighborhood of a point: high values allow thus to estimate intensive foraging behaviors of the predator. It was found that the distance from the closest front of FSLE drops significantly during HRT periods, i.e. during putative foraging activities. This can be seen in the two panels below (box plot on the left, and distance from the closest front along the turtle at-sea time on the right).

to assess how this relationship could be simply due to the fact that the fishery grounds were chosen by the vessels looking directly at satellite data, as recently shown by [Scales et al., 2018, Watson et al., 2018]. Industry dependent data then present other biases which are difficult to quantify, such as differences due to trawls and other factors as explained in Section 1.5.1. Furthermore, actual works on mid trophic levels do not provide any mechanistic explanation capable of identifying the direct role of fronts as aggregating hotspots for fish, and not from a quantitative point of view. Indeed, actual explications are based on *bottom-up* effect, associating for instance submesoscale features to vertical movements [Capet et al., 2008a, Klein et al., 2005], and thus to nutrient pulses capable of enriching the trophic chain [Lévy et al., 2012, Mahadevan et al., 2012, McGillicuddy Jr et al., 1998, Bakun, 2006]. The role of the horizontal transport is therefore actually not taken into account, neither its direct effect on fish movement. The latter has been studied only from a mechanistic [Bainbridge, 1958, Sfakiotakis et al., 1999, Gui et al., 2014] or schooling [Radakov, 1973, Parrish and Hamner, 1997, Grünbaum, 1998, Pavlov and Kasumyan, 2000] point of view, i.e. on distances ranging from few tens to hundreds

of meters, but not at larger scales like the ones that characterize the (sub)mesoscale dynamics (i.e. few to tens of kilometers). Therefore, as assessed by [St. John et al., 2016], it is important to describe "the links between oceanographic regimes and mesopelagic biomass and biodiversity (species, traits, population genetics and habitats) thus enabling the prediction of species dynamics relative to oceanographic regimes which will be impacted as their environment alters under climate change" .

1.5   The importance of intermediate trophic levels in the marine ecosystem and for societal issues

Although in my work I focused only on two specific aspects of micronekton dynamics (aggregation and sampling) it is instructive to briefly review they general importance. Intermediate trophic levels (or equivalently "mid trophic organisms") constitute a central element in the marine environment, for a large number of reasons. From an ecological point of view, micronekton connects plankton to the top predators, transferring thus production from lowest to apex levels of the trophic chain [Cury et al., 2000, Shannon et al., 2000, Jahncke et al., 2004, Frederiksen et al., 2005, Crawford et al., 2007, Smith et al., 2011]. For instance, myctophids, one of the most abundant fish worldwide, and reference fish of the present thesis (Section 1.6), are main prey of many apex predators [Sabourenkov, 1991, Kozlov, 1995, Hopkins et al., 1996, Beamish et al., 1999]. They feed mainly on crustacean and gelatinous zooplankton [Gordon et al., 1985, Kinzer et al., 1993]. With their nycthemeral cycle, defined as "the largest daily migration of animal on earth" [Hays, 2003, van Haren and Compton, 2013], and their huge biomass [Irigoien et al., 2014], micronektonic organisms play a central role in the carbon export to the depths, participating to the so called "biological pump". During this process the carbon, captured by the phytoplanktonic photosynthesis close to the surface, "falls" toward the seabed where it is trapped for geological-long times. The biological pump is responsible for the $\sim$50% of the carbon export in the depths of the ocean [Parekh et al., 2006], influencing in turn the atmospheric CO_2 concentrations. Indeed, just changing some parameters describing the biological pump process in the mesopelagic zone, studies such as the one of [Kwon et al., 2009] shown that CO_2 concentrations can vary of $\sim$100ppm. It is thus fundamental to take into account for the role of the vertical migration of micronekton, that instead only recently has been included in model simulations [Benway et al., 2014]. Thus, affecting the carbon sequestration into the depths, micronekton in turn plays also an unsuspected role in climate regulation [Hidaka et al., 2001a, Hudson et al., 2014].

In spite of the general lack of information on these organisms [Robison, 2009], micronekton potentially plays a key role in the mesopelagic biodiversity and interactions within the ecosystem [Tittensor et al., 2010, Webb et al., 2010].

Micronekton is one of the less exploited resources by fishery industries, but is threatened to be in the near future [St. John et al., 2016]. Indeed, fish are among the world's most traded food resources, with a business of around $ 130 billions per year (FAO State of World Fisheries and Aquaculture, 2014). Three billion people rely on fish as their primary source of protein, and, in some cases, fishing activity is essential to the survival of communities, not only for its importance in the daily diet, but also as main source of income and as integrating part of cultural identity [Ansell et al., 1996, Bell et al., 2018, Dunstan et al., 2018]. Actually, according to FAO estimates, 29% of the commercially important marine fish stocks are fished over biologically sustainable levels, with 61% of stocks fished at their maximum capacity. The quantity of fish eaten by people keeps raising and has doubled between 1960 and 2012. Even recreational fishing brings a source of fishing pressure and mortality for many fish stocks [Coleman et al., 2004, Tracey et al., 2016]. It is not surprising that therefore mesopelagic fish, and in particular myctophids, has started to receive attention as potentially harvestable resource ([Gjøsaeter and Kawaguchi, 1980], FAO 1997, 1998, 2001). In a recent work, [St. John et al., 2016] indicate as 2.7 the percentage of estimates of mesopelagic fish necessary for maintaining the whole global aquaculture production. They furthermore state that, fishing around the 50% of the actual mesopelagic biomass, would correspond to $\sim$ 4.6kg of fish biomass per person per day. Micronekton has started to receive lot of attention also for its high concentration in fatty acids [Lea et al., 2002, Koizumi et al., 2014], important for the demand of "Omega-3" useful for human health [Kris-Etherton et al., 2002].

In this scenario, it is thus important to move toward a more sustainable management of fisheries. This could lead to many advantages, as stated by FAO report of 2014 (State of World Fisheries and Aquaculture). Global fish harvest could be 40% higher if managed in a sustainable way, leading to an extra $ 50 billions of income. However, the information on ecological dynamics, interactions, biomass and so on, necessary to a healthy management, is difficult to obtain, especially at large scales [Handegard et al., 2012]. Satellite products are not useful for direct measurements of fish stocks and can only be used for chlorophyll observations. The time gap necessary for the development of the trophic chain between primary production and micronektonic organisms [Cotté et al., 2015] makes them difficult to interpret in this way. Also top predators are better studied than smaller size organisms. Occupying by definition the end of the trophic chain, any perturbation on the ecosystem is expected to affect them, and they are thus often defined as *integrators* of the trophic chain [Cury et al., 2003, Camphuysen, 2006, Sala, 2006, Heithaus et al., 2008, Estes et al., 2011]. Therefore, generally strong economic

[Pauly et al., 1998, Christensen et al., 2003, Reynolds et al., 2005, Shephard et al., 2012] or patrimonial [Tyler et al., 2011] interests are directed toward them. Therefore, less informations are available on micronekton, and often sampling measurements present different types of bias [Pakhomov and Yamamura, 2010a]. In the next Subsection we review some of the methods actually used for sampling fish.

1.5.1 Sampling techniques of intermediate trophic levels

1.5.1.1 Fishery data

One of the most important source of information about intermediate trophic levels are the data coming from fishery measurements. In this framework, it is possible to distinguish two different types of data: the industry dependent, and the industry independent data. The first type usually consists in a logbook, containing informations about the quantity, the type of fish, the location and the catch time. The main advantage of this type of data is that it usually has broad coverage, with relative low costs. However, industrial dependent data presents many potential problems [Faunce et al., 2015]. First of all, the fishery methods are not standardized between different industries, and therefore different catches do not necessarily correspond to differences in the ecosystem. It is then difficult to obtain information about the type of trawls used, and to estimate the differences in catches due to that [Zeller and Pauly, 2018]. Industries interest is addressed toward marketable fishes, and this implies a neglecting of other species that could be very important for the ecosystem. The presence on board of an independent observer makes instead this data industry independent. The risk is in fact that the compilation of the logbook stays uncompiled, or with wrong informations. These can be due to the fact that catches are declared in different areas, or at different times (fishing blocks), to respect locations and periods of fishing. The industry independent data presents therefore usually a smaller covering and a stronger dependence from availability of resources, but allow to obtain more informations (length, age and other biological parameters), with reduced risks for bias.

One of the first parameters used to assess the health of a stock is the "catch per unit of effort". This parameters estimates the cost of energy necessary to capture a certain quantity of fish. Assuming that the catch of fish is proportional to this effort E and to the size of the stock N (catch$= q\,E\,N$, q costant of proportionality), a proper estimate of the level of effort (e.g., number of days employed) can allow to obtain N. However, fishing seasonality, location and efficiency must be carefully taken into account to avoid strong biases.

1.5.1.2   Nets

Nets are traditional sampling tools, which allow to capture and bring to the surface fish samplings. Nets make possible to measure biological parameters such as size, weight, sex and so on, and taxonomic characterizations, all essential informations for the understanding of their ecology. Nets provide punctual measurements, i.e. reveal informations on a certain position and at a certain depth. One of the main problem of this method is related to the high costs necessary [Ariza et al., 2015]. Indeed many micronektonic organisms are too small to be captured by traditional trawls, and too fast to be captured by planktonic nets [Brodeur and Yamamura, 2005], and therefore specific tools are necessary for their sampling. Even with specific instrumentations, many problems occur [Pakhomov and Yamamura, 2010a]. One of the main issues is the bias due to different types of gears, which can lead to order-of-magnitude of differences between different samplings [Pakhomov and Yamamura, 2010b]. Secondly, the escaping rate of micronekton to nets is difficult to estimate [Pearcy, 1983], and make the measurements of their abundance probably underestimated with this method [Kaartvedt et al., 2012]. Another issue is due to the fact that during the recovery of the net other captures contaminates the sampling, making difficult to establish the vertical distribution of the organisms, even if some types of nets allow to avoid this [Pearcy, 1983]. The precision which can be obtained via nets depends also on the "patchiness" of the distribution [Wiebe, 1971]. This in turn depends on the time of the day, the season or the life stage of the individual [Pearcy, 1983]. Finally, nets measurements require a certain time, due to the handling difficulties and to the necessity to acquire a consistent biomass into the depth monitored. This limits the spatio-temporal scales detectable with this method to the medium-large ones.

1.5.1.3   Aerial surveys and logging programs

Other sampling methods consist in aerial surveys and logging programs. Aerial surveys are used for large size fish, such as tuna [Fromentin et al., 2003, Bauer et al., 2015], and therefore are not useful for small size organisms such as micronekton. Tagging programs can be addressed directly to fish, or to their predators. In the first case, populations are sampled at specific times along the year, and individuals characteristics are analysed. With this method it is possible to measure biological factors such as growth and mortality rates, movement, or population size [Neuheimer et al., 2011], and build effective monitoring regimes [Ewing et al., 2014]. These, however, are mainly devoted to coastal areas. Satellite tagging programs are instead used on largest and valuable species, to collect informations about abiotic factors characterising their environment such as temperature or salinity, or to measure vertical depth distributions, since they permit to
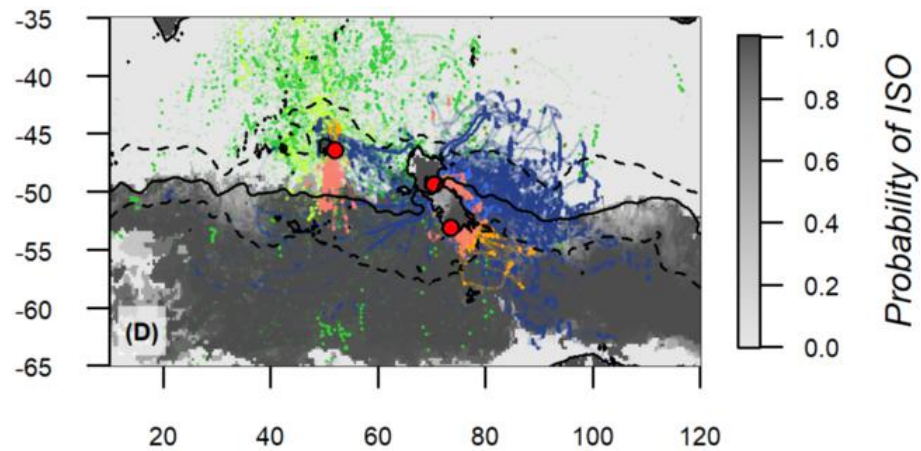
FIGURE 1.5: In collaboration with M. O'Toole et al. (submitted to PNAS, Appendix B). Biologging programs have allowed to target a large number of top predators. Here, we combine a large number of species of predator trajectories and 2° C isotherm map in order to define which predators target the isotherm and which do not. The map represents the probability of encountering the 2° C isotherm in the first 500m, while the different colors of the trajectories characterise a different species: king penguins (salmon), macaroni penguin (orange), Antarctic fur seal (blue), southern elephant seal (dark blue), dark-mantled albatross (light green), wandering albatross (green) and black-browed albatross (dark green). Red dots locate the top predators colonies here considered.

follow the fish position for relatively long time periods [Tracey et al., 2016]. Biologgers have been applied also to top predators such as fur seals [Lea et al., 2006, Nordstrom et al., 2013], elephant seals [Cherel et al., 2008], sea turtles ([Chambault et al., 2017], see Fig. 1.4, or [Polovina et al., 2006]), whales [Cotté et al., 2011a], or penguins [Cotté et al., 2007, Deagle et al., 2007, Bon et al., 2015], allowing to measure many different quantities (fluorescence, oxygen, swimming speed etc.). This has allowed, for instance, to combine these "in-situ" measurement with environmental data measured via satellite, and to characterize the foraging habitats of these predators ([Bost et al., 2009, Dragon et al., 2010, Hindell et al., 2011, Bailleul et al., 2007, Boehme et al., 2008], see also my contribution to the work in Fig. 1.5). From the micronekton sampling point of view, the introduction of accelerometers, capable of measuring the number of capture attempts, has been an important novelty. In [Della Penna et al., 2015], the relationship between the number of capture attempts and oceanographic features was analysed. This helped to shed some light on the characteristics of the favorable hotspots, rich of micronektonic organisms prey of these predators. However, one of the main limits of the biologging data is the limitation to the point of view of the predator (for instance, physiological constrains), that, even if it can help to study its ecology and those of its preys, is however restrictive for the analysis and with potential biases. For instance, one of the main limitations of accelerometers is that they risk to overestimate the number of preys present, since they can detect only the attempts of capture. Furthermore, this tool does not provide yet any indications about the size or the taxonomy of the preys.
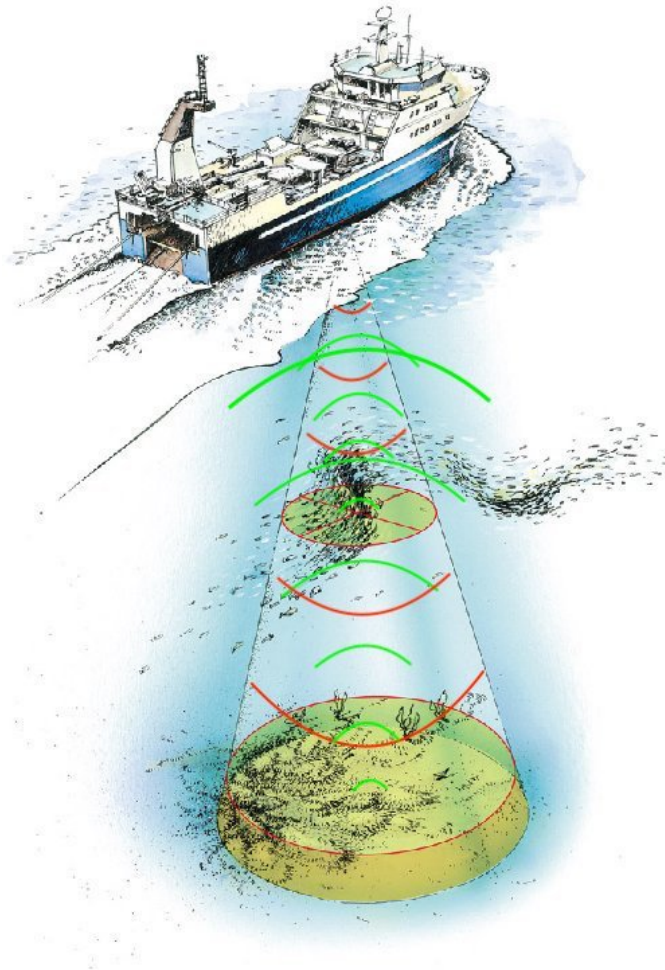
FIGURE 1.6: Illustrative scheme of the functioning of an acoustic sonar. Acoustic waves are emitted by an echosounder fixed on the boat. The wave propagates into depth and, when encountering particle matters or organisms, is backscattered. By measuring the intensity of the backscattered signal and the amount of time after which it has come back, the echosounder is able to identify the abundance and depth of ecological organisms (image from C. Cotté)

1.5.1.4 Acoustic data

So called "active acoustic" is a sampling method that has started to be largely used in ecology studies in the last two decades, thanks to the development of new sonar models. The basic principle of acoustic is the deployment of an acoustic wave which is sent from the sonar placed on the boat toward the bottom of the sea floor. Objects or organisms eventually present along the trajectory of the acoustic wave will absorb but also reflect the wave, according to their size and physical properties. The sonar, analysing therefore the signal rebounded and the amount of time after which it has come back, will be able to trace a profile of the objects present in correspondence of the sonar, indicating their size and depth (Fig. 1.6). Repeating this procedure, it is possible to obtain a profile or "transect", as shown in Fig. 1.9. Acoustic thus provide a time continuous information
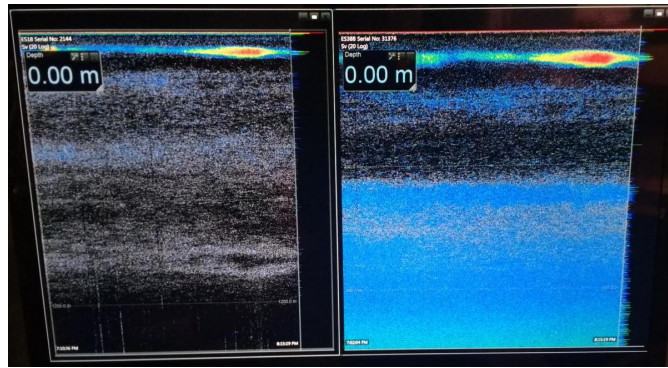
FIGURE 1.7: Repeating in time the procedure explained in the caption of Fig. 1.6, it is possible to trace a continuous profile or "transect". The picture shows two transects measured in about half an hour. The left screen shows the measure obtained employing an acoustic wave of 18kHz frequency, while the right screen the 38kHz frequency. Indeed, by changing the wavelength, it is possible to detect organisms of different sizes. In the upper right part of both screens, it is possible to see a strong backscattering signal, identified by a red patch, revealing the presence of a dense fish school at about 100m of depth. Photography by A. Baudena taken during the THEMISTO cruise in January-February 2017.

on the whole water column until a certain depth. This depth is inversely proportional to the frequency of the acoustic wave employed. Different frequencies can be used and combined together [Logerwell and Wilson, 2004], providing further informations on size, presence of swimbladder (Subsec. 1.6), and sometimes on general taxonomic parameters [Benoit Bird, 2006]. Acoustic measurements provide data which are generally more precise than those obtained with traditional nets [Catul et al., 2011]. Indeed the latter technique measures systematically lower levels of biomass [Kloser et al., 2009, Pakhomov and Yamamura, 2010b, Lara-Lopez et al., 2012], probably because of the high escape rates, leading to an underestimation of the total biomass [Kaartvedt et al., 2012].

1.6   Physiology of myctophids

In my thesis work I focus on a specific taxon: the myctophids. Myctophids are mesopelagic fish that belong to the family of *Myctophidae*, and are constituted by $\sim$250 species and 33 genera. They are considered as an important resource at planetary level [Gjøsaeter and Kawaguchi, 1980]. Possessing high energetic values [Benoit-Bird, 2004], they have been identified as a potential unexploited stock which could contribute to the *Blue Growth* strategy set by the European Union (e.g. [Gjøsaeter and Kawaguchi, 1980, Valinassab et al., 2007]). Their abundance in the Southern Ocean is estimated to about 70$\sim$200 million tonnes [Catul et al., 2011]. A recent study of [Irigoien et al., 2014], performed with acoustic measurements, underlined how this assessment and previous ones can underestimate of at least one order-of-magnitude the mesopelagic fish biomass, highlighting

FIGURE 1.8: Few individuals of *Electrona Antarctica*, a species belonging to the family of *Myctophidae*, and one of the most diffused in the Southern Ocean [Greely et al., 1999]. Photograph by A. Baudena.

even more their importance. Among the most diffused species in the Southern Ocean, we find the *Electrona Antarctica* (Fig. 1.8), the *Gymnoscopelus nicholsi* and the *Electrona calsbergi* [Pakhomov et al., 1994, Pusch et al., 2004, Loots et al., 2007, Collins et al., 2008, Flores et al., 2008, De Broyer et al., 2014, Gauthier et al., 2014]

One of the prominent characteristic of myctophids is the presence of photophores, small luminescent glandular organs, on their ventral and lateral part of their body [Tsuji and Haneda, 1971, Haddock et al., 2010], which makes them called also "lanternfishes". Leaving in the depths, between ∼150 and 1000m, they present a strong adaptation to low oxygen environments [Catul et al., 2011] and are nycthemeral fish. They spend the day at depth, between 500 and 1000m, and migrate vertically in the upper 200m at night, where they feed [De Broyer et al., 2014]. To perform this vertical translation, they are helped by the *swimbladder*, a gas-filled structure by which they are able to alter the amount of contained air and consequently their own specific gravity. They can thus move vertically relatively faster than horizontally [Hall, 1924, Kuhn et al., 1963]. The swimbladder makes myctophids more easily detectable with acoustic instruments. It is however important to note that this structure is not present on all myctophids species, and that furthermore its presence depends on the growth stage of the individual [Neighbors and Nafpaktitis, 1982].

Myctophids represent an intermediate level of the food web, with a trophic level between 3 and 4.6 [Irigoien et al., 2014]. Their main preys are zooplankton organisms such as euphasiids, ostacods and amphipods [Pakhomov et al., 1996, Gordon et al., 1985, Kinzer et al., 1993]. They are in turn main prey of many apex predators [Cherel et al., 2010, Sabourenkov, 1991, Kozlov, 1995, Hopkins et al., 1996, Beamish et al., 1999], from piscivorous fishes [Polovina, 1996, Potier et al., 2007, Pusineri et al., 2008, Flynn and Paxton, 2013], to marine mammals [Casaux et al., 1998, Brophy et al., 2009, Pereira

et al., 2011] and sea birds [Kooyman et al., 1992, Jansen et al., 1998, Deagle et al., 2007].

1.6.1   Orientating capacity of fish

In the present Subsection, I aim at showing the capacity of myctophids to identify, orientate, and follow a tracer cue in an aquatic environment, a central hypothesis in the present thesis. To do so, I first illustrate the state of art on the knowledge about fish perceiving capacities of the environment in which they live, in particular on their olfactive and visual sensibilities. I then expose some advantages of living in schools in comparison to solitary individuals. Even if there are no many direct experimental data on myctophids, it is reasonable to conclude that, thanks to the bibliography on many other species, this family of fish is capable of identifying sources of food and to follow them even for several kilometers.

1.6.1.1   Actual knowledge on fish orientating and feeding behavior.

One of the biggest problem encountered by aquatic animals during foraging and migratory activities is the fact that the resources they need varies on large spatial scales (tens of kilometers), while their sensitive capabilities allow them to achieve information only on a small volume of water around them [Atema, 1988, Royce, 2013]. This is valid in particular in presence of noisy fluctuations overlying the gradient. However, even in apparently disadvantageous conditions, fish have developed fine-tuned sense capacities and social interactions that help them to face these difficulties.
In fact, when looking at fish behavior during the research for feeding spots, two main factors must be kept into account. The first one is the olfactory reception [Kasumyan, 2004, Grimm, 1960, Hara, 1975, Kasumyan and Döving, 2003], that, in fish, is involved in almost all behavioral forms, from spawning, to locating food, to homing, to migrating, to defending, etc. [Kleerekoper, 1969, Malyukina et al., 1969, Malyukina et al., 1980, Døving, 1986, Hamdani et al., 2001, Kasumyan and Marusov, 2003]. It is recognized that this system is even more central for those species that base their feeding activities at night, thus in a dim environment, both for close and remote food searching activity [Kasumyan, 2004].
The olfactory organ in fish is a paired structure located in most species on the dorsal surface of the head. It is constituted by a chemosensory epithelium inside an olfactory bulb. Its surface consists in folds, lamellae or rosettes, that host the receptor cells. The water that enters the olfactory bulb comes in contact with this rugose surface, and brings thus in contact the substances dissolved in it with the receptor cells [Hara, 1975, Kasumyan, 2004].

Fish possess an extremely high sensitivity to scents. The concentration threshold for perception, i.e. provoking significant electrophysiological responses, can have extremely low values (10^{-9}–10^{-13} M, where M is the molar concentration, *mol/l*). [Døving, 1989] demonstrated that a sensitivity of 10^{-11}M means that a salmonid fish is able to react to a single drop poured in a $25 \times 10 \times 2$m basin (500 000 liters). In some cases, even few molecules can induce an electric response in the eel *Anguilla anguilla* [Teichmann, 1959]).

These extremely high sensibilities allowed the fish to develop different mechanisms of orientation. The most important widely accepted is the *klinotaxis*, by which a fish moves to the source of interest by swimming against the currents. It consists in a series of lateral movements, with the comparison of intensities of scent at different places, that allow the fish to proceed along a gradient, from low concentrations to higher ones [Kasumyan, 2004]. Among the other mechanisms of orientation, we cite the *tropotaxis*, that is the comparison of scents perceived by the paired olfactory organs. However, for an efficient research with this method, the two organs need them to be properly separated, or a strong gradient must be present. Another mechanism is the *rheotaxis*, by which the fish turns to face to a oncoming current and keeps its position rather that being advected by the current [Hara, 1975].

A second element to consider when analyzing the food seeking strategies of fish is the fact that they typically live in schools. Schools are groups of aquatic animals of the same species that move together displaying strong synchronicity in behavior and a large range of adaptive functions [Radakov, 1973, Pitcher, 1986, Grünbaum, 1998, Pavlov and Kasumyan, 2000]). Different dynamics can lead a fish school to climb gradients more efficiently than individuals. One of them is the so called "imitation behavior", a key ability for fish school formation, by which a fish tends to copy the behavior of a neighbor. This can lead a school of fish to reach a feeding spot that they would have not been capable of reaching alone [Radakov, 1972]. Another interesting dynamic takes place during exploratory behavior, when some fish leave the school, and rapidly come back, several times. When a source of food is identified, this movements repeats with more fishes and for larger distances. This leads to the formation of "tentacles" structures, that can disappear or improve in size. In fact, in favourable conditions, the fish can eventually convey in this tentacles, that will thus inflate and form the new school [Pavlov and Kasumyan, 2000]. This mechanism shows how collective research can help averaging the environmental noise and improve the gradient climbing capacity of schools compared to isolated individuals. Other mechanisms leading in this direction have been identified, theoretically or experimentally [Shaw and Sachs, 1967, Okubo, 1986, Grünbaum, 1998, Ogren et al., 2004, Vicsek and Zafeiris, 2012].

Finally, there have been some studies highlighting the hydrodynamical advantages of

swimming in schools. Even if the mechanisms of the hydrodynamic interrelationship between the fish are poorly understood, some indirect proofs pointed out that there is an energy saving when displacing inside a school rather than outside. Experiments reported that some schools in facts are capable of maintaining cruising speeds 3-5 times higher than individuals, with higher endurance [Breder, 1967]. It has been shown furthermore that the heading fish of a school consume more energy than the others, with higher caudal movements [Herskin and Steffensen, 1998].

1.6.1.2   Focus on myctophids

The studies shown in the previous Subsubsection illustrate the strong capacities of fish in orientating and climbing gradients even at large scales. Even if there are not many studies on myctophids concerning these issues (see for instance [Saunders et al., 2013] about school behavior in lanternfishes), however, [Lawry, 1973], describes the olfaction organ in *Tarletonbeania crenularis*, a lanternfish. The description of the organ and its epithelium does not differ substantially from the classical one given in the previous section. Myctophids are furthermore a worldwide diffused fish and their biomass is one of the greatest in the Southern Ocean, constituting the dominant bulk [Pakhomov et al., 1996, Cherel et al., 2010]. They are constituted by more than 250 species in 33 genera and two subfamilies [Catul et al., 2011], and they have diversified at higher rates than other families [Davis et al., 2014]. Some authors supposed that this diversification has been possible thanks to great adaptive capacities. In particular, [de Busserolles and Marshall, 2017] shown the great visual capacity of lanternfishes, in particular measuring their optical sensitivity with the Land formule for monochromatic light [Cronin et al., 2014, De Busserolles et al., 2014]. The authors obtained that myctophids possess a 10-100 times higher sensitivity than human eyes.

It is thus presumably to conclude that myctophids capacities do not differ significantly from the ones of other fish exposed in Subsubsec. 1.6.1.2. On the contrary, the dim-light environment in which they live and forage, along with their success in spreading worldwide and diversificate, suggest that they may possess significant capacities to adapt to different and hostile environments, both physiologically, both through social interactions.

This is why, in the following, I will assume that the myctophids simulated in the present thesis are capable of detecting a tracer and trying to follow it, in respect of their swimming capacities (cruising speed: 1 body length per second).
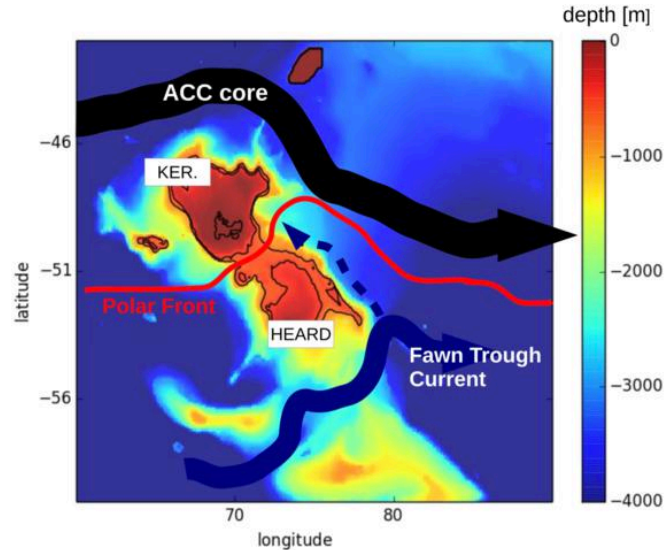
FIGURE 1.9: Schematic illustration of the circulation in the Kerguelen region, from [d'Ovidio et al., 2015], adapted from [Park et al., 2014]. The black thick lines, at 500 and 750, identifies the Kerguelen and Heard plateaux and the shelf break respectively.

1.7   The Kerguelen region

The Kerguelen basin is the region surrounding the Kerguelen archipelago, constituted by more than $\sim$300 small islands, and situated in the Indian sector of the Southern Ocean. The Northwest-Southeast shallow Kerguelen plateau ($\sim$500 m) forms a major barrier for the westerly coming Antarctic Circumpolar Current, which it separates in 3 major branches (see for instance [Park et al., 2014] for further details): the Kerguelen-Amsterdam passage, north of Kerguelen, which carries the majority of the transport ($\sim$150Sv, $\sim$60% of total transport) and which often overlaps with the Subantarctic front, the Fawn Trough and the Princess Elizabeth Trough. The Kerguelen plateau is instead characterised by weak currents, with a pretty stagnant situation. The Kerguelen region presents a strong annual phytoplanktonic bloom which, with an extension of about 1000 km, is one of the vastest of the Southern Ocean [Mongin et al., 2008]. The Southern Ocean is known to be a "high-nutrient low-chlorophyll" region, in which therefore the primary production is constrained by the presence of key limiting factors, in particular iron [Blain et al., 2001, Martin, 1990, De Baar et al., 1995, de Baar et al., 2005, Blain et al., 2007, Boyd et al., 2007, Blain et al., 2008a, Boyd et al., 2012]. Several works have recently suggested the importance of the currents into the modulation of this bloom. Indeed, the Antarctic Circumpolar Current, coming from the west meets the barrier constituted by the plateau and erodes it, becoming enriched in iron. The study of [d'Ovidio et al., 2015] shown how the patterns of chlorophyll detected by satellite can be qualitatively reconstructed simply advecting the water parcels that touched the plateau, and looking at their age. This diagnostic, called "age of waters", constitutes

thus an efficient proxy for describing the spatial organisation of the primary production of the region. It is however important to note that other mechanisms are responsible for the modulation and structure of the phytoplanktonic bloom, such as vertical intense upwellings associated to high (sub)mesoscale features [Rosso et al., 2014], grazing [Smetacek et al., 2004], and silicate limitation [Sullivan et al., 1993].

Primary production in Kerguelen region is mainly driven by large diatoms [Armand et al., 2008, Blain et al., 2008a]. These in turn sustain a relatively simple food web, which starts from a vast range of zooplankton, such as copepods, euphausiids, salps and amphipods [Carlotti et al., 2015, Bocher et al., 2001], to a large community of mesopelagic fish. In particular, myctophids constitutes a large part of this community [Pakhomov et al., 1996, Duhamel et al., 2005, Hulley et al., 2011], organised by the position of the major frontal structures of the region [De Broyer et al., 2014]. In this sense, the position of Kerguelen in respect to these fronts is responsible for a strong latitudinal variation of the pelagic communities [Koubbi et al., 1991, Koubbi, 1993, Duhamel, 1998], and in general of the whole trophic chain [Koubbi et al., 2016b, De Broyer et al., 2014, Koubbi et al., 2011a], from Subtropical to Antarctic ones. Myctophids play a key role in the trophic chain, being consumed and therefore sustaining many top predators based on the archipelago of Kerguelen and Heard Islands [Hindell et al., 2011, Koz, 1995, Lea et al., 2006, Lea et al., 2008, Deagle et al., 2007, Cherel et al., 2008]. Some species of these apex predators are endemic of the island, and several of them have been declared as vulnerable or near threatened by IUCN [Koubbi et al., 2016a].

Despite its remoteness, the Kerguelen region has been object of many research studies, from oceanographic campaigns, regional products for satellite (CLS, Collective Localisation Satellite, http://www.cls.fr/en/), a yearly monitored station, KERFIX [Jeandel et al., 1998], and several works concerning animal tracking [Bailleul et al., 2007, Dragon et al., 2010, d'Ovidio et al., 2013, Guinet et al., 2014]. In 2006 the Kerguelen archipelago was declared as marine protected area. In 2016, following the indication of a scientific commission [Koubbi et al., 2016a] (Appendix C) and [Koubbi et al., 2016b], the protected area was extended also to the Economic Exclusive Zone, covering thus $672\,000\text{km}^2$, and making it among the 10 largest marine protected area in the world. Furthermore, with $120\,\text{km}^2$ of no fishing zone, it is the second halieutic reserve in the world (http://www.taaf.fr). Indeed, Kerguelen region constitutes an important resource for fisheries industries. In the last ten year, about $10\,000$ metric tonnes of fish were captured each year in Kerguelen Islands [Palomares and Pauly, 2011].

1.8   Ecoregionalisation

As explained in the previous Section, in my thesis I focus on a vast region. When studying such a large domain from an ecological point of view, it is useful to split it according to its biogeographical characteristics, in order to study the different ecological systems separately. This is necessary particularly when working with acoustic datasets as in the present work. Indeed, a difference in the backscattering signal measured in two different sites could be due simply to the different backscattering capacity of the organisms present there, and not to a larger biomass. The branch of science which deals with the partition of a certain area in so called "ecoregions" is referred to as ecoregionalisation. It can be applied to global or regional scales [Bryce et al., 1999]. An ecoregion can be defined as a zone with a"relative homogeneity in ecosystems" [Omernik and Bailey, 1997], or also areas of the ocean which host different species assemblages or communities [Spalding et al., 2007] which "are presumed to share a common history of co-evolution" [Sutton et al., 2017].

The importance of ecoregionalisation is widely recognized, for several reason. One of the most important is the contribution it gives to marine conservation planning [Lourie and Vincent, 2004], helping identifying priority areas to protect, allowing to detect distinct contributions each area gives for a specific target, providing informations where not available through model analysis. The latter point can be a crucial insight when studying marine food web, and in particular pelagic ecosystems, for which only 1% of the habitat has been sampled [Webb et al., 2010, Mora et al., 2011, Appeltans et al., 2012, Costello et al., 2012, Higgs and Attrill, 2015, St. John et al., 2016]. Their importance to societal issues, such as their role in the carbon cycle or other major contributions, or their vulnerability to global change, commercial fishing, deoxygenation [Sarmiento et al., 2004, Koslow et al., 2011, Ramirez-Llodra et al., 2011, Mengerink et al., 2014] etc., is acknowledged even if poorly understood, as explained in Sec. 1.5. This is why the work of [Sutton et al., 2017] is important for my study. In the paper, the authors provide a partition of the global ocean in 33 ecoregions, according to the mesopelagic ecosystems. In order to do it, water masses, identified with fields of temperature, salinity and oxygen are taken in consideration. Indeed, water masses and circulation patterns influence faunal distributions and structure their regional limits [McGowan, 1974, Backus, 1986, Goetze and Ohman, 2010, Olivar et al., 2017]. Other parameters were taken into account, such as oxygen minimum zone, temperature extremes, or biotic factors such as primary production or local informations available on faunal composition. The result is shown in Fig. 1.10. In my study I will focus on 5 zones: the *Mid Indian Ocean* (18), the *Southern Indian Ocean* (19), the *Circumglobal Subtropical Front* (31), the *Subantarctic Waters* (32) and in particular on the *Antarctic Southern Ocean* (33) region. A detailed description of the region, in particular in the neighborhood of Kerguelen archipelago,
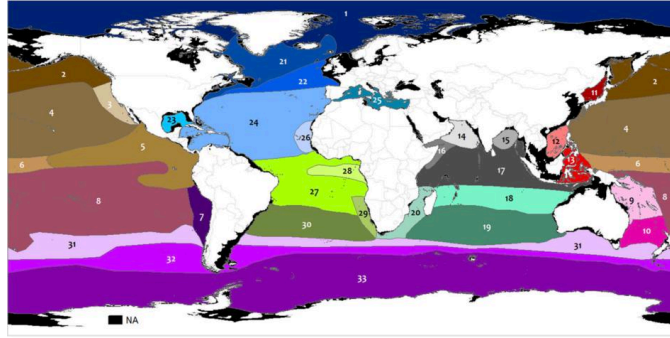
FIGURE 1.10: Mesopelagic ecoregionalisation of the global ocean, from [Sutton et al., 2017].
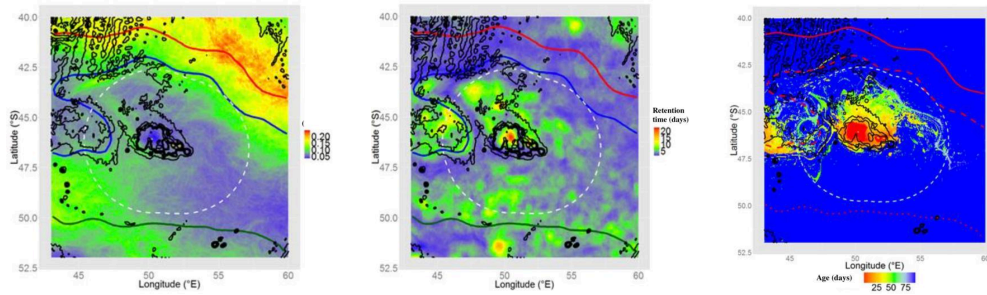
FIGURE 1.11: Lagrangian diagnostic can help identifying barrier to transport and highlight regions that, besides being important for their physical charactersitics, are pivotal also for ecobiological purposes. This is why, with a collaboration with O. da Silva, we computed different climatologies of Lagrangian quantities in the area of Crozet and Kerguelen. These helped in the eco-regionalization of the area of Crozet and Kerguelen, that was used to determine priority areas that should be protected with the incoming of a new Marine Protected Area (MPA). Here it is possible to see a climatology of FSLE (left panel), retention time (central panel) and water age (right panel) over the years 2010-2014. Images from [Koubbi et al., 2016b], see also [Koubbi et al., 2016a] (Appendix C).

and of the dynamics characterising it, can be found in Sec. 1.7.

A similar method to the one of [Sutton et al., 2017] was applied for the partition of the economic exclusive zone of Kerguelen, and Crozet, for the extension of the marine protected area of the islands (Fig. 1.11 and [Koubbi et al., 2016a, Koubbi et al., 2016b] for more details).

Chapter 2

Mesoscale fronts as hotspots of fish aggregation.

This Chapter will be submitted as *Mesoscale fronts as hotspots of fish aggregation.* by A. Baudena et al. at *Journal of the Royal Society Interface*, 2018.

Marine organisms are not distributed homogeneously across the ocean. One of the main reasons for this heterogeneity is due to the turbulent nature of the ocean, which influences deeply marine life abundance, distribution and diversity. Physical features at the (sub)mesoscale (few to hundreds of kilometers, days to several weeks) have indeed proved to play a central role into regulating lower trophic levels and top predators behavior, ecology and distribution. However, less is known on the relationship between fine scale structures and intermediate trophic levels, and how they regulate fish distribution and aggregation. In this Chapter I analyze acoustic transects acquired in the Southern Ocean, and co-localize them to satellite-derived fine scale features, finding high fish concentrations in correspondence of Lagrangian fronts. I then develop a simple fish aggregating mechanisms, over a frontal feature, capable of explaining the increased concentrations observed. The main finding is that fronts represent necessary but not sufficient conditions for high fish concentrations, and we confirm this with the acoustic measurements. Applications and limits of the present study are discussed.

2.1   Introduction

Marine biomass distribution is highly patchy and displays lot of variability, both from a spatial and temporal point of view, and far from being homogeneously distributed across all the trophic web [Gasol et al., 2003, Sakshaug et al., 1994, Simard and Lavoie, 1999,

Lavoie et al., 2000, McManus and Woodson, 2012, Lee et al., 2012]. This aspect presents a first evident consequence on the foraging strategies of marine predators. Indeed, in a hypothetical homogeneous ocean, a fast swimming organisms would probably not survive because the resources would be too sparse, and the energy budget necessary to move and forage too high compared to the energetic gain [MacArthur and Pianka, 1966, Schoener, 1971, Pyke, 1984, Abrahms et al., 2018].

Arguably, the patchy distribution of the marine biomass and the dynamical character of the ocean processes thus favored the emergence of competitive strategies for the survival. These see their peak with the complex foraging strategies of marine top predators, whose main preys are composed by nektonic (i.e. actively swimming) organisms such as fish. Apex predators have been indeed observed concentrating their foraging effort on specific regions [Scales et al., 2014b, Worm et al., 2003, Block et al., 2011, Davoren, 2013, Ceriani et al., 2017], (O'Toole et al. submitted, see also Appendix B) often targeting specific circulation features [Della Penna et al., 2015, Cotté et al., 2015, Chambault et al., 2017]. For instance, King penguins (*Aptenodytes patagonicus*) of Crozet Island colony forage in an area approximatively 400 km south of the Island, following each year the displacement of the Polar front [Bost et al., 2015]. Elephant seals (*Mirounga Leonina*) have been observed in intense foraging activities along some fine scale structures of the circulation, such as eddy peripheries and filaments [Della Penna et al., 2015]. The previous studies gave some indications on the spatial distribution of the nektonic organisms targeted by the predators, suggesting the existence of possible spots of increased fish concentration in specific sites. This is one of the reason why, along with animals, fishery industries have developed several methods and technologies to identify fishery grounds, from aerial surveys [Fromentin et al., 2003, Bauer et al., 2015], to use of Fish Aggregating Devices (FAD, [Capello et al., 2016, Moreno et al., 2016]), and satellite products [Scales et al., 2018, Watson et al., 2018].

The heterogeneous distribution of marine organisms across the oceanic landscape is in part due to biological reasons, such as growth and mortality processes, reciprocal interactions between the different elements of the trophic chain, etc. (see for instance [Abraham, 1998]), and partly due to physical factors. On the seafloor, physical factors such as sand particle size or material can condition the ecology [McLachlan, 1996, Harriague and Albertelli, 2007, Barboza et al., 2017], while close to the coast the conformation of the bathymetry can induce local upwellings [Fiúza, 1983, Huyer, 1983, Figueroa and Moffat, 2000, Su and Pohlmann, 2009], in a dynamic similar to the action played by topography on the terrestrial ecosystems [Turner, 1989]. In the open ocean, instead, far from the shore and from the bottom, a peculiar characteristic of the oceanic environment emerges: its dynamical nature. Further details can be found in Chapter 1 (Subsec

1.2), where I provided also information on the Lagrangian approach (Subsec 1.3). La-grangian tools have been applied successfully to study the lower and higher elements of the trophic web. For more information, please refer to Subsec 1.4.

Compared to plankton and top predators, information on intermediate trophic levels is poor, in particular in the open ocean. One of the main reasons is due to the ac-cessibility of pelagic organisms. These can not be tagged as large predators, neither observed directly via satellite as chlorophyll. Their measurement therefore presents sev-eral difficulties, as exposed in Subsec. 1.5.1. The studies of [Prants, 2013, Prants et al., 2014a, Prants et al., 2014b] have been the first attempt to relate fish measurements and Lagrangian diagnostics, showing a good correlation between the *Pacific saury* catches and Lyapunov exponents. The results, performed with the use of declared fish catches by commercial fishing vessels, leave however some concerns about the possible bias due to the use, by the fishing industry, of satellite data to select the foraging grounds [Watson et al., 2018]. The development of new technologies, and in particular of acoustic sonar measurements and data processing algorithms [Béhagle et al., 2017] provided however new interesting possibilities to fill the knowledge gap toward intermediate trophic levels.

Here, in my knowledge for the first time, we attempt to relate on-ship acoustic measure-ments and satellite derived diagnostics, in order to highlight the organization of spatial patterns of fish concentration according to fine scale structures of the circulation. The statistical analysis provided suggest that Lagrangian fronts can play an important role in the organization of nektonic resources. We suggest that Lagrangian fronts are fine scale structures necessary but not sufficient for the presence of high nektonic aggregations. We then develop a simple one dimensional mathematical mechanism for the coupling between fish behavior and Lagrangian transport. This model is based on a cue pursuing dynamic, and explains the observed enhanced concentrations of nekton biomass across frontal systems. We split the mechanism in two parts: the first is linked to the orientat-ing capacities of the fish, which must identify the noisy cue properly. The second takes into account the fact that the cue is advected and smoothed by the current over the same timescales over which the research takes place.

This Chapter is organized in this way. Sec. 2.2 contains informations on data acquisi-tion and analysis, the methodologies and techniques applied in the present paper, and biological knowledges on the reference fish studied. Sec. 2.3 illustrates the results ob-tained. The first part is dedicated to the analysis of the correlation between the acoustic data and satellite derived diagnostics. The second part illustrates a simple mechanisms of fish aggregation, which could explain the results observed in the first part of Sec. 2.3. Discussions about the results obtained, limits of the present study and possible implementations and perspectives are presented in Sec. 2.4.

2.2 Data and Methods

2.2.1 Acoustic measurements

Acoustic data were collected within the Mycto-3D-MAP program during 6 campaigns in 2013 and 2014, both in summer and in winter (see Tab. 1 for more details), using split-beam echo sounders at 38 and 120kHz. Details of data collection and processing are provided in [Béhagle et al., 2016]. The data were then treated with a bi-frequency algorithm, applied to the 38 and 120kHz frequencies, as described in [Béhagle et al., 2017]. This allows us to obtain a quantitative estimation of the fish concentration in the water column. The depth range goes from 10 to 300 meters (30 layers in total), with a vertical transect every 1,1 km on average. A second slice of higher resolution data (a vertical transect every 206 m), collected between the 22nd of January and the 5th of February 2014, and processed as the other dataset, is used for the computation of the zooplankton gradient, since it is all collected in in the Kerguelen region. The gradient of a point i of the boat transect is computed as:

$$\frac{\partial Z}{\partial x}(i) = \frac{1}{2}\left(\frac{Z_i - Z_{i-1}}{d_{i-1}} + \frac{Z_{i+1} - Z_i}{d_i}\right)$$

where Z_i is the cubic spline interpolation in an around of 2 km of the zooplankton concentrations (to smooth the noise effects and preserve the fronts), and d_i the kilometric distance between the point $i + 1$ and i.

Acoustic campaigns details

Cruise	Season	St. Date	End Date	Distance (km)
LOGIPEV193_RUNKER	Summer	09/02/2013	17/02/2013	2752
LOGIPEV193_KERMAU	Summer	04/03/2013	10/03/2013	3781
OP2013-2_RUNKER	Winter	30/08/2013	10/09/2013	3310
LOGIPEV197_RUNKER	Summer	06/01/2014	13/01/2014	2800
LOGIPEV197_KERMAU	Summer	06/02/2014	18/02/2014	2045
OP2014-2_RUNKER	Winter	24/08/2014	04/09/2014	3677

TABLE 2.1: Details of the acoustic transects analysed.

2.2.2 Biogeographical partition

The dataset employed presents a large latitudinal and longitudinal range, going from 16 to 50 °S and 43 to 83 °E. The transects analysed cross regions with different dynamics and characteristics, both from a physical and an ecobiological point of view (see Fig. 1.10 in the Introduction Chapter). Data are thus divided in different subsets, according to the

ecopartition of [Sutton et al., 2017]. Data fall in 5 different ecoregions; the *Mid Indian Ocean*, the *Southern Indian Ocean*, the *Circumglobal Subtropical Front*, the *Subantarctic Waters* and the *Antarctic Southern Ocean* region (Fig. 2.1). We will however take in consideration only the points belonging to the *Antarctic Southern Ocean* region, because of its ecological importance (Subsec. 1.7). We note that the ecoregionalisation of [Sutton et al., 2017] is also consistent with the ecopartition of [Koubbi et al., 2011b], since all the transects considered as being part of the *Antarctic Southern Ocean* ecoregion are in the same ecological group (group 5) identified in the work of [Koubbi et al., 2011b]. This is particularly important for our case study because the ecoregionalisation by Koubbi et al. is obtained through model species assemblages based on myctophids measurements, which are the family of fish considered in the present study. I described some of the general characteristics of myctophids in the Introduction. In the following Subsection I recall the features that are of specific interest for the analysis described in this Chapter".

2.2.3 Myctophids

Myctophids are small mesopelagic fish diffused worldwide and particularly in the *Antarctic Southern Ocean* region considered in this study. They present a diel vertical migration, living, during the day, in the twilight zone ($\sim$200 to 1000m), and ascending at dawn in the upper euphotic layer where they spend the night [Duhamel, 1998, Catul et al., 2011]. They feed mainly on copepods, euphasiids, ostacods and amphipods [Gordon et al., 1985, Kinzer et al., 1993, Hopkins et al., 1993, Koz, 1995, Pakhomov et al., 1996, Shreeve et al., 2009] and their vertical migration plays a major role in the carbon export into the depths [Hidaka et al., 2001b, Hudson et al., 2014]. Myctophids dominate the mesopelagic community and likely constitute one of the largest biomass of fishes in the world [Irigoien et al., 2014]. Their great importance is also due to the consumption by top predators such as piscivour fishes [Polovina, 1996, Potier et al., 2007, Pusineri et al., 2008, Flynn and Paxton, 2013], marine mammals [Casaux et al., 1998, Brophy et al., 2009, Pereira et al., 2011] and sea birds [Kooyman et al., 1992, Jansen et al., 1998, Deagle et al., 2007], for which they constitute a key resource [Cherel et al., 2010, Sabourenkov, 1991, Kozlov, 1995, Hopkins et al., 1996, Beamish et al., 1999]. They thus constitute a crucial element in the marine trophic chain, playing an intermediate role of connection and energy transfer between primary and secondary production, and apex predators. Recently, the study of [St. John et al., 2016] has underlined the gaps of knowledge actually present on the mesopelagic community, which could be soon being exploited for commercial use. The authors stress, amongst others issues, the necessity of a better understanding of "the links between oceanographic regimes and mesopelagic biomass".
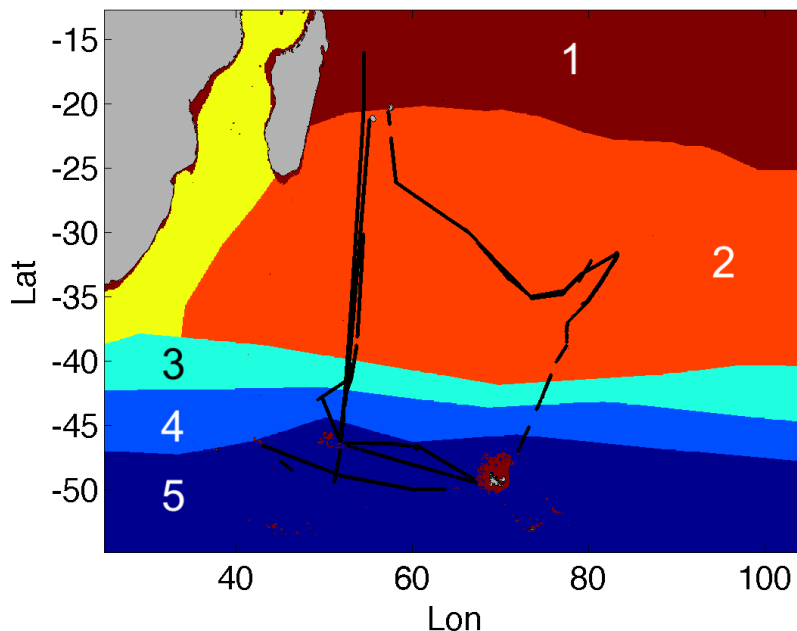
FIGURE 2.1: Biogeographic partition (from [Sutton et al., 2017]), with, superposed in black, the acoustic transects analysed. Each region is identified by a number. 1: *Mid Indian Ocean.* 2: *Southern Indian Ocean.* 3: *Circumglobal Subtropical Front.* 4: *Subantarctic Waters.* 5: *Antarctic Southern Ocean*

2.2.4 Satellite data.

Velocity current data and processing

Velocity currents are obtained from the Sea Surface Height (SSH), which is measured by satellite, through the geostrophic approximation. Data, which were downloaded from E.U. Copernicus Marine Environment Monitoring Service (CMEMS, http://marine.copernicus.eu/), are obtained from DUACS (Data Unification and Altimeter Combination System) delayed-time multi-mission altimeter, and displaced over a regular grid with spatial resolution of $\frac{1}{4} \times \frac{1}{4}^{\circ}$ and a temporal resolution of 1 day [Pujol et al., 2016].

Trajectories were computed with a Runge-Kutta scheme of the 4th order, with an integration time of 3 hours. Lyapunov Exponents (finite size) were computed following the methods in [d'Ovidio et al., 2004], with initial and final separation of 0.04° and 0.4° respectively. Betweenness, computed following the methods in Ser-Giacomi et al. (in preparation), was obtained from a regular grid with spatial separation of 0.025° and integration time of 30 days.

Temperature field

The temperature field was downloaded from the OSTIA global foundation Sea Surface Temperature product (SST_GLO_SST_L4_NRT_OBSERVATIONS_010_001). The data

are provided over a regular grid with spatial resolution of $0.05 \times 0.05°$ and daily-mean maps.

2.3 Results

2.3.1 Acoustic fish concentration and satellite-derived diagnostics

In this subsection, we look at the correlation between satellite derived diagnostics and the acoustic backscattering obtained through the bifrequency algorithm (Subsec. 2.2.1) representative of the fish mass in the water column. We will refer to the latter as Acoustic Fish Concentration (AFC). We will consider also the Acoustic Zooplankton Concentration (AZC). We consider as AFC (or AZC) of the point (x_i, y_i) the average of the bifrequency acoustic backscattering on the whole column on the point (x_i, y_i), with the exclusion of the first layer which is not considered due to surface noise.

Concerning the satellite derived oceanographic features, in order to reduce the error due to the resolution of the satellite measurement, we consider as value of the diagnostic (Lyapunov exponent, temperature gradient,..) the average value over a disc of $0.2°$ around the point (x_i, y_i). Due to the diel vertical migration of the myctophids, we split the values, according to the twilight index, in day and night. Finally, we separate the data according to the biogeographical partition of [Sutton et al., 2017], as explained in Subsec. 2.2.2.

The explanatory variables are 2 Lagrangian and 2 Eulerian diagnostics: the finite-size Lyapunov exponent, the betweenness, the SST gradient and the Kinetic Energy. For the quantile regression, the AZC was considered also as explanatory variable.

Fig. 2.2 shows two illustrative examples of the boat trajectory, on the 29th of August 2014 and 31st of August 2013 respectively. They are superposed to a field of Finite-size Lyapunov exponents computed as explained in Subsec. 2.2.4. Each dot of the boat trajectory is colored proportionally to the AFC in that point. On both the panels, AFC values show a qualitative agreement with the FSLE, increasing in correspondence of the frontal features identified by high values of the Lyapunov exponents. According to the biogeographical partition, we focus only on the *Antarctic Southern Ocean* region, which is of main interest because it includes the Kerguelen region (see also Subsec. 1.7 in the Introduction Chapter). Fig. 2.3 shows the scatter plots of the AFC against three different diagnostics, with both the axis in logarithmic scale. In the first row of Fig. 2.3, the scatter plot with the FSLE is reported, with, respectively, AFC values during day (left) and night (right). From now on, if not specifically declared, we will report only the values measured during the night. Indeed, the AFC values measured go from the surface to 300m. However, the nektonic organisms of the region, such as the myctophids,
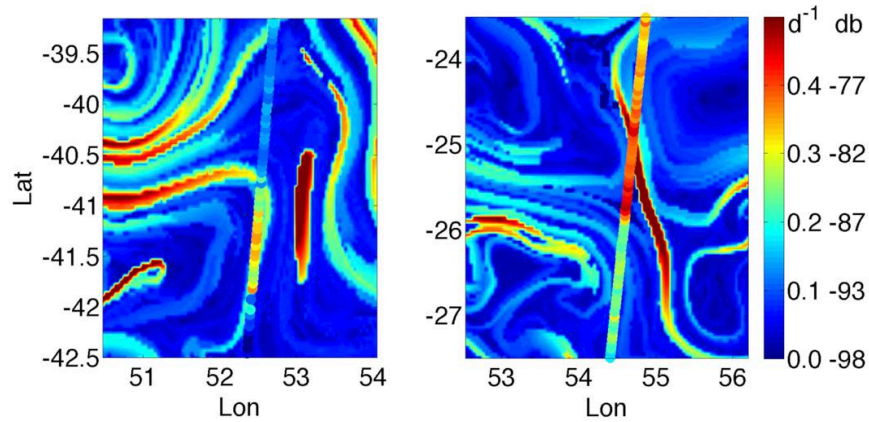
FIGURE 2.2: Illustrative examples of two transects of the boat trajectory. The color of each dot is proportional to the Acoustic Fish Concentration (in decibel: please refer to the right part of the colorbar ticks for the scale). The transects are superposed to a field of Finite-Size Lyapunov Exponents (FSLE) computed with altimetry derived velocities (days^{-1}, refer to the left part of the colorbar ticks for the scale). Left panel: August, 29th, 2014, biogeographic region: *Circumglobal Subtropical Front.* Right panel: August, 31st, 2013, biogeographic region: *Southern Indian Ocean.*

presents a nycthemeral cycle, and, living in the depth during the day, are not observed by the acoustic equipment. It is not surprising therefore that the data measured at night present a better spatial organization compared to the ones measured during the day, which is confirmed looking at the respective correlation coefficients. Finally, in the second row of Fig. 2.3, the diagnostics reported are the betweenness and the SST
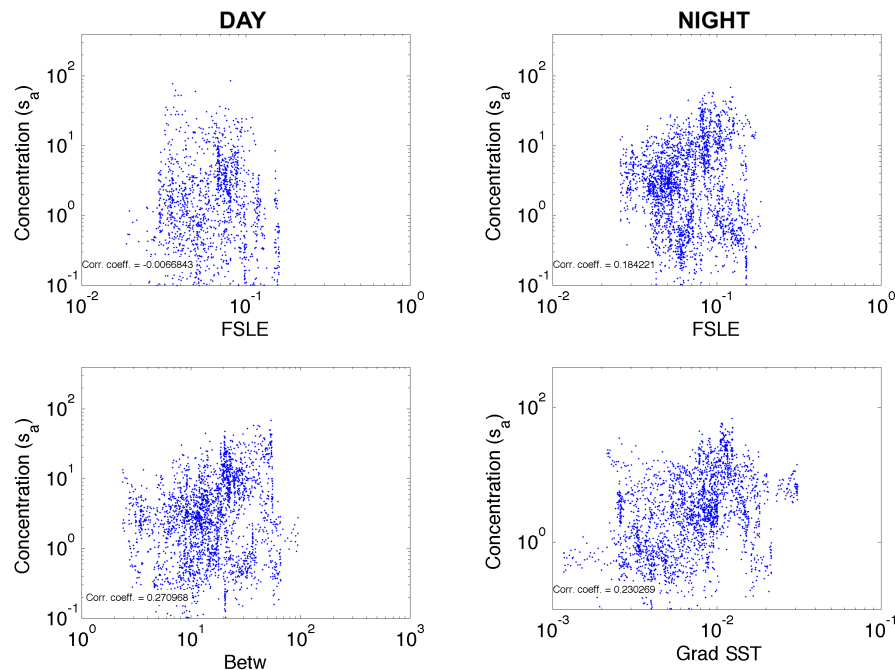
FIGURE 2.3: Scatterplots of AFC (s_a) against some diagnostic. Upper panels: FSLE (days^{-1}) during day (left panel) and night (right panel). Lower left panel: betweenness. Lower right panel: SST gradient ($°/km$). Each panel reports the correlation coefficient.

gradient. Kinetic Energy (not shown) presents a correlation coefficient of -0.15.

Bootstrap method

In order to see if the AFC values present significant differences in proximity of fine scale features, bootstrap analysis is applied, following the methodologies in [De Monte et al., 2012]. In order to identify the frontal features, the following diagnostic values are chosen as thresholds for representing the front: for the FSLEs, we use 0.08 days^{-1}, threshold value consistent with those chosen in [De Monte et al., 2012] and obtained from [Lehahn et al., 2007, Kai et al., 2009]. For the SST gradient, we consider as representative of a thermal front values greater than 0.9°C/100 km, which is about the half of the value chosen in [De Monte et al., 2012]. In that work however, the SST gradient was obtained from the advection of the SST field with satellite derived currents for the previous 3 days, which structures it in high resolution features that therefore present higher gradient values. For the betweenness, the threshold value is set to 30 and for the Kinetic Energy to $0.02\frac{m^2}{s^2}$.

The threshold value splits the AFC in two groups, over and under the threshold, whose independency is tested using a Mann-Whitney or U test. The results are reported in
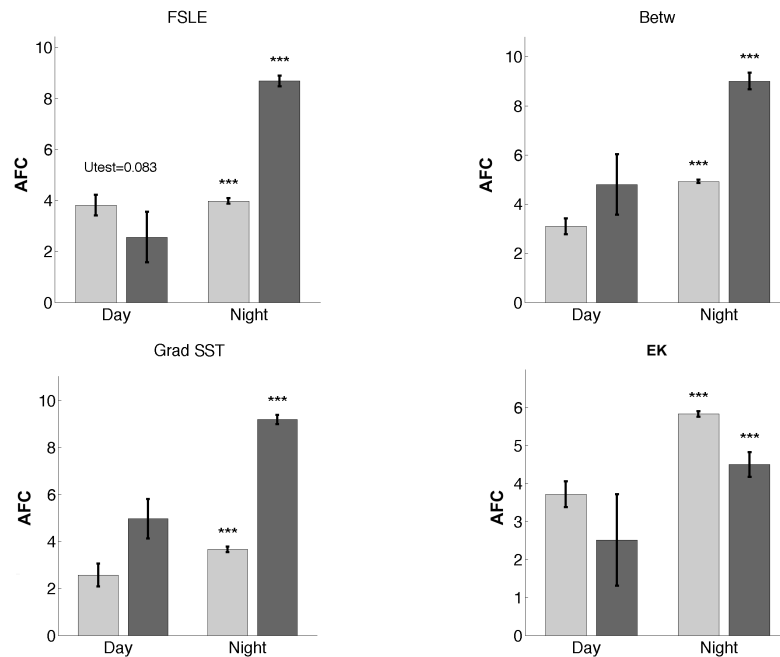
FIGURE 2.4: Bootstrap method results. Upper row: FSLE and Betweenness. Row below: SST gradient and Kinetic Energy averaged over 60 days. For each plot, the light gray columns represent the mean AFC under the threshold, and the dark gray columns the mean AFC over the threshold. On the left the bootstrap test is computed for the AFC values during the day, while on the right for the AFC values taken during the night.

Fig. 2.5. As expected, during the day no significant differences are recorded over or under the fixed threshold, due to the impossibility to measure the AFC deeper than 300m where instead the fish spend their daytime. Concerning the FSLE, the betweenness and the SST gradient during the night, highly significant differences (p-value < 0.001), with higher AFC value over the thresholds, are obtained. Interestingly, the Kinetic Energy presents an opposite trend, with significant higher AFC values present in regions of smaller EK.

Quantile regression

Quantile regression method, as applied for instance in [Sankaran et al., 2005], is employed with the 4 explanatory variables and the AZC. The quantile regression is applied, for each case, to the 50, 90 and 99 percentiles. The results are shown in Fig. 2.5. The best values of pseudo R^2, visible in the scatter plots, are all the over the 99 percentile, with the betweenness having $R^2 = 0.26$, the FSLE 0.20, the SST gradient 0.11 and the AZC 0.04. Kinetic Energy (not reported) presents instead a pseudo R^2 of 0.06 at the 99 percentile.

2.3.2   Frontal mechanisms of fish aggregation

Why fish aggregate along frontal features? I address this question by proposing a mathematical model based on a searching behavior of the fish, specifically of myctophids,
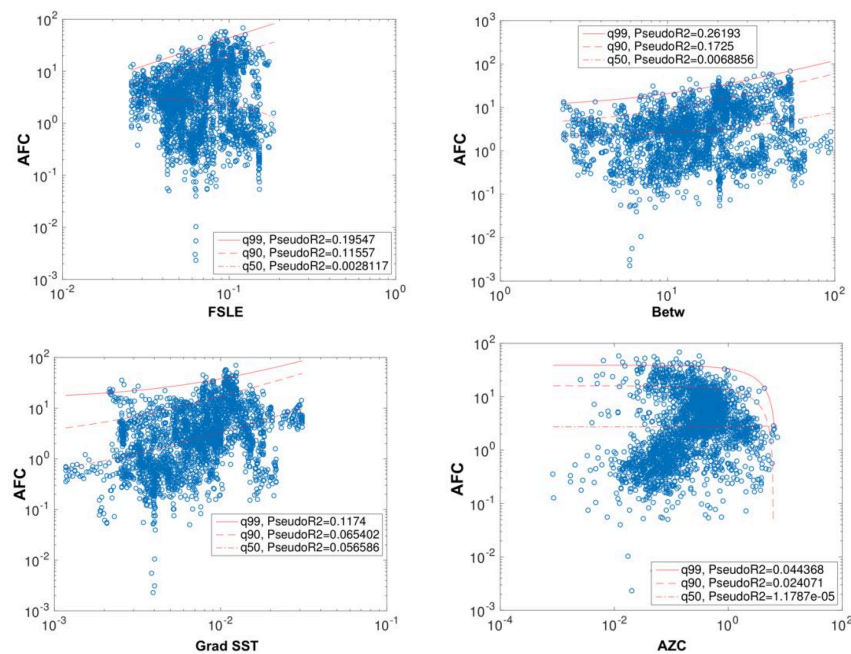
FIGURE 2.5: Quantile regression results. Upper row: FSLE and Betweenness. Row below: SST gradient and AZC.

whose orientating capacities have been presented in Subsec. 1.6.1 of Introduction Chapter. An obvious characteristic of fish, which becomes peculiar when analyzing their behavior in respect to lower trophic levels, is that they can swim, along the horizontal dimension, with velocities often comparable with those of the currents [Sfakiotakis et al., 1999, Bainbridge, 1958]. This allows them to move actively through the flow, performing different tasks such as escaping from predators, migrating, feeding, orientating and so on [Beamish, 1978, Stobutzki and Bellwood, 1994, Drucker, 1996, Watkins, 1996, Domenici, 2001]. In particular, swimming (often through the organization in schools) plays a central role in the research of hotspots with favorable taxis [Grünbaum, 1998, Drucker, 1996], such as foraging grounds, temperature, salinity or chemicals hotspots, during which the fish have to move actively. Often, we can suppose that the signature identifying those hotspots is a generic cue, advected passively by the currents. This is the case for instance of zooplankton, main prey of many fish species [O'Brien, 1979, Gordon et al., 1985, Pakhomov et al., 1996], which (at the scale we consider here, of 10s of km) possesses swimming capacities restricted to the vertical direction [Genin et al., 2005] and which thus can be approximated, along the horizontal direction, as a passive tracer. When searching for an optimal site, a swimming organism faces in general two difficulties. The first one is due to the fact that the individual can not know exactly the location of the hotspot is looking at. In our case, this is due to the fact that the capacity of the fish to observe the surrounding environment is limited to a certain spatial range around it, usually smaller than the scales over which the research takes place (see Subsec. 1.6.1). Furthermore, the presence of noise in the cue, a characteristic recurrent in many tracer observations in the ocean [Grünbaum, 1998, Shraiman and Siggia, 2000], can in principle lead the fish to follow the wrong direction. Other misleading factors can be inaccuracies in the sensorial field of the individual.

The second kind of difficulty is due to the oceanic turbulence, which makes the tracer cue evolve during the period of the research, and which has an effect on the fish trajectory. Turbulence can potentially dissipate hotspots of interest before the fish have the time to reach them, or create them elsewhere.

Thus, from one side, the fish must be able to identify properly the direction along which it has to swim and, on the other, it has to do it fast enough to reach the desired place before the cue faded. As a first step, we decouple the search dynamics from the tracer evolution. In Chapter 4 I will discuss how these two processes can occur at the same time, and I present some preliminary encouraging results.

In the next paragraph we describe a hypothetical fish behavior in a noisy environment, analyzing then the consequences on their spatial distribution. Next, we study the action of horizontal stirring and diffusion on the evolution of an optimal hotspot for fish, represented by a passive tracer, and the effects on fish concentration.

Gradient climbing effect.

In order to obtain a simple vision of the problem, we first describe the search as a one dimensional, individual based, Markovian process. In order to analyse this process, we discretize the time in timesteps of length $\Delta\tau$. We suppose that, at each timestep, the fish (or the fish school) chooses between swimming in one of the two directions or being advected by the currents without actively moving. This decision depends on the comparison between the quantity of tracer at its actual position and the one perceived at a distance f_W from it, where f_W is the field view of the fish. We consider the fish immersed in a tracer which concentration is described by the function $T(x)$.

We try now to derive an expression for the average velocity of the fish $U_F(x)$, supposing two type of different behaviors.

Behavior 1: observation along a random direction.
In a first, more simple scenario, we consider that, at each timestep, the fish is able to observe the tracer only along a random direction (that, in a one dimensional system, is just right or left). Along this direction, the fish will observe a different value of the tracer in which it is swimming. We introduce a noise in the tracer concentration, so that the effective value perceived by the fish will be

$$\tilde{T}(x_0 \pm \Delta x) = T(x_0 \pm \Delta x) + \xi$$

in which we consider a uniform distribution of the noise, with a range of values $-\xi_{MAX} < \xi < \xi_{MAX}$, with $\xi_{MAX} > 0$.
We assume then that, if $\tilde{T}(x_0 \pm \Delta x) > T(x_0)$, the fish will move in the new position $x_0 \pm \Delta x$, and, otherwise, will stay in the old one. We hypothesize that the observational range is small enough to consider the tracer variation as linear, as illustrated in Fig. 2.6, so that

$$\tilde{T}(x_0 \pm \Delta x) = T(x_0) \pm f_W \frac{\partial T}{\partial x} + \xi \ .$$

In case of absence of noise, or with $\xi_{MAX} < f_W \frac{\partial T}{\partial x}$, the fish will always stay right in case of rightward observation, and won't move in a leftward observation. Considering that the probability of observing right or left (P_{OR} and P_{OL} respectively) is equal $\frac{1}{2}$, on average, the net velocity of the fish school $U_F(x)$ will be $\frac{1}{2}V$, assuming V as the cruising swimming velocity of the fish.
Let's now assume $\xi_{MAX} > f_W \frac{\partial T}{\partial x}$. We will have the following scenario:

Jump on the right:
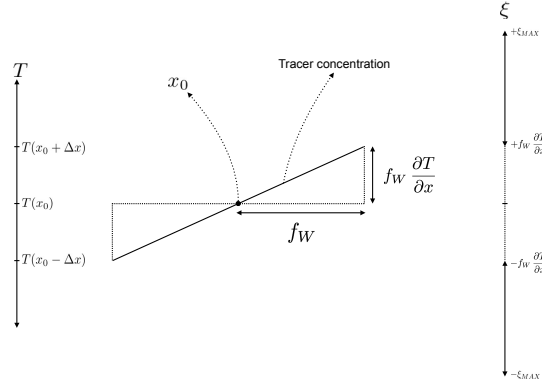
FIGURE 2.6: Schematic representation of the behavior of a fish. Each timestep, it can observe the tracer, according to its field view capacity, up to a distance f_W. We assume a small field view, so that the tracer variation can be considered linear, and a positive gradient. The tracer value in the new position will be affected by a noise, ranging between $-\xi_{MAX}$ and ξ_{MAX}. Behavior 1: if the fish observes a value of tracer higher in a randomly selected direction, it will move there, otherwise it will stay in the actual position x_0. Behavior 2: the fish observes both the directions, and swims toward the one with higher tracer.

if $\xi > 0 \rightarrow$ the fish goes right

if $-f_W \frac{\partial T}{\partial x} < \xi < 0 \rightarrow$ the fish goes right

if $-\xi_{MAX} < \xi < -f_W \frac{\partial T}{\partial x} \rightarrow$ the fish does not move

Jump on the left:

if $\xi < 0 \rightarrow$ the fish does not move

if $0 < \xi < +f_W \frac{\partial T}{\partial x} \rightarrow$ the fish does not move

if $+f_W \frac{\partial T}{\partial x} < \xi < +\xi_{MAX} \rightarrow$ the fish goes left

The probability of moving right is given by the product of P_{OR} and the probability that the noise will lead to a rightward moving. The latter is the ratio between the length of the interval of noise for which the fish is staying in the new position and the range of the noise. The procedure is analog for $P(L)$.
Thus:

$$P(R) = P_{OR} * \frac{1}{2\xi_{MAX}}[\xi_{MAX} + f_W \frac{\partial T}{\partial x}]$$

$$P(L) = P_{OL} * \frac{1}{2\xi_{MAX}}[\xi_{MAX} - f_W \frac{\partial T}{\partial x}]$$

The difference between $P(R)$ and $P(L)$

$$P(R) - P(L) = \frac{1}{4\xi_{MAX}}\left[\xi_{MAX} + f_W\frac{\partial T}{\partial x} - \xi_{MAX} + f_W\frac{\partial T}{\partial x}\right]$$

$$= \frac{1}{4\xi_{MAX}}\left[2f_W\frac{\partial T}{\partial x}\right]$$

$$= \frac{f_W}{2\,\xi_{MAX}}\frac{\partial T}{\partial x} \tag{2.1}$$

gives us the frequency of rightward moving. Thus, the average velocity of the fish school $U_F(x)$ will be

$$U_F(x) = \frac{1}{2}\frac{V\,f_W}{\xi_{MAX}}\frac{\partial T}{\partial x} \ . \tag{2.2}$$

We then assume that, over a certain value of tracer gradient $\frac{\partial T}{\partial x}_{MAX}$, the fish are able to climb the gradient without being affected by the noise. This assumption, from a biological point of view, means that the fish does not live in a completely noisy environment, but that under favorable circumstances is able to identify correctly the swimming direction. This means that

$$f_W * \frac{\partial T}{\partial x}_{MAX} = \xi_{MAX} \ . \tag{2.3}$$

Substituting (2.3) in (2.2):

$$U_F(x) = \frac{1}{2}V\frac{\frac{\partial T}{\partial x}}{\frac{\partial T}{\partial x}_{MAX}} \ . \tag{2.4}$$

Finally, we can include the effect of the currents speed U_C, considering that the tracer is transported passively by them, simply adding U_C to Expr. (2.4).

Behavior 2: observation along two directions.

We now suppose that, at each timestep, the fish is able to observe the environment that surrounds it. It will thus observe simultaneously the tracer at its right and its left. It will then move toward the point of higher observed tracer, avoiding to stay in the starting position.

The tracer observed at its left and its right, will be, respectively:

$$\tilde{T}(x_0 - \Delta x) = T(x_0) - f_W \frac{\partial T}{\partial x} + \xi_1$$
$$\tilde{T}(x_0 + \Delta x) = T(x_0) + f_W \frac{\partial T}{\partial x} + \xi_2$$

The fish will swim leftward if

$$\xi_1 - \xi_2 > 2 f_W \frac{\partial T}{\partial x} \; .$$

Since ξ_1 and ξ_2 range both between $-\xi_{MAX}$ and ξ_{MAX}, the probability that their difference is greater than $2 f_W \frac{\partial T}{\partial x}$ is

$$P(L) = \frac{1}{8\xi_{MAX}^2} \left(2\xi_{MAX} - 2 f_W \frac{\partial T}{\partial x} \right)^2$$
$$= \frac{1}{2} \left(1 - \frac{f_W}{\xi_{MAX}} \frac{\partial T}{\partial x} \right)^2$$

The probability of moving right will be

$$P(R) = 1 - P(L)$$

and their difference, analog to Eq. (2.1)

$$P(R) - P(L) = 1 - 2P(L) = 1 - \left(1 - \frac{f_W}{\xi_{MAX}} \frac{\partial T}{\partial x} \right)^2$$
$$= \frac{f_W}{\xi_{MAX}} \frac{\partial T}{\partial x} \left(2 - \frac{f_W}{\xi_{MAX}} \left| \frac{\partial T}{\partial x} \right| \right)$$

where the absolute value of $\frac{\partial T}{\partial x}$ has been added to preserve the correct climbing direction in case of negative gradient. The above expression leads to:

$$U_F(x) = \frac{V f_W}{\xi_{MAX}} \frac{\partial T}{\partial x} \left(2 - \frac{f_W}{\xi_{MAX}} \left| \frac{\partial T}{\partial x} \right| \right) \; . \tag{2.5}$$

Substituting then (2.3) into (2.5):

$$U_F(x) = V \frac{\frac{\partial T}{\partial x}}{\frac{\partial T}{\partial x}_{MAX}} \left(2 - \frac{\left| \frac{\partial T}{\partial x} \right|}{\frac{\partial T}{\partial x}_{MAX}} \right) \; . \tag{2.6}$$

Also for this case, we can take into account the effect of the currents by adding their speed U_C to U_F.

The representations showed until now are individual based, with each individual representing a single fish. We note here that however all the considerations done are valid also if we consider an individual representing a fish school. U_F will then simply represent

the average velocity of the fish schools. It is important to underline this aspect since in Subsec. 1.6.1 we observed that many fish species live and feed in groups.

Continuity equation in one dimension

Let?s now study the solution of this model. We consider the continuity equation in one dimension. The starting scenario is simply an initially homogeneous distribution of fish, that are moving in a one dimensional space with a velocity given by $U_F(x)$.

We suppose that, in the time scales considered (few days to some weeks) the fish biomass is conserved, so we neglect for instance fishing mortality or growing rates. In that case, we can express the evolution of the concentration of the fish ρ by the continuity equation

$$\frac{\partial \rho}{\partial t} + \nabla \cdot \mathbf{j} = 0 \tag{2.7}$$

in which $\mathbf{j} = \rho \, U_F(x)$, so that Eq. (2.7) becomes

$$\frac{\partial \rho}{\partial t} + \nabla \cdot \big(\rho \, U_F(x) \big) = 0 \ . \tag{2.8}$$

In one dimension, the divergence is simply the partial derivate along the x-axis. Eq. (2.8) becomes simply

$$\frac{\partial \rho}{\partial t} = -\frac{\partial}{\partial x} \bigg(\rho \, U_F \bigg) \tag{2.9}$$

Now, we decompose the fish concentration ρ in two parts, a constant one and a variable one $\rho = \rho_0 + \tilde{\rho}$. Eq. (2.9) will become

$$\frac{\partial \rho}{\partial t} = -U_F \frac{\partial \tilde{\rho}}{\partial x} - \rho \frac{\partial U_F}{\partial x} \ . \tag{2.10}$$

Estimation of the biological parameters.

Eq. (2.10) is numerically simulated using the Lax method [Press et al., 1988]. In Expr. (2.4) and (2.6) we impose that, $U_F(x) = V$ when $U_F(x) > V$. This means that, when the tracer gradient is very strong, the velocity of the fish is still limited to the cruising swimming speed V of the fish, which has sense from a biological point of view. We consider a cruising swimming speed V of about one body length per second [Bainbridge, 1958, Sfakiotakis et al., 1999, Domenici, 2001, Gui et al., 2014]. As the reference fish considered are the myctophids, whose size is about 10 cm ([Pakhomov et al., 1996] and Andrea Walters, pers. comm.), V is set to $0.1 \frac{m}{s}$. As expression of the tracer
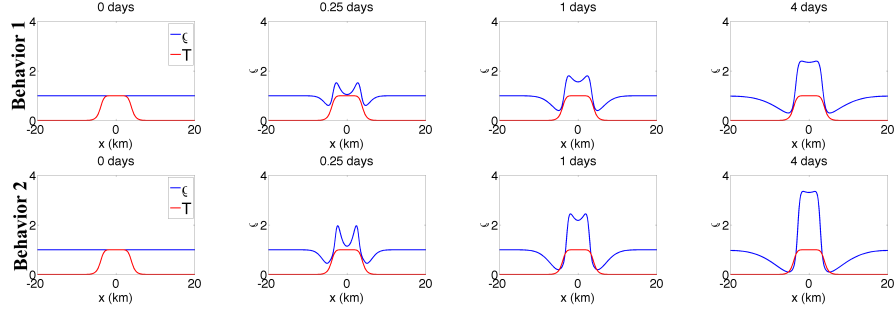
FIGURE 2.7: Time evolution of the fish concentration ρ (blue line) according to Eq. (2.10). The tracer (red line) is fixed in time according to Expr. (2.11). c =0 km, $2a = 8$ km (plateau width), $f = 5$ km (front length). Each row represents 4 different snapshots at 0, 6 hours, 1 and 4 days, respectively for the behavior 1 (upper row) and behavior 2 case (row below).
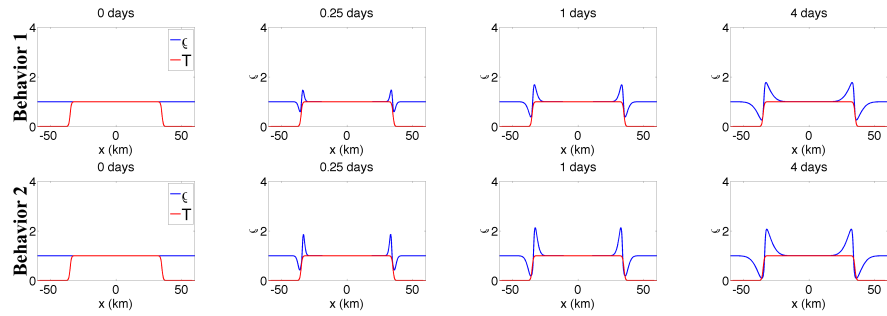
FIGURE 2.8: Time evolution of the fish concentration as reported in Fig. 2.7, with $2a$ that has been changed to 70 km.

concentration, we take a symmetric sigmoid function, defined as:

$$T(x) = \frac{1}{1 + \left(\frac{x-c}{a}\right)^{\frac{10a}{f}}} \tag{2.11}$$

where $c = 0$ m is the centre of the curve, $2a = 8$ km is the width of the plateau, and f the width of the front, i.e. the region characterized by a gradient in the tracer. We consider a window of spatial range [-20 +20] km with periodic boundary conditions, with integrating time step $\Delta t = 1$s (which is not the time decision of the fish $\Delta \tau$, introduced only for illustrative purposes) and spatial separation between two contiguous points of $100 \, \Delta t \, V$, in order to respect the Courant condition.

$\frac{\partial T}{\partial x}_{MAX}$ is determined from the 90 percentile (the choose of 90 percentile is arbitrary) of the distribution of the normalized zooplankton gradient, leading to a value of $\frac{\partial T}{\partial x}_{MAX} = 0.3475$ km^{-1}.

Simulation of the continuity equation

Eq. (2.10) is simulated considering a front $f = 5$ km, with starting condition $\rho(x) = 1$,
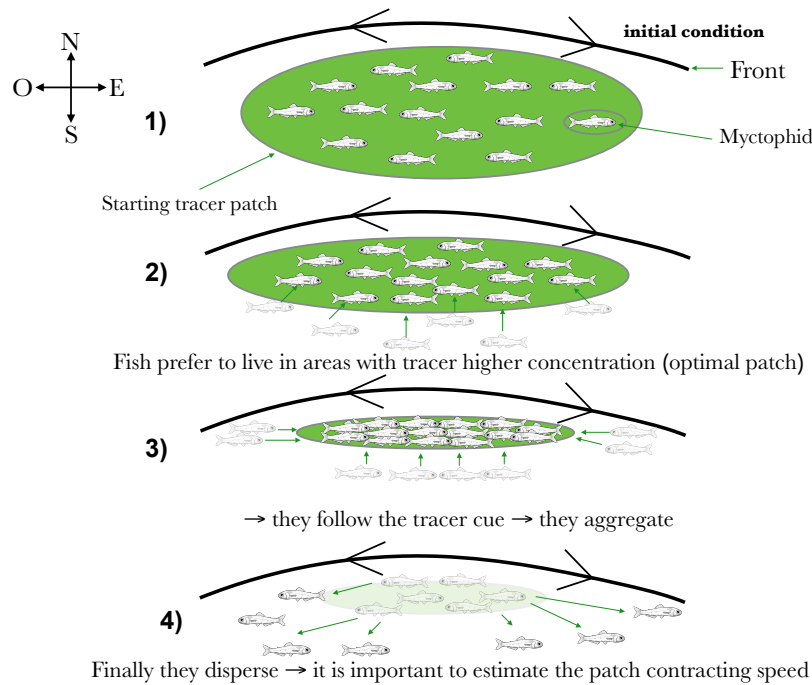
FIGURE 2.9: Illustrative scheme of the hyperbolic dynamic analysed: the green patch represents an optimal region for fish to live in, while the black line indicates the front, corresponding to a stretching region. After a certain amount of time, the patch will be compressed along the N-S direction and enlarged along the W-E, due to stirring. Then, due to the diffusion effect, the patch will start to reduce also in this direction. If the fish have a swimming capability able to follow the patch, their local density will improve and thus they will aggregate. When the green patch disappears, the fish disperse again.

for a time of 4 days. In Fig. 2.7, 4 different snapshots (at 0, 6 hours, 1 and 4 days) for each behavior are reported. After only 6 hours, two peaks are present in correspondence of the margins of the tracer plateau, with a concentration which has doubled for the behavior 2 case. In the following days the two peaks decrease their growing rate, while the concentration between them increase until they are merged together. The fish concentration is thus homogeneous over the 8 km of the plateau, presenting values between 2.5 and 3.5 times higher than the initial concentration. In case of a larger plateau ($2a = 70$ km, Fig. 2.8), the merging between the peaks occurs over longer timescales, and the peaks reach their maximum value after the first day, with the creation of two regions of increased concentration at the margins of the plateau. Not surprisingly, the behavior 2 leads to higher values of concentration, showing a better performance of the behavior 1.

Hyperbolic dynamic effect.

The results reported in the previous paragraph are identical if the whole system (fish+tracer) is transported leftward or rightward by a uniform current $U_C(x) =$ const. However, this is typically not the case of submesoscale frontal features, characterized by high

stirring rates and in which diffusion plays a consistent role [Nencioli et al., 2013]. A typical dynamic of this type is the one represented by the so-called hyperbolic points [Haller, 2001, Mancho et al., 2004, Lehahn et al., 2007]. These are characterised by a compression-elongation dynamic along two stretching directions, called respectively the stable and unstable manifold. A patch of tracer in proximity of this structure, is typically compressed along the stable manifold and elongated along the other. Eventually, diffusion acts on the thinning of the tracer by dissipating it, and reducing its concentration until it is below the threshold detected by the fish. Note that, due to the effect of diffusion, an isoconcentration contours of the tracer eventually retracts, even if the tracer is stretched along the unstable manifold. If we suppose that fish are interested in the region with high values of the concentration, they will swim in order to follow the contracting patch, and thus their concentration will improve (Fig. 2.9). Do myctophids have swimming capabilities strong enough to counter the dynamics of the reducing patch? We address this question by estimating the speed of an isoconcentration contour of a passive tracer under typical diffusion and stretching conditions of the Southern Ocean. We do it in the following way.

We analyse the evolution of a patch in the reference system of its center of mass over an unstable manifold. In this case, the velocity field can be written as:

$$
\begin{aligned}
u &= +\lambda x \\
v &= -\lambda y
\end{aligned}
\tag{2.12}
$$

in which λ is the strain rate given by the Lyapunov exponents.

Taking in consideration the horizontal diffusivity k, the patch, represented by a tracer concentration T, evolves in time following the advection-diffusion equation. The latter, considering the velocity field given by (2.12) can be written as:

$$
\frac{\partial T}{\partial t} + \lambda x \frac{\partial T}{\partial x} - \lambda y \frac{\partial T}{\partial y} = k \left(\frac{\partial^2 T}{\partial x^2} + \frac{\partial^2 T}{\partial y^2} \right) + \mathcal{S} \, .
\tag{2.13}
$$

Neglecting eventual source or sink terms, represented by $\mathcal{S}$, and assuming T as gaussian, Eq. (2.13) can be solved analytically:

$$
T(x,y,t) = \frac{M}{\sigma_u(t) \, \sigma_s(t)} \, exp \left[-\frac{x^2}{2\sigma_u^2(t)} - \frac{y^2}{2\sigma_s^2(t)} \right]
\tag{2.14}
$$

with M the total mass of the tracer and

$$
\begin{aligned}
\sigma_u^2(t) &= \left(\sigma_{u_0}^2 + \frac{k}{\lambda}\right)e^{2\lambda t} - \frac{k}{\lambda} \\
\sigma_s^2(t) &= \left(\sigma_{s_0}^2 - \frac{k}{\lambda}\right)e^{-2\lambda t} + \frac{k}{\lambda}
\end{aligned}
\tag{2.15}
$$

that are, respectively, the standard deviation of the tracer concentration along the unstable and stable manifold. We assume $M = \sigma_{u_0}\sigma_{s_0}$, so that the maximum starting value of the distribution (adimensional) is 1.

We define as *optimal patch* for the fish the ensemble of the points with tracer concentration greater than a certain threshold T_t (their detection threshold), $0 < T_t < 1$. The position of the points with tracer concentration $T = T_t$ delimit therefore the *optimal patch*. Their positions, along the stable $(x = 0)$ and unstable manifold $(y = 0)$, can be obtained inverting Eq. (2.14):

$$
p_u(t) = \sqrt{2\sigma_u^2(t)Log\left(\frac{M}{\sigma_u(t)\sigma_s(t)T_t}\right)}
\tag{2.16}
$$

$$
p_s(t) = \sqrt{2\sigma_s^2(t)Log\left(\frac{M}{\sigma_u(t)\sigma_s(t)T_t}\right)}
\tag{2.17}
$$

and their velocities $\dot{p}_u(t)$, $\dot{p}_s(t)$, deriving Eq. (2.16) and (2.17) in time (not reported). $\dot{p}_u(t)$ and $\dot{p}_s(t)$ thus represent the expanding (positive values) or contracting (negative values) speed of the boundaries of the *optimal patch*. Since the myctophids swim in a current flow, we consider their relative swimming speed S_{rs} as:

$$
S_{rs} = V + U_C
$$

where $U_C = -\lambda x$ along the unstable manifold, and $+\lambda y$ along the stable one, and V is the cruising swimming speed $(0.1\,\frac{m}{s})$. We evaluate the S_{rs} at the limits of the *optimal patch*, thus

$$
x = p_u(t) \qquad\qquad y = p_s(t)\,.
\tag{2.18}
$$

To do this, we consider a patch of $\sigma_{u_0} = \sigma_{s_0} = 5$ km. A typical value of Lyapunov exponent calculated using satellite-derived velocity currents is of the order of 0.1 days^{-1} (see for instance [d'Ovidio et al., 2015]). This value is representative of the ocean upper layer. Because myctophids do not live in the mixed layer, we follow the indications in [Bettencourt et al., 2012] for the estimation of the Lyapunov exponents in the column
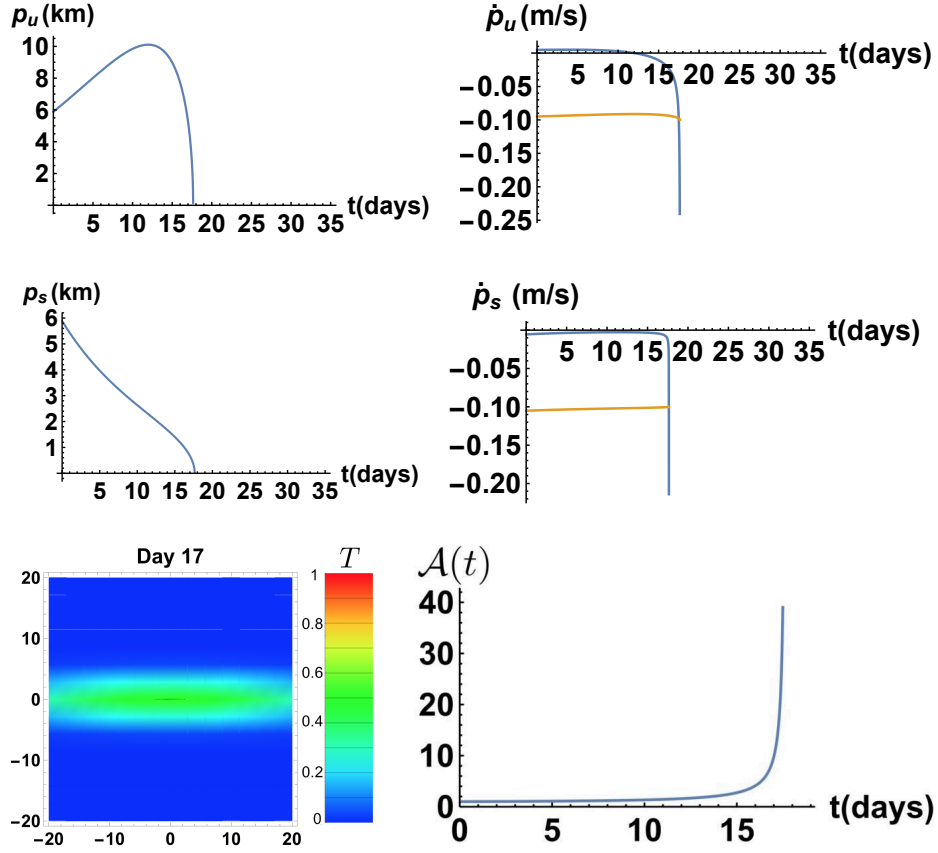
FIGURE 2.10: *Optimal patch* boundary position (p) and velocity ($\dot{p}$) along the unstable (first row) and stable (second row) manifold, according to the advection-diffusion equation (Eq. 2.13). K=4 m^2/s, $\lambda = 0.1$ days^{-1}, T with starting gaussian concentration with $\sigma_{u_0} = \sigma_{s_0} = 5$ km. In the plots reporting $\dot{p}_u$ and $\dot{p}_s$, the orange line represents the relative swimming speed of the fish (S_{rs}). Third row, left plot: *optimal patch* (delimited by the gray thin line) evolution after 17 days, just before it disappears: for 17 days, the fish have a S_{rs} greater than $\dot{p}$ along both the directions, thus potentially aggregating as showed in the right below panel, which illustrates the evolution of the aggregating estimate $\mathcal{A}$ (Eq. 2.19) in time, where 1 represents the starting fish aggregation value.

water. We consider therefore as λ the 75% of the surface value, i.e., $\lambda = 0.075$ days^{-1}, which is indicative of a depth of ~ 200 m. As value of horizontal diffusivity, we consider the average value $k = 4 \frac{m^2}{s}$ obtained from the estimates across an ocean front with Laypunov intensity as here by [Nencioli et al., 2013]. The optimal patch threshold T_t is set to 0.5 (the choice of the value is arbitrary). Results are shown in Fig. 2.10. Along the unstable manifold (panel A), the *optimal patch* expands for the first two weeks, then it decreases until it disappears after a "lifetime" of 17.65 days. The fish have a S_{rs} greater than $\dot{p}_u(t)$ (in absolute value) for $t_u = 17.49$ days (panel B). Along the stable manifold (panel C), the *optimal patch* decreases regularly for all the period, and the S_{rs} is greater than $\dot{p}_s(t)$ (in absolute value) for $t_s = 17.64$ days (panel D). The situation of the tracer after 17 days is reported in Fig. 2.10, panel E, with the contour identifying the *optimal patch*. In panel F we show the aggregation estimate $\mathcal{A}$, defined as the ratio

between the starting surface of the *optimal patch* and its value after a time t:

$$\mathcal{A}(t) = \frac{p_u(0)\,p_s(0)}{p_u(t)\,p_s(t)} \tag{2.19}$$

with $0 < t < min(t_u, t_s)$. The aggregation $\mathcal{A}$ improves slowly in the first two weeks, reaching a value of ~ 4 times after 15 days, and then improving dramatically in the last 2 days of life of the *optimal patch*, reaching a maximum value of 39 times the starting aggregation.

We note that (2.18) is a limiting aggregating condition, because it supposes that fish swim only if they are at the boundaries of the *optimal patch*, and not always toward the area of maximum tracer concentration. Nevertheless, it is possible to suppose that fish continuously swim, as described in the previous Subsection: in that case, their aggregation could improve more (not showed).

2.4   Discussion

Understanding the driving factors of the heterogeneity of marine biomass distribution across the oceanic landscape is a major issue for conservation purposes and fight against climate change [Hoegh-Guldberg and Bruno, 2010, Edwards and Richardson, 2004, Hays et al., 2005, Bradbury et al., 2008, Gaines et al., 2010]. In the open ocean, where no topographic frames of reference are present, this question is very complex, especially because of the simultaneous action of biological processes and physical dynamics, which may overlap [Lévy et al., 2012, McGillicuddy Jr, 2016, Lehahn et al., 2017]. Indeed, fine scale processes (few to hundreds of kilometers, days to several weeks) characterizing the horizontal circulation such as mixing and horizontal stirring, have showed to play a central role into conditioning and advecting planktonic biomass and regulating the community composition and biodiversity ([Lehahn et al., 2017, Lehahn et al., 2007, d'Ovidio et al., 2010, De Monte et al., 2013, McGillicuddy Jr, 2016], see also Ozier et al., in prep.). These questions have been addressed in the last 15 years, one approach being the use of Lagrangian methods, that allow one to identify kinematic features of the fine scale circulation which organize any advected tracer – so called Lagrangian Coherent Structures [Haller and Yuan, 2000, Boffetta et al., 2001, d'Ovidio et al., 2004, Beron-Vera et al., 2008, Haller, 2015]. In the recent years, this approach has been successfully applied also to the apex elements of the trophic chain, i.e. the top predators, leading to the emergent believe that fine structures do not modulate only primary production, but play an important role also into influencing predator behavior and movements (e.g. [Kai et al., 2009, Dragon et al., 2010, Cotté et al., 2015, Della Penna et al.,

2015]). However, knowledges on intermediate trophic levels are actually still missing, mainly because pelagic organisms can not be detected via satellite as primary production, neither tagged as for the case of larger predators, while several problematics are encountered during their samplings [Pearcy, 1983, Brodeur and Yamamura, 2005, Pakhomov and Yamamura, 2010b, Kaartvedt et al., 2012, Ariza et al., 2015, Faunce et al., 2015, Zeller and Pauly, 2018]. Recent development in technologies, in particular with acoustic sonar measurement and data analysis applied to marine ecology [Logerwell and Wilson, 2004, Benoit Bird, 2006, Béhagle et al., 2017], provided larger and more precise data availability, opening novel interesting opportunities. A Lagrangian approach to the analysis of fish catches measurements has been applied by Prants et al. [Prants, 2013, Prants et al., 2014a, Prants et al., 2014b], showing higher Pacific saury catches in proximity of frontal structures, leaving however the doubt that satellite data were used by the same fishery vessels to identify the fronts. Apart from that, possible mechanisms which may explain higher trophic abundances along frontal systems have not been described to our knowledge. Classical explanations (e.g., [Yoder et al., 1994]) are based mainly on *bottom-up* mechanisms along fronts with intense upwelling, which however do not take into account the fact that a maturation time is needed, time which can be greater that the lifetime of the front.

In my knowledge, the results presented in this Chapter are the first study which compares acoustic-derived fish concentration with Lagrangian (FSLE and betweenness) and Eulerian (SST gradient and mean Kinetic Energy) features. We do this by considering acoustic transects taken in the *Antarctic Southern Ocean* region (according to the ecopartition of [Sutton et al., 2017]) during night. This is related to the fact that the nektonic organisms present in the area, and in particular the myctophids, have often a nycthemeral cycle, migrating therefore into the depths during the day, where they are not detectable by the sonar employed (maximum depth achieved: 300m). Applying the bootstrap method, we show that a significant ($p<0.001$) higher fish concentration is present along frontal features, identified with FSLEs, betweenness and SST gradient.

The main limitation of this analysis is linked to the satellite resolution, which we tried to smooth by averaging over an around of $0.2°$. Future satellite missions such as SWOT (https://swot.cnes.fr) will help improving the resolution of the currents, being able to detect directly structures at the submesoscale, and providing also interesting possibilities for the detection and inclusion of 3D dynamics.

We then analyze the role of the frontal systems into enhancing fish aggregations, by taking into account the swimming capability of the fish, and looking at the two main difficulties that arise during the searching activity of an optimal hotspot in a dynamic environment. The first is related to the correct identification of the location of the hotspot, which in a noisy environment can be difficult, while the second is related to

the velocity of the fish, which must be able to reach it quick enough before the hotspot is dispersed. Concerning the first difficulty, we analyze a stationary frontal situation, simulating the fish density evolution assuming that the fish try to climb a noisy gradient along a realistic sized front in order to reach the higher concentration zones. We incorporate noise as a threshold dynamics, supposing that for values of the tracer gradient over a certain threshold, the fish are able to orientate without being affected by the noise. We estimate this threshold using the zooplankton gradient distribution obtained with the acoustic data employed in the first part of the paper. We obtain that, starting from a homogeneous fish distribution, the response to a frontal structure can be very quick, allowing the formation of two peaks of doubled concentration after only 6 hours, which then merges after 4 days (Fig. 2.7). We note that this "merging" scenario implies that the fish spread homogeneously in the whole region with high tracer values and do not convey all toward the highest tracer value at the center. This is interesting from a biological point of view because is in accordance with on-going studies of the myctophids response to food. Myctophids indeed are supposed to ingest always the same quantity of food over a certain threshold of prey concentration (P. Koubbi et A. Hulley, personal communication), so-called, Holling type III, [Holling, 1959].

The second kind of difficulty encountered by fish during their search process ? how they overcome currents - is analyzed through the simulation of the dispersion of an *optimal patch* of a passive tracer, represented by the collection of points with a concentration value over a certain threshold. The *optimal patch* is located over a frontal system, characterized by a hyperbolic dynamic, and is subjected to the action of stirring and diffusion simulated through the advection diffusion equation as it evolves in time.

The aim of the simulation is observing if fish possess a sufficient cruising velocity speed in order to follow the contracting patch and stay inside it. In this case, we do not include the noise effect considered previously which can limit the orientating capacity of the fish. We use strain rates and diffusion coefficients representative of Southern Ocean frontal features, an *optimal patch* starting size consistent with those of fine scale structures, along with a fish cruising speed representative of the myctophids swimming capability. We obtain that fish are possibly capable to follow and stay inside the *optimal patch* for about two weeks, time comparable with the timescales of the lifetime fine scale features. During this time, fish concentration grows about 40 times. Furthermore, the hyperbolic dynamic compress and slightly elongates the *optimal patch*, distributing thus the fish over a thin filament along the unstable manifold (which identifies the front). This is in accordance with the recent study of [Della Penna et al., 2015], which shows an increased capture rate of an elephant seal over a thin and elongated surface at an eddy periphery, for a similar time window ($\sim$ 10 days). Eddy peripheries are furthermore regions generally characterized by the hyperbolic dynamic analysed here [Lehahn et al.,

2007] and elephant seals feed mainly on myctophids [Cherel et al., 2008, Cherel et al., 2010, Daneri and Carlini, 2002]. The horizontal organization of the foraging ground of the elephant seals along an elongated filament is confirmed also by the three dimensional study of [Bras et al., 2017], which shows how density preys are associated to a strongly anisotropic behavior. In particular, high prey densities are recorded when the elephant seals swim along a single direction.

An additional interesting consideration arises when considering the results of the quantile regression of Subsec. 2.3.1. Indeed, with the gradient climbing effect and the hyperbolic dynamic, we assessed that frontal features can enhance aggregation of nektonic organisms. The starting condition of our hypothesis is the presence of a tracer which represents an element of interest for the fish (for instance, zooplankton) and, of course, of the fish themselves. Obviously, these conditions are not always verified in the ocean. Therefore, a strong "aggregating" front, failing these conditions, will not present high fish densities. The consistent R^2 tests obtained with the quantile regression analysis provides a confirmation of the limiting role of the fronts over the fish aggregation. The front can be seen as a necessary but not sufficient condition for high fish densities.

The mechanisms reported here constitute therefore, to our knowledge, the first attempt to identify and quantify the horizontal role of currents and frontal systems into creating hotspots of high fish concentration, by creating gradients in the distribution of tracers of interest which can be climbed quickly ($\sim$6 hours), and by advecting and smoothing them, conditioning the movement of the fish which improve their local aggregation over timescales which are relatively longer ($\sim$15 days).

The present study however includes several assumptions which must be taken carefully in consideration, and does not intend to provide an overall mechanism of fish aggregation which includes all the ocean dynamics. First of all, our mechanisms do not include any vertical dynamic, which can instead constitute an important factor into the organisation of the marine biota through nutrient upwellings [Lévy et al., 2012, Mahadevan et al., 2012, McGillicuddy Jr, 2016]. The choice of neglecting the vertical velocities arises from the fact that 3D observations of oceanic currents are still not available, while knowledge on oceanic horizontal dynamics is more advanced. This is why we started to analyse some simple 1D scenarios.

Another limitation of our study comes from the fact that we neglect the nycthemeral cycle which characterises the majority of myctophids species [Duhamel, 1998], which therefore live in depth during the day, where the circulation dynamics can be different. This choice is driven by the difficulty in parameterising such a non linear behavior, which however opens the possibility for further analysis. Furthermore, when we parameterise the tracer, we do not take into account for possible interactions of the fish with it. This

is not a strong assumption if the tracer represents a physical parameter such as temperature or salinity, but can be a constraint if it parameterises a nutrient, which could be consumed by the fish and thus reduced more quickly. In that case, however, we consider that, on the timescales considered, eventual reductions of the nutrient are compensated by source terms (like blooms), but further studies are required to assess the contribution of this phenomenon.

Finally, here I analyzed separately the searching dynamics and the dispersion of the tracer. This is probably the single most important aspect that should be addressed in the future. An interesting perspective in particular should be the study of the simultaneous interaction of the two mechanisms together, developing a model which takes into account the fact that a noisy gradient evolves in time due to horizontal stirring, and analysing it along two dimensions. In Chapter 4 I will develop further this point, presenting some preliminary but promising results.

Chapter 3

Aggregation over time: the "crossroadness"

This Chapter has been submitted as *Crossroads of the mesoscale circulation* by A. Baudena et al. at *Journal of Marine Systems*, 2018.

In the last Chapter, I showed how frontal systems can act as hotspots of increased fish concentration, and I provided a explanation for that, based on horizontal currents. The analysis is however limited to a specific region, the *Antarctic Southern Ocean*, which furthermore is characterised mostly by a single fish family, the *myctophidae*, even if largely diffused. It would be thus important to extend the previous analysis also to other oceanic regions, characterised by different ecologies and physical dynamics. This is not obvious because the *Antarctic Southern Ocean* region and, in particular, the Kerguelen sector is, despite its remoteness, a relatively well studied area, as explained in Sec. 1.7. Furthermore, as explained in Sec. 1.5, information on mid trophic levels at large scales is difficult to obtain, and often only ship-based measurements are available, which however can present biases. It is therefore essential to build new effective sampling strategies in order to monitoring optimally mid trophic levels, in order to increase data availability on them, and fill the knowledge gap actually present toward lower and higher elements of the trophic chain. In this Chapter, therefore, I address the problem of optimally intercepting a flux coming from, or going to, a target region, in order to build a network of fixed station capable of monitoring the largest surface possible, and of estimating furthermore its provenance.

3.1 Abstract

Quantifying the mechanisms of tracer dispersion in the ocean remains a central question in oceanography, for problems ranging from nutrient delivery to phytoplankton, to the early detection of contaminants. Until now, most of the analysis has been based on Lagrangian concepts of transport, often focusing on the identification of features that minimize fluid exchange among regions, or more recently, on network tools which focus instead on connectivity and transport pathways. Neither of these approaches, however, allows us to rank the geographical sites of major water passage, and at the same time, to select them so that they monitor waters coming from separate parts of the ocean. These are instead key criteria when deploying an observing network. In this Chapter this issue is addressed by estimating at any point the extent of the ocean surface which transits through it in a given time window. With such information it is possible to rank the sites with major fluxes that intercept waters originating from different regions. I show that this allows us to optimize an observing network, where a set of sampling sites can be chosen for monitoring the largest flux of water dispersing out of a given region. When the analysis is performed backward in time, this method allows us to identify the major sources which feed a target region. The method is first applied to a minimalistic model of a mesoscale eddy field, and then to realistic satellite-derived ocean currents in the Kerguelen area. In this region I identify the optimal location of fixed stations capable of intercepting the trajectories of 43 surface drifters, along with statistics on the temporal persistence of the stations determined in this way. I then identify possible hotspots of micro-nutrient enrichment for the recurrent spring phytoplanktonic bloom occurring here. Promising applications to other fields, such as larval connectivity, marine spatial planning or contaminant detection, are then discussed.

3.2 Introduction

Suppose that a contaminant is released in a region of the open ocean. Where should a set of monitoring stations must be deployed to maximize the chances of detecting and eventually restricting the contaminant spill? Characterizing the evolution of tracers dispersed by the oceanic currents is indeed a central question in several areas of oceanography. In some cases it is possible to partially address this point by tracking a given tracer using satellite images or model simulations, but often *in situ* measurements and adaptive sampling strategies are required.

Relevant examples range from the retrieval of contaminants and their basins of attraction [Vrana et al., 2005, Froyland et al., 2014], larval dispersal and marine populations connectivity [Carreras et al., 2017, Bradbury et al., 2008, Planes et al., 2009, Andrello et al., 2013, Melià et al., 2016, Monroy et al., 2017], the planning of oceanographic surveys [Bellingham and Willcox, 1996], monitoring systems design [Mooers et al., 2005, de Jonge et al., 2006, Muñoz et al., 2015], to the characterization of Marine Protected Areas [Cowen et al., 2006, Siegel et al., 2008, Shanks, 2009, Rossi et al., 2014, Dubois et al., 2016, Bray et al., 2017], or to the so called Marine Spatial Planning (MSP, [Viikmäe et al., 2011, Delpeche-Ellmann and Soomere, 2013a, Ehler, 2018] which integrates all the above.

Horizontal transport at the ocean surface is one of the key mechanisms controlling the dispersion of tracers, in particular on scales of the order of days to weeks. In this time frame, a heuristic but very common assumption is that vertical velocities are weak enough so that the motion of a water parcel can be considered two-dimensional. Strictly speaking, horizontal transport affects any advected tracer through two main processes: mixing, which reduces and smooths the gradients, and horizontal stirring, which instead enhances the tracer gradients [Eckart, 1948, Okubo, 1978, Garrett, 1983, Sundermeyer and Price, 1998]. Horizontal stirring is one of the main mechanism for which an initial homogeneous water mass is stretched by the currents and deformed into elongated and convoluted filaments. These features can intrude into some regions far apart from their origin, while other areas close to the source location may be shielded by circulation features, the so-called transport barriers. This filamentation process eventually enhances mixing by creating longer contact surfaces between water masses of contrasting properties.

Several tools have been proposed to achieve a better understanding of the role horizontal transport plays in tracer dispersion. Most of these approaches focus on the Lagrangian analysis of the ocean currents based on dynamical system theory [Ottino, 1989, Haller and Yuan, 2000, Mancho et al., 2004, Shadden et al., 2005, Wiggins, 2005]. These methods are mainly devoted to the detection of barriers to transport in flow systems [Boffetta et al., 2001, Abraham and Bowen, 2002, d'Ovidio et al., 2004, Beron-Vera et al., 2008, Prants et al., 2014a, Prants et al., 2014b] or coherent regions [Lehahn et al., 2007, Froyland et al., 2007, d'Ovidio et al., 2013, Berline et al., 2014, Hadjighasem et al., 2016, Miron et al., 2017] with minimal leaking to surrounding water masses. Interestingly, during the last years, network theory approaches to geophysics [Phillips et al., 2015], flow transport and mixing [Ser-Giacomi et al., 2015a, Lindner and Donner, 2017, Fujiwara et al., 2017, Molkenthin et al., 2017, Padberg-Gehle and Schneide, 2017, Ser-Giacomi et al., 2017, McAdam and van Sebille, 2018], and turbulence [Iacobello et al., 2018, Gopalakrishnan Meena et al., 2018] have also attracted lot of interest.

Recently, more attention has been given to a problem that is complementary and somehow opposite to the identification of transport barriers: how to detect regions that enhance fluid exchanges across a flow system [Ser-Giacomi et al., 2015b, Ser-Giacomi et al., 2015c, Costa et al., 2017, Lindner and Donner, 2017, Rodríguez-Méndez et al., 2017, Koltai and Renger, 2018]? This issue has been developed particularly in the framework of networks built from Lagrangian trajectories [Ser-Giacomi et al., 2015a]. In such studies, spatial sub-areas of the ocean are represented by network nodes while links parameterize the amount of water exchanged among them. Networks constructed in this way, called Lagrangian Flow Networks (LFNs), provide thus a topological description of the transport dynamics in the ocean allowing to describe features of the flow by using several network methods and tools.

In particular, it has been shown the existence of localized "bottlenecks"whose presence maintains connections between areas of the seascape that would be otherwise almost disconnected. Borrowing from Network Theory the concept of betweenness centrality, it has been possible to quantify explicitly how much LFN nodes act as bottlenecks for the oceanic flow by counting the number of paths passing through them during a fixed interval of time [Ser-Giacomi et al., 2015b].

The main limitation of the betweenness centrality concept, however, is that it identifies bottleneck regions that, even if topologically relevant for the connectivity geometry, do not present necessarily an important water flux. This is related to the fact that the betweenness measures the number of connections crossing a node, regardless of connectivity strength. Therefore, to pinpoint hotspots that maximize the incoming or outgoing flux in a given time window, one should focus on strong "passage points"of water, instead of only topological bottlenecks.

In this Chapter I aim to detect these hotspots, which act as "crossroads"of the circulation, being traversed by the largest amount of water coming from (or going to) a focal region. This is achieved by defining a quantity, which I call *crossroadness*, which is the surface flow through each spot of the domain considered in a specific temporal window.

Moreover, the calculation preserves the information on the original location of each passing trajectory. Based on the *crossroadness* analysis, I introduce an algorithm for designing a sampling network with minimal redundancy, i.e. in which the flow of a given source region through the network is maximized and the number of stations minimized. Reversing the analysis backward in time, it is possible to use the same method to find the major "source"points from which the water distributes over a target area. The paper is organized as follows: Sec. 3.3 describes the methodological framework, the theoretical model and the dataset employed for the computation and the validation of the results. In particular, Subsec. 3.3.1 introduces the crossroadness and its fluid dynamical
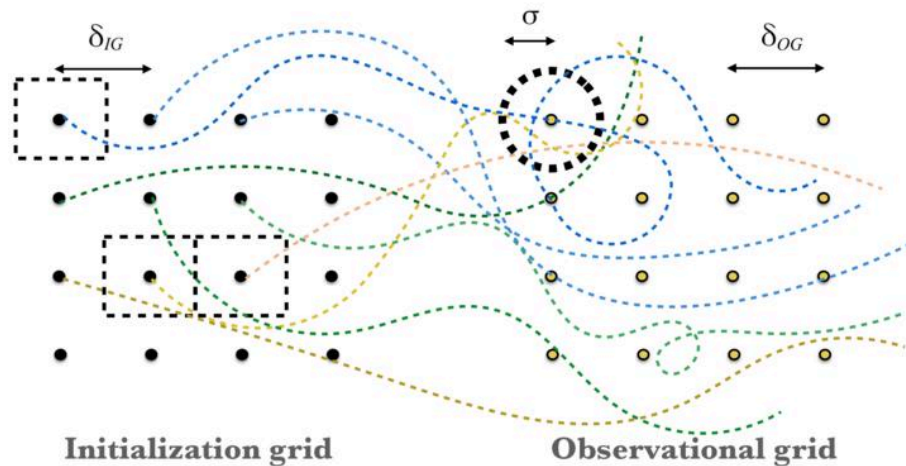
FIGURE 3.1: Illustrative example for the calculation of the crossroadness. Colored dotted lines correspond to different trajectories originating from the *initialization grid* (left), advected for a time τ. The circle (thick dotted line) represents the detection range of the station of the *observational grid* (right), while the rectangles (thin dotted line) contain the surface of water that passes through the station.

and oceanographic interpretation. I then determine a ranking method (Subsec. 3.3.3) that provides the sites with the major passage of water dispersed from a source region or feeding a target region, when computed forward or backward in time, respectively. Validation and case studies are then described in Sec. 3.4. In Subsec. 3.4.1, I first analyse the crossroadness properties of a simple steady vortex configuration obtained from the 2D Navier Stokes equation. In Subsec. 3.4.2, the method is applied to satellite altimetry data and validated against the trajectories of real SVP drifters in the Southern Ocean. In Subsec. 3.4.3, the relationship between the surface being monitored and the number of stations employed is examined. An analysis of the persistence of the observing network is reported in Subsec. 3.4.4. In Subsec. 3.4.5, the method is used to identify possible sites from which nutrients are delivered offshore the Kerguelen plateau, fuelling the open ocean planktonic bloom. A summary of the results, along with an illustration of the perspectives and possible fields of application is given in the Discussion (Sec. 3.5). Finally, the paper is completed by two appendices, extending the analysis of the sensitivity of the diagnostic introduced to changes in the dates of the velocity field used (Appendix A), and giving some demonstration of the link of the new diagnostic, under particular hypotheses, to averages of velocity and of kinetic energy (Appendix B).

3.3 Data and Methods

3.3.1 The crossroadness: characterizing regions by the amount of water crossing them

I define a new metric, which is called *crossroadness* (CR), measuring the surface crossing a region of a given size in a fixed temporal window.

To do this, two grids are considered, the *initialization* and the *observational grid* (Fig. 3.1), of cell sizes δ_{IG} and δ_{OG} respectively, where each cell is represented by its central point. If δ_{IG} is small enough, one can consider every central point as representative of the content of the cell.

Each central point of the *initialization grid* is advected and defines a trajectory. The *observational grid* represents instead the domain over which the crossroadness is computed (see also Subsec. 3.3.7). For each point $\mathcal{P}$ of this grid, I count the number of trajectories passing below a distance σ from $\mathcal{P}$. This is done by computing the Euclidian (or spherical when working with spherical coordinates) distance between $\mathcal{P}$ and the first point of the trajectory, then the second one, the third one and so on. One obtains thus N_{PT} values. I consider as distance between the trajectory and $\mathcal{P}$ the minimum among the N_{PT} values. σ represents the neighborhood radius (the detection range) of each point in the *observational grid*. In spherical coordinates, if σ is given in radians, this radius is indeed $R\sigma$. As the dimensions of a cell in the *initialization grid* are relatively small, one can consider that the trajectory is representative for the whole content of the cell from which it is originated (therefore, $\sigma \geq \delta_{IG}$). Thus, if the number of trajectories counted is multiplied for the surface of an initialization cell, Δ, one will obtain an estimation of the total water surface that passed through the node during the period τ. I call this total water surface flowing inside the detection range of the point $\mathcal{P}$ the "crossroadness" ("CR") at $\mathcal{P}$. In this way I define a CR field on all points of the *observational grid*. A representative scheme of this concept is illustrated in Fig. 3.1, where the crossroadness of the point in the circle is 3Δ since there are three trajectories entering its detection range. Because of the quasi-twodimensional nature of ocean circulation at the scales considered here, the amount of surface is proportional to the volume and then to the mass of the water transported in the upper ocean layers. The same procedure can be applied backwards: the *initialization grid* is advected backward in time, and, over the *observational grid*, I count for each point how many trajectories pass closer than the detection range σ. In this way I obtain the crossroadness field backwards in time.

3.3.2 Theoretical relation of the crossroadness with absolute velocity and mean kinetic energy

Intuitively, one can expect higher crossroadness values in points where the velocity is higher, because the corresponding particle fluxes are also larger. The situation is in fact more complex because a map of crossroadness is associated only to the trajectories stemming from a specific region. It is however instructive to study the case in which the trajectories stem from the entire domain (i.e., when the initialization grid coincides with the observational grid), because in this case the crossroadness has a direct proportionality relation with the kinetic energy.

To show this relation, I note that every circle of radius σ around an observational station presents a cross section (more properly a cross-length) 2σ perpendicular to the flow coming from any direction. If σ is sufficiently small to allow considering the velocity field constant on the whole observational circle, the amount of surface crossing that station in a short interval of time dt is $2\sigma|v|dt$, with $|v|$ the velocity modulus at the station. Integrating during a time τ I find that the CR at that point can be written as

$$CR = \int_{D_0}^{D_0+\tau} 2\sigma|v|dt = 2\sigma\tau < |v| > , \tag{3.1}$$

with $< |v| >$ the temporal average of the speed $|v|$ in the time interval τ. If the temporal fluctuations of $|v|$ during the time interval τ can be neglected, i.e. $< v^2 > \approx < |v| >^2$ then a relationship with the temporal average of the kinetic energy per unit of mass of the flow, $< E_K >=< v^2/2 >$, would hold:

$$CR \approx 2\sigma\tau\sqrt{2 < E_K >}. \tag{3.2}$$

The formulas above present the announced approximate relationship between the crossroadness and the flow speed. For a validation of Eq. (3.1) and (3.2), please refer to Appendix B.

As we shall see, more complex crossroadness patterns arise when the trajectories do not originated from the entire domain.

3.3.3 Ranking method for the optimization of a network of CR stations

In the study of the dispersion of a passive tracer one of the main questions is the definition of an effective sampling strategy. Considering the tracer (e.g. a contaminant) with a finite life time, I want to know what would be the best distribution of monitoring sites (referred to as "stations") that can intercept the largest fraction of the advected tracer.

In a turbulent pattern of circulation, the answer to this question is not obvious, since the patch can be redistributed irregularly through the domain considered.

Sampling on a regular grid is a possible choice. However, depending on the circulation patterns, one can easily imagine that some retrieving sites may convey water from larger regions than others. The crossroadness provides implicitly a simple method for the definition of a sampling strategy. In fact, if one wants to choose the best monitoring station, it will simply select the site crossed by the largest number of trajectories originated by the source region of the tracer, i.e. the one with the higher value of crossroadness. In order to define the second most important monitoring station, I exclude the trajectories already monitored by the first station. I consider only independent trajectories, i.e. originated from different locations of the *initialization grid*, and I determine also the second station. Proceeding iteratively in this way I identify a network of *CR stations* (Fig. 3.2).

The calculation can be performed backward in time as well. The initialization region becomes a target region. In this case, the network of CR stations represents the ensemble of locations which maximize the surface water feeding the target region.

3.3.4 A simple steady vortex field

I consider a numerical simulation of the Navier Stokes equation in two dimensions, which, for the scalar vorticity field $\omega = \nabla \times \mathbf{u}$ of an incompressible fluid ($\nabla \cdot \mathbf{u} = 0$, in which $\mathbf{u}$=(u,v) is the velocity field), can be written as:

$$\frac{\partial \omega}{\partial t} + \omega \cdot \nabla \mathbf{u} = \nu \nabla^2 \omega - \alpha \omega + f_\omega \tag{3.3}$$
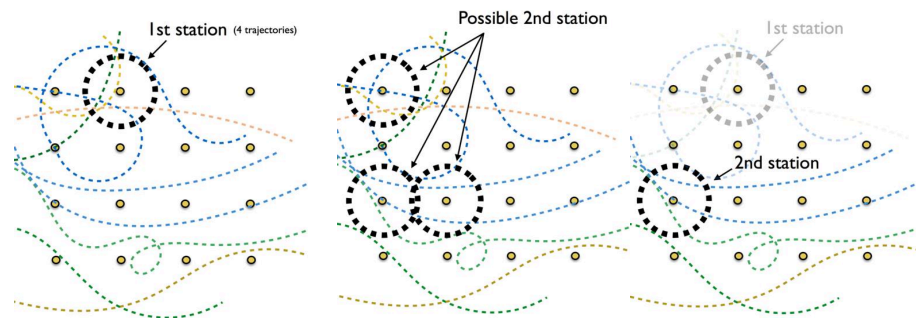
FIGURE 3.2: Illustrative scheme for the determination of the position of a network of observing stations which maximize the detection of a dispersed tracer. The first station is the one that collects the largest number of trajectories, in this case the one circled in the left panel (4 trajectories). Then, there are 3 possible second stations, each with 3 trajectories passing near them (middle panel). But since I consider only independent trajectories, I have to exclude the ones already sampled by the first station (panel on the right). In this way I have only one second possible station.

in which ν is the kinematic viscosity, $-\alpha\omega$ is a friction term removing energy at large scales and f_ω represents a forcing term necessary to maintain a stationary state. All the quantities are adimensionalised. I use a forcing on a narrow band of wave numbers around $k_f=2$ in Fourier space which is constant in time and acting with a fixed phase $\theta = \pi$. I take $\nu = 0.5$, $\alpha = 0.025$ and I integrate Eq. 3.3 with a pseudospectral code on a box of size $L_x = L_y = 2\pi$ with periodic boundary conditions and 512^2 grid points. Starting from a null vorticity field, the model is run for 15600 steps (dt= $5\cdot10^{-4}$, t = 7.8), until the energy of the system is constant ($E = 0.06$) and a steady vorticity (and velocity) field is reached. More details on the model are provided in [Boffetta et al., 2002, Boffetta and Musacchio, 2010].

The stationary vorticity field obtained is in Fig. 3.3. It is formed by a series of anti-clockwise (in blue) and clockwise (in red) rotating vortexes. Particles, disposed on a regular grid of 256^2 points, are then advected using a second order Runge Kutta method as explained in Subsec 3.3.7. The vorticity field is considered to cover periodically the full horizontal plane, on which the particle move, although I will only display and analyze the subdomain $[0,2\pi]\times[0,2\pi]$. Finite Time Lyapunov Exponents (FTLE) forward (λ^f) and backward (λ^b) in time are computed from the trajectories, following the definition in [Shadden et al., 2005].
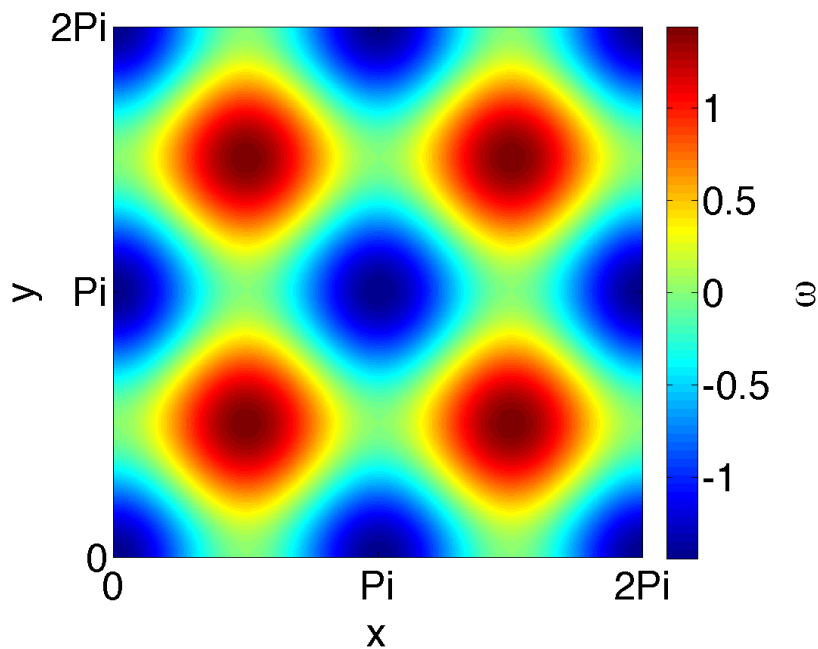
FIGURE 3.3: Two-dimensional steady vorticity field as obtained from Eq. 3.3. The box size are $L_x = L_y = 2\pi$ and the vorticity field was integrated with a resolution of 512^2 grid points regularly spaced.

3.3.5 Ocean satellite-derived velocity field and chlorophyl data

I focus on the Kerguelen region of the Southern Ocean, where in 2011 the KEOPS2 campaign released, over 20 days, a set of 48 Surface Velocity Program (SVP) drifters. These could represent waters hypothetically rich in myctophids larvae. I use a set of stations, defined by the method introduced previously, for a virtual "search and rescue"of these drifters. For their computation, I use satellite-derived velocity fields, which are obtained through the geostrophic approximation from the measurement of the Sea Surface Height (SSH). This approximation and the relatively low spatial and temporal resolution of satellite products often risk to smooth mesoscale structures [Bouffard et al., 2014], especially close to the coast [Nencioli et al., 2011]. The comparison between satellite-derived crossroadness and real drifter trajectories is thus a realistic assessment of the capacity of the algorithm described here to identify points with enhanced passage of particle trajectories.

The Kerguelen region is also characterized by a massive spring-time phytoplanktonic bloom, extended for hundreds of kilometres, preconditioned by the redistribution of micro-nutrients (in particular iron) advected by the Antarctic Circumpolar Current (ACC) from the Kerguelen plateau margin out into the open ocean [d'Ovidio et al., 2015]. Satellite-derived chlorophyll is therefore a useful tracer of transport pathways, and an opportunity for pinpointing likely sources of iron by employing the theoretical concepts developed in this paper.

For the velocity field I use the DUACS (Data Unification and Altimeter Combination System) delayed-time multi-mission altimeter gridded products defined over the global ocean with a regular $\frac{1}{4} \times \frac{1}{4}^{\circ}$ spatial sampling [Pujol et al., 2016] and available from the E.U. Copernicus Marine Environment Monitoring Service (CMEMS, http://marine.copernicus.eu/). An experimental product, which used an improved mean dynamic topography and for which the altimetric tracks have been interpolated with optimized parameters, is also considered. It corresponds to the AVISO regional Kerguelen product, velocities computed from altimetry in delayed time on a (higher resolution) $\frac{1}{8} \times \frac{1}{8}^{\circ}$ regular grid (http://www.aviso.altimetry.fr/duacs/).

The field of chlorophyll was downloaded from the Oceancolour product (OCEANCOLOUR_GLO_CHL_L at CMEMS. These data are provided by a map computed from satellite observations over a period of 8 days (to limit cloud coverage), and with a spatial resolution of 4 km× 4km.

3.3.6 SVP drifters

During the KEOPS2 campaign in October-November 2011, 48 Surface Velocity Program (SVP) drifters were released within the Kerguelen region. The SVP drifting buoy is a Lagrangian current-following drifter, composed of a spherical surface float of 35 cm in diameter, which contains the battery, a holey sock drogue of about 6 meters that tracked the water currents at a nominal depth of 15 m, representative of the surface circulation, and a satellite transmitter which relays the data through the Iridium system. All the buoys address the World Ocean Circulation Experiment (WOCE) benchmarks.

In the present Chapter I consider only the drifters released on the eastern part of the Kerguelen plateau, i.e. at a longitude greater than 68°E. I therefore consider 43 drifters trajectories of the 48 drifting buoys originally deployed. I assume the 11th of November 2011 as the release date. The duration of the trajectories ranges between 63 to 93 days (average of 81 days), with a temporal resolution of 1 day.

3.3.7 Initialization and observational grids

I describe here the details of the construction of the two grids used for the computation of the crossroadness.

For the Navier Stokes model, particles start over an *initialization grid* of 256^2 regularly displaced points ($\delta_{IG} = 0.0246$) and are advected with a second order Runge-Kutta scheme for a period t=11.7, corresponding to 23400 steps.

When working with altimetric velocities, the points of the *initialization grid* are advected using DUACS altimetric velocities with a 4th order Runge-Kutta integration scheme, for a period between 30 and 90 days and a time step of 3 hours. Each trajectory thus computed contains 8 points per day ($N_{PT} = 8\,N_D$ in total, N_D number of days). I remind that the period of integration is chosen so that the vertical motion can be neglected. Indeed, below 2-3 months, and excluding some peculiar regions of convection, the vertical velocity is usually 2∼3 orders of magnitude smaller than the horizontal one, and thus the ocean surface motion can be approximated as two dimensional [d'Ovidio et al., 2004, Rossi et al., 2014].

I note here that, when working with altimetric velocities, and thus in spherical coordinates, I impose that all the cells have the same size. The initial angular separation between two contiguous particles (δ_{IG}) used in the computations varies from 0.1 to 0.4 degrees. By initial separation δ_{IG} I mean the difference in latitude among contiguous rows of particles. Along the longitudinal (LON) direction, to keep the same distance, the

separation is thus corrected by the cosine of the latitude LAT ($\delta_{LON} = \delta_{IG}/\cos(LAT)$). In this way all the cells have the same lateral sizes, $R\delta_{IG}$, and area $\Delta = R^2\delta_{IG}^2$ (with δ_{IG} in radians, and R the Earth radius). The *observational grid* in spherical coordinates is built in the same way as the *initialization grid*.

In Sec. 3.4 I will always refer to them as *initialization* or *observational grid*, but keeping in mind their difference (for Navier Stokes and altimetric velocities) in Euclidian and spherical coordinates.

3.4 Results

3.4.1 The crossroadness in the steady Navier-Stokes 2D vortex configuration

To gain some insights on the interpretation of the crossroadness and on its differences in respect to other Lagrangian methods, I present here the analysis of the flow associated to the vorticity field shown in Fig. 3.3, obtained from the numerical simulation of Eq. (3.3), as explained in Subsec. 3.3.4. The flow contains 4 vortices rotating clockwise (positive vorticity, red patches) and a central vortex rotating anti clockwise (in blue). 9 other anti clockwise rotating vortices are present partially on the edges of the box. The vortices are surrounded by separatrices made of the stable and unstable manifolds of fixed hyperbolic points, arranged in a square lattice. To visualize these separatrices I compute in Fig. 3.4 Finite Time Lyapunov Exponent fields (FTLE, defined as in [Shadden et al., 2005]). Forward (λ^f) and backwards (λ^b) FTLE are calculated for an integration time $\tau = \pm 11.7$ on a grid of 256^2 points, and I plot their sum. The ridges of such field clearly identify the stable and unstable manifolds and its maxima highlight the position of the correspondent hyperbolic points.

As a first step, I compute the crossroadness field and the associated monitoring stations considering as *initialization grid* 256^2 particles regularly displaced on the entire domain ($\delta_{IG} = 0.0246$). The *observational grid* is made of 128^2 points ($\delta_{OG} = 0.0490$). Particles in the initialization grid are advected forward in time for t= 11.7, i.e. the same period considered for the computation of the FTLE of Fig. 3.4A. Finally, I consider as detection range $\sigma = 0.1$. The result is shown in Fig. 3.4B. The crossroadness pattern in itself does not contain much valuable information, because (as explained in Subsec. 3.3.2) when the *initialization grid* covers the entire domain the crossroadness closely matches the kinetic energy (except for points very close to the border). The position of the monitoring stations selected by the ranking algorithm (the set of points crossed by the largest number of independent trajectories) however is not trivial. They are shown as

black dots in each panel. For the first five, I plotted also their detection range and order of importance (white number inside the circle). Although in general FTLE ridges have large crossroadness values, only the first two stations (white numbers 1 and 2) fall over a manifold. This fact can be understood noting that multiple stations over the manifolds would be redundant, because they would sample trajectories intercepted by other stations. Interestingly, 173 stations were found to be necessary in order to sample the whole region. Multiplying this value for the surface of a station, i.e. $\pi\sigma^2$, I obtain that they cover only 14% of the total box surface. When considering instead a $\sigma = \delta_{OG}$, 632 stations, covering just the 3% of the total surface, were needed to sample the whole region.

I then changed the *initialization grid*, considering all the particles belonging to an ellipse of center $x_C = \pi$, $y_C = \frac{3}{2}\pi$, with semi-axes $r_x = 1$, $r_y = 0.5$. I note that the ellipse is thus centered exactly over a hyperbolic point. Finally, σ is set to 0.3. The results are reported in Fig. 3.4C-D. Contrary to the previous case, The pattern of the crossroadness is intimately linked to the choice of the *initialization grid* and also to the direction of the advection (forward or backward).

Looking at the disposition of the CR stations for the backward-in-time case it is possible to note that the first two stations are situated over the regions of highest crossroadness, and in symmetric positions in respect to the starting ellipse (dotted line). However, they do not fall exactly on the manifolds. The subsequent stations are not displaced symmetrically, and their disposition does not appear obvious. For instance, the 3rd station is on a branch of the crossroadness pattern far away from the ellipse and, interestingly, does not fall in any of the two regions with relatively high values of CR (the one at $x \simeq 5$, $y \simeq 4$ and the other at $x \simeq 1$, $y \simeq 5.5$). As in the previous case, this is due to the fact that the fluxes passing there have already been intercepted by the first two stations. The 4th station, instead, falls almost totally inside the starting ellipse. Finally, the last station (not numbered) falls in a region of higher crossroadness than the previous three.

3.4.2 SVP drifters and crossroadness in the Kerguelen region

In order to test the crossroadness and the ranking method as defined in Subsec. 3.3.1 and 3.3.3 in a real oceanic environment, I use the dataset from the KEOPS2 campaign, in which 43 drifters were released in a relatively small area (the eastern margin of the Kerguelen plateau), approximately in the same period of time (around the 11th of November 2011), and advected for a similar window of time ($\tau_D = 81$ days on average) by the currents, as shown in Fig. 3.5. I use thus 43 real drifter trajectories.
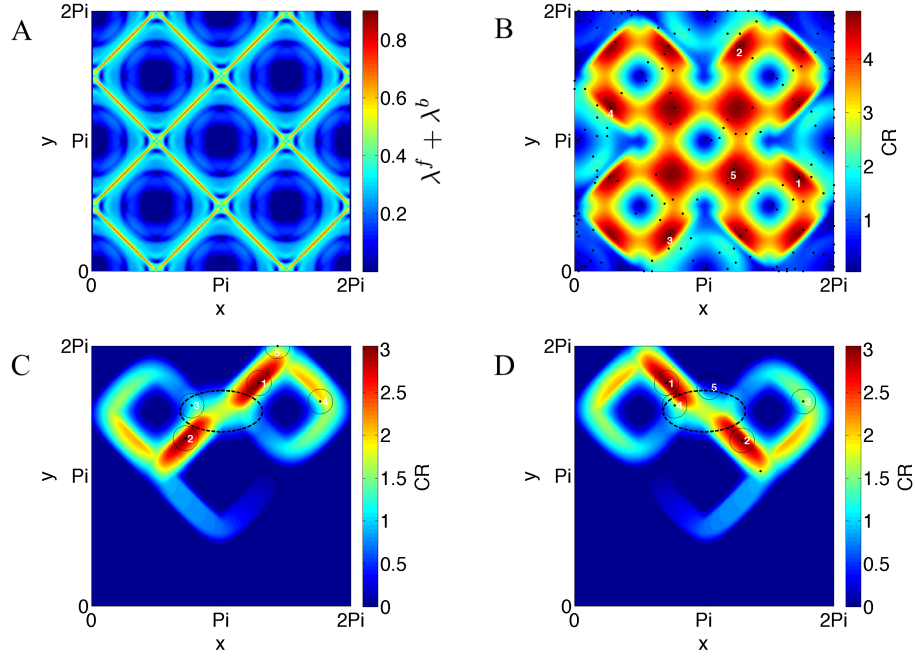
FIGURE 3.4: Panel A: Forward (λ^f) and backwards (λ^b) FTLE fields, computed with integration times $t = \pm 11.7$ respectively, and over a 256^2 regular grid. They identify the locations of stable and unstable manifolds and the associated hyperbolic points. The quantity actually plotted is $\lambda^f + \lambda^b$ Panel B: crossroadness forward in time, obtained from the advection of a 256^2 regular *initialization grid* for a time $t = 11.7$, computed over a 128^2 *observational grid* covering the same domain. $\sigma = 0.1$. Panel C-D: cross-roadness, forward and backward in time respectively, computed from the advection of the points started at the ellipse (black dotted line) centered in $x_C = \pi$, $y_C = \frac{3}{2}\pi$, with semi-axes $r_x = 1$, $r_y = 0.5$ and spatial separation between two contiguous particles $\delta_{IG} = 0.0246$, for a time $t = \pm 11.7$, respectively. The *observational grid* is the same of panel B. For B,C,D, each black dot represents a CR station. The detection range of each of the 5 most important stations is displayed as a black circle, and contains the order of priority of each station (white number).

The aim is to compare the regions of densest passage of these real buoys with the ones predicted by the CR method, which is based on oceanic currents estimated from satellite altimetry. Therefore, the *initialization grid* consists in a series of virtual drifters displaced in the following way: I consider the region of release of the real drifters (between [-51, -47]°S, and [70, 75]°E). I cover it with rows of virtual tracers, separated by $\delta_{IG} = 0.1°$ along the latitude. In order to preserve the same angular distance (0.1°) among tracers of the same row, I make a latitudinal correction on their longitudinal separation, so that $\delta_{LON} = \delta_{IG}/\cos(LAT(row))$, as explained in Subsec 3.3.1. I put in each row the same number of virtual drifters. Thus, the longitude range of the southern row (at latitude 51°S) is [70,75.4]°. For simplicity I will denote in the following this type of geographic region as a *rectangle* of coordinates longitude=[70, 75]° and latitude=[-51, -47]°.

I use the altimetry-derived velocities to advect these points forward in time for a period of $\tau = 60$ days, comparable with τ_D. I compute the CR values at all points separated

by the same distance δ_{IG} on the Kerguelen region, i.e. a *rectangle* of boundaries longitude=[68, 92]° and latitude=[-53, -42]°, which constitutes the *observational grid*. The resulting CR field is displayed in Fig. 3.6. I see a remarkably good agreement between features in the drifters trajectories and the ones in the CR field: areas of denser buoy passage correspond with higher values of the field, suggesting a good qualitative match between CR high values and areas of drifters passage. More quantitative results are

Drifters Intercepted

	CR Stations		
	Global product	Regional product	**Grid**
$\sigma = 0.1°$	30.5(25.5)	30.0(23.5)	12.0(11.0)
$\sigma = 0.2°$	53.0(34.0)	68.3(37.3)	28.0(22.0)
Total mean	**41.2(30.6)**	**51.0(31.8)**	**21.6(17.6)**

TABLE 3.1: Number of drifters intercepted (out of 43) using six CR stations (left columns) or six stations disposed on a 3×2 regular grid. The value is an average obtained changing the different parameters used (the advection time τ, the detection range σ and the resolution of the *initialization* and *observational grids* δ_{IG} and δ_{OG}, which were kept equal). For each cell, the two values correspond respectively to the total number of drifters intercepted by the stations and, in parenthesis, to the independent ones. First column: global product for altimetric velocities. Second column: regional product. Third column: stations on a regular grid.

obtained by considering a set of 6 best-ranked CR stations (the choice on the quantity of stations is arbitrary) with the method explained in the previous section. The number of real drifters intercepted by the CR stations is compared to the result obtained by a set of stations placed on a regular grid. This last set is constituted by 3×2 stations
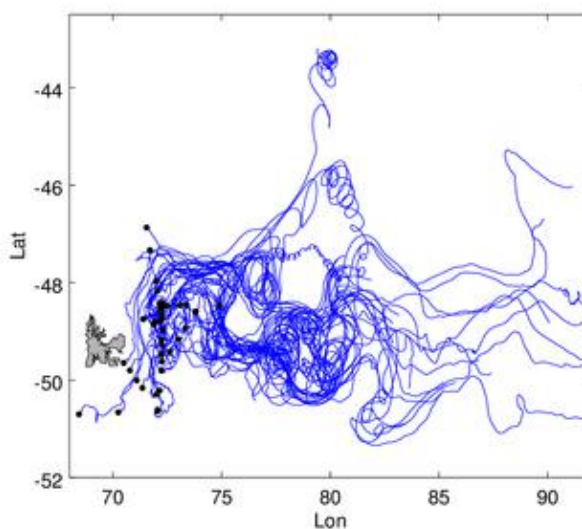
FIGURE 3.5: Trajectories of the 43 drifters of the KEOPS2 Campaign. Black dots represent the starting positions of the drifters.
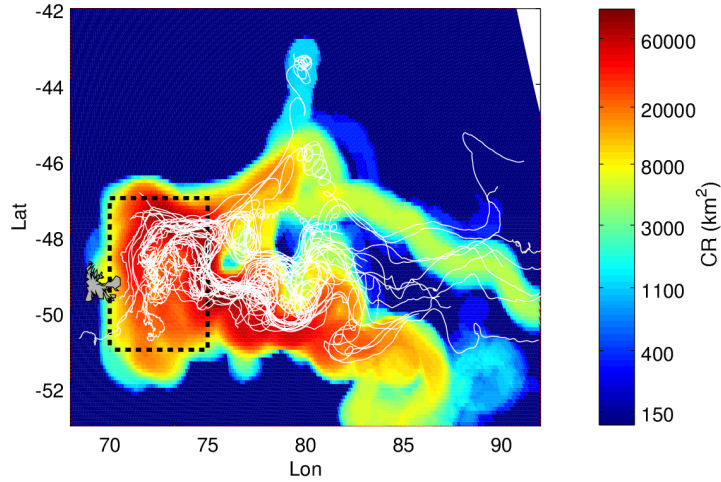
FIGURE 3.6: Crossroadness field derived from satellite altimetry ($\tau = 60$ days, $\delta_{IG} = \delta_{OG} = 0.1°$, $\sigma = 0.4°$), with superimposed trajectories of SVP drifters released during the 2011 KEOPS2 campaign. The CR field was computed advecting only the small *rectangle* (longitude: [70, 75]°; latitude: [-51, -47]°, black dotted line) in which the drifters have been released.
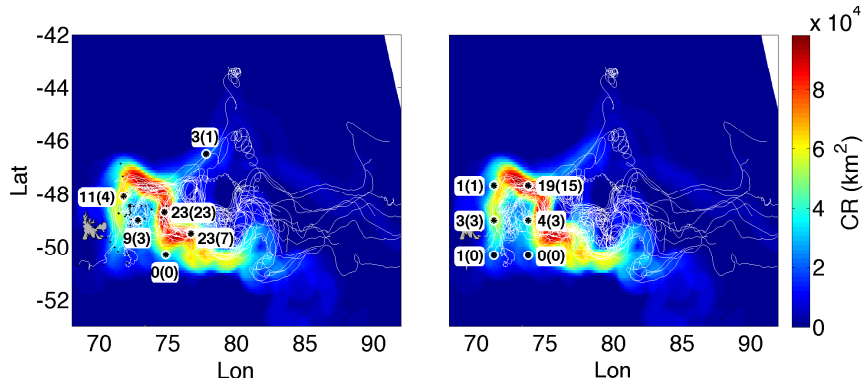
FIGURE 3.7: Left panel: first 6 CR stations (black stars) superimposed on the CR field computed advecting the same region as in Fig. 3.6, using the regional product for the velocity field ($\tau = 60$ days, $\delta_{IG} = \delta_{OG} = 0.1°$, $\sigma = 0.2°$). Right panel: same CR field, this time the black stars identify 6 stations disposed on a regular grid. For each station, the first number identifies the amount of total drifters intercepted, the value in brackets the number of independent drifters. Amount of drifters intercepted by the CR stations (total and in parenthesis the independent): 69 (38). Regular grid: 28 (22).

distributed over the area of the drifters motion, separated longitudinally by 2.5° and 1.23° latitudinally.

The measure is repeated several times and for different parameters, changing the advection time τ (at 30, 60 and 90 days), the detection range σ (at 0.1, 0.2 and 0.4°) and the resolution of the *initialization* and *observational grids* $\delta_{IG} = \delta_{OG}$ (at 0.1 and 0.2°). An illustrative example is reported in Fig. 3.7, where $\sigma = 0.4°$, $\delta_{IG} = \delta_{OG} = 0.1°$ and $\tau = 60$ days.

For each station, the total number of intercepted drifters is computed, as well as the number of drifters first detected by this station (independent ones). The results are reported in Table 3.1. The first two columns show the number of drifters (total and independent) intercepted with the CR stations, the third one the values obtained with a regular grid. The efficiency of the method introduced in this work is about twice the result obtained with a regular grid. A lower value of sigma corresponds not surprisingly to a lower number of catches for both the CR and the regularly spaced *observational grid*, but to an improved ratio in favor of the CR network.

3.4.3 Dependence of the surface monitored on the number of monitoring CR stations

I present here a statistical analysis in order to assess the efficacy of a CR based detection network with respect to a set of stations randomly chosen or arranged on a regular grid. The benchmark that I use is the CR, i.e. the ocean surface crossing the CR observing network as a function of the number of the monitoring stations.

Figure 3.8 displays a map of forward crossroadness computed around Kerguelen Island, advecting particles starting from November 1st, 2011, for a time of 60 days. Superimposed, white circles identify the first four CR stations. Black dots identify the monitored
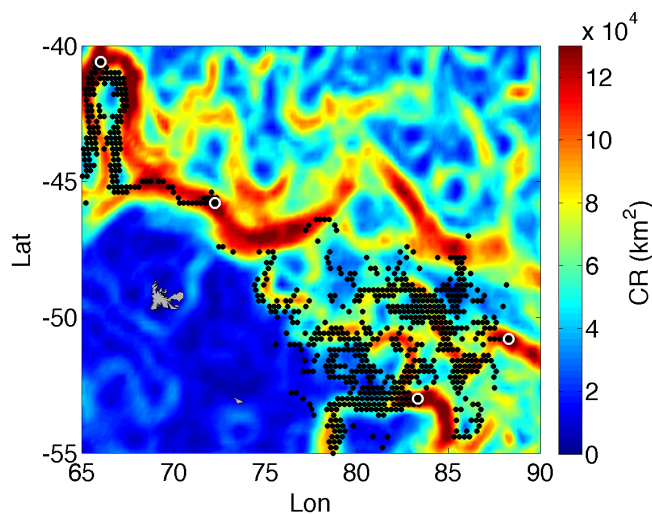
FIGURE 3.8: For this plot and the ones showed in Appendix A, the *initialisation grid* is the *rectangle* between longitude=[55, 100]°, latitude=[-36, -59]°, while the *observational grid* corresponds to the domain showed, if not specified differently. Crossroadness computed with an advection time $\tau = 60$ days, $\delta_{IG} = \delta_{OG} = \sigma = 0.2°$, with, superimposed, the first four CR stations (white circles) and the surface that they control (black dots on the corresponding *initialization grid* points). Note that some black dots can be outside the plot, since I advected a larger region than the observational domain showed in the panel, in order to take into account the particles upstream.
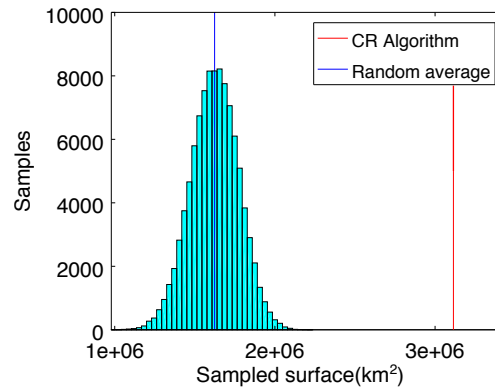
FIGURE 3.9: Histogram, computed from 100000 experiment repetitions, of the surface detected choosing each time $N = 20$ stations randomly displaced. The vertical red line on the right is instead the surface scanned choosing the stations with CR algorithm. Here $\sigma = 0.4°$. The distance between the mean value of the distribution (vertical blue line) and the vertical red line is 9.96 times the standard deviation of the distribution.
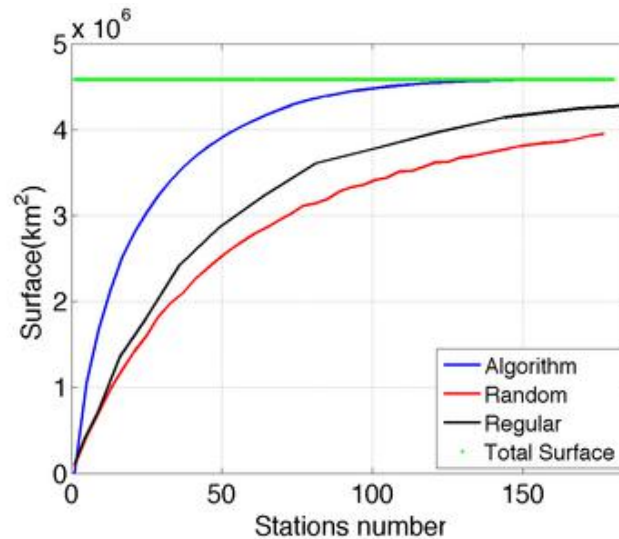
FIGURE 3.10: Surface sampled varying the number of stations considered ($\tau = 60$ days, $\delta_{IG} = \delta_{OG} = 0.1°$, $\sigma = 0.4°$), chosen randomly (red line), on a regular grid (black line) and with the CR method (blue line). Concerning the random choice and the regular grid, each value was obtained from the average of 1000 repeated measures. For the case of the regular grid, each time it was rigidly shifted along the longitude and the latitude of a random fraction of the distance between two grid points. The green line represents instead the total surface.

waters, namely the points that will pass in proximity of one of the four stations during the advection time τ.

First, I measure the surface monitored by 20 randomly selected stations with a detection range of $0.4°$ in a period of 60 days. The measure is repeated 100000 times and the results are reported in the histogram of Fig. 3.9. The vertical blue line is centered on the mean value of the distribution, while the red one is the value of the surface scanned with 20 stations chosen with my method. The distance between the two measures is about ten

times the value of the standard deviation of the distribution, an extremely significant ($p < 10^{-22}$) deviation with respect to the expected result of monitoring a larger surface with randomly selected stations.

The measure is repeated changing the number of stations selected, and the results are shown in Fig. 3.10. A sampling with a regular grid is performed as well. In this case, each measure is obtained by rigidly shifting the grid by a random fraction of the grid step along longitude and latitude. The use of the CR stations (blue dots) shows a better performance compared to the regular grid (black stars) and the random case (red circles) sampling. For instance, to scan a surface of $3 \times 10^6 \, km^2$ with a detection range of $R\sigma = 40km$, 25 stations selected with the CR method are needed, about 55 with a regular grid, and 75 randomly chosen.

3.4.4 Persistence of the monitoring network

The calculation of the crossroadness computed in the previous sections requires that at the moment of choosing the monitoring stations, the velocity that will disperse the tracer in the future is already known with good precision. As an example, in Subsec. 3.4.2 I calculated the CR stations used to intercept the SVP drifters using the velocity data of the days in which the buoys were advected by the currents. How much this impacts the CR stations ability to intercept the maximal surface of a stirred patch? Here I attempt to address this question by looking at the "persistence" of the CR stations i.e. the ability of a CR network, using velocity of the past, to intercept a tracer dispersed in the near future.

Surface monitored using past velocity field for the computation of the CR stations.

In general, I define

$$\mathcal{T}(\mathcal{R})_{D_0 \to D_f}$$

as the whole collection of trajectories $\mathcal{T}$ generated from the advection of all the points regularly initialized over a region $\mathcal{R}$, from the day D_0 until D_f. In general, from a set of trajectories $\mathcal{T}(\mathcal{R})_{D_0 \to D_0 + \tau}$, I can compute an ensemble of CR stations $\mathcal{S}(\mathcal{R})_{D_0 \to D_0 + \tau}$, as explained in Subsec. 3.3.3, that will be for construction the best choice in order to scan $\mathcal{T}$.

When the velocity field between the day D_0 and $D_0 + \tau$ is not known, I can use the stations computed with the velocity field in a time interval previous to D_0, e.g. $\mathcal{S}(\mathcal{R})_{D_0 - \tau \to D_0}$ to monitor the area, under the assumption that if the flow does not

change much in an interval of time of the order of τ the optimal stations will maintain approximately the same positions.
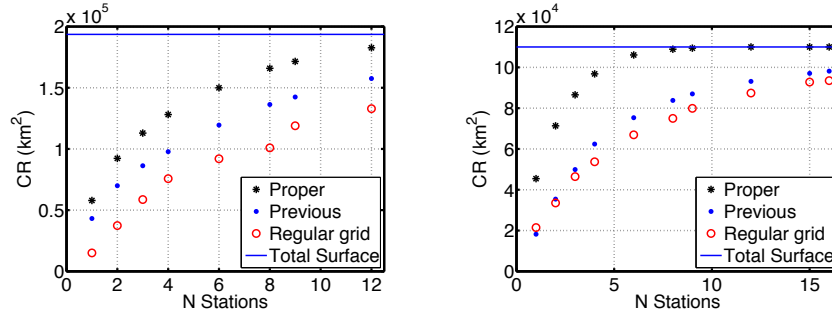
FIGURE 3.11: CR, i.e. surface monitored as a function of the number of stations. Each point is the average obtained changing D_0 over the first day of each month of 2011. Black stars represent the value obtained using the stations computed with the proper velocity field, i.e. $\mathcal{S}(\mathcal{R})_{D_0 \to D_0+\tau}$, while blue dots the ones computed with the previous τ days, (i.e. $\mathcal{S}(\mathcal{R})_{D_0-\tau \to D_0}$). Red circles are the values obtained with a regular disposition of the sampling sites. Left panel: $\mathcal{R} = \mathcal{R}_P$ (plateau region). Right panel: $\mathcal{R} = \mathcal{R}_T$ (turbulent area). $\delta_{IG} = \delta_{OG} = 0.2°$, $\tau = 60$ days, $\sigma = 0.2°$.

Thus, in this section I use the velocities between $D_0 - \tau$ and D_0 to compute a set of stations $\mathcal{S}(\mathcal{R})_{D_0-\tau \to D_0}$. I use then the latter to monitor $\mathcal{T}(\mathcal{R})_{D_0 \to D_0+\tau}$ and see how many trajectories (i.e. sea surface) they intercept.

I take as D_0 the 1st January, 2011 and $\tau = 60$ days. I change the number of stations considered between 1 and 16, analogously to what has been done in Subsec. 3.4.3. For comparative purposes, I also measure the surface intercepted with $\mathcal{S}(\mathcal{R})_{D_0 \to D_0+\tau}$, and then with a regular disposition of the stations. I then repeat the procedure using as D_0 the 1st February 2011, then the 1st March 2011 and so on, until the 1st of December 2011 and I consider the average of the 12 values obtained. In this way I obtain a more consistent statistics.

The results are reported in Fig. 3.11. I consider two different monitoring areas: the first one is the drifters release area, defined in Subsec. 3.4.2, situated mainly on the Kerguelen plateau and in which the bathymetry seems to affect the circulation pattern, making it more persistent in time. I will refer to it as $\mathcal{R}_P$. I then consider a more turbulent region situated offshore from Kerguelen, in which the current field should not be as constrained by the shallow shelf structures as in the former case, and in which the mesoscale structures affect deeply the variability of the currents [Park et al., 2014]. I take this turbulent region $\mathcal{R}_T$ to be the *rectangle* with longitude between 80 and 83°E, and latitude between 47 and 50°S.

Concerning the plateau region (left panel in Fig. 3.11), I see a stronger performance of the CR stations compared to the regular grid, even if they are computed with the trajectories of two months before. E.g., in order to monitor a surface of $100000\,km^2$, I

need 8 stations disposed regularly, while only 4 if I consider the stations obtained from the advection of the previous 60 days, and 3 if I consider the advection from time D_0 (i.e. the velocity field simultaneous to the surface advection).

The results are worse but surprisingly consistent for the turbulent region scenario (right panel in Fig. 3.11), with about 25% less CR stations needed than in the regular case. The analysis in this section is completed in Appendix A, in which the detection power of the CR stations is assessed against further changes in the dates used for the velocity field.

3.4.5 Identification of a source region

In the previous section I used CR for intercepting a tracer stirred from a given region. Here instead I study another typical problem arising when studying dispersion, namely the identification of the most important source regions connected by the circulation to a given target area.

This occurs, for instance, when I aim to determine the key regions that can affect vulnerable marine protected areas downstream, or in the identification of nutrient sources feeding a biogeochemical active region [Ciappa and Costabile, 2014, Suneel et al., 2016].

In order to showcase this application, I considered the area studied in the previous section, i.e. the Kerguelen plateau, that recent studies have stressed as a natural source of iron supply that sustains the primary production in the zone situated to the east of the island [d'Ovidio et al., 2015, Blain et al., 2008b, Christaki et al., 2008].

Large areas of the Earth oceans present waters with high quantities of nutrients, but low concentration of chlorophyll (HNLC). This is generally due to the absence of some micronutrients that act as limiting factors. In many cases one of the main constrains to the presence of chlorophyll is the low concentration of bioavailable iron. In this regime, injection of this micronutrient fuels the primary production [Boyd et al., 2007, Lam and Bishop, 2008, Martin et al., 2013]. In recent years, different studies have underlined the importance of continental margins as a subsurface source of iron that can thus fed the phytoplanktonic bloom in the waters downstream [Lam and Bishop, 2008]. Among them, the Kerguelen plateau is one of the clearest region to show this biogeochemical dynamics and its importance for primary production is now well established. Nevertheless, the hotspots of the continental shelf that may act as main iron sources are still unknown. Here I use the crossroadness computed backward in order to address this question.

Since I want to determine the possible iron sources on the Kerguelen plateau, delimited by the bathymetric line of 1000m, I examine only the region situated eastward to this
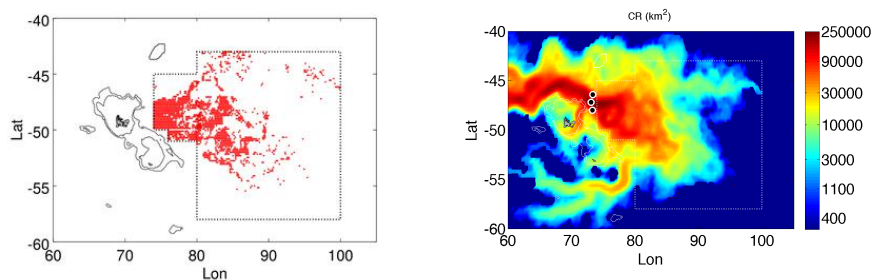
FIGURE 3.12: Left panel: Kerguelen plateau with the bloom area delimited by black dotted lines. Bathymetric lines at 500 and 1000 meters. The set of initializing points (shown in red) are selected by choosing the pixels that supported at least one value of chlorophyll greater than $1\,mg/m^3$ between November and December 2011 and are showed in red. Each initialization point is assumed to carry an amount of water given by a surface $\Delta = R^2\delta_{IG}^2$ (when R is the Earth radius and δ is in radians) for $\delta_{IG} = 0.15°$. Right panel: CR computed backward (in log scale), with advection time $\tau = 180$ days, from the red points showed on the left panel, that cover a total area of about $517000\,\mathrm{km}^2$. Black dots represent the first three source stations computed with the CR algorithm described above. Detection range $\sigma = 0.4°$

contour. This is approximated by considering only a region delimited by the perimeter reported in Fig. 3.12 (left panel, black dotted line). Furthermore, in order to consider only the waters that support a springtime bloom, I analyze satellite-derived images of the chlorophyll patch of spring 2011. I therefore consider as starting points only the pixels that, belonging to the area enclosed by the perimeter, present at least one value of chlorophyll concentration larger than $1\,mg/m^3$ during the peak of the bloom of November and December 2011. Note that, in this way, I do not have an *initialization grid*, but a set of initialization points. The selection is reported on the left panel of Fig. 3.12 (red points). These points are advected backward for a period of time $\tau = 180$ days, and the crossroadness field is reported in Fig. 3.12 (right panel). This map highlights a strong passage of water coming from the northern part of the plateau, underlining the central role of the Antarctic Circumpolar Current (ACC) in the advection of waters in proximity of the island platform, and shows also the Southern ACC Front (SACCF) that passes into the Fawn trough. I then use the ranking algorithm in order to locate the most important passage points which feed water to the blooming region. The first three CR stations are all in proximity of the northern part of the plateau, meaning that in the 180 days before the bloom, the largest part (about 70 %) of the water that will sustain primary production, passed through these three points. This analysis locates the Gallieni Spur as a strong candidate where to search for iron sources of the Kerguelen bloom. I note that in general the CR algorithm does not really determine *source* regions, but rather regions of dense trajectory passage. But since half lifetime of iron in these waters is of the order of about two-three weeks [d'Ovidio et al., 2015], for the value of τ used the CR method in this case should also locate source regions.

3.5   Discussion and perspectives

Studying dispersion problems, in particular at scales of $\sim 10 - 100$ kms, [Boyd et al., 2007, Olascoaga et al., 2013, Mahadevan, 2016], is a central issue in many oceanographic problems [Bellingham and Willcox, 1996, Mooers et al., 2005, Bradbury et al., 2008, Rossi et al., 2014, Dubois et al., 2016], whose aim is to achieve good characterization, managing and protective strategies of marine areas and resources. I stress their importance, in particular, for Marine Spatial Planning (MSP). The goal of MSP is indeed to identify the peculiarities, from an ecological or societal point of view [Crowder and Norse, 2008], of the different marine regions, and to map their spatial and temporal distributions in order to manage them in a sustainable way [Ansong et al., 2017, Ehler, 2018]. MSP has become, in the last 20 years, a fundamental process in sea management [Douvere, 2008, Muñoz et al., 2015] and is expected to play an increasing important role in the future (e.g., [Qiu and Jones, 2013, Magris et al., 2014]. An essential component of MSP is the necessity for an effective modeling and monitoring strategy [Ehler, 2017, Ehler, 2018], a question intimately related to the dispersion of tracers.

In this context, it is possible to identify two main questions.
From one side, there is the case of a passive tracer, advected by the currents. The chaotic and turbulent dynamics characterizing the ocean circulation can disperse the patch and make it spread over a large area (say, of size larger than 100 km) within a short time (days to weeks). In this case, a recurrent problem is to locate the sites where to deploy observing stations, capable of monitoring or collecting the dispersed tracer [Addison et al., 2018].
A second class of problems concerns the case of a sensible region that is influenced by the circulation upstream [Viikmäe et al., 2011, Delpeche-Ellmann and Soomere, 2013a, Delpeche-Ellmann and Soomere, 2013b, Soomere et al., 2015]. In this case, the identification of the "sources" that may affect and spread all over the target area is important for vulnerability assessment [Halpern et al., 2007].
Current methods, mainly based on Lagrangian advection of particles [d'Ovidio et al., 2004, Mancho et al., 2006], concern mostly the identification of coherent regions with minimal transfer of water toward the environs [Haller, 2001, Mancho et al., 2004, Shadden et al., 2005, Beron-Vera et al., 2008]. Nevertheless, the knowledge of the spots with enhanced exchanges amongst a flow system is a central issue in dispersion problems [Ser-Giacomi et al., 2015b, Monroy et al., 2017]. The latter question has been recently addressed in the study of Lagrangian Flow Networks [Ser-Giacomi et al., 2015a, Lindner and Donner, 2017, Rodríguez-Méndez et al., 2017, Fujiwara et al., 2017], in particular with the concept of Most-Probable-Path–betweenness [Ser-Giacomi et al., 2015b]. This

diagnostic identifies the choke points in the topology of a flow system. These, nonetheless, are not necessarily spots of major water passage.

Furthermore, to my knowledge, current notions do not solve the problem of displaying and sorting a series of stations in order to answer the two questions mentioned above.

To address these issues, I introduced here a new diagnostic, the crossroadness, which measures the water surface flowing in the neighborhood of a point in a given time window. This has permitted us to develop a ranking method that estimates the places where the majority of the flux passes, and that at the same time sees waters coming from different locations.

This allowed us to design an optimal monitoring system, because each station identified in this way intercepts independent patches of water. I stress that this independence is important for retrieval strategies, for example in the recovering of a contaminant. In fact, in that case the series of the recuperation stations has to be set so that each of them recaptures a different portion of the pollutant that is dispersed. Thus, there is no interest that a station monitors again some waters that have already been intercepted upstream by another one. The same logic is valid in sampling strategies, in which the analysis of the largest surface possible is preferred, and in which sampling twice the same portion of water may be a waste of resources.

Reversing the analysis backward in time it is possible instead to quantify, for each point of the domain, the amount of surface that, passing nearby, will feed a target region. In this case the ranking method identifies the major "source"points from which the water distributes over a vast surface, with each source "irrigating"different areas. The independence of the destinations allows us to maximize the surface covered with a minimal identification of source stations. This is an important factor for the assessment of vulnerable points whose contamination can lead serious damages: for instance, for the protection of Marine Protected Areas [Rengstorf et al., 2013, Ciappa and Costabile, 2014] or hotspots of biological importance [Hobday and Pecl, 2014], like a region with a recurrent bloom that sustains the local trophic chain [Lehahn et al., 2007, Mongin et al., 2008, d'Ovidio et al., 2015]. In those cases, it is central to determine the main sites upstream feeding the whole areas.

I first explored the properties of the crossroadness using a steady velocity field obtained from the Navier-Stokes equation [Boffetta et al., 2002, Hairer and Mattingly, 2006], characterized by eddies surrounded by hyperbolic points and manifolds. I showed that the crossroadness is strongly linked to the choice of the *initialization grid* region. Furthermore, the disposition of the CR stations is not obvious, since they do not necessarily fall on Lagrangian Coherent Structures identified by ridges of Lyapunov exponents, neither their disposition is symmetric, even if the flow stream analyzed is stationary. Interestingly, I found that the stations necessary to monitor all the box cover just the 3% of its surface.

I then applied the previous concepts to the Kerguelen region by considering satellite derived velocity fields. I validated the forward-in-time case by analyzing the trajectories of 43 SVP drifters from KEOPS2 campaign. I showed that 6 stations computed with the crossroadness would have been able to intercept on average about the double of the drifters captured with a regular grid, using the same number of detecting sites. Interestingly, the ratio seemed to improve when diminishing the detection range. I then studied the persistence of an optimal crossroadness network, by looking at how its intercepting capacity degrades when the network is computed from a velocity field previous to the one that disperses the tracer. Even in this case, the crossroadness stations show better performances than regular grids. This is valid also when considering a region with stronger turbulence. These facts demonstrate how stations computed from past velocity fields can be applied to future circulation patterns, validate furthermore the algorithm proposed and show its robustness when applied to an oceanic environment. It is in fact presumable that, for growing levels of turbulence, the performances of the CR stations, those of a regular grid or a random disposition of the stations would tend to coincide, due to the chaotic activity. However, even when considering a zone with a very strong turbulence (the Kerguelen region), the algorithm showed better performances than a regular grid, meaning that the levels of turbulence activity in ocean do not affect the capacity of the algorithm. The effectiveness of the algorithm does not rely either on a strong detecting power of the stations employed, but on the contrary it improves when diminishing it. The only limitation is the fulfillment of the condition stated in Subsec 3.3.1, i.e. $\sigma \geq \delta_{IG}$, which could lead potentially to a decrease in the algorithm performance if the detection range considered is smaller than the resolution of the velocity field.

I use the backward-in-time method to analyse the Kerguelen spring primary production during November-December 2011, showing that about the 70% of the waters that supported the bloom had passed in the vicinity of just 3 sites on the Kerguelen plateau during the previous 6 months, in proximity of the Gallieni Spur.

In the analyses of the present Chapter I focused on the properties of the crossroadness considering two-dimensional dynamics. 2D turbulence is in fact present in nature over a large range of scales in which the ratio of lateral and vertical length is very large [Kraichnan and Montgomery, 1980, Tabeling, 2002, Boffetta and Ecke, 2012]. When applying these concepts to the oceanic cases, I considered periods of advection sufficiently small in order to neglect vertical velocities. Furthermore, several relevant tracers (in a first approximation) such as plastic, oil and chlorophyl are present almost only in the upper ocean layers, and for their study the 2D approximation can be considered very robust. I note also that all the analyses provided here can be integrated in a three-dimensional environment, delineating interesting perspectives for future studies.

I note that in a recent paper, [Rypina and Pratt, 2017] introduced a "mixing potential" approach which exploits ideas similar to the crossroadness. The main difference is that the *mixing potential* is a Lagrangian quantity attached to each fluid parcel, whereas the crossroadness uses Lagrangian trajectories but is assigned to each fixed location in space. Thus, whereas the diagnostic in [Rypina and Pratt, 2017] may be more appropriate to assess mixing, my approach aims to deploy observation networks and identify sources of transported substances.

There are then several other cases looking interesting for future applications of the crossroadness and its ranking method, and I list here some. For the dispersion of pollutants, the forward in time crossroadness allows us to estimate the most important points in which position a fix station in order to retrieve the contaminant. The aforementioned method can also be used for sampling strategies in order to maximize the surface intercepted and the probability of encountering elements of interest and thus to improve the cost-effectiveness quality [Elliott and Jonge, 1996, Elliott, 2011]. In search and rescue operations, if the exact missing point is lacking, and the information available is just on the area of disappearance, computing the forward CR could establish optimal observing stations to look for the lost target. Regarding the backward calculation, this can be used for prioritizing survey locations upstream to vulnerable regions (like Marine Protected Areas), or identifying most likely hotspots close to the shore from which fish larvae may span to a large recruiting area. My diagnostic provides a direct and simple way to sort a series of stations in order to survey with good performances even very turbulent regions, taking furthermore explicitly into account the detection range.

Acknowledgements
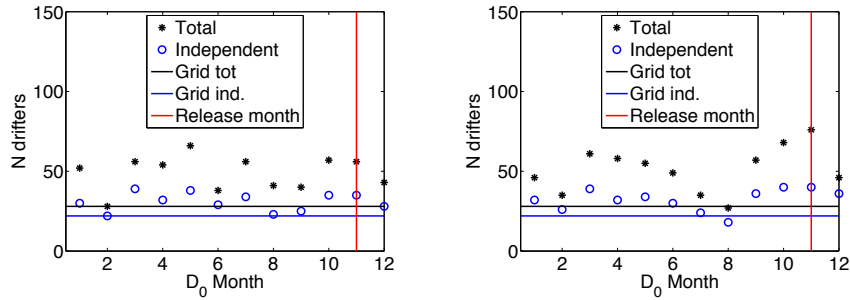
FIGURE 3.13: Number of drifters intercepted using the different months along the year. $\delta_{IG} = \delta_{OG} = \sigma = 0.2°$. Left panel: $\tau = 30\,days$. Right panel: $\tau = 60\,days$ Horizontal lines: values obtained with a regular grid, total (black) and independent (blue line). Note that the release period of the drifters is November 2011.

Appendix A. Temporal persistence of the CR stations along the year

In this Appendix I extend the analysis of Subsec. 3.4.4 on the possibility of using known velocity fields from the past to obtain sets of CR stations able to monitor transport by future velocity fields.

Drifters intercepted with stations computed along the year.

The SVP drifters release region $\mathcal{R}_P$ is advected taking as starting day D_0 January, 11th, 2011, for a period τ of 30 and 60 days, from which 6 CR stations were calculated. They are then used to see how many real drifters from the dataset released on November 2011 they would have intercepted. The computation is repeated changing D_0, using each time a different month until December, 2011. The results, reported in Fig. 3.13, show a better performance of the CR stations compared to the regular grid, along all the year, with a number of drifters intercepted always higher except for one case (August 2011, $\tau = 60$ days). The case of 60 days advection presents a linear decrease of drifters intercepted for calculations using the three months previous to November, and then a regular increase again, showing a sort of annual cycle, while the 30 days results shows a more irregular trend.

Surface monitored with stations computed along the year.

As in the former case, the region $\mathcal{R}_P$ is advected starting from D_0 January, 11th, 2011, for a period τ of 30 and 60 days, and 6 CR stations were computed. This time the stations are not used to see how many SVP drifters they would have collected, but how many trajectories of the set $\mathcal{T}(\mathcal{R})_{D_R \to D_R + \tau}$, with $D_R =$ November, 11th, 2011, they would have intercepted. D_0 is varied taking each time the 11th day of a different month of 2011.
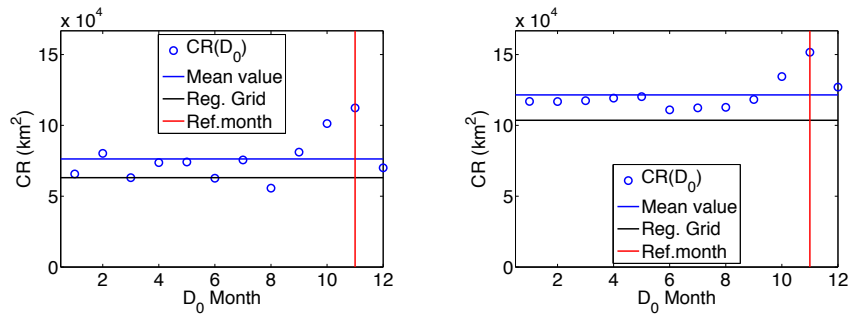
FIGURE 3.14: Surface of $\mathcal{R}_P$, advected from D_R = November, 11th, 2011, monitored using the stations computed with velocity currents of different months along the year. $\delta_{IG} = \delta_{OG} = 0.1°$, $\tau = 60\,days$. Left panel: $\sigma = 0.1°$. Right panel: $\sigma = 0.2°$ Horizontal lines: surface of November monitored using a regular grid (black line) or 6 CR stations (blue line, mean value of the blue circles)

The results are reported in Fig. 3.14 and display in both cases a temporal decrease of the surface sampled with the CR stations for the first three months. Generally, the surface monitored with this method is about 15% greater than with a regular grid.

Appendix B. Relation with absolute velocity and mean kinetic energy

A validation of Eqs. (3.1) and (3.2) is reported in Fig. 3.15, where a map of crossroadness, of kinetic energy and of absolute velocity field, averaged for the month of November, is shown. There, the patterns look pretty identical. This is confirmed by the scatter plot of Fig. 3.16, in which the expressions (3.1) and (3.2) are represented by the red line. The correlation coefficients of the two plots are very similar, confirming the validation of the assumptions leading to these equations.

Nevertheless, the kinetic energy or speed presents two main differences with the crossroadness, that make them less suitable for monitoring purposes in dispersion problems. In fact, even if these quantities are very similar to CR when the advected area is larger than the domain of calculation, this ceases to be true for smaller advected domains. This is seen in Fig. 3.15, lower right panel. There, the crossroadness is computed with the same parameters as in the left upper panel ($\tau = 30$ days, $\delta_{IG} = \delta_{OG} = \sigma = 0.1°$) and on the same *observational grid*, but the *initialization grid* is the one used Subsec. 3.4.2, i.e. much smaller than the observational one. it is possible to notice that the two patterns differ radically, confirming the importance of the fulfillment of the hypothesis leading to Eqs. (3.1) and (3.2). Furthermore, simple maps of kinetic energy or speed do not allow to track the origin of the particles that passed through each point, and thus to establish a hierarchy of importance for observing stations.
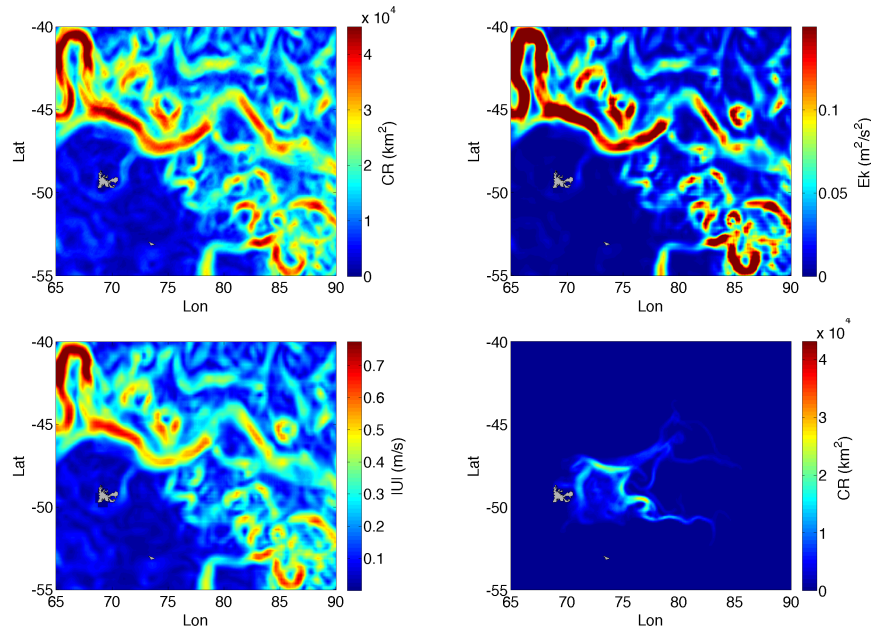
FIGURE 3.15: Top left panel: crossroadness relative to November 2011 computed with an advection time $\tau = 30$ days, $\delta_{IG} = \delta_{OG} = \sigma = 0.1°$. Top right panel: mean kinetic energy $< E_K >$ of November 2011. Lower left panel: mean absolute velocity field $< |v| >$ of November 2011. Lower right panel: CR field computed over the same *observational grid* as in the left upper panel, with same parameters, but the *initialization grid* is only the drifter release region (*rectangle* of longitude: $[70, 75]°$ and latitude: $[-51, -47]°$) as in Subsec. 3.4.2
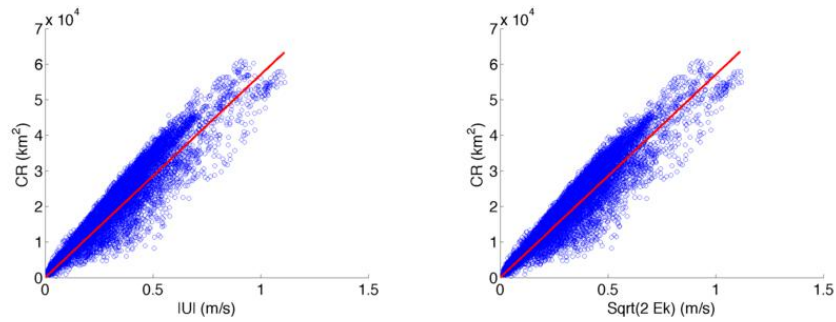
FIGURE 3.16: Scatterplot of values of CR vs $< |v| >$ (left panel, correlation coefficient: 0.969) and CR vs $\sqrt{2 < E_K >}$ (right panel, correlation coefficient: 0.967) of Fig. 3.15

Chapter 4

Discussion and perspectives

4.1 Discussion

When studying the marine environment, a central aspect which must be faced is its chaotic nature. This makes it evolve and change over the same timescales of the marine organisms which live there, contrary to what happens on land. Indeed, during their life time marine organisms see the environment that surrounds them changing over relatively short timescales, and have to develop peculiar characteristics and behaviors adapted to such a fluid habitat. This is why, when studying biological processes in the ocean, it is essential to couple them together with the physical dynamics. This can have several implications, from the fight against climate change [Orr et al., 2005, Halpern et al., 2008, Domingues et al., 2008, Iudicone et al., 2016], the conservation of marine populations [Viikmäe et al., 2011, Delpeche-Ellmann and Soomere, 2013a, Ehler, 2018], marine spatial planning [Viikmäe et al., 2011, Delpeche-Ellmann and Soomere, 2013a, Ehler, 2018] and design of marine protected areas [Cowen et al., 2006, Siegel et al., 2008, Shanks, 2009, Rossi et al., 2014, Dubois et al., 2016, Bray et al., 2017], to the comprehension of the role of ocean on global climate.

The influence of fine scale processes on the trophic chain

One of the oceanic regimes whose temporal scales overlap substantially with the ecological ones goes by the name of "fine scale" features. This regime is characterized by eddies and filaments with sizes from few to hundreds of kilometers, and typical timescales between a few days and a few weeks. These are for instance the duration of phytoplankton blooms, whose images from satellite provide a remarkable signature of the fine scale physics. An additional difficulty in the analysis of the biophysical processes is due to the fact that, contrary to terrestrial environment, in the ocean it is difficult to establish

an absolute frame of reference. This happens because because water parcels are continuously transported and rearranged by the chaotic dynamic present. In this regard, the Lagrangian approach has been proved to provide a natural framework for the analysis of these questions, because it follows particles along their trajectories and does not focus on fixed points like in the Eulerian system of reference, providing information on parcels history and diagnostics describing the properties of the flow transport. Lagrangian methods have allowed to successfully describe some of the influence of fine scale structures on lower and upper ends of the trophic chain, i.e. on plankton and top predators. Indeed, several studies assessed how lower trophic levels (such as phytoplankton and krill) distribution, abundance, community composition and biodiversity are deeply influenced and regulated by transport mechanisms identified with Lagrangian tools [Lehahn et al., 2017, Mahadevan and Campbell, 2002, Martin, 2003, Fach and Klinck, 2006, d'Ovidio et al., 2010], while in the last years there is an emerging indication of the role of fine scale features also into modulating apex predator behavior and displacement [Polovina et al., 2006, Kai et al., 2009, Bailleul et al., 2010, De Monte et al., 2012, Della Penna et al., 2015, Chambault et al., 2017].

A lack of knowledge on intermediate trophic levels

However, the relationship of these processes with the ecology of intermediate trophic levels, which are fundamental in marine ecosystem functioning [Hidaka et al., 2001a, Frederiksen et al., 2005, Tittensor et al., 2010, Webb et al., 2010, Smith et al., 2011, Hudson et al., 2014], is largely not known [Robison, 2009]. This is mainly due to the sampling difficulties of mid trophic levels at large scales. These can not be monitored through satellite observations as chlorophyll, neither tagged with biologgers as large predators. Information on them is available mainly through ship-based measurements. These however can present several biases [Pakhomov and Yamamura, 2010a, Brodeur and Yamamura, 2005] and the necessity of a "spatial vs temporal" interpretation. Therefore, efficient strategies are required for their monitoring and the acquisition of large data sets. Furthermore, while mid trophic levels and, more generally, ocean resources, are not distributed homogeneously through the marine landscape, the contribution of fine scale processes to this heterogeneity, through eventual aggregating mechanisms, is not clear, neither, it has been explored previously, to my knowledge. Technologies recently applied to marine ecology studies, like acoustic sonar measurements, along with refined satellite observations of the physical phenomena, integrated with novel methodologies such as Network Theory applied to flow networks and complex systems tools, provide however interesting perspectives in order to address these questions in a Lagrangian framework.

In this thesis, I choose to work on the Kerguelen region, in the Indian sector of the Southern Ocean. The importance of the area is recognized both from an ecological and physical point of view. The Kerguelen archipelago hosts several species of apex predators. Most of them are declared as vulnerable or near threatened by IUCN (the International Union for Conservation of Nature). The Marine Protected Area has also been recently extended also to the Economic Exclusive Zone. It now constitutes the second halieutic reserve in the world (http://www.taaf.fr). Furthermore, despite its remoteness, this area has received significant scientific attention.

Kerguelen region represents therefore the perfect "natural laboratory" in order to address the aforementioned multidisciplinary questions.

Observed fish concentration on frontal systems

In Chapter 2, therefore, I analyse acoustic transects acquired in 2013 and 2014 in the Antarctic Southern Ocean, revealing the fish concentration in the water column (acoustic fish concentration, AFC). There is a significative difference of the AFC values in correspondence of a front, identified by values of the Eulerian and Lagrangian diagnostics over a prefixed threshold. In particular, high AFC values are observed in correspondence of high finite-size Lyapunov exponents, betweenness and sea surface temperature gradient values, while the trend is opposite for the Kinetic Energy.

Aggregating mechanism of frontal systems

In the second part of the Chapter, I explore a possible mechanism of fish aggregation along fronts, by analysing the two main difficulties faced when searching for an optimal hotspot in the ocean: the capability to orientate and correctly identify the position of patches of interest, and the ability to reach one of those patches before they fade out because of the mixing. By using realistic parameters estimating fish behavior and its environment characteristic, on one side, I study the fish capacity to orientate by climbing a noisy gradient, showing that this behavior leads to the formation of two peaks of increased concentration in a relatively short period (∼6 hours). The peaks then smooth over the area with high tracer concentration. Therefore, not all fish converge toward the highest value of tracer, but they redistribute homogeneously in the frontal region. This strategy makes sense from a biological point of view because it implies a better repartition of the tracer/resource between the individuals. On the other hand, I analyse a time evolving tracer, which represents an *optimal patch* for the fish. This patch, subjected to stirring and diffusion, is eroded and eventually fades out. I analyse if the fish are able to follow the reducing *optimal patch* and thus aggregate. I find that fish are able to stay inside the *optimal patch* for about 2 weeks, a timescale characterising many fine scale processes. After that time window, their concentration has risen up to 40 times

the starting value, and the fish patch is mainly disposed along the front, in a way that is compatible with the results of [Della Penna et al., 2015]. Indeed, the authors observe an increasing foraging effort of an elephant seal along a long thin structure at the eddy periphery, which is also a region characterised by the hyperbolic dynamic analysed here.

Fronts as necessary but not sufficient conditions for high fish biomass

The hypothesis at the basis of the two aforementioned mechanisms of fish aggregation is the initial presence of a hotspot of interest for the fish. This could be a nutrient gradient, a temperature or a salinity patch, and, of course, the presence of the fish themselves, which are initially distributed over a vast surface. If these two conditions are verified, I show that horizontal fine scale processes can increase fish concentration by modulating the gradient of the patch of interest and by reducing the optimal area available, thus promoting fish aggregation. The front presence is thus a condition for increased fish concentrations: nonetheless, in absence of one of the two starting conditions, a frontal system would not be able obviously to aggregate the fish. It is therefore possible to identify the front as a necessary but not sufficient condition for having consistent fish aggregations. Interestingly, this is what emerges from the quantile regression analysis of the AFCs with the explanatory variables. This analysis gives significant pseudo R^2 correlations, showing that the AFC peak intensities are limited by the corresponding diagnostic value.

Sampling of mid trophic levels

The previous results shed a novel light on the interactions between fine scale structures and intermediate trophic levels. The analyses illustrated in Chapter 2 are however focused only on the Kerguelen region. One of the main reason for this choice is that Kerguelen region is a deeply studied area, where several at-sea campaigns and scientific programs are conducted, as exposed in Sec. 1.7, and in which the ecological dynamics are relatively well known. However, it would be interesting to extend the previous analysis to other oceanic regions, with different biological and physical characteristics. This is not obvious, especially because data availability on mid-trophic levels is limited to ship-based campaigns. The latter present biases and, through their use, it is difficult to obtain information over large scales. It is therefore necessary to increase data collection on mid trophic organisms by implementing optimal sampling strategies.

Design of an efficient monitoring network: the crossroadness

In Chapter 3 I analyse the problem of efficiently intercepting the flux of a tracer coming from, or going to, a certain region. This problem is linked not only to an efficient

monitoring strategy of intermediate trophic levels, but has also applications in larval connectivity studies [Carreras et al., 2017, Andrello et al., 2013, Monroy et al., 2017], retrieval of contaminants [Rengstorf et al., 2013, Ciappa and Costabile, 2014], design of marine protected areas [Rossi et al., 2014, Dubois et al., 2016, Bray et al., 2017] and, in general, to all those thematics linked with Marine Spatial Planning [Viikmäe et al., 2011, Delpeche-Ellmann and Soomere, 2013a, Ehler, 2018]. Drawing inspiration from Lagrangian Flow Networks [Ser-Giacomi et al., 2015a, Costa et al., 2017, Lindner and Donner, 2017], I design a novel Lagrangian diagnostic, which I call *crossroadness* (CR). CR forward (backward) in time measures the quantity of flow which comes from (goes to) a predetermined target region in a given time window. Crossroadness is expressed in units of a surface. Furthermore, the CR keeps the information on the origin (destination) of the parcels advected. This allows one, if the CR is computed forward in time, to build a network of fixed stations which optimally intercepts the water coming from the target region. Backward in time, this network identifies instead the neuralgic points of the system, i.e. in which the water flows and spreads all over the domain. The method takes into account explicitly the extension of the neighborhood which a station is able to monitor, i.e. the detection range.

I analyse the CR properties and the efficiency of the proposed algorithm with a theoretical model, characterised by a series of eddies rotating alternatively clockwise and anti-clockwise, and separated by manifolds crossing into hyperbolic points. I find that, in order to monitor the whole surface, a series of stations disposed with the proposed algorithm covers only the 3% of the whole domain. Furthermore I show that the disposition of the stations is not obvious, i.e. not systematically falling on regions of high CR values, neither exactly in correspondence of manifolds identified with maps of Finite Time Lyapunov Exponents. I validate then the algorithm considering a real case study, such as the KEOPS2 experiments, in which 43 real SVP drifters were released on the Kerguelen plateau in 2011, and which can represent the trajectories of water masses hypothetically rich in myctophids larvae spawned close to the archipelago shore. I use therefore 6 stations computed with the CR algorithm, applied to satellite derived velocities, in order to see how many drifters they would have intercepted, and I obtain that this value is about the double of the amount of drifters observed with a regular grid. It is intuitive to imagine that the performance of the CR stations compared to a regular grid could coincide in a very turbulent dynamical regime. However, this is not the case for the turbulent activity typical of the ocean, even in extreme cases like the chaotic region eastward of the Kerguelen plateau. Indeed, there, I test the persistence of the CR network in time, looking at the amount of surface intercepted if I use CR stations computed using the velocity field in the past. Also in that case, better performances are obtained with the CR algorithm than with a regular grid. This confirms the robustness of the CR algorithm in time, even for high levels of chaoticity. Finally, CR backward in

time is applied to the study of the Kerguelen spring bloom, identifying the main passage points in which water parcels transited before supporting high chlorophyll values. In this case, CR stations may identify local sources of iron enrichment along the Kerguelen plateau.

It is important to stress that the good performance of the CR algorithm resides in the independence of the water parcels intercepted by each CR station. The justification for this choice is driven by the fact that, if the parcel must be sampled or a contaminant in it retrieved, once the water has been monitored, it is not necessary that it must be sampled again by another station. Another important novelty of the CR method is that the detection range of each station is explicitly taken into account. More interestingly, I show that, for small detection ranges, only $\sim$3% of the surface must be covered with stations in order to survey all the domain. This can have a positive feedback on the performance of monitoring systems.

4.2   Limitations of the works presented...

I argue here about some of the limitations of the studies presented, as discussed also in Sec. 2.4 and 3.5 of Chapter 2 and 3.

The mechanisms of aggregation illustrated in Chapter 2 do not intend to provide a complete view of the aggregating dynamics present into the ocean, but aim at opening a new perspective on the role of horizontal currents and fine scale structures by analysing two simplistic case and evidencing a possible reason for the observed increased concentrations. Indeed, many aspects have not been included during this work. First, I decided to focus only on the horizontal dimension, noting that fish possess strong capabilities of vertical displacement, along with zooplankton. Therefore, while along the horizontal dimension currents have intensities in the order of the cruising swimming speed of the fish, on the vertical dimension these are generally several orders of magnitude smaller. Furthermore their effect for the temporal scale considered in the study (two weeks) can often be neglected. However the role of vertical dynamics could be important on the evolution of the *optimal patch*, for instance through the induction of submesoscale instabilities which provoke nutrient upwelling [Capet et al., 2008a, Lévy et al., 2012, McGillicuddy Jr, 2016] and thus possible sources of tracer. The reason of this choice is due to the fact that vertical velocities are still very difficult to estimate and parameterise.

Secondly, eventual presences of source or sink terms have not been taken into account. This can be the case, for instance, if they balance each other or are small. However, while source terms can be induced by vertical upwelling, sink terms can be provoked by the consumption of tracer by the fish through grazing, and can important in the total

balance.

Concerning the study of Chapter 3, there again I focused only on 2D dynamics, assuming that during the time windows considered for the study of the crossroadness (from 30 to 90 days), vertical motions could be neglected. In Lagrangian literature, this choice is often justified by the fact that, in certain cases, vertical motions are orders of magnitude smaller than horizontal velocities [d'Ovidio et al., 2004, Rossi et al., 2014]. Admittedly, however, the neglecting of vertical velocities responds also to the theoretical and observation difficulty of including such components when analysing stirring scales [Sulman et al., 2013]. Even if, from an heuristic point of view, this approximation often seems to work, there are certainly cases in which vertical velocities contribute importantly to the transport dynamic. This is the case, for instance, of subsurface motions. However, it is important to note that many taxis object of interest, such as plastic debris, oil and chlorophyll, are present almost only close to the surface.

Robustness of the crossroadness and of the selecting method of the stations has been tested, showing that the proposed algorithm provides efficient performances even for very intense ocean turbulence, which makes the crossroadness suitable for oceanographic applications. The only condition which must be respected is that the step grid of the target region advected must be smaller or equal to the detection range of the stations.

4.3 ...and some ways forward

In Chapter 2, I analyse two aggregating mechanisms separately. In the first one, fish climb a gradient which does not change in time. Even if one assumes that temporal changes can be neglected over the short timescales analysed there, it is however important to analyze the phenomenon on larger time windows. In the second mechanisms, instead, the simulated tracer evolves, but it is supposed that the fish can always orientate correctly, as in a noiseless environment, which is typically not the case when studying fine scale processes [Lévy et al., 2015, Kern and Coyle, 2000]. Furthermore, it is important to pass from a one dimensional analysis, such as the one concerning the gradient climbing scenario, to a two dimensional study, in which both the mechanisms are integrated together to study their reciprocal interactions. Indeed, current trends in conservation studies is to include ecological components in circulation models. The main purpose is to predict future changes on aquatic environment due to the effects of global change, in order to protect the threatened marine biota. In this context, a great leap forward for the prediction and comprehension of phytoplankton dynamics has been achieved with DARWIN model [Follows et al., 2007, Dutkiewicz et al., 2009, Barton et al., 2010]. Such a model indeed integrates the effect of fine scale circulation structures and phytoplankton dynamics, allowing to represent changes in diversity due to

latitudinal gradients [Barton et al., 2010], the role of fine scale processes into regulating nutrient availability through mixing [Barton et al., 2014] and community assemblage and diversity [Lévy et al., 2015, Soccodato et al., 2016].

The frontier is now represented by the extension of the previous consideration to intermediate trophic levels. Two examples are given by the SEAPODYM ([Sibert et al., 1999, Lehodey et al., 2002], http://www.seapodym.eu/) or Ecopath [Woodson and Litvin, 2015] models, which integrate physical and biological parameters in order to characterise the distribution and evolution of fish populations. This type of models aim to represent how oceanic dynamics affect biomass transfer through the trophic chain, and their role on larval dispersal. On the other hand, they do not take into account for aggregating mechanisms. However, as showed in the present thesis, these mechanisms can be important, influencing local concentration values up to one order of magnitude higher than expected. Increasing resolutions and realism of the physical circulation models suggest interesting possibilities in order to include them into the modeled dynamics.

In the present Section, thus, I illustrate some of the preliminary results obtained from the analysis of aggregation patterns of fish in a numerical simulation, which models at the same time fine scale processes and individual behavior. This model is built from the Navier-Stokes equation, and is similar to the model illustrated in Subsec. 3.3.4. The main difference is that the vorticity field evolves in time, and simulates an oceanic environment, containing typical mesoscale structures (left panels of Fig. 4.1). I use the vorticity field as representative of the zooplankton concentration, since its spectral slope is consistent with that of zooplankton field ([Lévy and Klein, 2004] but see also [Mackas and Boyd, 1979, Abraham and Bowen, 2002]). In this environment, 4096 fish are simulated, supposing that they try to climb the gradients of zooplankton, searching for regions with highest concentration. Their sensorial capacities are limited to a certain field view. Furthermore, the zooplankton value perceived by the fish is affected by a white noise. The range of the white noise is identified from previous studies on zooplankton distribution [Johansson et al., 1993, Coyle and Jr, 2000, Kern and Coyle, 2000, Reese et al., 2005]. Finally, I suppose that for zooplankton gradient values over a certain slope, fish are able to orientate without being affected by the noise. The fish considered, as in Chapter 2, are the myctophids, with cruising swimming speed of 0.1 m/s.

In Fig. 4.1, I report a preliminary analysis obtained from the simulation of the model described, run for a time of 25 days, starting from a homogeneous distribution of N=4096 fish. Looking at fish disposition (left column of Fig. 4.1), no intense qualitative structures of aggregation emerge. However, looking at the fish density plot on the right column, and considering that the starting density condition is $\sim$ 0.4 fish per cell, where

each cell is 8 km wide, it is possible to identify some patterns of increased fish concentration. These preliminary results seem encouraging, highlighting areas of ~ 10 times more fish concentration than at the beginning of the simulation.

However, further analysis are needed. Indeed, if one looks at the zooplankton perceived, on average, by each fish in time, it seems that no energetic advantages emerge, as it is possible to see from Fig. 4.2 (panel A). The zooplankton perceived increase lightly in
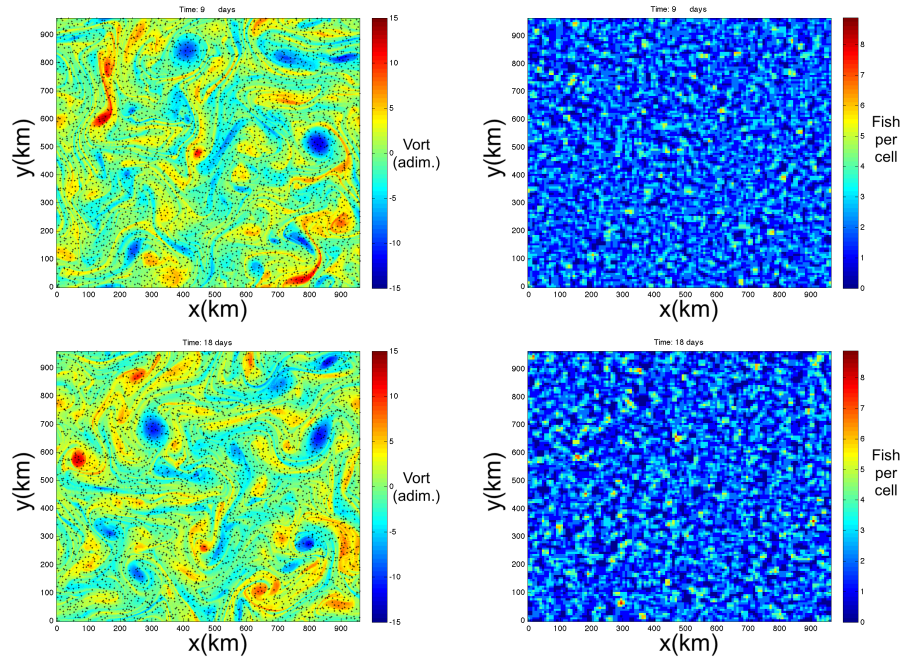
FIGURE 4.1: Preliminary results. The 2D model simulates the evolution in time of a vorticity field. This is characterized by mesoscale structures of around ~ 100 km. The vorticity is used to represent a zooplankton field, prey of 4096 simulated fish. These swim toward high levels of zooplankton values. They are initially disposed on a regular grid and the model is run for about 3 weeks. Panels on the left column show the vorticity/zooplankton field after 9 and 18 days, with fish position indicated by black crosses. Right column shows the density plot of the fish, in number of fish simulated per cell (each cell is 10×10 km^2)..
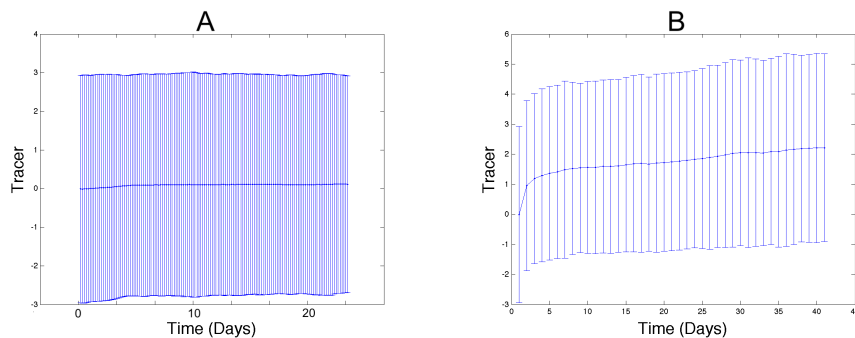
FIGURE 4.2: Preliminary results. In order to estimate the energy gain of the fish, mean zooplankton value in correspondence of the fish positions is computed for each day simulated.

time, but keeps close to 0, while the standard distribution is still very wide. In order to understand this issue, a simulation without noise, thus with $\xi_{MAX} = 0$, is made. The fish aggregation patterns, identified through the density plot are, not surprisingly, more intense (not showed). The zooplankton perceived instead shows an increasing trend, growing exponentially for the first 5 days and then relaxing at a value of ~ 2. However, the standard deviation is still very high. A possible explanation for that is that fish can orientate easily, but are "trapped" by relative local maxima. These however do not present very high zooplankton values. This is due to the relatively short field view of the fish, which does not allow them to identify the higher peaks of zooplankton. Further investigations on the orientating strategies of the myctophids simulated are thus required.

4.4 Final remarks

Future works are needed to integrate the effect of vertical dynamics. The latter can indeed play an essential role on the ecology of the marine ecosystems. It will be thus interesting to integrate and extend the previous results to 3 dimensional dynamics, in order to analyse also the effect of submesoscale structures on vertical movements and, by consequence, on marine biota, and integrate the results with ecosystem marine model already present, such as DARWIN. This could, on one side, help better characterising the fish prey field, which is now represented through the vorticity. On the other hand, it could reveal possible mechanisms of aggregation also on the vertical direction: indeed, some interesting patterns of fish aggregation along this dimension have already been observed [Bras et al., 2017].

Concerning the acoustic backscattering measurements, it would be interesting to extend the previous analysis to a larger area, an to a larger temporal window. It would be important also to analyse separately the different seasons, to understand the underlying annual intra-variability. Furthermore, biological factor must be included as explanatory variables, in order to sharpen the prediction. This would allow to assess potential global change impacts on intermediate trophic levels populations, and provide information which could be used for conservation purposes.

Finally, it would be interesting to apply the methodologies of the crossroadness also to other diagnostics, to study the performance of non fixed stations, and to extend, also in this case, the analysis to 3 dimensions.

4.5 Conclusions

In the present thesis I analyse the problem of the coupling between physical and biological processes in the ocean, in particular concerning the intermediate trophic levels. These are actually by far the less known elements of the trophic chain in this coupled analysis. In this work I present an analysis which shows an interesting relationship between fish measurements and frontal systems. On the other hand, front emerge as as structures which are necessary but not sufficient for finding high fish concentrations. This allows to shed some light on the role of fine scale processes as aggregating structures for fish, and open the doors to future interesting perspectives, with the integration of the highlighted dynamics in global models of circulation and marine ecology. Furthermore, I developed an optimal monitoring strategy which could help, on one hand, to better sample mid trophic organisms. This may fill the knowledge gap actually present toward the other elements of the trophic chain. On the other hand, the work presented could help to build effective networks which can protect peculiar marine regions.

Appendix A

Appendix A: The Gulf Stream frontal system: A key oceanographic feature in the habitat selection of the leatherback turtle?

This appendix has been published as *The Gulf Stream frontal system: A key oceanographic feature in the habitat selection of the leatherback turtle?* by P. Chambault, A. Baudena et al. at *Deep Sea Research I*, 2017.
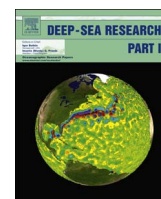
The Gulf Stream frontal system: A key oceanographic feature in the habitat selection of the leatherback turtle?

Philippine Chambault[a,*], Fabien Roquet[b], Simon Benhamou[c], Alberto Baudena[d], Etienne Pauthenet[b], Benoît de Thoisy[e], Marc Bonola[a], Virginie Dos Reis[e], Rodrigue Crasson[e], Mathieu Brucker[a], Yvon Le Maho[a], Damien Chevallier[a]

[a] Université de Strasbourg, IPHC UMR 7178 F-67000 Strasbourg, France
[b] Stockholm University, Department of Meteorology (MISU), Sweden
[c] Centre d'Étude Fonctionnelle et Évolutive, CNRS, 1919 route de Mende, 34293 Montpellier Cedex, France
[d] Sorbonne Universités, UPMC Université Paris 06, CNRS-IRD-MNHN-IPSL Laboratory, 4 Place Jussieu, F-75005 Paris, France
[e] Association Kwata, 16 avenue Pasteur, BP 672, F-97335 Cayenne Cedex, France

ARTICLE INFO

ABSTRACT

Although some associations between the leatherback turtle *Dermochelys coriacea* and the Gulf Stream current have been previously suggested, no study has to date demonstrated strong affinities between leatherback movements and this particular frontal system using thorough oceanographic data in both the horizontal and vertical dimensions. The importance of the Gulf Stream frontal system in the selection of high residence time (HRT) areas by the North Atlantic leatherback turtle is assessed here for the first time using state-of-the-art ocean reanalysis products. Ten adult females from the Eastern French Guianese rookery were satellite tracked during post-nesting migration to relate (1) their horizontal movements to physical gradients (Sea Surface Temperature (SST), Sea Surface Height (SSH) and filaments) and biological variables (micronekton and chlorophyll *a*), and (2) their diving behaviour to vertical structures within the water column (mixed layer, thermocline, halocline and nutricline). All the turtles migrated northward towards the Gulf Stream north wall. Although their HRT areas were geographically remote (spread between 80–30 °W and 28–45 °N), all the turtles targeted similar habitats in terms of physical structures, i.e. strong gradients of SST, SSH and a deep mixed layer. This close association with the Gulf Stream frontal system highlights the first substantial synchronization ever observed in this species, as the HRTs were observed in close match with the autumn phytoplankton bloom. Turtles remained within the enriched mixed layer at depths of 38.5 ± 7.9 m when diving in HRT areas, likely to have an easier access to their prey and maximize therefore the energy gain. These depths were shallow in comparison to those attained within the thermocline (82.4 ± 5.6 m) while crossing the nutrient-poor subtropical gyre, probably to reach cooler temperatures and save energy during the transit. In a context of climate change, anticipating the evolution of such frontal structure under the influence of global warming is crucial to ensure the conservation of this vulnerable species.

1. Introduction

Oceanic fronts are transition areas between water masses of contrasting properties (Belkin et al., 2002; Scales et al., 2014). These sharp boundaries are generally characterized by physical and biological discontinuities in terms of temperature, salinity and nutrient gradients (Le Fèvre, 1986; Reul et al., 2014; Scales et al., 2014; Greer et al., 2015), and occur across a variety of spatial and temporal scales, from sub-mesoscale (1–10s km) to ocean basin scales (1000s km). Oceanic fronts can be generated by various physical processes, ranging from the presence of an estuary or a shelfbreak, the occurrence of locally enhanced tidal mixing, wind-induced upwelling or convergence patterns, the presence of sea ice or the western intensification of gyre circulations (Belkin et al., 2009).

The physical processes (upwelling, mixing, stirring) generating oceanic fronts lead to increased primary and secondary productivity (Olson and Backus, 1985; Olson et al., 1994), enhancing in most cases the activity at higher trophic levels via bottom-up processes (Le Fèvre, 1986; Largier, 1993; Acha et al., 2004). Frontal systems are therefore commonly associated with a diverse range of marine vertebrates such

as seabirds (Haney and McGillivary, 1985, van Franeker et al., 2002; Cotté et al., 2007; De Monte et al., 2012; Scheffer et al., 2012; Thorne and Read, 2013; Whitehead et al., 2016), pinnipeds (Bradshaw et al., 2004; Bailleul et al., 2010; Nordstrom et al., 2013), cetaceans (Moore et al., 2002; Etnoyer et al., 2006; Doniol Valcroze et al., 2007; Druon et al., 2012; Murase et al., 2014) and sea turtles (Eckert et al., 2006b; Fossette et al., 2010a; Witherington, 2002; Polovina et al., 2004; Polovina and Howell, 2005).

The largest frontal system in the North Atlantic Ocean is associated with the Gulf Stream, one of the World hydrodynamic oceanic currents (Schmitz and McCartney, 1993; Lozier et al., 1995; Ducet et al., 2000). Forming the western boundary current system of the North Atlantic Ocean subtropical gyre, this fast current originates in the Gulf of Mexico and intensifies along the south-east coast of the United States before leaving the coastline to cross the Atlantic Ocean at about 40 °N. A strong thermal boundary occurs at the intersection of the warm, salty Gulf Stream waters and the cold and less salty waters of the Labrador Current (Fuglister, 1963). Like in other frontal systems, some associations have been observed between the Gulf Stream and marine megafauna (Olson et al., 1994) such as seabirds (Haney and McGillivary, 1985; Thorne and Read, 2013), fish (Block et al., 2001, 2005; Wilson et al., 2004; Skomal et al., 2009; Potter et al., 2011) and sea turtles (loggerhead: Witherington, 2002; leatherback: Eckert et al., 2006b; Fossette et al., 2010a; Lutcavage, 1996; Dodge et al., 2014).

While the leatherback turtle (*Dermochelys coriacea*) has often been tracked in the Atlantic Ocean (Bailey et al., 2012b; Eckert et al., 2006b; Fossette et al., 2010b, 2010a; James et al., 2005a, 2005b; Ferraroli et al., 2004; Hays et al., 2004; McMahon and Hays, 2006; López-Mendilaharsu et al., 2009; Dodge et al., 2014), only a few studies have suggested that this species may associate with the Gulf Stream frontal system (Eckert et al., 2006b; Fossette et al., 2010a; Lutcavage, 1996). More recently, Dodge et al. (2014) have shown a relationship between leatherback movements and strong Sea Surface Temperature (SST) gradients, highlighting some affinities for the Gulf Stream front, but only for a limited number of individuals (n=2), and not in the vertical dimension. Given that the Gulf Stream frontal system is marked by strong SST gradients and pronounced vertical mixing, aggregating therefore low trophic level organisms such as jellyfish (Sims and Quayle, 1998; Greer et al., 2013; Powell and Ohman, 2015), it would be logical to expect North Atlantic leatherback turtles to interact with the Gulf Stream frontal system during their post-nesting migration across the North Atlantic. We propose in this study to examine more systematically the potential affinities of leatherback turtles with this frontal system based on detailed 3D oceanographic data, investigating both the geographical patterns and the vertical dive behaviour in relation to physical and biological ocean conditions.

This study assesses the role of the Gulf Stream frontal system in the selection of preferentially used areas by the leatherback turtle via the satellite tracking of 10 adult females, equipped between 2014 and 2015 from the Eastern French Guianese rookery. This is one of the two major rookeries for the leatherback turtle on the west coast of the equatorial Atlantic (Fossette et al., 2008), showing a different genetic structuration (Molfetti et al., 2013). Note that several female leatherback turtles from the Western French Guianese population have been tracked in the past (Fossette et al., 2010b, 2010a), but it is the first time tracks from the Eastern rookery are documented. After identifying high residence areas (a proxy of foraging grounds), we used a series of biological and physical variables provided by 3D ocean reanalysis products to relate (1) the horizontal movements of the leatherback turtles to physical properties (SST and Sea Surface Height (SSH) gradients and filaments) and biological variables (micronekton and chlorophyll *a*), and (2) their diving behaviour to vertical structures within the water column (mixed layer, thermocline, halocline and nutricline).

2. Materials and methods

2.1. Ethics statements

This study met the legal requirements of the country in which the work was carried out (France), and followed all institutional guidelines. The protocol was approved by the "Conseil National de la Protection de la Nature" (CNPN, http://www.conservation-nature.fr/acteurs2.php?id=11), which is under the authority of the French Ministry for ecology, sustainable development and energy (permit Number: 2015133-0022), and acts as the ethics committee for French Guiana. The fieldwork was carried out in strict accordance with the recommendations of the Police Prefecture of Cayenne (French Guiana, France), to minimize any disturbance of the animals.

2.2. Study area and tag deployment

During the 2014 and 2015 nesting seasons, 11 adult female leatherback turtles were equipped with satellite tags on the beaches of Rémire-Montjoly (4.53°N–52.16°W, Cayenne, French Guiana). One Argos Fastloc GPS tag (SPLASH10-F-296A, Wildlife Computers Redmond, WA, USA) was deployed in August 2014 and 10 Satellite Relay Data Loggers (SRDL, Sea Mammal Research Unit, University of St. Andrews, Scotland) were deployed in June 2015. These tags were attached during night-time egg laying, i.e. at the only moment when individuals are static while ashore. Harnesses were not used to attach the satellite tags in order to minimize hydrodynamic drag. Prior to attachment, the tags were moulded into a resin mount to match the shape of the central dorsal ridge, and two holes were drilled into the resin mount for the stainless steel cable. The attachment area was disinfected with Betadine then locally anesthetised with Lidocaïne © spray. Two < 0.5 cm diameter holes were drilled into the central dorsal ridge. The tags were then fixed by threading a stainless steel cable through the holes in the dorsal ridge and the resin tag mount. Stainless steel crimps were used to secure the cable and were covered with an epoxy resin to ensure solidity, preventing the tag from being released before the return of the turtles to the nesting site (French Guiana) in 2–4 years.

2.3. Data collected from the tags

Both tag types recorded horizontal (Argos and/or GPS locations) and vertical movements (diving behaviour) of the turtles, but at different resolutions.

2.3.1. Argos Fastloc GPS tag

The single Argos Fastloc GPS tag deployed in 2014 recorded both Argos and GPS locations (every 4-h), as well as depth data describing specific diving parameters, namely maximum dive depths, dive durations, and *in situ* temperature data, binned as 4-h period histograms. The wet/dry sensor of the tag was used to identify the beginning and end of each dive. The sensor entered haul-out state after 20 consecutive dry minutes, and exited haul-out state if it remained wet for 30 s or more. Maximum depths were collected in different bins, every 10 m from 10 to 100 m, then every 50 m from 100 to 250 m with a depth sensor accuracy of 1% of reading. Similarly, maximum dive durations were stored from 30 s to 1 min, then every minute from 1 to 5 min, every five minutes from 5 to 20 min, and *in situ* temperatures from 20 to 32 °C were recorded during dives with a resolution of 1 °C, with a temperature sensor accuracy of 0.1 °C. This tag also supplied Time At Depth (TAD), defined as the proportion of time (in %) spent at each depth.

2.3.2. SRDL tags

One of the 10 SRDL tags deployed in 2015 did not transmit any data, and was therefore excluded from the analysis. The other nine SRDL tags provided Argos-based location data, as well as data about

diving behaviour including dive depth (with a depth sensor resolution of 0.5 m), dive duration and duration of post-dive surface intervals. The wet/dry sensor of the tag was used to identify the beginning and end of each dive. Dives started when the sensor was wet and below 1.5 m for 20 s, and ended when dry or above 1.5 m. The SRDL tags were programmed to send summarized dive profiles using the compression algorithm described by Fedak et al. (2001), with 4 depth records for each dive (instead of 1 maximum depth per dive for the Argos Fastloc GPS tag).

2.4. Data pre-filtering

As all tags were deployed during the nesting season, they recorded movements and diving behaviour for both the nesting and migration phases. Following the procedure described in Chambault et al. (2015), we excluded the nesting phase to focus on the migration phase alone. A Kalman filtering algorithm (Silva et al., 2014; Lopez et al., 2014) provided by Collecte Location Satellites (CLS Toulouse, France) was applied to estimate Argos locations. Basically, the algorithm uses a correlated random walk model to predict the next location and its associated error based on the previous positions and estimated error. To each Argos location was assigned a Location Class (LC): 3, 2, 1, 0, A, B or Z. Approximately 17% of the locations of our study were associated with an estimated error (from > 250 m to > 1500 m, LC 3: 2.1%, 2: 4.3%, 1: 5.6% and 0: 5.7%), 83% had no accuracy estimation (LC A: 20.5% and B: 61.7%), and 1% were invalid (LC Z). The GPS locations (provided by the single tag deployed in 2014) were associated with an accuracy < 100 m (0.1% recorded). We used the General Bathymetric Chart of the Oceans (GEBCO) database (http://www.gebco.net/, resolution 30 arc-second, ~1 km grid) to discard any locations on land. As described in Fossette et al. (2010a), we also discarded the Argos locations associated with a speed of over 10 km h^{-1} (9% in 2014 and 10% in 2015, Fossette et al., 2010b), as well as "type Z" (i.e. invalid Argos-based) locations.

2.5. Current correction of tracks

Tracks were first re-sampled according to the mean daily locations frequency obtained for both tag types: every 2 h (Argos-GPS) or 8 h (SRDL). We then corrected the ground-related (satellite-recorded) tracks for oceanic currents to estimate the movements of leatherbacks according to the water masses they cross, providing a more accurate picture of actual movement behaviour (Girard et al., 2006; Gaspar et al., 2006). Surface current velocity fields can be computed as the vectorial sum of geostrophic and Ekman components (Sudre et al., 2013). The geostrophic component results from the balance between the horizontal pressure gradient force and the Coriolis force. It was computed from the Ssalto/Duacs maps of absolute dynamic topography data available daily on a 1/4 ° grid (www.aviso.altimetry.fr/en/data/products/sea-surface-height-products/global/madt-h-uv.html) based on an updated assessment of the sum of sea level anomalies and mean dynamic topography, both being referenced over a twenty-year period in the Duacs 2014 version (V15.0). The Ekman component results from the balance between friction by wind and the Coriolis force. It was estimated from wind stress data provided daily on a 1/4° grid by CERSAT IFREMER (Ascat daily gridded mean wind field: http://cersat.ifremer.fr/data/products/catalogue). Both geostrophic and Ekman components were computed using a recent model (GEKCO product) developed by Joël Sudre and underwent a bi-linear spatial interpolation and a linear temporal interpolation to estimate their "meridional" (i.e. E-W) U and "zonal" (i.e S-N) V components at every turtle's location (velocity field data and a user-friendly program to interpolate local values at any location and time are freely available at www.legos.obs-mip.fr/sudre). It is worth noting however that the Ekman component becomes negligible under the mixed layer (e.g. within the thermocline, Marshall and Plumb, 2007). We therefore estimated the proportion P of time spent above the thermocline for

each dive of each turtle, and computed the real current velocity as:

$$U_{actual} = U_{geostrophic} + P. U_{Ekman} \text{ and } V_{actual} = V_{geostrophic} + P. V_{Ekman}$$

The time spent above the thermocline could not be calculated for the Argos-GPS tag deployed in 2014 due to the coarser resolution of the diving data. For this turtle, P was estimated as a function of the location based on the diving data provided by the 9 other tags. Finally, the water mass-related (i.e. "motor") step lengths for each turtle were computed as:

$$\Delta X_{motor} = \Delta X_{track} - \Delta t. U_{actual} \text{ and } \Delta Y_{motor} = \Delta Y_{track} - \Delta t. V_{actual}$$

where ΔX_{track} and ΔY_{track} are ground-related step lengths based on coordinates of the satellite-recorded locations (converted from longitude and latitude to an orthonormal metric system X and Y), and Δt is the time of movement between a given location and the next (see Girard et al., 2006 for details).

2.6. Residence time analysis

We inferred high residence time (HRT) phases (and therefore HRT areas) by applying Residence Time (RT) analysis (Barraquand and Benhamou, 2008; Benhamou and Riotte-Lambert, 2012) to the current-corrected movements. The RT for a given location indicates the time spent within a circle centred on this location with a given radius R. It is therefore computed as the difference between forward and backward first passage times at distance R from the centre, plus possible additional backward and/or forward times spent within the circle provided that the animal does not leave the circle for more than a given time (set to 8 h in the present study), before returning within the circle. The circle runs along the path in this approach, providing a more contrasted and less noisy time series (with respect to simpler analyses based on first passage times). As advised in Barraquand and Benhamou (2008), we computed RT time series with a radius r ranging between 10 and 100 km to explore different scales. The low residence time (hereafter LRT) and HRT areas for the migration of each turtle were then inferred by segmenting RT time series using Lavielle (2005) segmentation method.

2.7. Environmental data

2.7.1. Horizontal variables

We extracted a series of environmental variables from both remote sensed data and model simulations to characterize the habitat of leatherback turtles at their HRT areas. The variables selected were those most likely to influence the distribution of jellyfish (Graham et al., 2001). We extracted the surface sea water chlorophyll *a* concentration at each turtle location from the *Global ocean biochemical analysis and forecast* product (BIO 001–014) at a 0.5 ° spatial resolution (from U.E Copernicus Marine Service Information: http://marine.copernicus.eu/services-portfolio/access-to-products/).

As the *Spatial Ecosystem And Population Dynamics Model* (SEAPODYM) predicts the spatio-temporal distribution of micronekton (Lehodey et al., 2008, CLS Toulouse), the smallest pelagic organisms capable of swimming against sea currents (individuals measuring from 2 to 25 cm), it was used to estimate the distribution of leatherback prey. It includes the diet of leatherback turtles and encompasses different micronekton groups, including jellyfish (Brodeur et al., 2005). Micronekton is modelled using current and temperature data provided by the *GLobal Ocean ReanalYsis and Simulations* product (GLORYS-2v1), and net primary production and euphotic depth derived from ocean colour satellite data (http://www.science.oregonstate.edu/ocean.productivity/) using the *Vertically Generalised Production Model* (VGPM). Due to the lack of micronekton predictions in nearshore mesopelagic and bathypelagic layers, we estimated only the epipelagic layer using this model. To investigate variations in the vertical accessibility of leatherback prey, we also extracted the euphotic depth weekly on a grid of 0.25 °×0.25 °.

Table 1

Summary of the horizontal post-nesting movements of the 10 leatherback turtles tracked. Speed values are Mean ± SD. PTT refers to the turtle's ID, Nloc to the number of locations, HRT to high residence time.

Ptt	Tag type	Start date	End date	Nloc	Tracking duration (d)	Distance (km)	Daily speed (km d^{-1})	Duration to HRT areas (d)
131347	SPLASH10-F	28/08/2014	25/01/2015	1798	150	6794	44.9 ± 29.0	92
149680	SRDL	30/07/2015	06/11/2015	297	99	4957	49.6 ± 25.9	65
149681	SRDL	06/07/2015	12/12/2015	479	159	7122	44.5 ± 21.4	92
149682	SRDL	18/07/2015	03/02/2016	579	200	8080	40.8 ± 34.0	111
149683	SRDL	16/07/2015	12/11/2015	357	119	5093	42.4 ± 19.6	79
149684	SRDL	08/07/2015	07/12/2015	454	152	7093	46.3 ± 22.8	115
149685	SRDL	14/07/2015	21/02/2016	665	222	11640	52.2 ± 27.1	73
149687	SRDL	26/06/2015	26/12/2015	547	183	11181	60.8 ± 24.8	66
149688	SRDL	08/07/2015	14/04/2016	844	281	11066	39.2 ± 21.2	87
149689	SRDL	24/06/2015	20/12/2015	537	179	12746	70.8 ± 34.6	75
Mean ± SD				655 ± 429	174 ± 52	8577 ± 2842	49.1 ± 9.8	85 ± 17

To assess the effect of horizontal physical gradients on the foraging behaviour of leatherback turtles (associated with HRT areas), we extracted at each turtle location the associated SST and SSH from the *Global sea physical analysis and forecast* product (PHYS 001–024) at a resolution of 0.08 ° (from U.E Copernicus Marine Service Information). We then calculated the values of SST gradient (SSTgrad) and SSH gradient (SSHgrad) at the locations of each turtle. We then used the areas with the highest SSTgrad and SSHgrad magnitude (≥ quantile 0.95) to identify the locations of oceanic fronts. Then we assessed the use of frontal zones by leatherback turtles based on the distance to the closest frontal zone identified. We repeated the analysis to determine whether the turtles directly targeted SST fronts or if they were attracted by another oceanographic feature present at frontal regions. This procedure used *Finite-Size Lyapunov Exponents* (FSLE, D'Ovidio et al., 2004) and focused on pure transport diagnostics. The FSLE method provides a direct measurement of local stirring by sub-mesoscale currents, and the separation of waters coming from different regions by the FSLE ridges makes it possible to identify water masses with different physical properties (D'Ovidio et al., 2010; De Monte et al., 2012). FSLE diagnostics were computed as described in Bon et al. (2015) and the FSLE diagnostics were extracted at each turtle location at a 0.08 ° horizontal resolution. For the SST and SSH fronts, the distance to the closest FSLE filament with a gradient magnitude ≥ quantile 0.95 was then calculated for each turtle location.

2.7.2. Vertical variables

We assessed the habitat use of leatherback turtles in the vertical dimension by extracting sea water temperature, sea water salinity, mixed layer depth (MLD) and sea water chlorophyll *a* concentration from Copernicus Marine Service Information. These parameters were extracted at each dive location and for each maximum depth reached by all turtles equipped in 2015. The use of vertical habitat by the turtle equipped in 2014 could not be characterized due to the coarse resolution of the diving data (only 1 maximum dive depth per location). We extracted temperature, salinity and MLD (using Kara et al.'s method (2000a)) data from June 2015 to April in 2016 from the *Global physical analysis and coupled system forecast* product (PHY 001–015), available from Copernicus, at a 0.25 ° horizontal resolution and depths of 0–400 m. Similarly, we extracted sea water chlorophyll *a* concentration data from the BIO 001–014 product at a 0.5 ° horizontal resolution and depths of 0–400 m. We then used these data to locate the thermocline, halocline and nutricline depths. The seasonal thermocline was defined as the layer comprised between the MLD (upper layer of the thermocline) and the maximum MLD during the previous winter peak below (e.g. lower layer, in February 2015 for the tags deployed in June 2015). We also estimated the halocline and nutricline depths of each dive location from the salinity and chlorophyll *a* gradients, respectively.

2.8. Diving behaviour analysis

An indication of dive shape was obtained through the Time of Allocation at Depth (TAD) index, calculated by using the four inflection points of the summarized profiles provided by SRDL tags deployed in 2015. We used Fedak et al.'s method (2001) to calculate the TAD and thus estimate the type of activity the turtles displayed during the dives. Exploratory dives commonly corresponded to V-shaped dives with $0.5 \leq$ TAD < 0.75, and foraging activity at the bottom of the dive corresponded to U-shaped dives with $0.75 \leq$ TAD<1. We fixed the average rate of change of depth at 1.4 m s^{-1}, as values above this speed are considered biologically unreliable.

3. Results

3.1. Migratory routes and high residence time (HRT) areas

The tracked turtles measured (mean ± SD) 160 ± 8.1 cm in curved carapace length, 116 ± 6.4 cm in curved carapace width and 206 ± 13.7 cm in circumference. We obtained 655 ± 429 (mean ± SD) locations per turtle, for a tracking duration ranging from 99 (#149680) to 281 days (#149688, Table 1). The total distance travelled varied from 4957 km (#149680) to 12746 km (#149689, mean ± SD: 8577 ± 2842 km). The actual daily speed (corrected for oceanic currents) ranged from 39.2 ± 21.2 to 70.8 ± 34.6 km d^{-1} (#149688 vs. #149689, respectively, mean ± SD: 49.1 ± 9.8 km d^{-1}). The average elapsed time to reach the HRT areas (putative foraging grounds) was 85 ± 17 d (mean ± SD; range: 65–115 d, #149680 vs. #149684, respectively).

The 10 females tracked in this study left French Guiana between late June and late August, and occupied HRT areas between August and November. They headed in various directions towards mid-latitude areas, i.e. south-eastern US continental shelf, Newfoundland-Labrador, the Azores or even pelagic waters in the North Atlantic (Fig. 1a). The areas that were identified as putative foraging grounds based on a HRT were spread between 30–45 °N, and were located either in neritic or pelagic zones. Three turtles used a coastal HRT area located off the shores of the south-eastern US shelf (#149680, #149682 and #149689). Another (#149687) remained in the neritic HRT area of Newfoundland-Labrador, at the mouth of the Saint Lawrence River, and the six remaining turtles spent most of their time in pelagic waters. The running circle providing the best contrast in terms of residence time series analysis had a radius of 80 km. The largest HRT percentage was observed from October (n=10) to December (n=8) (Fig. 1b).

3.2. Associations with biological features

The initial part of the migration within the core of the North Atlantic subtropical gyre corresponded to low RT (hereafter 'transit
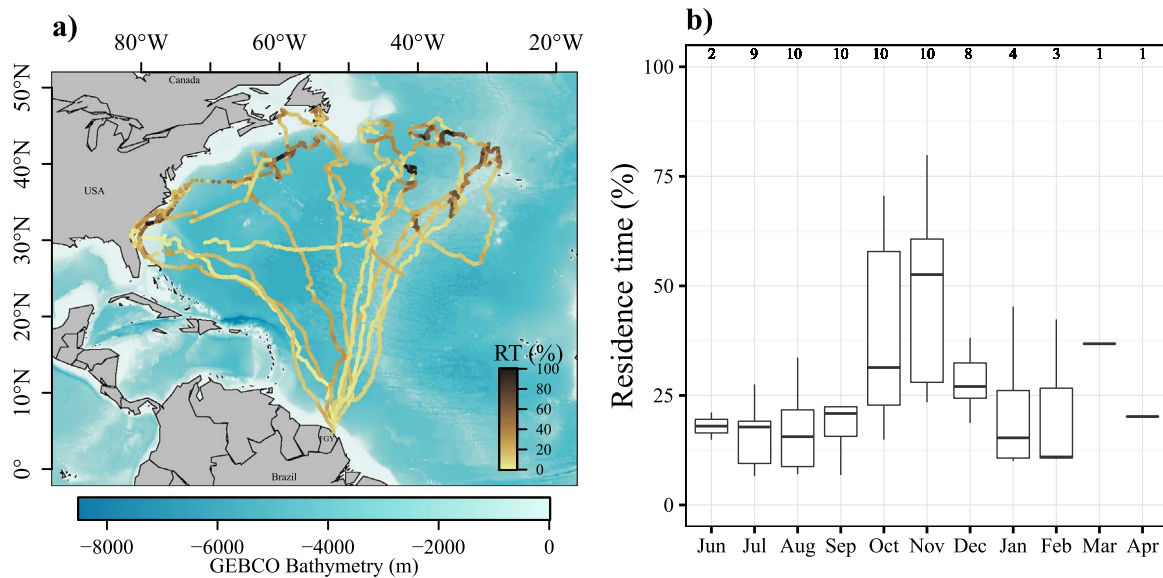
Fig. 1. (a) Proportion of residence time (RT in %) calculated along the 10 leatherback tracks in 2014 (*n*=1) and 2015 (*n*=9) and (b) box plots of RT (in %) according to the months of tracking. The RT (initially expressed in days) was converted into a percentage based on the maximum value obtained for each individual to obtain a comparable scale across individuals. (b) The locations associated with the highest values in (a) were considered to be potential foraging areas. FGY indicates the departure point and tagging site located in French Guiana. The numbers in (b) refer to the sample size of each box plot (i.e. the number of turtles; note that only one turtle was still tracked in March and April).

phase') for all females in scantily productive waters containing low levels of micronekton biomass and chlorophyll *a* concentration (Figs. 2a and 2d). When all the transit phases were taken into account, the micronekton biomass was significantly lower than that found in HRT areas (mean ± SE: 0.56 ± 0.04 vs. 1.31 ± 0.25 g m^{-2}, respectively, Wilcoxon test, V=35, *p* < 0.05, Fig. 3a). Similarly, the chlorophyll *a* concentration was significantly lower at locations where the turtles transited (mean ± SE: 0.18 ± 0.04 vs. 0.53 ± 0.13 mg m^{-3}, respectively, Wilcoxon test, V=28, *p* < 0.05, Fig. 3b).

Locations at higher latitudes (> 30 ºN) correspond to areas where the turtles spent most of their migration time, and highly productive waters for both the micronekton biomass and the chlorophyll *a* were recorded (Figs. 2b, 2e and 5b). However, most of the leatherback turtles headed southward on leaving these mid-latitude feeding grounds, remaining in waters of expected high chlorophyll *a* concentration (Fig. 2f) rather than high micronekton biomass (Fig. 2c). The euphotic depth was significantly shallower in HRT areas (mean ± SE: 77.9 ± 3.3 vs. 55.5 ± 4.8 m; Wilcoxon test, V =36, *p* < 0.005) – see Figs. 3c, 2g, 2h, 2i. Waters of shallower euphotic depth were associated with higher latitudes (> 30 ºN), where the turtles were assumed to feed intensively (Fig. 2h).

3.3. Associations with physical discontinuities

Our turtles experienced warm waters (~30 ºC) when crossing the core of the North Atlantic subtropical gyre (see Fig. 4a). After reaching HRT areas at higher latitudes in November, they remained in cooler waters ranging mainly between 15 and 23 ºC (Fig. 4b). At the beginning of winter (January), the cold waters coming from the Labrador Current extended further south and the four remaining turtles tracked at this period tended to follow the 20 ºC isotherm southward (Fig. 4c). The SSH and SST were significantly lower when the turtles occupied HRT areas (mean ± SE: 9.4 ± 2.8 vs. −14.1 ± 3.4 cm; Wilcoxon test, V=55, *p* < 0.005, Figs. 3g, 4d, 4e, 4f, and mean ± SE: 25.7 ± 0.5 vs. 20.5 ± 1.2 ºC; Wilcoxon test, V=55, *p* < 0.005, Fig. 3h, respectively).

During the first and final parts of the migration, corresponding to the low RT phases, the turtles crossed waters associated with low horizontal gradients (SST and SSH fronts), as illustrated in Figs. 6a, 6c, 6d and 6f. They crossed waters associated with low FSLE (Figs. 6g and 6i). In contrast, they remained close to stronger SSH and SST gradients while occupying HRT areas at mid-latitudes (Figs. 6b and 6e). The SST

gradient was up to three times higher when on HRT areas (mean ± SE: 0.01 ± 0.002 vs. 0.03 ± 0.006 ºC km^{-1}, Wilcoxon test, V=1, *p* < 0.01) - see Figs. 6a, 6b and 6c. The SSH gradient was up to twice as high when the turtles occupied HRT areas (mean ± SE: 0.14 ± 0.01 vs. 0.25 ± 0.05 cm km^{-1}, Wilcoxon test, V=1, *p* < 0.05) - see Figs. 6d, 6e and 6f. The distance to the SST front was significantly shorter when the turtles were in HRT areas than when they were on low RT areas (mean ± SE: 379 ± 32 vs. 37 ± 7.5 km; Wilcoxon test, V=55, *p* < 0.005) – see Figs. 3d and 5c. Similarly, the distance to the SSH front was significantly shorter when the turtles were in HRT areas (mean ± SE: 474 ± 44 vs. 86 ± 22 km, Wilcoxon test, V=55, *p* < 0.005) – see Figs. 3e and 5d). However, the FSLE was not significantly higher when the turtles occupied HRT areas (mean ± SE: 0.13 ± 0.02 vs. 0.21 ± 0.05 days^{-1}, Wilcoxon test, V=4, *p*=0.1094) - see Figs. 6g, 6h and 6i. The distance to the FSLE (filaments) was significantly shorter when the turtles were in HRT areas (mean ± SE: 253 ± 34 vs. 64 ± 22 km; Wilcoxon test, V=54, *p* < 0.005) – see Figs. 3f and 5e.

3.4. Diving behaviour and vertical structures

3.4.1. Turtle maximum depth and dive duration

The Argos-GPS tag recorded 4539 depths and 4614 dive durations. Among the 720 summarized dives transmitted (the tags have not recorded the dives continuously) by the 9 SRDL, on average 80 ± 33 dives per individual were transmitted (range: 41–137 dives per turtle, #149680 vs. 149688). Over the 10 tags, 27% of the dives were less than 10 m deep (Fig. 7a). Maximum dive depths were significantly different between individuals (Kruskal-Wallis rank sum test, χ^2=49, *p* < 0.001). The turtles dove significantly deeper when occupying low RT areas (mean ± SE: 82.4 ± 5.6 vs. 38.5 ± 7.9 m, Wilcoxon test, V=55, *p* < 0.005) – see Fig. 7a. Dive durations varied from 0.5 to 85 min, with 26% of the dives lasting less than 10 min, and 31% between 20 and 45 min (Fig. 7b). Dive durations differed significantly between individuals (Kruskal-Wallis rank sum test, χ^2=57, *p* < 0.001). The turtles performed longer dives when in low RT areas (mean ± SE: 27.0 ± 1.3 vs. 14.3 ± 2.4 min, Wilcoxon test, V=54, *p* < 0.005) – see Fig. 7b.

3.4.2. Surface interval and TAD

Among the 720 dives recorded by the SRDL tags, 76% of the surface intervals lasted less than 5 min (mean ± SE: 13.1 ± 2.4 min). Surface
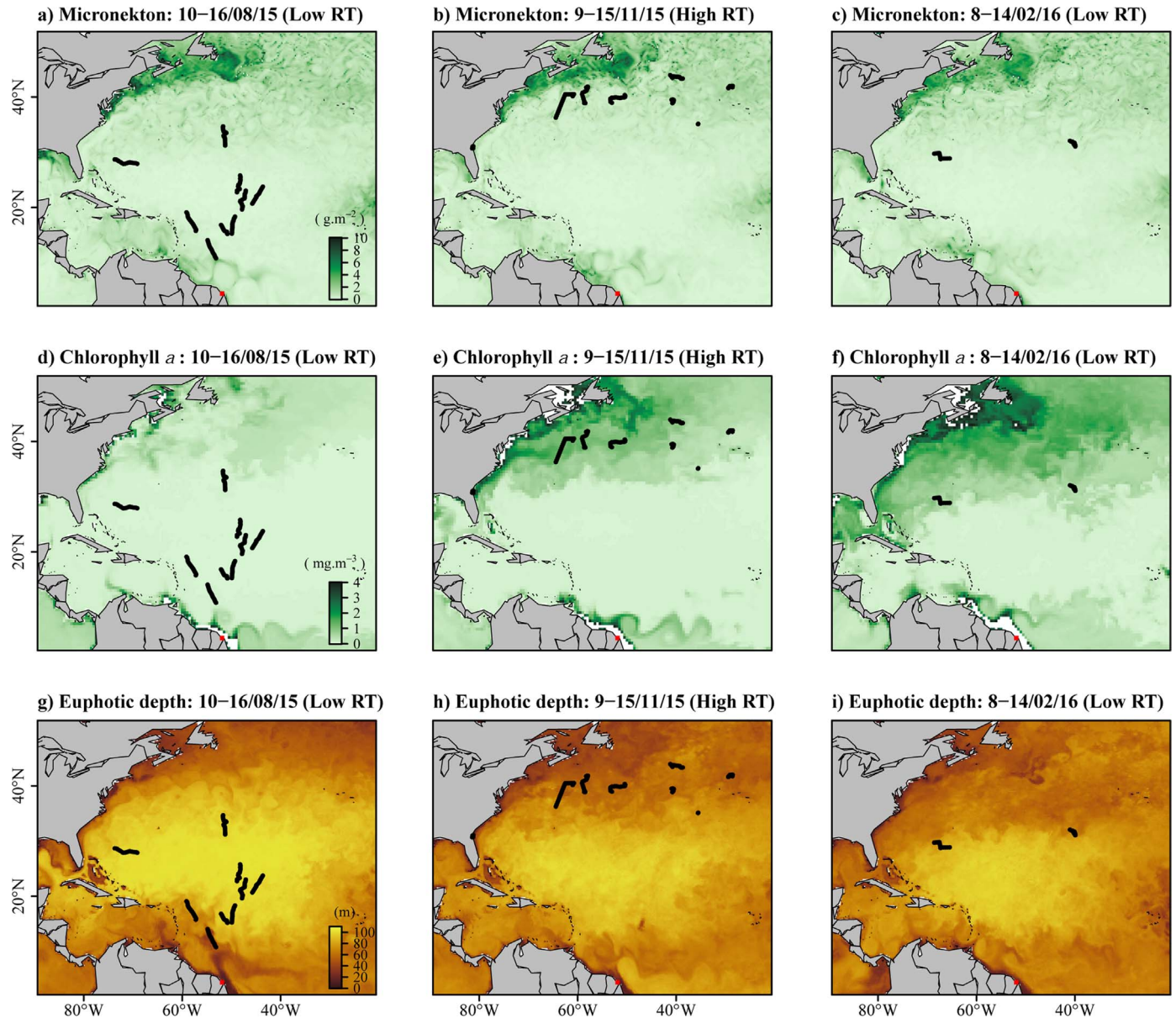
Fig. 2. Maps of the weekly averaged micronekton biomass predicted from SEAPODYM (a, b, c), the chlorophyll *a* concentration extracted from Copernicus (d, e, f) and the euphotic depth (g, h, i) predicted by SEAPODYM during three phases: the crossing of the North Atlantic gyre (a, d, g: low RT, *n*=10), the high RT period at mid-latitudes (b, e, h, *n*=10) and after leaving the high RT areas (c, f, i, *n*=3). The black dots correspond to the locations of the leatherback turtles tracked from French Guiana for the corresponding week and the red square to the migration starting point. (For interpretation of the references to color in this figure legend, the reader is referred to the web version of this article.)

intervals recorded by the 9 SRDL tags differed significantly between individuals (Kruskal-Wallis rank sum test, χ^2=68, $p < 0.001$) but did not differ significantly according to the type of behaviour (mean ± SE: 12.9 ± 2.6 vs. 11.3 ± 2.6 min, Wilcoxon test, V=18, p=0.6523). The Time of Allocation at Depth (TAD) varied from 0.25 to 0.92 and was on average (± SE) 0.59 ± 0.004. With a TAD below 0.5, 11% of the 720 dives recorded by the SRDL tags could not be assigned to a U or V dive shape, whereas 85% corresponded to V-shaped dives and 4% to U-shaped dives.

3.4.3. SST and temperature at turtle maximum depth

The values for SST and temperature at the maximum recorded depth of each turtle decreased over the tracking period, with the highest values recorded during the first month of tracking in June (mean ± SE: 28.1 ± 0.3 and 27.6 ± 0.1 °C, SST and temperature at maximum dive depth respectively) and the lowest in November (mean ± SE: 21.1 ± 3.1 and 20.7 ± 3.1 °C) – see Fig. 8. The difference between SST and temperature at maximum depth varied between 0 and 6.2 °C, and was at its highest in July (mean ± SE: 3.6 ± 1.4 °C) and lowest in February (0.09 ± 0.1 °C). This

smaller difference between SST and temperature at maximum depth coincides with the strong deepening of the mixed layer from October to February (Fig. 8).

3.4.4. Mixed layer depth and thermocline

The deepness of the mixed layer at turtles' locations increased substantially between August and November (mean ± SE: 31.6 ± 10.7 vs. 96.1±49.7 m) – see Figs. 8 and 9. The lower limit of the thermocline also deepened from June (9.4 m, *n*=2) to November (mean ± SE: 260.3 ± 121.7 m, *n*=8), then became slightly shallower (February mean ± SE: 175.5 ± 43.3 m, *n*=3). The turtles remained above it while occupying HRT areas (from October). Before reaching HRT areas (June to October), the turtles dived mainly below the mixed layer (Fig. 9). Afterwards, they performed shallower dives from October to February, remaining within the mixed layer (Fig. 9).

3.4.5. Nutricline and halocline

Turtle maximum dive depth was positively correlated to the vertical
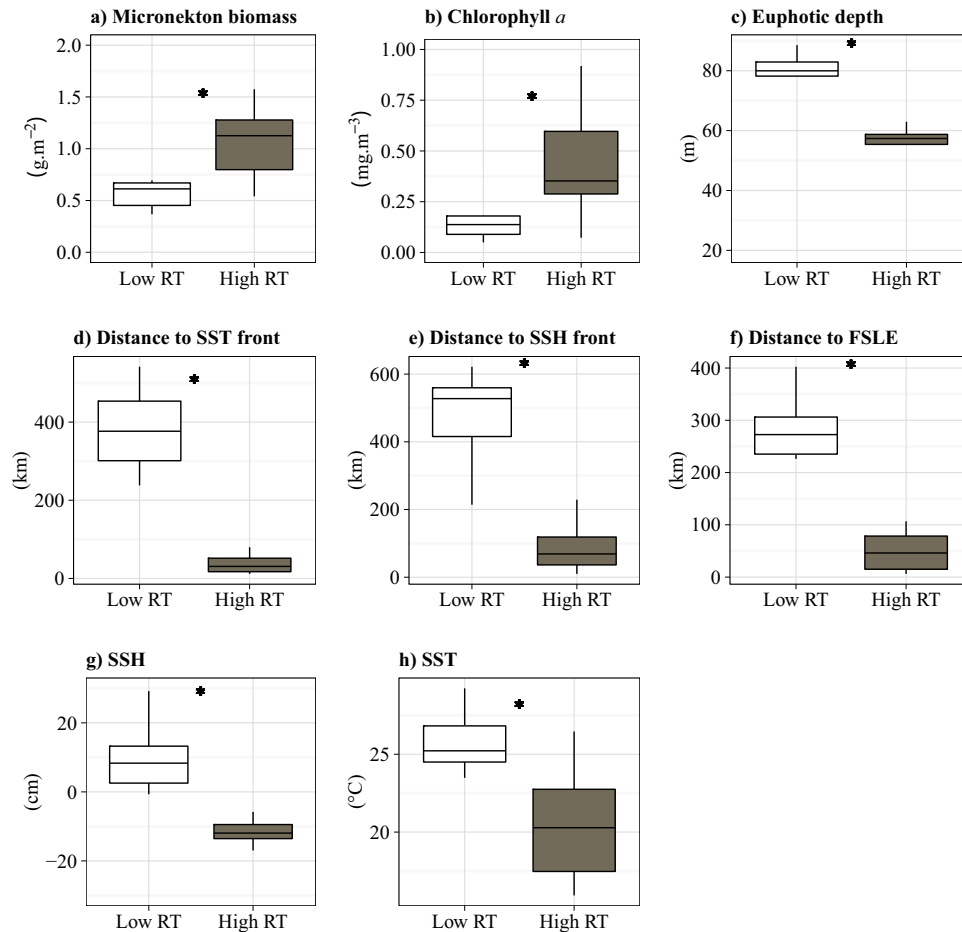
Fig. 3. Box plots of micronekton biomass (a), chlorophyll *a* concentration (b), euphotic depth (c), distance to the closest SST front (d), distance to the closest SSH front (e), distance to the closest FSLE filament (f), SSH (g) and SST (h) for both modes (low RT in white and high RT in dark grey). The stars in each plot indicate the significant differences between the two modes for each variable.

chlorophyll *a* gradient magnitude (nutricline depth derived from model forecast, Spearman correlation test: $R^2=0.34$, $p<0.001$) and to the depth at which chlorophyll *a* concentration is maximum (Spearman correlation test: $R^2=0.41$, $p<0.001$). However, the maximum dive depth reached by the leatherback was not correlated to the magnitude of the vertical salinity gradient (halocline depth derived from model forecast, Spearman correlation test: $R^2=-0.015$, $p=0.682$).

4. Discussion

The use of satellite tracking together with a set of environmental variables (from remote sensing data and model simulations) in this study allowed us to shed light on the role played by the Gulf Stream frontal system in the selection of areas eliciting high residence times (HRT) by the North Atlantic leatherback turtle.

4.1. Migration across the North Atlantic basin

The movement and diving behaviours of the leatherback turtle have been comprehensively investigated on an international scale over the past decade, with particular attention paid to their migration cycle across the Atlantic Ocean (Bailey et al., 2012b; Eckert et al., 2006b; Fossette et al., 2010b, 2010a; James et al., 2005a, 2005b; Ferraroli et al., 2004; Hays et al., 2004; McMahon and Hays, 2006; López-Mendilaharsu et al., 2009; Dodge et al., 2014). Although numerous studies have been conducted in populations from western French Guiana (Fossette et al., 2008, 2010b, 2010a), the present study is the first to investigate the movements and diving behaviour of individuals

from the Eastern population. Despite the genetic differences between the two French Guianese populations (Molfetti et al., 2013), the eastern and western individuals showed similar movement patterns. Indeed, like adult females from the Western population (see Fossette et al., 2010b, 2010a; Ferraroli et al., 2004), our tracked individuals migrated northward to reach relatively higher latitudes (> 30 °N) where they tended to display movement behaviour leading to a local increase in residence time during autumn and winter, in either coastal or pelagic habitats. The HRT spent in some particular areas at mid-latitudes indicate that these areas may correspond to foraging grounds. The importance of these potential foraging grounds for this species is reinforced by previous studies that have already reported same hot-spots for the leatherback in Florida, Nova Scotia and the Azores (Eckert et al., 2006b; Fossette et al., 2010a, 2010b; Ferraroli et al., 2004; James et al., 2006; Hamelin et al., 2014). After occupying HRT areas at mid-latitudes, the two turtles that transmitted data for the longest tracking durations headed back southward. While in high RT areas, these two individuals have experienced low SST reaching up to 12 °C. Despite these occasional SST encountered, for most of our tracked turtles, the thermal barrier seemed to occur between the 15–20 °C SST isotherm while foraging, with 77% of the turtles remaining in warmer water than 15 °C. These findings are in accordance with the 15 °C thermal tolerance suggested by McMahon and Hays (2006) for this species. Indeed, despite their endothermic capacity (James and Mrosovsky, 2004), it has been suggested that temperature thresholds might limit the amount of time the leatherback turtles can spend in some cold water areas (Witt et al., 2007). The relatively short tag life (6 ± 2 months) was however a drawback for this study, which would

a) SST: 10−16/08/15 (Low RT) **b) SST: 9−15/11/15 (High RT)** **c) SST: 8−14/02/16 (Low RT)**

d) SSH: 10−16/08/15 (Low RT) **e) SSH: 9−15/11/15 (High RT)** **f) SSH: 8−14/02/16 (Low RT)**
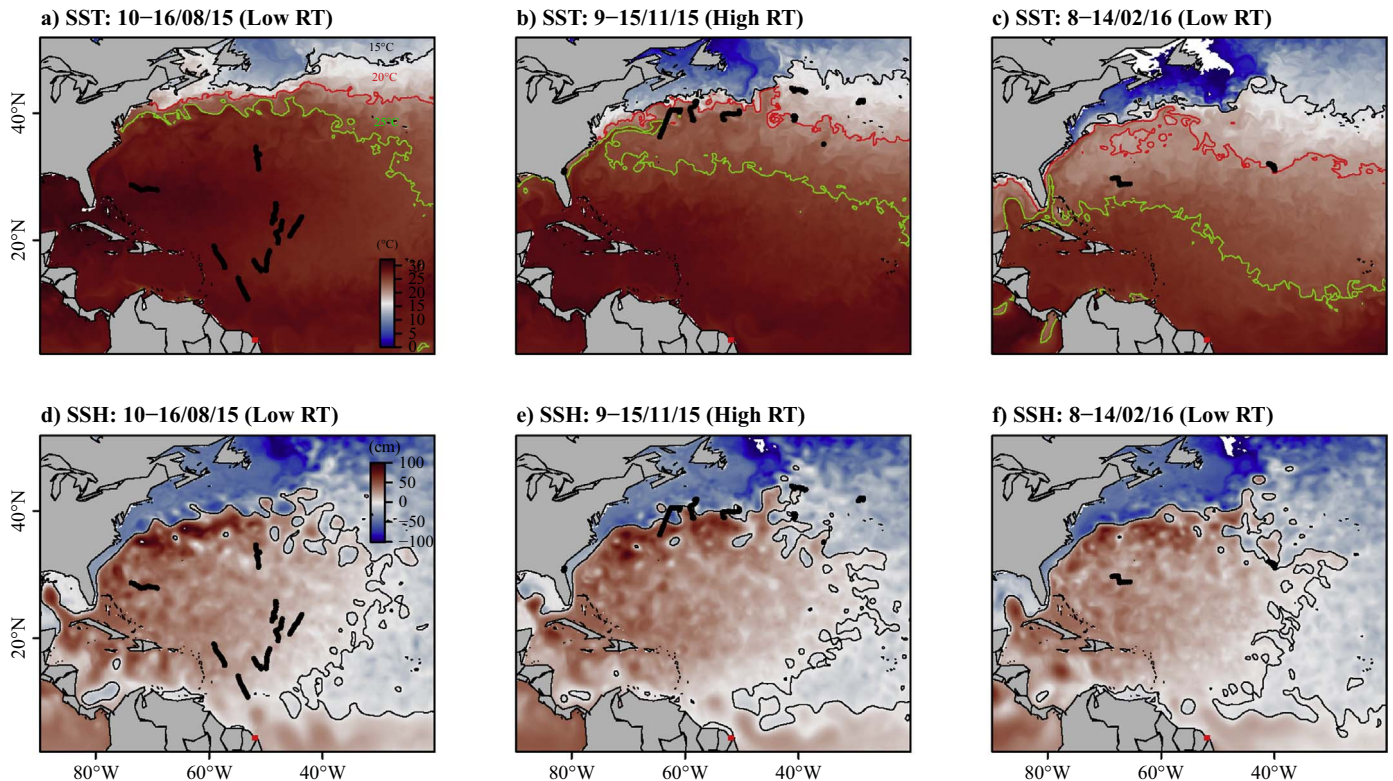
Fig. 4. Maps of the weekly averaged SST (a, b, c) and SSH (d, e, f) derived from Copernicus during three phases: the crossing of the North Atlantic gyre (a, d: low RT, *n*=10), the high RT period at mid-latitudes (b, e, *n*=10) and after leaving the high RT areas (c, f, *n*=3). Three SST contours were superimposed: 15 °C, 20 °C and 25 °C, and the SSH contour (0 cm) refers to the location of the Gulf Stream front. The black dots correspond to the locations of the leatherback turtles tracked from French Guiana for the corresponding week and the red square to the migration starting point. (For interpretation of the references to color in this figure legend, the reader is referred to the web version of this article.)

require a period of 2−4 years to track the entire remigration cycle across the North Atlantic Basin. There is thus a clear need for further tag deployment to identify the different habitats targeted by this species during post-nesting migration.

4.2. Associations with biological variables

In this study, the leatherback turtles travelled at high speed when crossing the nutrient-poor North Atlantic subtropical gyre, reflecting a transit behaviour. This area is considered as an 'ocean desert' (Tomczak and Godfrey, 2013), due to its scant primary productivity (0.50 mg C m^{-2} d^{-1}, Marañón et al., 2000). In contrast, the turtles spent more time and concentrated searching in HRT areas in the colder waters of upwelling and mid-latitude regions (Marañón et al., 2000), where primary productivity can reach up to 1000 mg C m^{-2} d^{-1}. There is a lack of documentation concerning the spatial distribution of jellyfish (Houghton et al., 2006), but primary production or chlorophyll *a* concentration were evidenced to be good proxies for leatherback prey availability (Fossette et al., 2010a; Dodge et al., 2014). The probability to forage was shown to increase with chlorophyll *a* concentration (up to 2.5 mg m^{-3}) for the Western Pacific (Bailey et al., 2012b) and the North Atlantic populations (Dodge et al., 2014). Similar results were found in our study, where values of chlorophyll *a* on assumed foraging grounds (corresponding to HRT areas) reached concentrations up to three times higher than those recorded in transit areas (0.18 ± 0.04 vs. 0.53 ± 0.13 mg m^{-3}, respectively). Furthermore, a clear match was observed between the high chlorophyll *a* concentrations and the HRTs, evidencing a remarkable synchronization of this species with areas of high productivity in the North Atlantic. However, as chlorophyll *a* concentrations come from forecasting ocean models (Copernicus database), we can observed some discrepancies, such as the subtropical gyres of the North Atlantic that are predicted slightly too oligotrophic, or the over-estimation of the chlorophyll *a* in the tropical band. Such differences may lead to misinterpretation of tracking data when looking at fine-scale

movements (1−10 s of km). But the purpose of our study was to look at mesoscale patterns (10−100 km) and consider relative chlorophyll *a* values (and not absolute values) to fit the accuracy of our tracking data, making the output of Copernicus model adequate and reliable.

As mentioned by Fossette et al. (2010b), a more reliable picture of jellyfish distribution may be obtained by looking at a higher trophic level than chlorophyll *a* (Strömberg et al., 2009). In this context, SEAPODYM recently appeared as a promising model to provide estimations of the spatio-temporal distribution of micronekton, including cephalopods, crustaceans, fishes and jellyfish (Lehodey et al., 2010). We therefore hypothesized that the micronekton biomass provided by this model would match locations of foraging leatherbacks better than chlorophyll *a*. Although the presence of chlorophyll *a* seemed to better match the occurrence of HRT areas, levels of micronekton at these locations were more than twice higher than those found in low RT areas (0.55 ± 0.04 vs. 1.31 ± 0.25 g m^{-2}). SEAPODYM predictions were based on the maturation time of pelagic organisms, i.e. 1−2 months for zooplankton and 10 months for micronekton (both at 15 °C; Conchon, unpublished data), but the maturation time of jellyfish is shorter than 10 months. This may explain why the concentration of micronekton biomass was not at its highest in HRT areas at mid-latitudes. A further study including the zooplankton output updated from SEAPODYM may nevertheless provide a better explanation for the habitat selection by leatherbacks.

4.3. Associations with physical discontinuities

The Eastern French Guianese leatherback turtles we tracked tended to display HRT behaviour mainly along physical discontinuities at mid-latitudes (> 30 °N), probably because such interfaces correspond to nutrient-rich waters where jellyfish aggregate (Sims and Quayle, 1998; Greer et al., 2013; Powell and Ohman, 2015). At the northern edge of the Gulf Stream, its warm waters meet the cold Labrador Current

a) Residence time

b) Chlorophyll *a*

c) Distance to SST front

d) Distance to SSH front

e) Distance to FSLE
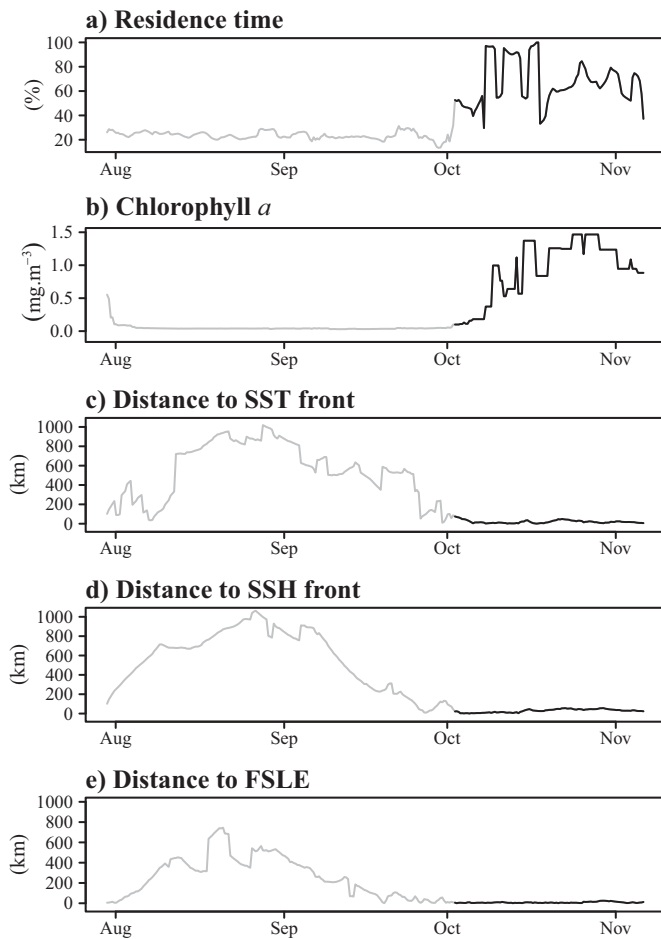
Fig. 5. Proportion of RT (a, in %) and four environmental variables (b, c, d, e) extracted along the track of turtle #149680, namely: chlorophyll *a* concentration (b), distance to the closest SST front (c), distance to the closest SSH front (d) and distance to the closest FSLE filament (e). The highest RT values (from October onwards) were considered to be a foraging activity, and the black parts of the lines refer to the putative foraging mode.

waters, creating a sharp temperature gradient in an area referred as the Gulf Stream north wall (GSNW, Sanchez-Franks et al., 2015). The shelf-slope front (SSF), a front located off the northeast coast of the United States and Canada, separates colder, less saline continental shelf waters from warmer and more saline slope waters (Bisagni et al., 2009), where most of our turtles (60%) displayed HRT behaviour. However, the HRT areas of three turtles were located on the shelf waters south of North Carolina-United States, in the South Atlantic Bight, where they used the lower branch of the Gulf Stream, characterized by much less extreme temperature gradients. Our results highlighted a surprising synchronization and aggregation of all the leatherback turtles between these two fronts before migrating back south.

HRT areas tended to occur preferentially along the SST and SSH gradients, as well as along the FSLE filaments. The identification of these frontal zones enabled us to delineate the frontal boundaries of the GSNW and the SSF. The strong association with these physical discontinuities was confirmed by the shorter distance to the closest front (SST gradient, SSH gradient and FSLE filament) while in HRT areas compared to transit periods. Several studies have already described the tendency for some sea turtles species (loggerhead and leatherback) to associate with frontal structures in the Pacific with the Kuroshio Current (Polovina et al., 2004, 2006; Polovina and Howell, 2005; Scales et al., 2015), or in Atlantic Ocean with the Gulf Stream (Eckert et al., 2006b; Fossette et al., 2010a; Lutcavage, 1996; Witherington, 2002). But to date, only one study has demonstrated such affinities between the leatherback movements and the Gulf Stream

frontal system using oceanographic data (Dodge et al., 2014), but such findings were limited to the horizontal dimension and true for a limited number of individuals (n=2). The associations with filaments at the sub-mesoscale in our study (identified via FSLE), in agreement with findings in previous studies conducted on penguins (Lowther et al., 2014; Bon et al., 2015; Whitehead et al., 2016) and seals (Nordstrom et al., 2013; Lowther et al., 2014), confirms the importance of frontal areas in the aggregation of prey.

Regions of high FSLE and strong SSH and SST gradients may all provide complementary data facilitating the interpretation of animal tracking (De Monte et al., 2012). Strong SSH gradients correspond to high kinetic energy and high FSLE to confluence/frontal regions, while a strong SST gradient corresponds to frontal regions marked by temperature difference, where upwelling/downwelling can occur. These three diagnostics can diverge in regions of intermediate or weak kinetic energy, where a confluence is the result of the interaction of multiple mesoscale features and of their temporal evolution and in which high SST gradients only occur at certain confluences (D'Ovidio et al., 2013). However, these diagnostics may be strongly correlated in highly energetic and contrasted regions where gradient intensification by the mesoscale currents arises on relative short time scales (i.e. days), and coincide with the occurrence of strong temperature gradients. This is the case for the branch of the Gulf Stream targeted by the turtles in our study, and may explain why the associations with frontal areas are similar in terms of SST gradients, FSLE, and SSH contours.

4.4. Affinities for vertical structures

The leatherback turtles we tracked performed shallower dives while in HRT areas (38.5 ± 7.9 m) than during transit (82.4 ± 5.6 m). This is in accordance with the behaviour of individuals of the Western French Guianese population (53.6 ± 33.1 vs. 81.8 ± 56.2 m, Fossette et al., 2010a). This behaviour should enable them to get an easier access to prey, which is assumed to concentrate in the upper layer (Hays et al., 2008). The analysis of residence time data showed that the tracked females started to display HRT behaviour during early autumn (October), when the phytoplankton bloom begins along the GSNW (Friedland et al., 2016) and the phytoplankton net growth rate increases in the subarctic Atlantic waters located further north (> 40 °N, Behrenfeld, 2010). We equipped our turtles at the nesting peak in June to obtain a reliable picture of the population trend. Despite the low light conditions in the North Atlantic during autumn and winter, the deep winter mixing of the upper layer favours the phytoplankton bloom formation via biomass accumulation (Behrenfeld, 2010). During low stratification months (October-May) in the South Atlantic Bight, where three turtles spent most of their time, the winds and small temperature differences between nutrient-rich water intrusions and the overlaying cold waters bring subsurface nutrient intrusions to the upper layers, as well as cold air outbreaks, favouring the frequent vertical redistribution of chlorophyll *a* and therefore avoiding nutrient depletion in this region (Martins and Pelegrí, 2006).

As our turtles performed mostly shallow dives while in HRT areas at mid-latitudes, the depths they reached during this period were mainly within the mixed layer. In the North Atlantic, the deepest mixed layer occurs between January and May during deep water formation at ~40 °N (Kara et al., 2003). The mixed layer started deepening in October at locations further south (30–40 °N) where the turtles aggregated, coinciding with the period when the turtles started performing shallower dives. The turtles remained within this mixed layer while in HRT areas over the winter period (n=4 in January to n=1 in April). A similar behaviour was observed by Fossette et al. (2010a) for the Eastern French Guianese leatherback turtles, and could be performed to get an easier access to their prey by maximizing energy gain while foraging. Reaching shallower depths while in HRT areas may also reflect the distribution of jellyfish, which is known to be more abundant in the upper layer in cold waters (Longhurst et al., 1995).
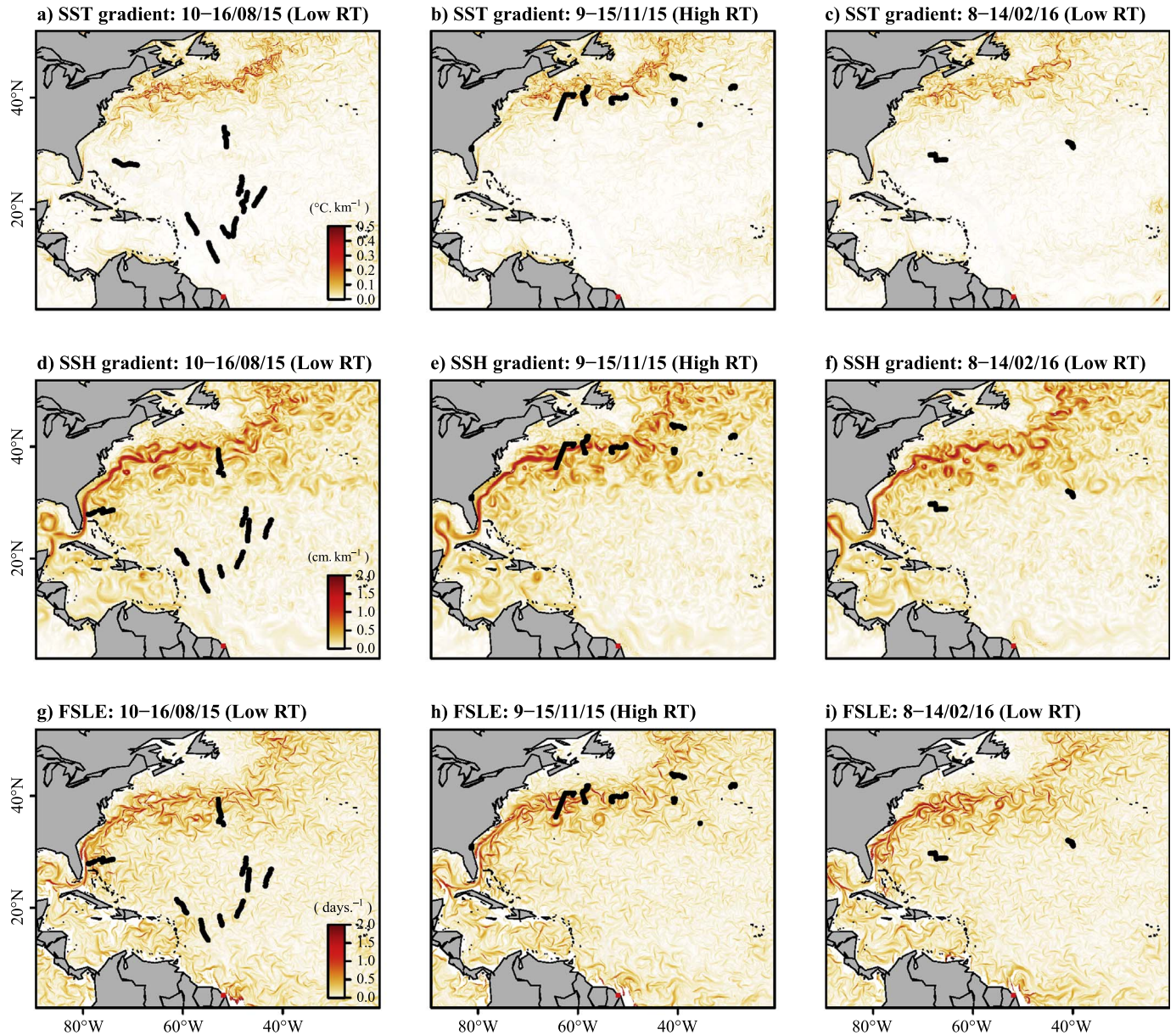
Fig. 6. Maps of the weekly averaged SST gradient (a, b, c), SSH gradient (d, e, f) and FSLE (g, h, i) during three phases: the crossing of the North Atlantic gyre (a, d, g: low RT, *n*=10), the high RT period at mid-latitudes (b, e, h, *n*=10) and after leaving the high RT areas (c, f, i, *n*=3). The oceanic frontal zones were associated with the highest values of the three gradients. The black dots correspond to the locations of the leatherback turtles tracked from French Guiana for the corresponding week and the red square to the migration starting point. (For interpretation of the references to color in this figure legend, the reader is referred to the web version of this article.)

This deep mixed layer, associated with high nutrient biomass, may therefore explain the remarkable aggregation of leatherback turtles at higher latitudes during autumn and winter. Although the deepest mixed layer commonly occurs during winter, it occurs during the austral autumn in the southern hemisphere in the Western Australia and coincides with high values of chlorophyll *a* (Rousseaux et al., 2012), thus enabling the replenishment of the surface waters via vertical mixing. The turtles in our study remained within the mixed layer while in HRT areas (i.e. above the upper limit of the thermocline) and dove below it while in other areas, and did not show any particular association with the thermocline or any other strong vertical gradient area (halocline or nutricline), contrary to findings in previous studies conducted on fur seals (Nordstrom et al., 2013), Atlantic olive ridleys (Chambault et al., 2016) and Atlantic leatherback turtles (Bailey et al., 2012a; Hamelin et al., 2014). This difference may be explained by the methodology used to calculate the vertical gradients: the thermocline is commonly defined based on the temperature gradient magnitude

(Bailey et al., 2012a), but this approach can be biased by incomplete temperature profiles (over the continental shelf) or insufficient depths reached by the individuals. To avoid a possibly biased identification of the thermocline depth, we decided to use the MLD provided by Copernicus as the upper limit, and the deepest mixed layer during the previous winter peak for the lower limit. In contrast, Hamelin et al. (2014) used *in situ* temperatures provided by CTD tags to determine the thermocline, which probably resulted in less errors and a better resolution than when using the outputs from ocean forecasts such as Copernicus.

In the North Atlantic, the breakdown of the seasonal thermocline under the effects of storms and winds during autumn leads to deep mixed layer that generates a quasi-uniform layer of temperature (isothermal layer) throughout the water column, with relatively homogeneous values between the upper layer of the thermocline and the surface (Lentz et al., 2003). Unlike the cooler SST encountered when performing HRT behaviour (20.0 ± 3.9 °C, range: 15.9–26.3 °C), the

a) Maximum dive depth   b) Dive duration
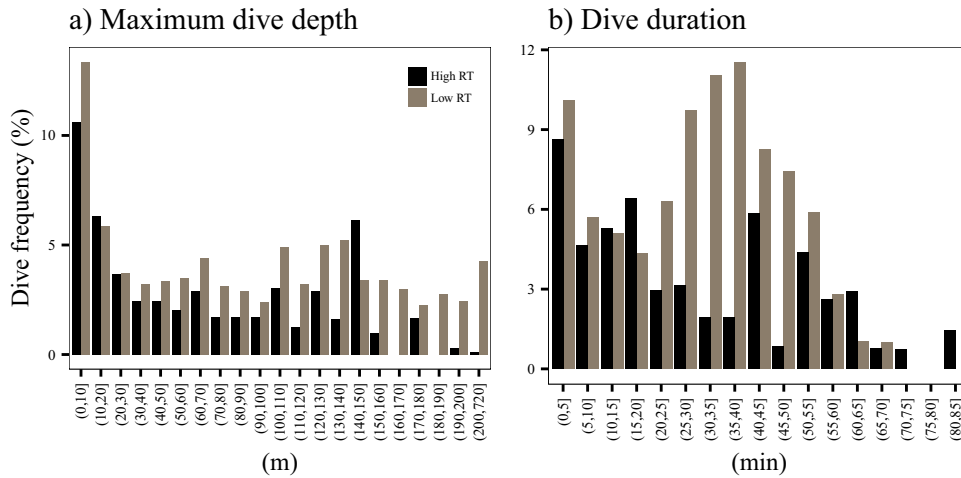
Fig. 7. Histograms of the maximum dive depth (a) and the dive duration (b) for the 10 tags deployed in 2014 (*n*=1) and 2015 (*n*=9) and for both modes (low RT in grey vs. high RT in black).
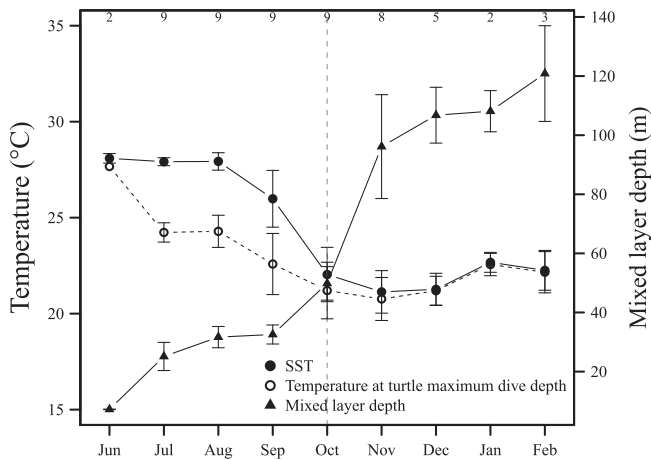
Fig. 8. Monthly mean (± SE) of SST (filled dots), *in situ* temperature at the turtle maximum dive depth (empty dots) and mixed layer depth (triangles) extracted for the 9 SRDL tags and from Copernicus database. The vertical dotted line refers to the beginning of the high RT period for the majority of the turtles. The numbers refer to the sample size of each box plot (i.e. the number of turtles).
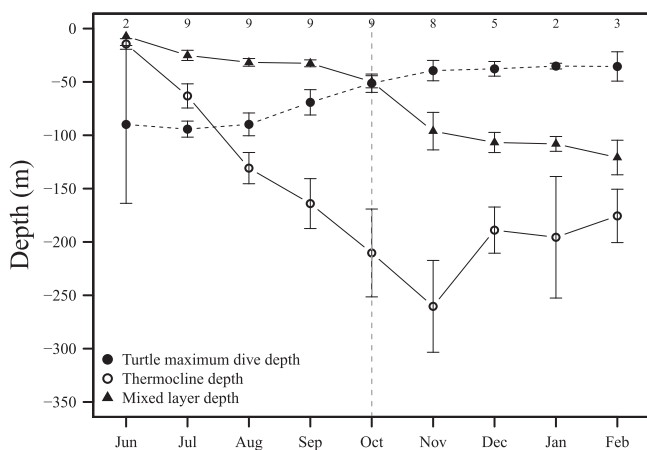
Fig. 9. Monthly mean (± SE) of turtle maximum dive depth (filled dots), lower limit of the thermocline (empty dots) and mixed layer depth (triangles) extracted for the 9 SRDL tags. The lower limit of the thermocline and the mixed layer depth were extracted from the Copernicus database. The vertical dotted line refers to the beginning of the high RT period for the majority of the turtles. The numbers refer to the sample size of each box plot (i.e. the number of turtles).

turtles experienced warm SST during their transit across the subtropical gyre (28.1 ± 1.8 °C, range: 20.9–30.9 °C). Besides the SST difference between the two movement modes, there was also a significant temperature difference of up to 4.2 °C between the surface and the maximum dive depth within the gyre. While crossing the gyre, the females therefore experienced shallow mixed layer and warm temperatures. As Fossette et al. (2010a) found for the western French Guianese population, our eastern French Guianese turtles performed deep dives (104 ± 80.7 m) in this nutrient-poor area (Marañón et al., 2000; Strömberg et al., 2009), which may indicate that they targeted cooler temperatures in deeper layers to save energy during the transit phase of their migration. The selection by these turtles of HRT areas located at mid-latitudes suggests a preference for cool waters (mean temperature at maximum depth: 19.1 ± 4.9 °C), as observed in leatherbacks from the East Pacific population (Bailey et al., 2012b). The long post-dive surface intervals (13.1 ± 2.4 min) observed in our study reinforce the hypothesis that some individuals may swim at the surface to process and eat large prey items in the Northwest Atlantic (James and Mrosovsky, 2004). The deployment of 3D-acceleration data loggers together with cameras should make it possible to identify prey catch attempts during the dives, and therefore relate this activity to leatherback diving behaviour. Despite the relatively low number of dives recorded by the 9 SRDL tags (*n*=720), the 4614 dives collected by the Argos-GPS tag provide complementary dive data to support the first evidence of the use of the mixed layer by the adult female leatherback turtles during post-nesting migration across the North Atlantic. While in high RT areas, the shallower diving behaviour of the turtles (within the first 55 m) was already evidenced by a previous study (Fossette et al., 2010b), which therefore reinforces the observed pattern of the turtles remaining mainly within the deep mixed layer. In a lesser extent, the low number of dives recorded could however prevent from observing some occasional deep dives performed below the mixed layer. To cope with this limitation, some additional SRDL tags programmed to collect several daily profiles need to be further deployed. The deployment of additional tags over longer periods (at least one year) is required to collect complementary data on both the horizontal and vertical movements, since leatherback behaviour shows inter-annual variability.

5. Conclusion

The present study is the first to document the post-nesting migration movements of the Eastern French Guianese population of leatherback turtles. Our findings highlight the crucial role of the Gulf Stream front in the selection of potential foraging habitats by this species. The use of innovative

and 3D ocean models for estimating SSH, temperature, salinity, chlorophyll *a*, FSLE (computed from satellite-derived currents), and micronekton biomass (from SEAPODYM) enabled us to investigate the link between leatherback movements and frontal structures in both the horizontal and vertical dimensions. Although the high residence time areas of the turtles were geographically remote (spread between 80–30 ºW and 28–45 ºN), these probable foraging grounds were all found in close proximity to the Gulf Stream frontal zone, a highly dynamic and productive physical discontinuity separating the warm and salty waters of the Gulf Stream from the cold and less-saline waters of the Labrador Current. As seen in other oceanic fronts, this extensive area is known to enhance primary production and thus aggregate low trophic level organisms such as jellyfish, which is the main food resource for leatherback turtles. In a context of climate change, anticipating the evolution of such frontal structure under the influence of global warming is crucial to ensure the conservation of this vulnerable species.

Acknowledgments

References

Acha, E.M., Mianzan, H.W., Guerrero, R.A., Favero, M., Bava, J., 2004. Marine fronts at the continental shelves of austral South America: physical and ecological processes. J. Mar. Syst. 44, 83–105.

Bailey, H., Benson, S.R., Shillinger, G.L., Bograd, S.J., Dutton, P.H., Eckert, S.A., Morreale, S.J., Paladino, F.V., Eguchi, T., Foley, D.G., Block, B.A., Piedra, R., Hitipeuw, C., Tapilatu, R.F., Spotila, J.R., 2012a. Identification of distinct movement patterns in Pacific leatherback turtle populations influenced by ocean conditions. Ecol. Appl. 22, 735–747.

Bailey, H., Fossette, S., Bograd, S.J., Shillinger, G.L., Swithenbank, A.M., Georges, J.-Y., Gaspar, P., Strömberg, K.H.P., Paladino, F.V., Spotila, J.R., Block, B.A., Hays, G.C., 2012b. Movement patterns for a critically endangered species, the leatherback turtle (*Dermochelys coriacea*), linked to foraging success and population status. PLOS ONE 7, e36401.

Bailleul, F., Cott, C., Guinet, C., 2010. Mesoscale eddies as foraging area of a deep-diving predator, the southern elephant seal. Mar. Ecol. Prog. Ser. 408, 251–264.

Barraquand, F., Benhamou, S., 2008. Animal movements in heterogeneous landscapes: identifying profitable places and homogeneous movement bouts. Ecology 89, 3336–3348.

Behrenfeld, M.J., 2010. Abandoning Sverdrup's critical depth hypothesis on phytoplankton blooms. Ecology 91, 977–989.

Belkin, I., Krishfield, R., Honjo, S., 2002. Decadal variability of the North Pacific Polar Front: Subsurface warming versus surface cooling. Geophys. Res. Lett. 29, (65–1).

Belkin, I.M., Cornillon, P.C., Sherman, K., 2009. Fronts in large marine ecosystems. Prog. Oceanogr. 81, 223–236.

Benhamou, S., Riotte-Lambert, L., 2012. Beyond the Utilization Distribution: identifying home range areas that are intensively exploited or repeatedly visited. Ecol. Model 227, 112–116.

Bisagni, J.J., Kim, H.-S., Chaudhuri, A., 2009. Interannual variability of the shelf-slope front position between 75° and 50°W. J. Mar. Syst. 78, 337–350.

Block, B.A., Dewar, H., Blackwell, S.B., Williams, T.D., Prince, E.D., Farwell, C.J., Boustany, A., Teo, S.L.H., Seitz, A., Walli, A., Fudge, D., 2001. Migratory movements, depth references, and thermal biology of Atlantic Bluefin Tuna. Science 293, 1310–1314.

Block, B.A., Teo, S.L.H., Walli, A., Boustany, A., Stokesbury, M.J.W., Farwell, C.J., Weng, K.C., Dewar, H., Williams, T.D., 2005. Electronic tagging and population structure of Atlantic bluefin tuna. Nature 434, 1121–1127.

Bon, C., Della Penna, A., Ovidio, F. d.', Y.P. Arnould, J., Poupart, T., Bost, C.-A., 2015. Influence of oceanographic structures on foraging strategies: macaroni penguins at Crozet Islands. Mov. Ecol. 3, 32.

Bradshaw, C.J.A., Hindell, M.A., Sumner, M.D., Michael, K.J., 2004. Loyalty pays: potential life history consequences of fidelity to marine foraging regions by southern elephant seals. Anim. Behav. 68, 1349–1360.

Brodeur, R.D., Seki, M.P., Pakhomov, E., Suntsov, A.V., 2005. Micronekton-What are they and why are they important. Pac. Mar. Sci. Org. Press 13, 7–11.

Chambault, P., Pinaud, D., Vantrepotte, V., Kelle, L., Entraygues, M., Guinet, C., Berzins, R., Bilo, K, Gaspar, P., Thoisy, B., de, Maho, Y.L., Chevallier, D., 2015. Dispersal and diving adjustments of the green turtle chelonia mydas in response to dynamic environmental conditions during post-nesting migration. PLOS ONE 10, e0137340.

Chambault, P., Thoisy, B. de, Heerah, K., Conchon, A., Barrioz, S., Dos Reis, V., Berzins, R., Kelle, L., Picard, B., Roquet, F., Le Maho, Y., Chevallier, D., 2016. The influence of oceanographic features on the foraging behavior of the olive ridley sea turtle *Lepidochelys olivacea* along the Guiana coast. Prog. Oceano. 142, 58–71.

Cotté, C., Park, Y.-H., Guinet, C., Bost, C.-A., 2007. Movements of foraging king penguins through marine mesoscale eddies. Proc. R. Soc. Lond. B Biol. Sci. 274, 2385–2391.

D'Ovidio, F., Fernández, V., Hernández-García, E., López, C., 2004. Mixing structures in the Mediterranean Sea from finite-size Lyapunov exponents. Geophys. Res. Lett. 31, L17203.

D'Ovidio, F., Monte, S.D., Alvain, S., Dandonneau, Y., Lévy, M., 2010. Fluid dynamical niches of phytoplankton types. Proc. Natl. Acad. Sci. 107, 18366–18370.

D'Ovidio, F., Monte, S.D., Penna, A.D., Cotté, C., Guinet, C., 2013. Ecological implications of eddy retention in the open ocean: a Lagrangian approach. J. Phys. Math. Theor. 46, 254023.

De Monte, S., Cotté, C., Ovidio, F. d.', Lévy, M., Corre, M.L., Weimerskirch, H., 2012. Frigatebird behaviour at the ocean–atmosphere interface: integrating animal behaviour with multi-satellite data. J. R. Soc. Interface 9, 3351–3358.

Dodge, K., Galuardi, B., Miller, T.J., Lutcavage, M.E., 2014. Leatherback turtle movements, dive behavior, and habitat characteristics in ecoregions of the Northwest Atlantic Ocean. PLOS ONE 9, e91726.

Doniol Valcroze, T., Berteaux, D., Larouche, P., Sears, R., 2007. Influence of thermal fronts on habitat selection by four rorqual whale species in the Gulf of St. Lawrence. Mar. Ecol. Prog. Ser. 335, 207–216.

Druon, J., Panigada, S., David, L., Gannier, A., Mayol, P., Arcangeli, A., Caadas, A., Laran, S., Mglio, N.D., Gauffier, P., 2012. Potential feeding habitat of fin whales in the western Mediterranean Sea: an environmental niche model. Mar. Ecol. Prog. Ser. 464, 289–306.

Ducet, N., Le Traon, P.Y., Reverdin, G., 2000. Global high-resolution mapping of ocean circulation from TOPEX/Poseidon and ERS-1 and −2. J. Geophys. Res. Oceans 105, 19477–19498.

Eckert, S.A., Bagley, D., Kubis, S., Ehrhart, L., Johnson, C., Stewart, K., DeFreese, D., 2006b. Internesting and Postnesting movements and foraging habitats of leatherback Sea turtles (*Dermochelys coriacea*) nesting in Florida. Chelonian Conserv. Biol. 5, 239–248.

Etnoyer, P., Canny, D., Mate, B.R., Morgan, L.E., Ortega-Ortiz, J.G., Nichols, W.J., 2006. Sea-surface temperature gradients across blue whale and sea turtle foraging trajectories off the Baja California Peninsula, Mexico. Deep Sea Res. Part II Top. Stud. Oceanogr. 53, 340–358.

Fedak, M.A., Lovell, P., Grant, S.M., 2001. Two approaches to compressing and interpreting time-depth information as collected by time-depth recorders and satellite-linked data recorders. Mar. Mammal Sci. 17, 94–110.

Ferraroli, S., Georges, J.-Y., Gaspar, P., Maho, Y.L., 2004. Endangered species: where leatherback turtles meet fisheries. Nature 429, 521–522.

Fossette, S., Kelle, L., Girondot, M., Goverse, E., Hilterman, M.L., Verhage, B., Thoisy, B. de, Georges, J.-Y., 2008. The world's largest leatherback rookeries: a review of conservation-oriented research in French Guiana/Suriname and Gabon. J. Exp. Mar. Biol. Ecol. 356, 69–82.

Fossette, S., Hobson, V.J., Girard, C., Calmettes, B., Gaspar, P., Georges, J.-Y., Hays, G.C., 2010b. Spatio-temporal foraging patterns of a giant zooplanktivore, the leatherback turtle. J. Mar. Syst. 81, 225–234.

Fossette, S., Girard, C., López-Mendilaharsu, M., Miller, P., Domingo, A., Evans, D., Kelle, L., Plot, V., Prosdocimi, L., Verhage, S., Gaspar, P., Georges, J.-Y., 2010a. Atlantic leatherback migratory paths and temporary residence areas. PLoS ONE 5, e13908.

Franeker, J.A. van, Brink, N.W. van den, Bathmann, U.V., Pollard, R.T., Baar, H.J.W. de, Wolff, W.J., 2002. Responses of seabirds, in particular prions (Pachyptila sp.), to small-scale processes in the Antarctic Polar Front. Deep Sea Res. Part II Top. Stud. Oceanogr. 49, 3931–3950.

Friedland, K.D., Record, N.R., Asch, R.G., Kristiansen, T., Saba, V.S., Drinkwater, K.F., Henson, S., Leaf, R.T., Morse, R.E., Johns, D.G., Large, S.I., Hjøllo, S.S., Nye, J.A., Alexander, M.A., Ji, R., 2016. Seasonal phytoplankton blooms in the North Atlantic linked to the overwintering strategies of copepods. Elem. Sci. Anthr. 4, 99.

Fuglister, F.C., 1963. Gulf stream '60. Prog. Oceano. 1, 265–373.

Gaspar, P., Georges, J.-Y., Fossette, S., Lenoble, A., Ferraroli, S., Maho, Y.L., 2006. Marine animal behaviour: neglecting ocean currents can lead us up the wrong track. Proc. R. Soc. B Biol. Sci. 273, 2697–2702.

Girard, C., Sudre, J., Benhamou, S., Roos, D., Luschi, P., 2006. Homing in green turtles *Chelonia mydas*: oceanic currents act as a constraint rather than as an information source. Mar. Ecol. Prog. Ser. 322, 281–289.

Graham, W.M., Pagès, F., Hamner, W.M., 2001. A physical context for gelatinous zooplankton aggregations: a review. Hydrobiologia 451, 199–212.

Greer, A.T., Cowen, R.K., Guigand, C.M., McManus, M.A., Sevadjian, J., 2013. Relationships between phytoplankton thin layers and the fine-scale vertical distributions of two trophic levels of zooplankton. J. Plankton Res. 35, 939–956.

Greer, A.T., Cowen, R.K., Guigand, C.M., Hare, J.A., 2015. Fine-scale planktonic habitat partitioning at a shelf-slope front revealed by a high-resolution imaging system. J. Mar. Syst. 142, 111–125.

Hamelin, K.M., Kelley, D.E., Taggart, C.T., James, M.C., 2014. Water mass characteristics and solar illumination influence leatherback turtle dive patterns at high latitudes. Ecosphere 5, 1–20.

Haney, J.C., McGillivary, P.A., 1985. Midshelf fronts in the south atlantic bight and their influence on seabird distribution and seasonal abundance. Biol. Oceanogr. 3, 401–430.

Hays, G.C., Houghton, J.D.R., Myers, A.E., 2004. Endangered species: pan-atlantic leatherback turtle movements. Nature 429, (522–522).

Hays, G.C., Doyle, T.K., Houghton, J.D.R., Lilley, M.K.S., Metcalfe, J.D., Righton, D., 2008. Diving behaviour of jellyfish equipped with electronic tags. J. Plankton Res. 30, 325–331.

Houghton, J.D.R., Doyle, T.K., Wilson, M.W., Davenport, J., Hays, G.C., 2006. Jellyfish aggregations and leatherback turtle foraging patterns in a temperate coastal environment. Ecology 87, 1967–1972.

James, M.C., Mrosovsky, N., 2004. Body temperatures of leatherback turtles (*Dermochelys coriacea*) in temperate waters off Nova Scotia, Canada. Can. J. Zool. 82, 1302–1306.

James, M.C., Eckert, S.A., Myers, R.A., 2005a. Migratory and reproductive movements of male leatherback turtles (*Dermochelys coriacea*). Mar. Biol. 147, 845–853.

James, M.C., Myers, R.A., Ottensmeyer, C.A., 2005b. Behaviour of leatherback sea turtles, *Dermochelys coriacea*, during the migratory cycle. Proc. R. Soc. Lond. B Biol. Sci. 272, 1547–1555.

James, M.C., Davenport, J., Hays, G.C., 2006. Expanded thermal niche for a diving vertebrate: a leatherback turtle diving into near-freezing water. J. Exp. Mar. Biol. Ecol. 335, 221–226.

Kara, A.B., Rochford, P.A., Hurlburt, H.E., 2000a. An optimal definition for ocean mixed layer depth. (July 15)J. Geophys. Res. Oceans 105, 16803–16821.

Kara, A.B., Rochford, P.A., Hurlburt, H.E., 2003. Mixed layer depth variability over the global ocean. J. Geophys. Res. Oceans 108, 3079.

Largier, J.L., 1993. Estuarine fronts: How important are they? Estuaries 16, 1–11.

Lavielle, M., 2005. Using penalized contrasts for the change-point problem. Signal Process 85, 1501–1510.

Le Fèvre, J., 1986. Aspects of the Biology of Frontal Systems, Advances in Marine Biology. Academic Press.

Lehodey, P., Senina, I., Murtugudde, R., 2008. A spatial ecosystem and populations dynamics model (SEAPODYM) – modeling of tuna and tuna-like populations. Prog. Oceanogr. 78, 304–318.

Lehodey, P., Murtugudde, R., Senina, I., 2010. Bridging the gap from ocean models to population dynamics of large marine predators: a model of mid-trophic functional groups. Prog. Oceanogr. 84, 69–84.

Lentz, S., Shearman, K., Anderson, S., Plueddemann, A., Edson, J., 2003. Evolution of stratification over the New England shelf during the Coastal Mixing and Optics study, August 1996–June 1997. J. Geophys. Res. Oceans 108, 3008.

Longhurst, A., Sathyendranath, S., Platt, T., Caverhill, C., 1995. An estimate of global primary production in the ocean from satellite radiometer data. J. Plankton Res. 17, 1245–1271.

Lopez, R., Malarde, J.-P., Royer, F., Gaspar, P., 2014. Improving argos doppler location using multiple-model kalman filtering. IEEE Trans. Geosci. Remote Sens. 52, 4744–4755.

López-Mendilaharsu, M., Rocha, C.F.D., Miller, P., Domingo, A., Prosdocimi, L., 2009. Insights on leatherback turtle movements and high use areas in the Southwest Atlantic Ocean. J. Exp. Mar. Biol. Ecol. 378, 31–39.

Lowther, A.D., Lydersen, C., Biuw, M., Bruyn, P.J.N. de, Hofmeyr, G.J.G., Kovacs, K.M., 2014. Post-breeding at-sea movements of three central-place foragers in relation to submesoscale fronts in the Southern Ocean around Bouvetøya. Antar. Sci. 26, 533–544.

Lozier, M.S., Owens, W.B., Curry, R.G., 1995. The climatology of the North Atlantic. Prog. Oceanogr. 36, 1–44.

Lutcavage, M.E., 1996. Planning your next meal: leatherback travel routes and ocean fronts. NOAA Tech. Memo. NMFS-SEFSC 378, 174–178.

Marañón, E., Holligan, P.M., Varela, M., Mouriño, B., Bale, A.J., 2000. Basin-scale variability of phytoplankton biomass, production and growth in the Atlantic Ocean. Deep Sea Res. Part Oceanogr. Res. Pap. 47, 825–857.

Marshall, J., Plumb, R.A., 2007. Atmosphere Ocean Climate Dynamics: an introduction text, International Geophysics 93. AP.

Martins, A.M., Pelegrí, J.L., 2006. CZCS chlorophyll patterns in the South Atlantic Bight during low vertical stratification conditions. Cont. Shelf Res. 26, 429–457.

McMahon, C.R., Hays, G.C., 2006. Thermal niche, large-scale movements and implications of climate change for a critically endangered marine vertebrate. Glob. Change Biol. 12, 1330–1338.

Molfetti, É., Vilaça, S.T., Georges, J.-Y., Plot, V., Delcroix, E., Scao, R.L., Lavergne, A., Barrioz, S., Santos, F.R. dos, Thoisy, B. de, 2013. Recent demographic history and present Fine-scale structure in the Northwest Atlantic leatherback (*Dermochelys coriacea*) turtle population. PLOS ONE 8, e58061.

Moore, S.E., Watkins, W.A., Daher, M.A., Davies, J.R., Dahlheim, M.E., 2002. Blue whale

habitat associations in the Northwest Pacific: analysis of remotely-sensed data using a Geographic Information System. Oceanography, 20–25.

Murase, H., Hakamada, T., Matsuoka, K., Nishiwaki, S., Inagake, D., Okazaki, M., Tojo, N., Kitakado, T., 2014. Distribution of sei whales (*Balaenoptera borealis*) in the subarctic–subtropical transition area of the western North Pacific in relation to oceanic fronts. Deep Sea Res. Part II Top. Stud. Oceano. 107, 22–28.

Nordstrom, C.A., Battaile, B.C., Cotté, C., Trites, A.W., 2013. Foraging habitats of lactating northern fur seals are structured by thermocline depths and submesoscale fronts in the eastern Bering Sea. Deep Sea Res. Part II Top. Stud. Oceano. 88–89, 78–96.

Olson, D.B., Backus, R.H., 1985. The concentrating of organisms at fronts: a cold-water fish and a warm-core Gulf stream ring. J. Mar. Res. 43, 113–137.

Olson, D.B., Hitchcock, G., Mariano, A., Ashjian, C., Peng, G., Nero, N., Podesta, G., 1994. Life on the edge: marine life and fronts. Oceanography 7, 52–60.

Polovina, J., Uchida, I., Balazs, G., Howell, E.A., Parker, D., Dutton, P., 2006. The Kuroshio extension bifurcation region: a pelagic hotspot for juvenile loggerhead sea turtles. Deep Sea Res. Part II Top. Stud. Oceano. 53, 326–339.

Polovina, J.J., Howell, E.A., 2005. Ecosystem indicators derived from satellite remotely sensed oceanographic data for the North Pacific. ICES J. Mar. Sci. J. Cons. 62, 319–327.

Polovina, J.J., Balazs, G.H., Howell, E.A., Parker, D.M., Seki, M.P., Dutton, P.H., 2004. Forage and migration habitat of loggerhead (*Caretta caretta*) and olive ridley (*Lepidochelys olivacea*) sea turtles in the central North Pacific Ocean. Fish Oceanogr. 13, 36–51.

Potter, I.F., Galuardi, B., Howell, W.H., 2011. Horizontal movement of ocean sunfish, Mola mola, in the northwest Atlantic. Mar. Biol. 158, 531–540.

Powell, J.R., Ohman, M.D., 2015. Covariability of zooplankton gradients with glider-detected density fronts in the Southern California Current System. Deep Sea Res. Part II Top. Stud. Oceano. 112, 79–90.

Reul, N., Chapron, B., Lee, T., Donlon, C., Boutin, J., Alory, G., 2014. Sea surface salinity structure of the meandering Gulf stream revealed by SMOS sensor. Geophys. Res. Lett. 41, (2014GL059215).

Rousseaux, C.S.G., Lowe, R., Feng, M., Waite, A.M., Thompson, P.A., 2012. The role of the Leeuwin Current and mixed layer depth on the autumn phytoplankton bloom off Ningaloo reef, Western Australia. Cont. Shelf Res. 32, 22–35.

Sanchez-Franks, A., Hameed, S., Wilson, R.E., 2015. The Icelandic low as a predictor of the Gulf stream North wall position. J. Phys. Oceanogr. 46, 817–826.

Scales, K.L., Miller, P.I., Hawkes, L.A., Ingram, S.N., Sims, D.W., Votier, S.C., 2014. REVIEW: on the Front Line: frontal zones as priority at-sea conservation areas for mobile marine vertebrates. J. Appl. Ecol. 51, 1575–1583.

Scales, K.L., Miller, P., Varo-Cruz, N., Hodgson, D.J., Hawkes, L.A., Godley, B.J., 2015. Oceanic loggerhead turtles *Caretta caretta* associate with thermal fronts: evidence from the Canary Current large marine ecosystem. Mar. Ecol. Prog. Ser. 519, 195–207.

Scheffer, A., Bost, C., Trathan, P., 2012. Frontal zones, temperature gradient and depth characterize the foraging habitat of king penguins at South Georgia. Mar. Ecol. Prog. Ser. 465, 281–297.

Schmitz, W.J., McCartney, M.S., 1993. On the North Atlantic circulation. Rev. Geophys. 31, 29–49.

Silva, M.A., Jonsen, I., Russel, D.J., Prieto, R., Thompson, D., 2014. Assessing performance of bayesian state-space models fit to argos satellite telemetry locations processed with kalman filtering. PLoS ONE 9.

Sims, D.W., Quayle, V.A., 1998. Selective foraging behaviour of basking sharks on zooplankton in a small-scale front. Nature 393, 460–464.

Skomal, G.B., Zeeman, S.I., Chisholm, J.H., Summers, E.L., Walsh, H.J., McMahon, K.W., Thorrold, S.R., 2009. Transequatorial migrations by basking sharks in the Western Atlantic Ocean. Curr. Biol. 19, 1019–1022.

Strömberg, K.H.P., Smyth, T.J., Allen, J.I., Pitois, S., O'Brien, T.D., 2009. Estimation of global zooplankton biomass from satellite ocean colour. J. Mar. Syst. 78, 18–27.

Sudre, J., Maes, C., Garçon, V., 2013. On the global estimates of geostrophic and Ekman surface currents. Limnol. Oceanogr. Fluids Environ. 3, 1–20.

Thorne, L.H., Read, A.J., 2013. Fine-scale biophysical interactions drive prey availability at a migratory stopover site for *Phalaropus spp.* in the Bay of Fundy, Canada. Mar. Ecol. Prog. Ser. 487, 261–273.

Tomczak, M., Godfrey, J.S., 2013. Regional Oceanography: An Introduction. Elsevier.

Whitehead, T.O., Kato, A., Ropert-Coudert, Y., Ryan, P.G., 2016. Habitat use and diving behaviour of macaroni *Eudyptes chrysolophus* and eastern *rockhopper E. chrysocome filholi* penguins during the critical pre-moult period. Mar. Biol. 163, 1–20.

Wilson, S.G., Lutcavage, M.E., Brill, R.W., Genovese, M.P., Cooper, A.B., Everly, A.W., 2004. Movements of bluefin tuna (Thunnus thynnus) in the northwestern Atlantic Ocean recorded by pop-up satellite archival tags. Mar. Biol. 146, 409–423.

Witherington, B., 2002. Ecology of neonate loggerhead turtles inhabiting lines of downwelling near a Gulf stream front. Mar. Biol. 140, 843–853.

Witt, M., Broderick, A., Johns, D., Martin, C., Penrose, R., Hoogmoed, M., Godley, B., 2007. Prey landscapes help identify potential foraging habitats for leatherback turtles in the NE Atlantic. Mar. Ecol. Prog. Ser. 337, 231–243.

Appendix B

Appendix B: Underlying physical mechanisms driving trophic niches in the open ocean

This appendix has been submitted as *Underlying physical mechanisms driving trophic niches in the open ocean* by M. O'Toole, A. Baudena et al. at *PNAS*, 2018.

1Underlying physical mechanisms driving trophic niches in the open ocean

2Malcolm O'Toole[1], Cedric Cotté[1], Alberto Baudena[1], Sara Sergi[1], Charles Bost[2], Christophe

3Guinet[2], Henri Weimerskirch[2], Mark A Hindell[3,4], Francesco d'Ovidio[1]

4[1]*Laboratoire d'Oceanographie et du Climat (LOCEAN-IPSL), Université Pierre et Marie Curie, Paris 75252, France | [2]Centre*

5*d'études biologiques de Chizé, Villiers-en-Bois 79360, France | [3]Institute for Marine and Antarctic Studies, University of*

6*Tasmania, Hobart, TAS 7001, Australia | [4]Antarctic Climate and Ecosystems CRC, Hobart, TAS 7001, Australia*

7

8Significance

9Despite our understanding of how ocean physics affect bottom-up biology processes,
10investigation into how these changes drive trophic niche is still limited by direct
11observations from ship-based surveys. We overcome this by using multi-satellite data and
12ocean models to infer the prey field and its availability to air-breathing marine predators in
13the subantarctic. When this information was integrated with a large marine predator
14telemetry data set our approach can reveal important physical processes that underpin
15broader ecosystem function.

16

17Abstract

18Understanding the bio-geography and functional role of diverse trophic habitats in the open
19ocean is a central question when studying the interactions between the marine biosphere
20and the climate system. Knowledge of ocean physics and its effect on bottom-up biology
21processes is now available thanks to the recent advancements in operational oceanography
22and multi-species animal telemetry. However, the bio-geography of mid-trophic organisms

23remains difficult to investigate, because it requires direct observation by ship surveys, which

24in turn provides information that is restricted in space and time. Based on the iron-limited

25biological production in the subantarctic ocean, we use, as a proxy of the prey field, ageing

26water masses fertilized by bathymetric features where primary and secondary production is

27likely to have developed. When integrated with physical information about prey

28accessibility, the water masses identified unfold the trophic niches of the regional top

29predators in a remarkably consistent way. The methods developed here for the subantarctic

30region can provide a tool for merging remote sensing with animal telemetry and explore

31trophic interactions in other pelagic regions.

32

33**Introduction**

34A fundamental question in ecological research is how the physical environment influence

35trophic interactions, and ultimately, the functioning of food webs as biomass (i.e. energy)

36flows from low to higher trophic levels (1). Pinpointing which physical features are the most

37ecologically relevant in the heterogeneous, and highly dynamic, marine environment is

38therefore a primary goal for ocean science and management (2). One important driver of

39ocean heterogeneity is the fact that nutrients are upwelled and stirred by the current

40systems, creating spatially contrasted patterns of primary production which then feeds into

41the trophic web. A dramatic example is provided by the subantarctic domain of the

42Southern Ocean. Primary production in this region is limited by bioavailable iron (3). Iron

43sources are located predominately on shallow bathymetric features like continental

44plateaux, seamounts, and thermal vents where internal tide mixing suspend iron from the

45sediments (4–6). From these sources, iron is spread downstream by the Antarctic

46Circumpolar Current (ACC) as large plumes stemming for hundreds of kilometres (7), to fuel

47intense phytoplankton blooms in spring.

48These iron plumes can be identified indirectly by analysing satellite-derived ocean currents.

49These advective pathways induced by the ocean circulation have been found to structure

50not only primary production (7, 8) but also the foraging habitat for upper-trophic species

51with well-developed dispersal capabilities and optimised feeding strategies for finding prey.

52It is tempting to interpret satellite-derived advective pathways in terms of resources, habitat

53vulnerability, and climate change. However, in order to proceed in this direction, it is

54necessary to incorporate into our interpretation biological data from trophic levels above

55primary production. To date, most of these attempts have addressed only single species and

56mainly underlined non-mechanistic (i.e. correlative) relations. These two limitations make it

57difficult to decipher the physical processes underpinning broader ecosystem function. A

58common obstacle in this regard is the fact that the information on the distribution of mid-

59trophic organisms, which make the link between the observations of primary production

60and distribution of predators is only available at much coarser resolution. Here we propose

61a novel approach for bridging this knowledge gap, by inferring from physical observations,

62information about the prey field in terms of "maturation" of water parcels and prey

63accessibility in terms of hydrographic properties of the vertical water columns. This

64approach attempts to describe the trophic niches of seven subantarctic marine predator

65species simultaneously. In total, our telemetry dataset includes over 800 animal tracks (see

66**Table 1**) with diverse foraging strategies and diet.

67Mesopelagic fish are major prey for four of the marine predator species in our study (Table

681). Fish feed on crustacean. Crustacean are transported by eastward advection. These are all

69air-breathing animals which are divided into swimming and flying predator groups. Three of 70the four swimming predator species feed on mesopelagic fish (Table 1 + (9, 10)) and may 71rely on extrinsic factors to access their prey: King penguins (*Aptenodytes patagonicus*) use 72cold isotherms (< 2C) that facilitate prey access (11, 12); Antarctic fur seals (*Arctocephalus* 73*gazelle*) forage at night when their prey migrate closer to the surface (ref); and southern 74elephant seals (*Mirounga leonina*) perhaps rely less on extrinsic factors to access prey 75because of their deep-diving capabilities (dive up to 1500 m (13)). These fish can be 76modulated vertically in the water column by hydrothermal conditions and will be accessible 77for air-breathing predators attempting to access them. The macaroni penguin () is the other 78swimming predator species, which instead feed on crustaceans.

79In order to create a satellite-based proxy of the prey field, we trace the dispersal of iron 80from known sources, and we assume it is incorporated in the food chain via bottom-up 81processes (14, 15). Indeed previous observations have shown that "older" water parcels – 82which have been in contact with an iron source since a longer time - have been found to be 83areas of preferred foraging activity for higher trophic levels (16), consistent with a 84mechanism of ecosystem maturation inside the drifting water mass. Regarding the proxy of 85prey accessibility, we look at the presence of the 2°C isotherm in the 500 m surface layer, 86which is the thermal discontinuity between the warmer summer Surface Mixed Layer (SML) 87and the previous winter's cooler mixed layer below (Winter Water; WW) (17). We focus on 88this hydrographic feature on the basis of past studies which have shown the vertical 89distribution of stenothermal fish (e.g. myctophid) is modulated by the presence of the 2°C 90isotherm, which acts as a thermal barrier to fish vertical migration (11). Without the 2°C 91isotherm, mesopelagic fish can migrate deeper, thus becoming less accessible to predators.

92Our aim here is to provide compelling evidence for how these two physical processes –

93"ageing" iron-enriched water parcels, and presence of 2°C isotherm in the upper layer –

94define different trophic niches by structuring the prey field in the subantarctic zone.

95

96**Methods**

97Physical ocean climatology

98We use altimetry-derived surface currents (Aviso product ID
99SEALEVEL_GLO_PHY_L4_REP_OBSERVATIONS_008_047) and sea temperature (product ID
100GLOBAL_REANALYSIS_PHY_001_025-TDS) from Copernicus (http://marine.copernicus.eu).
101These data cover the entire spatial extent of the study site daily from 2005 to 2015. A
102summary of these climatology data and their expected biological relevance is presented in
103**Table 2**. Details are provided below.

104We used a Lagrangian model based on altimetry to trace monthly averages of advected
105water parcels at 0.25° resolution backward in time and assign them a time stamp when they
106reach iron-enriched waters over a continental plateau (19) or open ocean seamount (see *SI*
107*Materials and Methods, Text 1)*. This model focuses on the summer period and has been
108extensively calibrated and validated in the Crozet and Kerguelen regions by integrating
109satellite data (altimetry and ocean colour), lithogenic isotopes, iron measurements and
110drifters (20). We assume that "young" water parcels (that is, water parcels which have been
111enriched since a few days only) are in an early blooming stage, and therefore are less rich in
112mid-trophic biomass than parcels with an "older" age. Finding a threshold separating young
113and old parcels is somehow arbitrary. We choose 60 days because this value corresponds to

114the time since the initial bloom in which the chlorophyll intensity starts to decline in satellite

115images (21), or post-bloom stage. This value also matches the peak foraging activity of

116elephant seals at sea (*SI Figures, Fig S1*); a major predator of mid-trophic species in the

117Southern Ocean. The sensibility of our results to the 60-day threshold is discussed in the

118Conclusions. The probability of post-bloom waters is therefore estimated from the

119percentage of iron-enrich water parcels older than 60 days present in each 0.25° grid cell

120over the 10-year data coverage period (**Fig 1B**).

121The sea temperature from the Glorys product produced by Mercator and available on

122Copernicus Marine Monitoring System (version: *global-reanalysis-phy-001-025-monthly*)

123was used to calculated the monthly depth average of the 2°C isotherm at 0.25° resolution.

124We remind that our hypothesis is that the presence of the 2°C isotherm in the upper 500 m

125surface layer will facilitate (i.e. shallower) access for predators feeding on mesopelagic mid-

126trophic prey. The probability of facilitated prey access is therefore estimated from the

127percentage of water parcels where the 2°C isotherm in the upper 500 m surface layer is

128present in each 0.25° grid cell over the 10-year data coverage period (**Fig 1C**).

129

130Identify habitat using tracking data from multiple species

131Seven marine predator species were fitted with Argos or GPS satellite transmitters on three

132subantarctic islands in the Indian Ocean during the austral summer between 1989 and 2016,

133totalling 821 useable tracks (**Table 1**). These deployments coincided with recurrent

134phytoplankton bloom events in the region. Bio-logging transmitters were fixed to the

135feathers on the back of seabirds with cyanolycrate adhesive securely fastened with cable-

136ties, and fixed to the head or back of pinnipeds with a two-part expoxy adhesive. The
137capture, release and handling procedures received the approval of the ethics committee of
138the French Polar Institute (IPEV), the French Environment Ministry and Australian
139government. All devices were hydrodynamically shaped to limit drag effect and weighed <
1402% of the mean adult weight. Transmission interval range varied by species but minimum
141daily transmission rate was > 10 for each individual. Details of instrumentation are provided
142in publications cited in **Table 1**. Published and unpublished data are sourced from Centre
143d'Études Biologiques de Chizé, Centre National de la Recherche Scientifique (CEBC-CNRS)
144and the Australian Antarctic Data Centre (AADC) (https://data.aad.gov.au/).

145Observed GPS measurement error seldom exceeded a few tens of kilometres (22) but Argos
146location estimates are associated with varying classes of error. To account for location error,
147all track data were fitted to a hierarchical first difference correlated random walk (hDCRW)
148state-space model using the R software package *bsam* (function *ssm_fit*) (23, 24). The fitted
149tracks data were used to map marine predator hotspots from kernel density estimates (see
150*SI Materials and Methods, Text 2*). However, to characterise the environment potentially
151available to individuals, and thus allowing a case-control design for habitat preference
152modelling (25), we simulated random or pseudo-tracks. For each observed track we
153simulated 20 pseudo-tracks by fitting a first-order vector autoregressive (AR) model
154characterised by the step lengths and turning characteristics of the observed track (26).
155Simulated tracks are therefore random movements constrained by the step length and turn
156angle of the observed track locations, and thus represent the space available to an animal if
157it had no habitat preferences. The R software package *availability* (27) provides an easy two-
158step process for generating these simulated tracks: (i) function *surrogateARModel* fits the

159AR model to each track; and (ii) *surrogateAR* simulates each new simulated track. Simulated

160locations falling on land were rejected and re-sampled. Population-level comparisons of the

161simulated tracks (available habitat) and observed tracks (selected habitat) are available in *SI*

162*Figures, Fig. S2*.

163

164Permutation test

165We performed a two-sided permutation analysis for each predator species to test if the

166probability of a mature ecosystem was significantly different between available predator

167habitat (H_1) and selected predator habitat (H_2). A *p*-value was estimated by calculating the

168mean probability difference (D_{obs}) between H_1 and H_2 and permuting the probability of a

169mature ecosystem for the two treatments (H_1,H_2) to obtain all possible permutations (ε =

1701000). The significance threshold was set at 0.05. A statistically significant value indicted

171whether or not the probability of a mature ecosystem in H_2 was different to those in H_1. The

172relative precision of D_{obs} was represented by its standard error. The same procedure was

173repeated for the probability of facilitated prey access.

174

175**Results**

176We start by listing the different uses of the two prey proxies species by species. Marine

177predator hotspots were mapped in the Indian sector of the subantarctic Southern Ocean

178and compared to the proxies of prey field and prey vertical accessibility (see section xxxx),

179that is, the probability of post-bloom waters and probability of presence of the 2C thermal

180barrier, hence where prey is facilitated by being closer to the surface (**Fig. 1**). Marine

181predators generally encountered mature ecosystems as they migrated east of the Kerguelen

182and Crozet Plateaux or south of Crozet (**Fig. 1B**), whereas areas where prey access could be

183facilitated by the 2°C isotherm were located south of the Polar Front (PF) (**Fig. 1C**). Pinnipeds

184and penguins (swimming predators) were regularly located south of the PF where large

185areas support facilitated prey access. In contrast, most albatross (flying predators) were

186north of the PF where facilitated prey access was negligible. The southern elephant seal was

187the marine predator species to migrate the furthest east from the Kerguelen Plateau, where

188other swimming predators (king penguins, macaroni penguins and Antarctic fur seals)

189alternatively used areas close to the shelf edge. However, the distribution of swimming

190predators was not only species specific, but also depended on the location of their colony.

191The king penguins from Crozet, for instance, migrated south of Crozet to the vicinity of the

192PF. However, king penguins from Kerguelen and Heard remained relatively close to the

193south-eastern or southern edge of the Kerguelen Plateau.

194We then attempted to unfold the trophic niches of the different species. This is achieved by

195plotting together a quantitative analysis of the physical differences between selected and

196available habitat (see Method). This main result of this analysis is depicted in Fig. 2. This

197figure shows how the use of mature ecosystems and areas of facilitated prey access was

198specific to species (**Fig. 2**). Swimming predators were more likely than flying seabirds to use

199mature ecosystems, areas of facilitated prey access, or both. All but one species of

200swimming predator (the macaroni penguin) used mature ecosystems ($\Delta > 0$, $p < 0.01$), but

201only the king penguin used areas of facilitated prey access ($\Delta > 0$, $p < 0.01$). The southern

202elephant seal was the only swimming predator toused areas where prey access was not

203facilitated by the 2°C isotherm ($\Delta < 0$, $p < 0.01$). Interestingly, the southern elephant seal,

204which typically migrated furthest from its colony, also used an area close to the eastern

205shelf edge of the Kerguelen Plateau that supported a mature ecosystem (**Fig 3**). Similar to

206the macaroni penguin, no flying predator used mature ecosystems or areas of facilitated

207prey access. Instead, the wandering albatross used areas where the ecosystem had not yet

208matured ($\Delta < 0$, $p < 0.01$) and, the dark-mantled albatross included, used areas where prey

209access was not facilitated by the 2°C isotherm ($\Delta < 0$, $p < 0.01$). All values of physical

210differences between selected and available habitat and associated statistical significances

211are provided in *SI Figures, Fig S3*.

212

213**Discussion**

214Our aim is to identify the trophic niches of different pelagic predators on the basis of the

215comparison of oceanic physical features and animal telemetry. First, we use bio-logging

216tracks of seven major marine predator species to observe the spatial structure of the prey

217field in the subantarctic. First, we observe advection of ageing iron and the 2C isotherm, two

218important drivers, which shape and maintain such ecological landscape. Then, we compare

219these proxies to the foraging grounds that we derive by analyzing the biologging

220trajectories. We found that they are in remarkable agreement   This conclusion is based on

221the observed coincidence between the boundaries of predator trophic niches and these

222physical processes on the timescale of a planktonic bloom. Lagrangian analysis shows the

223advection of iron can structure the prey field as the bloom's ecosystem develops over

224summer. The same horizontal transport of water modulates the landscape of dominant

225phytoplankton types (d'Ovidio et al 2010). The upward force of the 2C isotherm then

226separates mid-trophic prey field based on their accessibility to predators.

227These observations combined, unfold the trophic niches of the region's top predators in

228away which is remarkably consistent. In regions where productivity is limited by bioavailable

229iron, an eastward transition from young bloom waters to older post-bloom waters appeared

230to represent a shift in the prey field from predominately crustaceans to mid-trophic fish.

231Elephant seals using high retention mesoscale eddies seems to suggest the same thing: old

232post-bloom water patches are where the upper trophic prey field is likely to develop

233(d'Ovidio et al 2013, Cotte et al 2015). Three of the most abundant consumers of mid-

234trophic-level myctophid fish, including the king penguin (28), southern elephant seal (9, 10)

235and Antarctic fur seal (9), used post-bloom waters, where we assume enough time has

236passed for iron to pass through the food chain to mid-trophic fish. Conversely, macaroni

237penguins, which feed predominately on lower trophic level crustaceans (28, 29), are less

238likely to use post-bloom waters, including areas adjacent the iron-enriched shelf.

239Interestingly, macaroni penguins from Kerguelen which consume more fish than their Crozet

240counterparts (30), and were also more likely to use post-bloom waters (*Fig. S4*). However,

241this is only conjecture as the few track data we have for Crozet (n=4) makes this

242interpretation ambiguous. The squid-based diet of wandering and dark-mantled albatross

243(31), for instance, would let us assume that they use post-bloom waters. But in fact,

244wandering albatross are more likely to use bloom waters north of the SAF (see **Fig 1**) where

245they can rely on olfactory cues from dimethyl sulphide emitted by phytoplankton (32, 33) to

246locate their squid prey, suggesting more complex mechanisms. A similar foraging strategy is

247adopted by loggerhead turtles (34).

248The 2C isotherms upward forcing effect on the vertical distribution of mid-trophic fish can

249also play an important role in structuring the prey field of swimming predators (refs in Peron

250et al 2012) (11). The three swimming predators whose diet largely consists of myctophid fish

251fall into species-specific trophic niches according to how they rely on prey access facilitated

252by the 2C isotherm. King penguins are the only predator species to use the 2C isotherm to

253maximise feeding efficiency (12, 35). The pinnipeds in this study did not: Elephant seals are

254capable of diving far below the 2C isotherm (up to 1500 m, 13, 36) and Antarctic fur seals,

255although limited by their dive capabilities (up to 250 m, 37), typically feed at night (38, 39)

256when their prey migrate towards the surface(40). If Antarctic fur seals did use the 2C

257isotherm it is more likely to be during daylight hours when prey return to deeper waters

258(40), which may explain their use, albeit non-significant, of the 2C isotherm ($\Delta > 0$, p=0.67).

259However, as Antarctic fur seals feed mostly at night (38), this effect is expected to be small.

260Flying albatross species, incapable of diving more than a few meters below the surface (41,

26142), are unlikely to use subsurface isotherms to facilitate access to prey. Instead, wandering

262albatross (and possibly dark-mantled albatross) likely hunt live squid or scavenge floating

263squid carrion at the surface (43). Black-browed albatross, on the other hand, forage

264predominately in neritic waters on the shelf (31), which may have weaken any statistical

265response to our analysis conducted only in areas off the shelf. A summary of predator-prey

266trophic niches and the underlying ocean physics is presented in **Table 3**.

267

268Physical conditions shape trophic niches, but the effects of the physical environment on

269predator species are expected to be stronger for those with reduced dispersal capabilities.

270In summer, breeding constraint is a major factor that influences predator distribution and

271which physical conditions they will encounter. Stronger effects on income breeders.

272 • Elephant seals obtain all resources necessary to provision their offspring during one very long trip at

273 sea the previous winter (capital breeders) (Costa 1993) and are therefore capable of ranging over vast

274 spatial scales. Penguins and fur seals, however, must frequently return to provision their offspring and

275 are therefore limited to short trips of 1-2 weeks and a few hundred kilometres from the breeding

276 colony (income breeders) (Costa 1993, Trillmich and Weissing 2006, Houston et al 2007, Costa and

277 Shaffer 2012, Ludynia et al 2013). Furthermore, there is a premium on maximising energy gain while

278 minimising time spent foraging, so these predators typically occur in productive oceanic regions

279 (Costa and Shaffer 2012). ...

280 • Environmental forcing agents have greater effect on income breeders that depend on predictable and

281 profitable habitat – e.g. cold water tongue on the eastern shelf edge used by king penguins. ...

282 circulation and bathymetry interaction OR stable PF

283

284 Emphasis importance of isotherm in SO (physically and biologically)

285

286 We use specific parameters to demonstrate importance of two major physical processes

287 (age of iron and isotherm), but could modify parameters to examine specific predator

288 response - We expect predator species will respond to different variations of the two

289 parameters used in this study. A hypothetical analysis, for example, could test how each

290 predator species responds to the probability of an immature ecosystem dominated by

291 crustaceans (iron-enriched water parcels < 60 d) and the probability of a different isotherm

292 (e.g. the 3.5°C isotherm in the upper 100 m surface layer likely modulates the vertical

293 distribution of crustacean (44)).. In this scenario we may expect to find macaroni penguins

294 respond significantly to these two altered physical parameters, while many other predator

295 species will not.

296Our results provide an objective demonstration of how (sub)mesoscale physics structures

297the marine ecosystem, and hence, trophic interactions. That two physical ocean processes

298can reveal trophic patterns consistent with diverse foraging ecologies of marine vertebrates

299is remarkable. Such information is fundamental for ecological spatial planning, as we were

300able to identify the boundaries of ecologically-significant areas in the open ocean. For

301example, dynamic time-area MPAs could trace regions of ageing iron-rich waters and

302likelihood of a surface mixed layer that support trophic niches of interest to king penguins; a

303species likely facing increasing anthropogenic pressures over the next 50 years (12, 45).

304Predicting these provinces by key physical drivers will be important for optimizing climate

305models and designing future management solutions.Changing evaluation of climate change

306effect on marine environemnt.

307The sensibility of our results to the 60-day threshold is discussed in the Conclusions

308Open ocean habitat outside of management zones (Fig S5 – Sara Sergi). Detection of

309ecologically relevant ocean structures obtained with the integration of animal telemetry and

310multisatellite analysis has been proposed as a tool to support the design of pelagic marine

311protected areas (Scales et al 2014, Della Penna et al 2017).

312The literature exemplifies innumerable cases of species in terrestrial systems using different

313strategies to exploit a niche to avoid overlap with competitors (Silvertown 2004 TEE,

314Amarasekare 2003 + more refs). The principle physical drivers in this study could likely be

315the same for other open ocean areas. find evidence of trophic niches formed by ecosystem

316development and facilitated access to prey, which holds true for multiple predator species

317foraging in the Indian sector of the open Southern Ocean. Habitat selected by a diverse

318array of predator species – including swimming and flying predators, are described by

319various combinations of ecosystem maturity and facilitated prey access. Region well

320understood by past campaigns run over the past two decades (MYCTO, MEOP2, tagging

321programs). A summary of predator-prey trophic niches and the underlying ocean physics is

322presented in **Table 3**.

323

324**Acknowledgements**

326

327**References**

3281.   Lindeman RL The Trophic-Dynamic Aspect of Ecology. *Ecology* 23(4):399–417.

3292.   Della Penna A, et al. (2017) Lagrangian analysis of multi-satellite data in support of open ocean Marine
330   Protected Area design. *Deep Sea Res Part II Top Stud Oceanogr* 140:212–221.

3313.   Blain S, et al. (2007) Effect of natural iron fertilization on carbon sequestration in the Southern Ocean.
332   *Nature* 446(7139):1070–1074.

3334.   Park Y-H, Fuda J-L, Durand I, Garabato ACN (2008) Internal tides and vertical mixing over the Kerguelen
334   Plateau. *Deep Sea Res Part II Top Stud Oceanogr* 55(5):582–593.

3355.   van Beek P, et al. (2008) Radium isotopes to investigate the water mass pathways on the Kerguelen
336   Plateau (Southern Ocean). *Deep Sea Res Part II Top Stud Oceanogr* 55(5):622–637.

3376.   Tagliabue A, et al. (2014) Surface-water iron supplies in the Southern Ocean sustained by deep winter
338   mixing. *Nat Geosci* 7:314.

3397.   Ardyna M, et al. (2017) Delineating environmental control of phytoplankton biomass and phenology in
340   the Southern Ocean. *Geophys Res Lett* 44(10):5016–5024.

3418.   d'Ovidio F, De Monte S, Alvain S, Dandonneau Y, Levy M (2010) Fluid dynamical niches of
342   phytoplankton types. *Proc Natl Acad Sci* 107(43):18366–18370.

3439.   Cherel Y, Ducatez S, Fontaine C, Richard P, Guinet C (2008) Stable isotopes reveal the trophic position
344   and mesopelagic fish diet of female southern elephant seals breeding on the Kerguelen Islands. *Mar
345   Ecol Prog Ser* 370:239–247.

34610.   Authier M, Dragon A-C, Richard P, Cherel Y, Guinet C (2012) O{\textquoteright} mother where wert
347   thou? Maternal strategies in the southern elephant seal: a stable isotope investigation. *Proc R Soc
348   London B Biol Sci* 279(1738):2681–2690.

34911.   Charrassin J-B, Bost C (2001) Utilisation of the oceanic habitat by king penguins over the annual cycle.
350   *Mar Ecol Prog Ser* 221:285–298.

35112.   Peron C, Weimerskirch H, Bost C-A (2012) Projected poleward shift of king penguins' (Aptenodytes
352   patagonicus) foraging range at the Crozet Islands, southern Indian Ocean. *Proc R Soc B Biol Sci*
353   279(1738):2515–2523.

35413.   McIntyre T, et al. (2010) A lifetime at depth: Vertical distribution of southern elephant seals in the
355   water column. *Polar Biol* 33(8):1037–1048.

35614.   Christaki U, et al. (2014) Microbial food web dynamics during spring phytoplankton blooms in the
357   naturally iron-fertilized Kerguelen area (Southern Ocean). *Biogeosciences* 11(23):6739–6753.

35815.   Boyd PW, et al. (2007) Mesoscale Iron Enrichment Experiments 1993-2005: Synthesis and Future

359   Directions. *Science (80-)* 315(5812):612–617.

360 16.   Cotté C, d'Ovidio F, Dragon AC, Guinet C, Lévy M (2015) Flexible preference of southern elephant seals
361   for distinct mesoscale features within the Antarctic Circumpolar Current. *Prog Oceanogr* 131:46–58.

362 17.   Park Y-H, Charriaud E, Fieux M (1998) Thermohaline structure of the Antarctic Surface Water/Winter
363   Water in the Indian sector of the Southern Ocean. *J Mar Syst* 17(1):5–23.

364 18.   Catul V, Gauns M, Karuppasamy PK (2011) A review on mesopelagic fishes belonging to family
365   Myctophidae. *Rev Fish Biol Fish* 21(3):339–354.

366 19.   Bowie AR, et al. (2015) Iron budgets for three distinct biogeochemical sites around the Kerguelen
367   Archipelago (Southern Ocean) during the natural fertilisation study, KEOPS-2. *Biogeosciences*
368   12(14):4421–4445.

369 20.   d'Ovidio F, et al. (2015) The biogeochemical structuring role of horizontal stirring: Lagrangian
370   perspectives on iron delivery downstream of the Kerguelen Plateau. *Biogeosciences* 12(19):5567–5581.

371 21.   Arrigo KR, van Dijken GL, Bushinsky S (2008) Primary production in the Southern Ocean, 1997–2006. *J*
372   *Geophys Res Ocean* 113(C8). doi:10.1029/2007JC004551.

373 22.   Lopez R, Malardé JP, Royer F, Gaspar P (2014) Improving argos doppler location using multiple-model
374   kalman filtering. *IEEE Trans Geosci Remote Sens* 52(8):4744–4755.

375 23.   Jonsen ID, Flemming JM, Myers RA (2005) Robust state-space modeling of animal movement data.
376   *Ecology* 86(11):2874–2880.

377 24.   Jonsen I (2016) Joint estimation over multiple individuals improves behavioural state inference from
378   animal movement data. *Sci Rep* 6:20625.

379 25.   Aarts G, MacKenzie M, McConnell B, Fedak M, Matthiopoulos J (2008) Estimating space–use and
380   habitat preference from wildlife telemetry data. *Ecography (Cop)* 31(1):140–160.

381 26.   Raymond B, et al. (2014) Important marine habitat off east Antarctica revealed by two decades of
382   multi–species predator tracking. *Ecography (Cop)* 38(2):121–129.

383 27.   Raymond B, Wotherspoon S, Reisinger R (2016) availability: Estimating geographic space available to
384   animals based on telemetry data.

385 28.   Cherel Y, Hobson KA, Guinet C, Vanpe C (2007) Stable isotopes document seasonal changes in trophic
386   niches and winter foraging individual specialization in diving predators from the Southern Ocean. *J*
387   *Anim Ecol* 76(4):826–836.

388 29.   Deagle BE, Gales NJ, Hindell MA (2008) Variability in foraging behaviour of chick-rearing macaroni
389   penguins Eudyptes chrysolophus and its relation to diet. *Mar Ecol Prog Ser* 359:295–309.

390 30.   Delord K, et al. (2013) *Atlas of top predators from French Southern Territories in the Southern Indian*
391   *Ocean* doi:10.15474/AtlasTopPredatorsOI_CEBC.CNRS_FrenchSouthernTerritories.

392 31.   Jaeger A, et al. (2013) Stable isotopes document inter- and intra-specific variation in feeding ecology of
393   nine large southern Procellariiformes . *Mar Ecol Prog Ser* 490:255–266.

394 32.   Nevitt GA, Bonadonna F (2005) Sensitivity to dimethyl sulphide suggests a mechanism for olfactory
395   navigation by seabirds. *Biol Lett* 1(3):303–305.

396 33.   Nevitt GA, Losekoot M, Weimerskirch H (2008) Evidence for olfactory search in wandering albatross,
397   Diomedea exulans. *Proc Natl Acad Sci* 105(12):4576–4581.

398 34.   Endres CS, Lohmann KJ (2012) Perception of dimethyl sulfide (DMS) by loggerhead sea turtles: a
399   possible mechanism for locating high-productivity oceanic regions for foraging. *J Exp Biol*
400   215(20):3535–3538.

401 35.   Cotte C, Park Y-H, Guinet C, Bost C-A (2007) Movements of foraging king penguins through marine
402   mesoscale eddies. *Proc R Soc B Biol Sci* 274(1624):2385–2391.

403 36.   Bailleul F, Cotté C, Guinet C (2010) Mesoscale eddies as foraging area of a deep-diving predator, the
404   southern elephant seal. *Mar Ecol Prog Ser* 408:251–264.

405 37.   Lea MA, Hindell M, Guinet C, Goldsworthy SD (2002) Variability in the diving activity of Antarctic fur
406   seals, Arctocephalus gazella, at Iles Kerguelen. *Polar Biol* 25(4):269–279.

407 38.   Lea MA, Cherel Y, Guinet C, Nichols PD (2002) Antarctic fur seals foraging in the Polar Frontal Zone:
408   Inter-annual shifts in diet as shown from fecal and fatty acid analyses. *Mar Ecol Prog Ser* 245:281–297.

409 39.   Goldsworthy SD, Page B, Welling A, Chambellant M, Bradshaw CJA (2010) Selection of diving strategy
410   by Antarctic fur seals depends on where and when foraging takes place. *Mar Ecol Prog Ser* 409:255-
411   U273.

412 40.   Duhamel G, Koubbi P, Ravier C (2000) Day and night mesopelagic fish assemblages off the Kerguelen
413   Islands (Southern Ocean). *Polar Biol* 23(2):106–112.

414 41.   Prince PA, Huin N, Weimerskirch H (1994) Diving depths of albatrosses. *Antarct Sci* 6(3):353–354.

415 42.   Sakamoto KQ, Takahashi A, Iwata T, Trathan PN (2009) From the Eye of the Albatrosses: A Bird-Borne

416   Camera Shows an Association between Albatrosses and a Killer Whale in the Southern Ocean. *PLoS*
417   *One* 4(10):1–4.

41843. Croxall JP, Prince PA (1994) Dead or alive, night or day: how do albatrosses catch squid? *Antarct Sci*
419   6(2):155–162.

42044. Thiebot J-B, et al. (2014) Adjustment of pre-moult foraging strategies in Macaroni Penguins Eudyptes
421   chrysolophus according to locality, sex and breeding status. *Ibis (Lond 1859)* 156(3):511–522.

42245. Bost CA, et al. (2015) Large-scale climatic anomalies affect marine predator foraging behaviour and
423   demography. *Nat Commun* 6:8220.

42446. Guinet C, et al. (2001) Spatial distribution of foraging in female antarctic fur seals Arctocephalus gazella
425   in relation to oceanographic variables: A scale-dependent approach using geographic information
426   systems. *Mar Ecol Prog Ser* 219:251–264.

42747. Bailleul F, et al. (2007) Successful foraging zones of southern elephant seals from the Kerguelen Islands
428   in relation to oceanographic conditions. *Philos Trans R Soc B Biol Sci* 362(1487):2169–2181.

42948. Charrassin JB, Park YH, Maho Y Le, Bost CA (2002) Penguins as oceanographers unravel hidden
430   mechanisms of marine productivity. *Ecol Lett* 5(3):317–319.

43149. Hindell M, et al. (2011) Foraging habitats of top predators, and areas of ecological significance, on the
432   Kerguelen Plateau. *The Kerguelen Plateau: Marine Ecosystem and Fisheries*, pp 203–215.

43350. Thiebot J-B, Lescroël A, Pinaud D, Trathan PN, Bost C-A (2011) Larger foraging range but similar habitat
434   selection in non-breeding versus breeding sub-Antarctic penguins. *Antarct Sci* 23(2):117–126.

43551. Weimerskirch H, Mougey T, Hindermeyer X (1997) Foraging and provisioning strategies of black-
436   browed albatrosses in relation to the requirements of the chick: natural variation and experimental
437   study. *Behav Ecol* 8(6):635–643.

43852. Pinuad D, Weimerskirch H (2007) At−sea distribution and scale−dependent foraging behaviour of
439   petrels and albatrosses: a comparative study. *J Anim Ecol* 76(1):9–19.

44053. Weimerskirch H, Robertson G (1994) Satellite tracking of light-mantled sooty albatrosses. *Polar Biol*
441   14(2):123–126.

44254. Weimerskirch H, Salamolard M, Sarrazin F, Jouventin P (1993) Foraging Strategy of Wandering
443   Albatrosses through the Breeding Season: A Study Using Satellite Telemetry. *Auk* 110(2):325–342.

444
445

446 **Table 1.** Instrumentation of seven marine predator species in the Southern Indian Ocean. Deployments were
447 made on Crozet (C), Kerguelen (K) and Heard Island (H) during the breeding season (Oct – Mar). References
448 detail instrumentation of telemetry devices.

species	colony (no. of tracks)	deployment years (references)
Antarctic fur seal *Arctocephalus gazelle*	K (52), H (65)	1998-2001; 2004; 2006-2008; 2012 (39, 46)
Southern elephant seal *Mirounga leonina*	K (236)	2002; 2004-2016 (47)
King penguin *Aptenodytes patagonicus*	C (38) ,K (48), H (67)	1998-2004; 2006; 2011-2016 (12, 48, 49)
Macaroni penguin *Eudyptes chrysolophus*	C (4), K (10), H (28)	2004; 2009-2011; 2014-2015 (29, 50)
Black-browed albatross *Thalassarche melanophris*	K (18), H (28)	1995; 1999; 2003-2004 (49, 51, 52)
Dark-mantled albatross *Phoebetria fusca*	C (42)	2007-2009 (53)
Wandering albatross *Diomedea exulans*	C (161), K (24)	1989; 1990-1992; 1994; 1998-2003; 2007-2010 (52, 54)

449

450 **Table 2.** Physical ocean climatology used as proxies for ecosystem process in the subantarctic ocean.

physical ocean climatology	source of physical ocean climatology	biological relevance of ocean physics	ecosystem process
Trace iron-enriched water parcels that originate from shelf waters (< 750 m).	Lagrangian model based on altimeter products produced by CLS/AVISO, with support from CNES; http://www.avi-so.altimetry.fr/duacs/(20)	Water parcels enriched by iron more than 60 days ago represent an ecosystem in the late bloom phase; depleted in phytoplankton, but increasingly rich in mid-trophic biomass.	Probability of a mature ecosystem
2°C isotherm is the thermal discontinuity between the Surface Mixed Layer (SML) and Winter Water (WW)	Copernicus model based on the temperature product 'GLOBAL_REANALYSIS_PHY_0 01_025-TDS' (http://marine.c-opernicus.eu)	The 2°C isotherm is likely to modulate the vertical distribution of mid-trophic organisms.	Probability of facilitated prey access

451

452

453

454

455

456

457**Table 3.** Summary description of trophic niches and their underlying physical environment. Prey are based on
458summer diet of each predator (list of predators in Fig 1).

Trophic niche		Underlying physical environment	
Predator	Prey (trophic level)	Use mature ecosystem?	Use facilitated prey access?
	crustacean (lower)	No. Use young bloom waters that support zooplankton stock.	No. Find prey within the 100 m surface layer.
	fish (mid)	Yes. Use old post-bloom waters that support mid-trophic prey.	Maybe. More likely to access resources at night when prey migrate towards the surface.
	fish (mid)	Yes. Use old post-bloom waters that support mid-trophic prey.	Yes. 2°C isotherm facilitates prey accessibility.
	fish (mid)	Yes. Use old post-bloom waters that support mid-trophic prey.	No. Capable of reaching deep-sea prey without using the 2°C isotherm (dive up to 1500 m).
	fish (mid)	No preference. Feed predominately in shelf waters and only sometimes feed in pelagic waters.	No. Unable to use the 2°C isotherm (limited to dives < 10 m). Known to target neritic prey, presumably near the surface.
	squid (higher)	No. Use bloom waters. Predator likely uses olfactory cues from phytoplankton blooms north of the ACC to find higher-trophic prey.	No. Unable to use the 2°C isotherm (limited to dives < 2 m). Target prey near the surface.
	squid (higher)	No. Likely use a strategy similar to wandering albatross (i.e. find prey using olfactory cues from bloom). Also feed on terrestrial bird carrion.	No. Unable to use the 2°C isotherm (limited to dives < 5 m). Target prey near the surface.

459

460

461

462
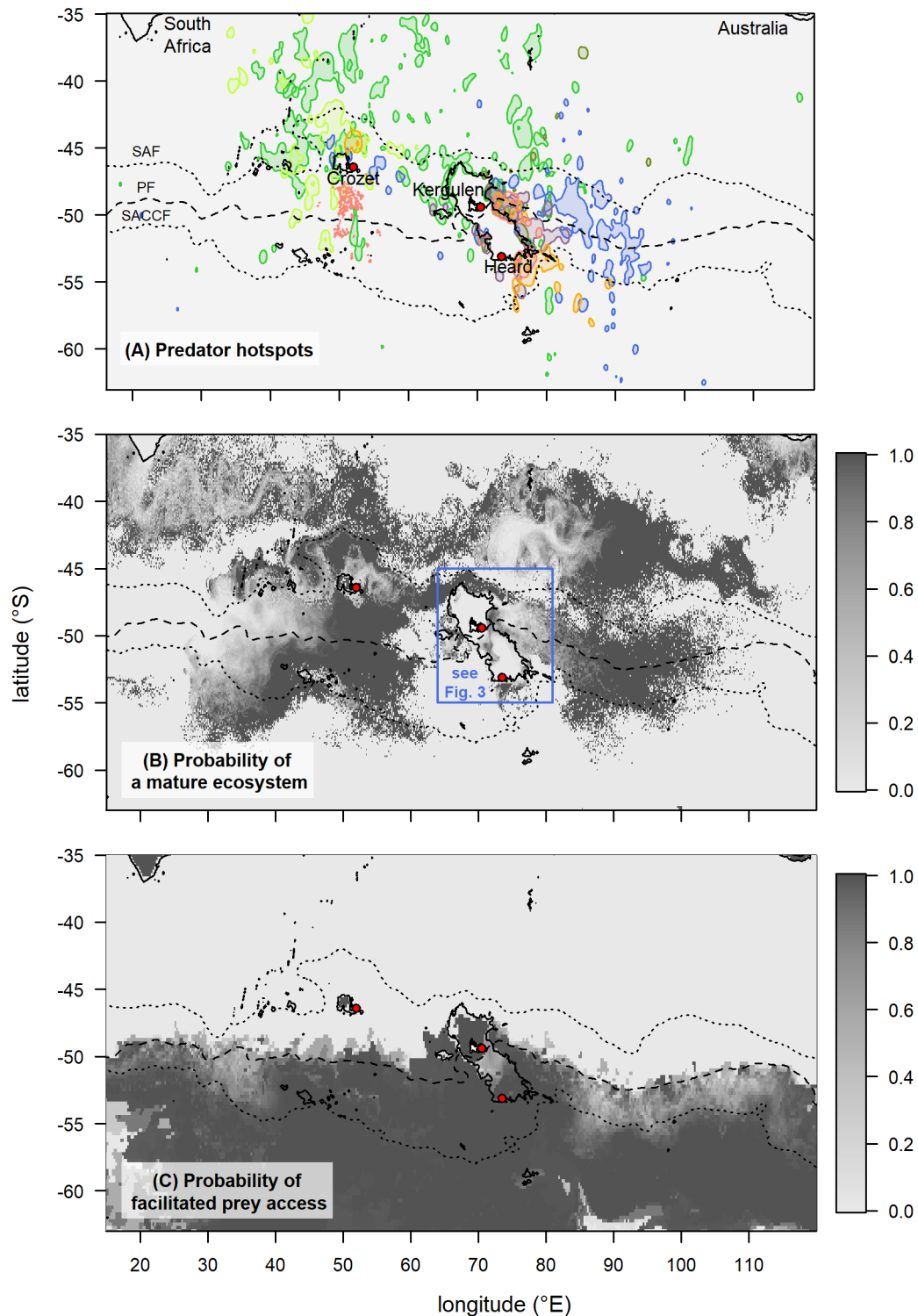
Fig 1. Predator hotspots (A) and climatology for probability of mature ecosystems (B) and facilitated prey access (C). Predator hotspots include king penguins (*salmon*), macaroni penguin (*orange*), Antarctic fur seal (*blue*), southern elephant seal (*dark blue*), dark-mantled albatross (*light green*), wandering albatross (*green*) and black-browed albatross (*dark green*). Antarctic Circumpolar Current fronts include the sub-Antarctic Front (SAF), Polar Front (PF) and southern Antarctic Circumpolar Current Front (SACCF). Red dots represent predator colonies (north to south) Crozet, Kerguelen and Heard. Shelf beak (1000 m bathymetric contour) is represented by a solid black line. Predator hotspots generated from kernel density values (see *SI Text 2*).

471
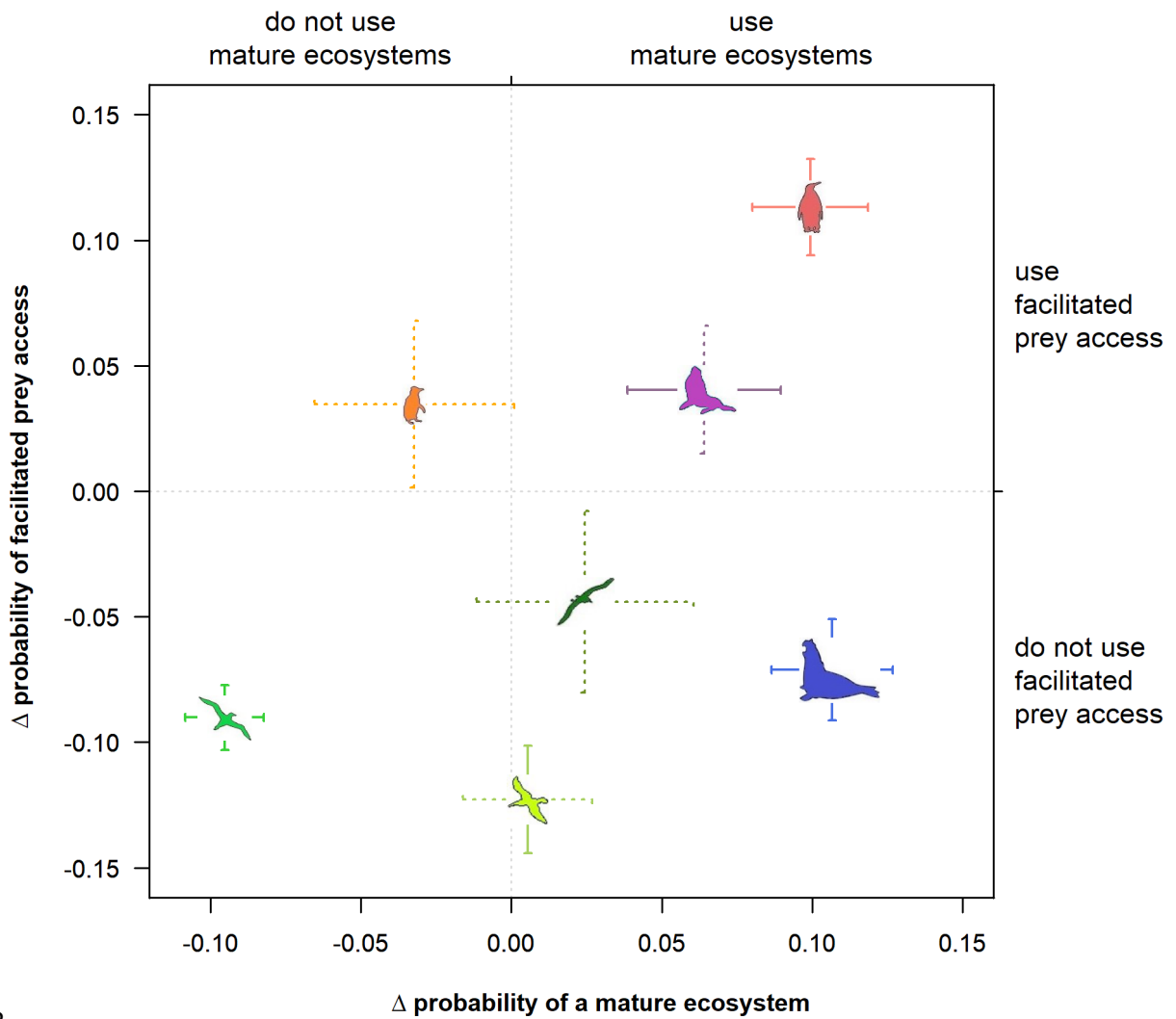
Fig 2. Trophic niche positions as driven by ecosystem maturity and presence of facilitated prey access. Each trophic niche is represented by the habitat use of a specific predator species (see **Table 3**). The use (or not) of mature ecosystems and facilitated prey access is represented by the statistical difference in probabilities between available and selected habitat (> 0 indicates use). Significant values (p < 0.05) are indicated by bold standard error bars.

473

474
475
476
477
478

479
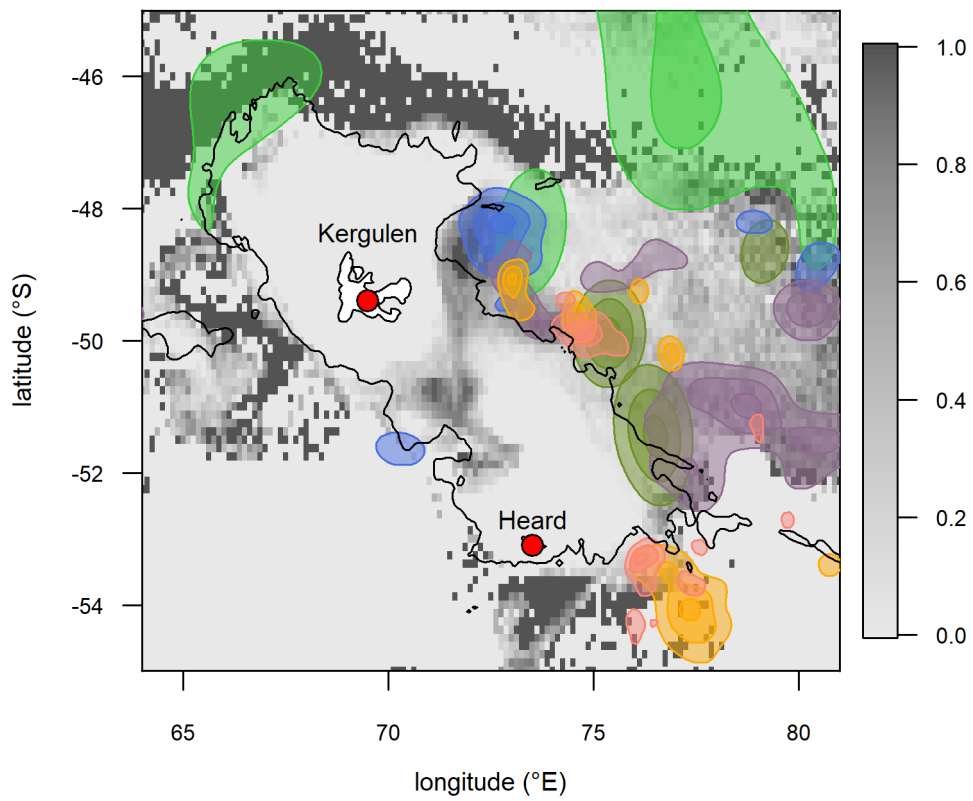
Fig 3. Insert from figure 1 of climatology for probability of a mature ecosystem superimposed by predator hotspots. Note the recirculated water (i.e. mature ecosystem) close to the eastern shelf break superimposed by a southern elephant seal hotspot (dark blue).

483

484

485
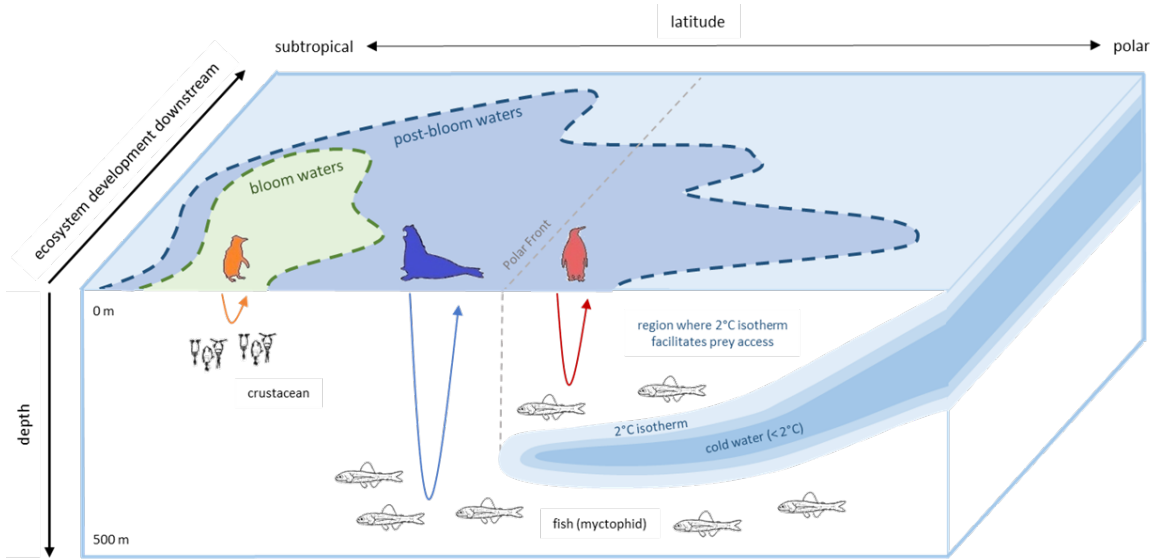
Fig 4. Schematic of the physical processes driving trophic niches of three swimming predator species, including macaroni penguins (orange), king penguins (red) and southern elephant seals (blue). Ecosystem development evolves downstream of the initial bloom site: from a crustacean-dominated system in bloom waters (dashed green) to a fish-dominated system in post-bloom waters (dashed blue). The vertical distribution of stenothermal fish (e.g. myctophid) is modulated by the upward force of the 2°C isotherm and downward pressure from air-breathing predators. King penguins use the 2°C isotherm in the upper 500 m surface layer to access deep-sea fish prey. The southern elephant seal is a deep-diving predator (up to 1500 m) and can access fish prey without the aid of the 2°C isotherm.

494

495

Appendix C

Appendix C: Ecoregionalisation of the Kerguelen and Crozet islands oceanic zone Part I: Introduction and Kerguelen oceanic zone

This appendix constitutes the technical report titled *Ecoregionalisation of the Kerguelen and Crozet islands oceanic zone Part I: Introduction and Kerguelen oceanic zone* written by P. Koubbi, A. Baudena et al. in 2016, and used for the extension of the marine protected area of Kerguelen and Crozet.

Ecoregionalisation of the Kerguelen and Crozet islands oceanic zone
Part I: Introduction and Kerguelen oceanic zone

Authors: Koubbi P.[1], Guinet C.[2], Alloncle N.[3], Ameziane N.[4], Azam C.S.[5], Baudena A.[6], Bost C.A.[2], Causse R.[1], Chazeau C.[1], Coste G.[5], Cotté C.[6], D'Ovidio F.[6], Delord K.[2], Duhamel G.[1], Forget A.[3], Gasco N.[1], Hautecœur M.[1], Lehodey P.[7], Lo Monaco C.[6], Marteau C.[5], Martin A.[1], Mignard C.[1,5], Pruvost P.[1], Saucède T.[8], Sinegre R.[1], Thellier T.[5], Verdier A.G.[5], Weimerskirch H.[2].

Affiliations:
1. Unité Biologie des organismes et écosystèmes aquatiques (BOREA, UMR 7208), Sorbonne Universités, Muséum national d'Histoire naturelle, Université Pierre et Marie Curie, Université de Caen Basse-Normandie, CNRS, IRD; CP26, 57 rue Cuvier 75005 Paris, France.
2. Centre d'Études Biologiques de Chizé, UMR 7372 du CNRS-Université de La Rochelle, 79360 Villiers-en-Bois, France.
3. Agence des aires marines protégées - 16 quai de la douane - CS42932 - 29229 Brest Cedex 2, France.
4. Unité Biologie des organismes et écosystèmes aquatiques (BOREA, UMR 7208), Sorbonne Universités, Muséum national d'Histoire naturelle, Université Pierre et Marie Curie, Université de Caen Basse-Normandie, CNRS, IRD; BP 225, 29182 Concarneau Cedex, France.
5. Terres Australes et Antarctiques Françaises (TAAF, Rue Gabriel Dejean, 97410 Saint-Pierre, La Réunion, France.
6. LOCEAN-IPSL, CNRS/MNHN/UPMC/IRD (UMR 7159), 4 place Jussieu, 75005, Paris, France.
7. CLS, Space Oceanography Division. 11 rue Hermes, 31520 Ramonville St Agne, France.
8. UMR 6282 Biogéosciences, Univ. Bourgogne Franche-Comté, CNRS, 6 boulevard Gabriel 21000 Dijon, France.

Corresponding author: Philippe Koubbi - philippe.koubbi@upmc.fr

Table of contents

ABSTRACT

A workshop was held in Paris from June 6 to 9th 2016. It was convened by Philippe Koubbi and Christophe Guinet. The main aim was to determine ecoregions in the Kerguelen oceanic zones to give orientations for extending the actual coastal natural reserve managed by the Terres Australes and Antarctiques Françaises. The workshop listed general conservation objectives to evaluate boundaries of ecoregions based on abiotic (geography, geomorphology and oceanography) and biotic features such as pelagic, benthic (including demersal ichthyofauna) and top predators species or assemblages. As biodiversity is not only species diversity, the workshop also considered the functional diversity (trophic web, essential habitats, life history traits,…).

This report is a summary of the conclusions based on expert knowledge. It is divided into three parts:

- A summary of the ecological characteristics of the Kerguelen oceanic zone;
- The ecoregionalisation of the pelagic realm, the benthic realm and the top predators;
- A final ecoregionalisation and recommendations for future works.

The workshop determined 12 main pelagic ecoregions based on oceanographic processes, pelagic assemblages and on keystone species distribution such as mesopelagic fish. Four Important areas for top predators were defined and 8 benthic ecoregions were drawn from the coast to the limit of the Kerguelen EEZ.

The experts found relevant to combine the pelagic and benthic ecoregions to obtain a global ecoregional map of 18 ecoregions based mainly on:

- Habitat characteristics (bathymetry, oceanography, primary production, biogeochemical parameters, …),
- Types of species assemblages with consideration of endemicity and conservation status,
- Functionality (essential habitats such as spawning grounds, nursery grounds or foraging habitats, areas of high primary and secondary production or, structure of the habitat by benthic species,…).

In this process, the workshop verified the superposition of the ecoregional synthetic map with specific habitats of species (birds and mammals distribution, essential fish habitats,...). It corrected some of the boundaries of ecoregions with these ecological parameters so that some essential species habitats are mainly within one region. For each of the final ecoregions, the workshop summarized the essential characteristics that support the creation of the ecoregion and estimated its ecological importance.

To conclude, the workshop indicated the need to continue research and monitoring over this vast area and to identify special research zones such as observatories to:

- Study the impacts of global change,
- Minimize knowledge gaps in ecology and environment,
- Consider natural variability,
- Study the resistance and resilience towards potential human impacts.

1 Introduction

A workshop was held in Paris from June 6 to 9th 2016 at the Université Pierre et Marie Curie with 29 persons. The workshop was convened by Philippe Koubbi, professor at UPMC (UMR BOREA) and Christophe Guinet, Director of Research at CNRS (CEBC).

The main aim of the week was to work on ecoregional process to:
- Give orientations for extending the actual coastal natural reserve of Terres Australes Françaises (CCAMLR-XXVI/BG/21, 2007),

- Evaluate if the process should be extended in the CCAMLR area in the planning domains 5 and 6.

1.1   Background of the workshop

Pr. Koubbi presented to the workshop the objectives of CCAMLR for defining a representative system of Marine Protected Areas in the Southern Ocean and recall paper SC-CAMLR-XXIX/13 (2010): "Contribution by France to work on bioregionalisation aimed at establishing marine protected areas in the CCAMLR area". Following this paper, different actions were held by French scientists to contribute to CCAMLR objectives concerning MPAs in the subantarctic area. The first initiative was to co-organize the CCAMLR workshop on MPAs in 2011 in Brest (France) where different papers were presented on the Kerguelen and Crozet areas:

- Améziane et al. (2011a). Estimating the biodiversity and distribution of the northern part of the Kerguelen Islands slope, shelf and shelf-break for ecoregionalisation: benthos and demersal fish. WS-PA11/09.

- Améziane et al. (2011b). Biodiversity of the benthos off Kerguelen Islands: overview and perspectives. WS-MPA-11/P03.

- Delord et al. (2011). Estimating the biodiversity of the subantarctic Indian part for the ecoregionalisation of CCAMLR areas 58.5.1 and 58.6: Part II. foraging habitats of top predators from French Antarctic Territories – areas of ecological significance in the Southern Ocean. WS-MPA-11/08.

- Duhamel et al. (2011a). Major fishery events in Kerguelen Islands: *Notothenia rossii*, *Champsocephalus gunnari*, *Dissostichus eleginoides* – current distribution and status of stocks. WS-MPA-11/P04.

- Koubbi et al. (2011). Estimating the biodiversity of the subantarctic Indian part for ecoregionalisation: Part I. Pelagic realm of CCAMLR areas 58.5.1 and 58.6. WS-MPA-11/10.

- Pruvost et al. (2011). PECHEKER-SIMPA – A tool for fisheries management and ecosystem modelling. WS-MPA-11/P02.

The second initiative was the organization with South Africa in 2012 in St-Pierre (La Réunion islands, France) of the CCAMLR workshop on Planning Domain 5 (Koubbi et al., 2012 WG-EMM-12/33 Rev.1) which gathered scientists from different countries.

From 2009 to 2011, a research project was carried out to collect all scientific data to summarize the ecology of Kerguelen and Crozet areas. This project was held with the financial support of the French Marine Protected Areas agency and the National Natural Reserve of TAF. The data used for this project came from different international and French database including results from French national polar projects supported by IPEV, the French Polar Institute, or from the fisheries researches.

Some of these data were transferred to *biodiversity.aq* and contributed to different chapters of the biogeographic atlas of the Southern Ocean (de Broyer et al., 2014). One of this chapter is the synthesis of Duhamel et al. (2014) on Fish.

1.2   Objectives of the workshop

The workshop held in June 2016 is based on the « best available science » for these subantarctic areas considering data quality and publications of the participants. The workshop evaluated as in the Census of Marine Life what is "known, unknown and unknowable" for achieving its task on ecoregionalisation.

The main objective was to determine ecoregions in both sectors. Ecoregions are the "assemblages of flora, fauna and the supporting geophysical environment contained within distinct but dynamic spatial boundaries" (Vierros et al., 2008). The result is a set of regions of distinct environmental conditions and species assemblages (Grant et al., 2006; Vierros et al., 2008; Koubbi et al., 2011).

For achieving this task, we used criteria of the CBD as the first step for identifying priority areas for future MPAs. These criteria were:

- Uniqueness / rarity;

- Special for life history of species;

- Importance for threatened, endangered or declining species / habitats;

- Vulnerability, fragility, sensitivity or slow recovery;

- Biological productivity;

- Biological diversity;

- Naturalness.

The workshop considered research and monitoring for identifying "special research zones" for long term ecological studies to understand impacts of climate change.

The workshop listed general conservation objectives to evaluate boundaries of ecoregions based on abiotic (geography, geomorphology and oceanography) and biotic features such as pelagic, benthic (including demersal ichthyofauna) and top predators species or assemblages. As biodiversity is not only species diversity, the workshop also considered the functional diversity (trophic web, essential habitats, life history traits,…).

The following general objectives for the workshop were to:

- Define representative ecoregions from:
  - Biogeochemical and oceanographic provinces, frontal zones, retention areas,
  - Pelagic and benthic spatial distribution of species assemblages,

- Identify species and habitats that are fragile, vulnerable or in danger,

- Identify key habitats (important bird areas IBAs, spawning habitats, nursery grounds, areas of high productivity, …),

- Identity special research zones for studying potential impacts of climate change and human activities.

The first document (Part I) is a summary of the conclusions of the workshop on the Kerguelen oceanic zone based on expert knowledge. It is divided into three parts:

- A summary of the ecological characteristics of the Kerguelen oceanic zone,

- The ecoregionalisation based on expert knowledge of the pelagic realm, the benthic realm and the top predators,

- A final ecoregionalisation and recommendations for future works.

The second document (Part II) is on the Crozet oceanic zone.

2 Ecological characteristics of the Kerguelen Islands oceanic zone

The abiotic and species diversity of the Kerguelen areas were described for the CCAMLR workshop on MPAs in 2011 for the benthic realm and demersal fish (Améziane et al., 2011a WS-MPA11/09 and 2011 b WS-MPA-11/P03; Duhamel et al., 2011a WS-MPA-11/P04), the pelagic realm (Koubbi et al., 2011 WS-MPA-11/10) and the top predators (Delord et al., 2011 WS-MPA-11/08). A new synthesis on top predators was published (Delord et al., 2013, background paper submitted to WG EMM, 2016). Additional information can be found in the special volume of the 1st international Science Symposium on the Kerguelen Plateau (Duhamel and Welsford, 2011).

2.1   Abiotic factors

2.1.1   Bathymetry and geomorphology

The Kerguelen Plateau separates the Enderby Basin and the Australian Antarctic Basin. It is one of the largest submarine mountain in the Southern Ocean and extends from 46°S to 62°S. It is divided into two parts by the Fawn Trough (sill depth: 2600 m; 56°S, 78°E). Further South, it is separated from the Antarctic continental shelf by the Princess Elizabeth Trough (sill depth: 3600 m; 64°S, 84°E) (Roquet et al., 2009). North of the Fawn Trough, the Plateau is subdivided into two main parts, the Kerguelen Islands shelf and the Heard islands shelf.

The marine geography of the Kerguelen and Heard EEZ differs from the other subantarctic islands. Both islands shelves are the largest ones of the Indian part of the Southern Ocean. The Kerguelen islands shelf represent 20% of the Kerguelen EEZ which is larger than Heard (10% of its EEZ) and the other subantarctic islands such as Crozet, Marion and Prince Edward (less than 3%). Importantly, 70% of the bathymetric range from 0 to 500 m of the Kerguelen-Heard Plateau is within the Kerguelen EEZ, it also includes the vast seamount of Skiff which is located in the west of the Kerguelen islands shelf.

The area between 500 and 1500 m represents 20% of the Kerguelen EEZ (Figure 1) which is also a large figure compared to other oceanic islands where this depth range represents only 5%. The deeper zone (> 1500 m) represents an area of 60% for Kerguelen towards, 65% for Heard and 95% for other subantarctic islands.
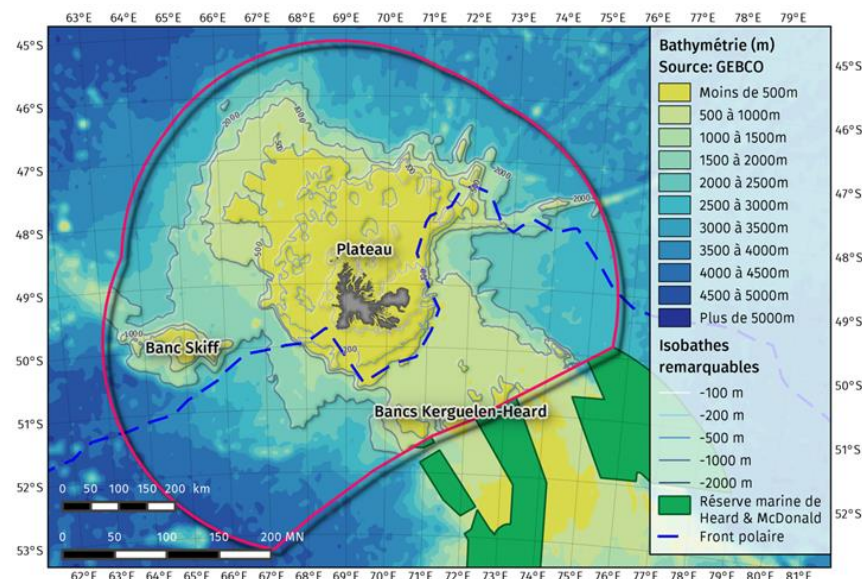
Figure 1: Bathymetry of the Kerguelen Exclusive Economic zone (EEZ).

2.1.2   Oceanography

The Kerguelen Plateau influences the position of the major frontal zones. Oceanographic features are characterized by a well-developed horizontal spatial gradient with a succession of frontal

zones from the north to the south that were summarized by Park et al (2008) and Koubbi et al. (2011). The following fronts are observed:

- The Subtropical Front (STF) which marks the northern limit of the Southern Ocean,

- The Subantarctic Front (SAF),

- The Antarctic Polar Front (PF) which is characterized by the northernmost position of the subsurface (200 m) temperature colder than 2 °C (Park et al., 1991, 1993; Orsi et al., 1995). Park et al. (1998) showed a meandering of this front in the Kerguelen area.

Between these fronts, large oceanographic regions are observed (Koubbi et al., 2011):

- The subantarctic zone lies between the STF and the SAF but this region is very limited in the Kerguelen EEZ and is more spread in the rest of the 58.5.1 CCAMLR area. There is a narrow band of approximately 2 ° of latitude caused by the juxtaposition of the STF and the SAF (Gambéroni et al. 1982; Charriaud and Gamberoni 1987; Park et al., 1991 and 1993). This unusual hydrological region is named the Transition Frontal Zone (TFZ),

- The Polar Frontal Zone (PFZ) lies between the PF and the SAF. The PF is closer to the TFZ in the Kerguelen shelf area than it is in the Crozet area,

- The Antarctic zone is located between the APF and the Southern Boundary of the Antarctic Circumpolar Current (ACC). It is at its largest extent south of Kerguelen with more than 15° in latitude, while in other sectors it extends only on few degrees.

The Kerguelen plateau is a major barrier to the eastward circulation of the ACC (Roquet et al., 2009). Most of the ACC transport in the region occurs either north of the Plateau along the SAF or through the Fawn Trough (close to Heard), but two other secondary branches cross the plateau (Figure 2). The first branch follows the PF and flows through a passage between the Kerguelen and Heard islands shelf (just south of the Kerguelen Island shelf). It continues south eastwardly in the oceanic zone to a permanent meander constrained northerly by the Gallieni Spur. The second branch transports colder and saltier water, passing south of the Heard shelf before curling northwest along the eastern edge of the Plateau and then joining the other branch at the meander of the PF. These two secondary branches bring the High Nutrient Low Chlorophyll (HNLC) water to the east of Kerguelen where they are in contact with iron sources of the plateau. This allows recurrent phytoplankton bloom to occur during springtime. This bloom allows productive hotspots over both the northern and Southern shelves and in the open ocean with a dynamical area which extends east along the ACC to approximately up to 90E.
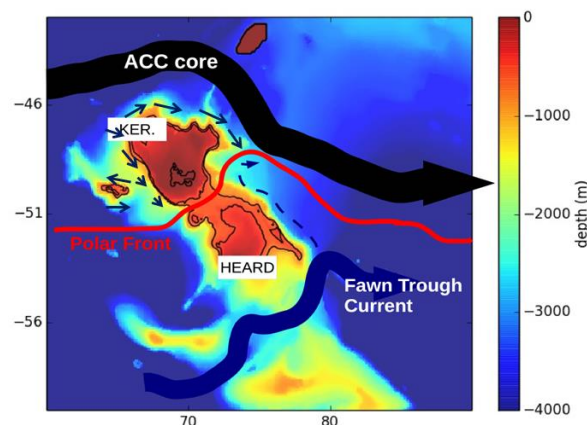
Figure 2: Circulation and position of the PF in the northern part of the Kerguelen Plateau (from d'Ovidio et al. 2015, adapted from Park et al. 2014).
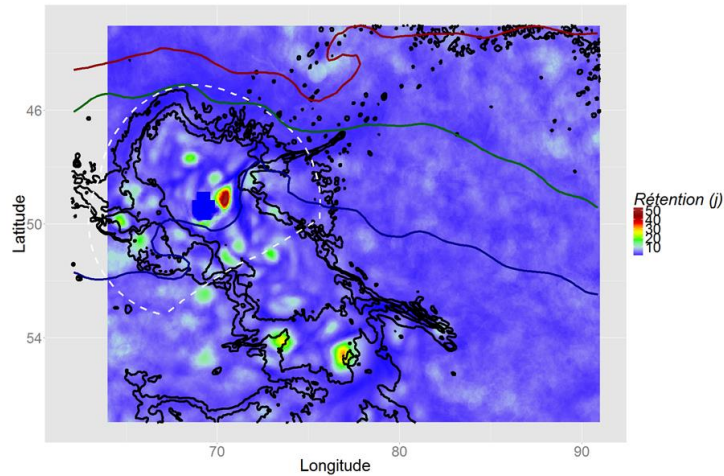
Figure 3: Average retention of eddy cores present in the region (in days) (d'Ovidio et al., 2013).

The springtime distribution of bioavailable iron, the main limiting factor for primary production, is heavily preconditioned by this current system and retention (Figure 3). It is very low west of the Plateau, high over the Plateau, and then decreases monotonically eastward with the exception of an iron moderate low area in the middle of the permanent meander of the PF (d'Ovidio et al., 2015).

2.2   Pelagic realm

2.2.1   Primary production

The Southern Ocean, South of the SAF is the largest HNLC area. This paradox is mainly due to the limitation of primary production by the low availability of micro-nutrients in Antarctic Surface Waters (notably dissolved iron) because of the distance from ice-free continents (Martin et al., 1990; Tagliabue et al., 2012). The Kerguelen region is one of the major exception, due to the input of iron and other trace metals from the island and from the shelf (Quéroué et al., 2015; van der Merwe, 2015). This induces a natural fertilization of Antarctic Surface Waters that promotes an important development of phytoplankton above the shelf and downstream (to the east) (Figure 4).
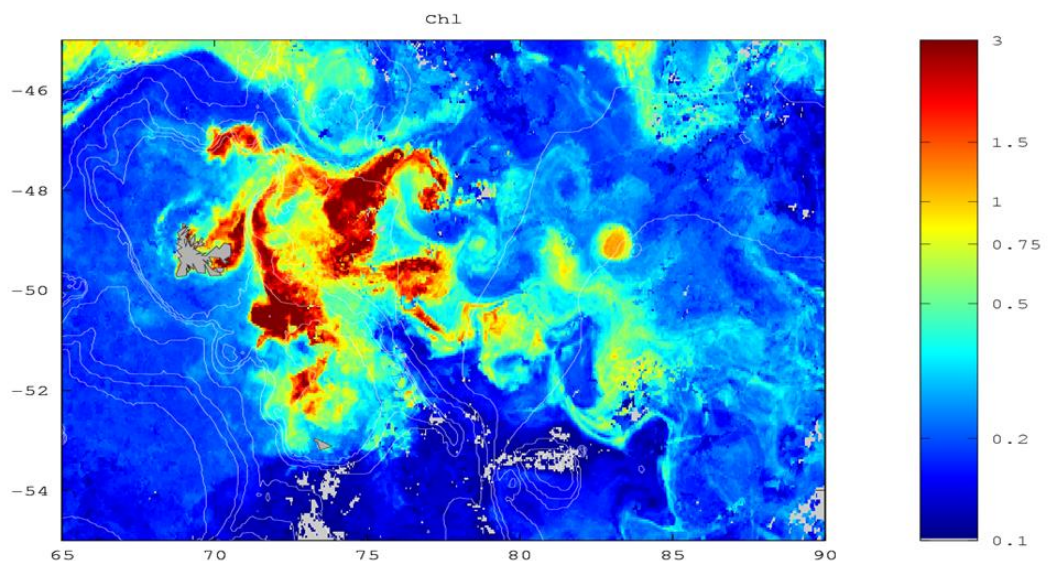
Figure 4: Chlorophyll-a concentration (mg/m3) proxy for primary production) around the Kerguelen shelf (from d'Ovidio et al., 2015).

The fertilization of surface waters around Kerguelen is highly constrained by ocean dynamics (d'Ovidio et al., 2015). The waters to the north and to the west (upstream) of the shelf are generally poor in iron and chlorophyll-a. The western part of the shelf being fed by these HNLC waters, it is also characterized by a low primary production (with the exception of coastal waters). On the contrary, the eastern part of the shelf shows higher chlorophyll-a concentrations, notably northeast of Kerguelen Island (possibly due to enhanced terrestrial inputs in Hillsborough Bay). An intense bloom is also observed every year above the deep passage between Kerguelen and Heard, probably due to the resuspension of sediments forced by internal waves (Park et al., 2008). These waters enriched with iron are transported offshore to the east by the ACC, thus fertilizing a vast region downstream of the Kerguelen Plateau. The complex recirculation pattern east of the Kerguelen Plateau, generates heterogeneity in the distribution of iron, which structures the phytoplanktonic bloom in this region (d'Ovidio et al., 2015). Waters trapped in the center of the recirculation region (within the PF meander) are characterized by relatively low primary production (due to reduced iron availability), whereas the jets associated with the PF (notably north of the meander) allow for a fast delivery of iron downstream, thus limiting the loss of iron by scavenging during the transit.

The phytoplanktonic bloom associated with the Kerguelen Plateau is observed every year in November and December (growing phase), and persists to a lower extent in January and February (declining phase) (Mongin et al., 2008). The duration of the bloom largely depends on ocean stratification in spring (caused by reduced winds and sea surface warming), and the availability of iron and silicate during summer. Brief events of destratification of the water column during summer (notably in response to summer storms) could also have a positive impact on primary production since it allows for the resupply of nutrients to the surface layer (including micro-nutrients recycled from biogenic matter synthesized during the growing season). The depletion of silicate and iron in surface waters, which characterises the decline of the bloom, is associated to a modification in the structure of the phytoplanktonic ecosystem (Mosseri et al., 2008 ; Lasbleiz et al., 2014) : during the growing phase, the bloom is dominated by heavily silicified diatoms, while smaller cells dominate the declining phase (small diatoms and nanoflagellates). The decline phase of the bloom is also associated with an increase in the abundance of grazers, which could be explain by linked to the quality of the phytoplanktonic resource since small organisms are more vulnerable to grazing than the large diatoms (Carlotti et al., 2015).

2.2.2 Plankton and pelagic fish

The biogeographic atlas of the Southern Ocean (de Broyer et al., 2014) gave synthesis on the presence of marine species including plankton (Kouwenberg et al., 2014 for copepods; Cuzin et al., 2014 for Euphausiids, …), fish (Duhamel et al., 2014) or cephalopods (Rodhouse et al., 2014). The large scale biogeographic patterns of these groups are linked to the latitudinal zonation due to the position of the major frontal zones (Koubbi et al., 2014).

In this context, the geographic position of the Kerguelen Islands in relation to these fronts induces high changes in pelagic assemblages over short distances. These assemblages are subtropical, linked to the Transition Frontal Zone, the Polar Frontal Zone or the Antarctic zone, respectively. The transition is not only latitudinal, it differs longitudinally because of the meandering of the PF around the Kerguelen island shelf. The spatial segregation of assemblages is also complex because of the juxtaposition of the SAF, the STF and in the eastern part the PF. Importantly, these fronts are at their most northern position in this area of the Indian part of the Southern Ocean. There is a pelagic diversity gradient that is observed for plankton (Koubbi et al., 2011), fish larvae (Koubbi et al. 1991; Koubbi, 1993) or pelagic fish (Duhamel et al., 1998 and 2014). We have demonstrated that the SAF is the main biogeographic barrier of Southern Ocean species whereas the PF is the main barrier to the subtropical fauna (Duhamel et al., 2014; Koubbi et al., 2014). This latitudinal pattern is not unique. There are also differences in species assemblages between subantarctic islands as these ones are located differently towards each major front. Crozet, for example, is well separated from the PF.

2.2.2.1 Plankton

There are neritic and oceanic assemblages (Figure 5) but also differences between the northern and southeastern part where waters are colder.
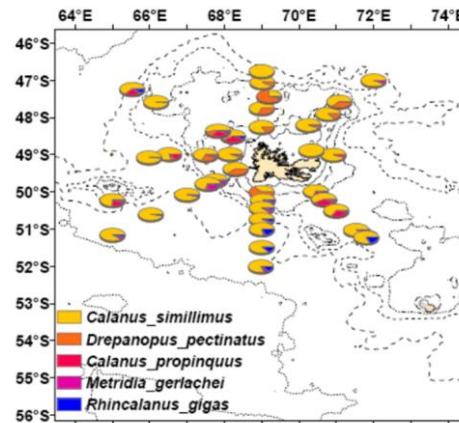
Figure 5: Proportion of copepods from the SKALP surveys (1987-88) in the oceanic zone of Kerguelen (Koubbi et al., 2011).

The neritic zone of Kerguelen is characterized by the presence of the endemic copepod species, *Drepanopus pectinatus*, which is also observed around Crozet. In the coastal zone, this species is the most abundant, especially in the Morbihan Bay, the largest inner bay of the archipelago which is open to the ocean the east by the Royal Passage. In this area, *D. pectinatus* dominates at more than 99% the copepods. This species has four generations per year and supports foraging of planktivorous species in the coastal zone.

The Kerguelen coastal zone is quite unique as there are a high numbers of bays of different sizes and fjords where other pelagic assemblages are observed. There are high seasonality in the plankton or the ichthyoplanktonic assemblages within the Morbihan Bay or in the other coastal areas (Koubbi, 1992; Koubbi et al., 2001)

The amphipod *Themisto gaudichaudii* or the euphausiid *Euphausia vallentini* are also distributed in the coastal zone and the oceanic zone where they can be very abundant as shown by recent results with the continuous plankton recorder (Figure 6). They are keystone species as they are the main preys of planktivorous species including seabird and fish.
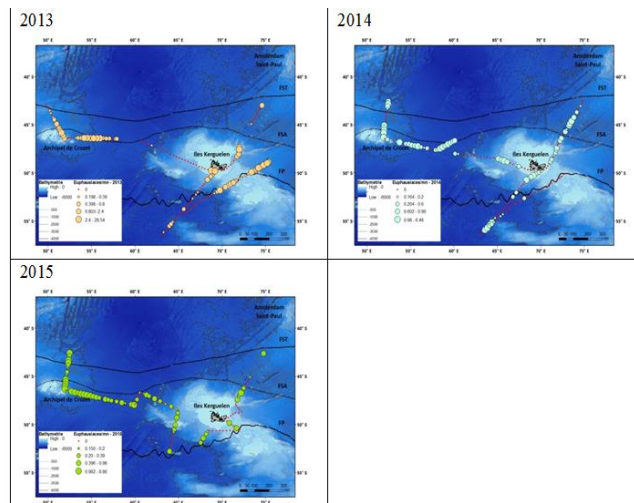
Figure 6: Abundance of Euphausiids collected by the CPR during summers 2013, 2014 and 2015 from the R/V "Marion Dufresne".

2.2.2.2 Mesopelagic fish

Myctophid fish larvae dominated the oceanic zone with mainly *Krefftichthys anderssoni*, *Gymnoscopelus* sp. and *Protomyctophum* sp. larvae (Koubbi et al., 1991). Nototheniids larvae occur over the island shelves whereas myctophid larvae are mainly found in the oceanic zone but also over the shelf. The larval taxonomic richness increased to the north in the TFZ and is greatest in the Agulhas Front region (Koubbi, 1993; Koubbi et al, 2011).

K. anderssoni larvae were the most abundant in the epipelagic zone, and are present throughout the year with maximal abundances observed during winter (Koubbi et al., 1991). Koubbi et al. (2003) showed that distribution is age dependent. The small larvae distribution might indicate an essential habitat (either hatching area and/or nursery area) in the meander of the PF in the east of the Kerguelen shelf.

In terms of their species richness, biomass and abundance, lantern fishes (family Myctophidae) are the dominant Fish in the mesopelagic and bathypelagic zones of the subantarctic Indian Ocean (Duhamel & Hulley, 1993; Duhamel et al., 2005). Adult specimens generally occur offshore of the 200m continental shelf-break around the island systems. With the exception of *K. anderssoni* and the bathypelagic species *Gymnoscopelus opisthopterus* and *Nannobrachium achirus*, all mesopelagic myctophids undertake diel vertical migration (Duhamel et al., 2014; Koubbi et al., 2011). About 26 species of lantern Fish are now known from the Crozet and Kerguelen regions (Hulley, 1990; Duhamel and Hulley, 1993). There are no endemic or rare species of lantern Fish either at Crozet or at Kerguelen. Here, the myctophid ichthyofauna is dominated by Antarctic (66%) and subantarctic species (34%), but convergence and bi-temperate species do occur (Koubbi et al., 2011). Habitat modelling showed the Kerguelen area host one of the most northern extent of Antarctic species such as *E. antarctica* (Figures 7 and 8). This is specially observed in the meander of the PF east of the shelf. Recent samplings realized in this region reported a high diversity of Fish, particularly myctophids, in the PF area.
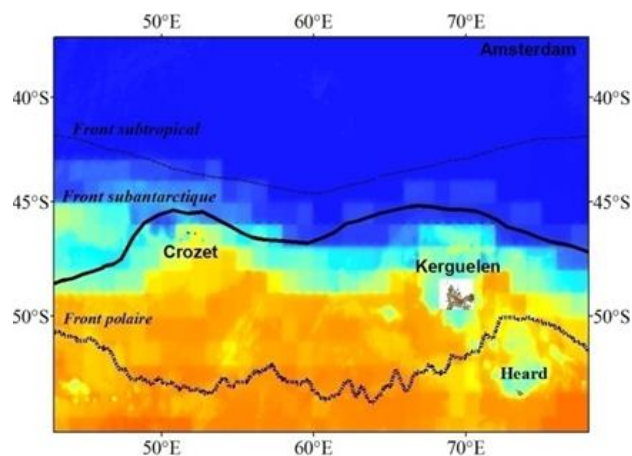
Figure 7: Potential habitat of *Electrona antarctica* estimated with Boosted Regression Trees (adapted from Duhamel et al., 2014).
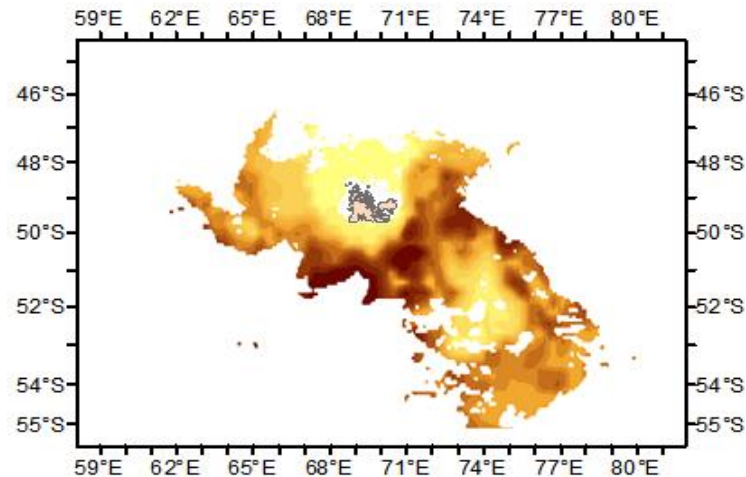
Figure 8: Modelled abundances of *Electrona antarctica* in the Kerguelen oceanic zone showing areas of high concentration (in dark brown) in the eastern part of the area in the oceanic zone. This species does not occur over shelves (yellow) (Loots et al., 2007).

2.2.2.3   Secondary production

Synoptic views of the secondary pelagic production at the large regional scale of Kerguelen EEZ can be explored through ecosystem modelling. One model of lower and mid-trophic functional groups of the ocean ecosystem (Lehodey et al 2010; 2015) provides predicted distributions of biomass for one group of zooplankton and 6 groups of micronektonic organisms (~1-20 cm in size) defined according to their nycthemeral vertical behaviour between surface and ~1000 m depth. The vertical dimension is simplified with three layers: the epipelagic layer (~0-150m), and the upper- (~150-400m) and lower- (~400-1000 m) mesopelagic layers. The model is forced by water temperature, horizontal currents and primary production (based on satellite ocean colour data). It provides hindcast simulations at resolution of ¼ to 1/12°. The dynamics is based on functional relationships between the time of development of the organisms and their ambient temperature. During their development the organisms are redistributed by the currents and a diffusion coefficient representing their own random movements.

The differences in temperature and circulation combined with these times of developments produce quite different biomass distributions according to the layer and group considered (Figure 9). Following the spring bloom of productivity in the eastern Kerguelen EEZ region, the zooplankton peak of productivity is predicted to occur in Dec-Mar period in the eastern region also. However the dynamics is quite different for the deep micronekton group that is less impacted by seasonality due to a longer lifespan and show high concentration on the western edge of the plateau. If the model predictions capture the key patterns of the small pelagic organisms dynamics, they should match predators overall distributions according to their targeted prey. It is for instance interesting to note that the distribution of observed sperm whales around Kerguelen (see section below) shows higher density along the west coast coinciding with high predicted biomass of deep potential prey species.

	Zooplankton	Lower mesopelagic micronekton
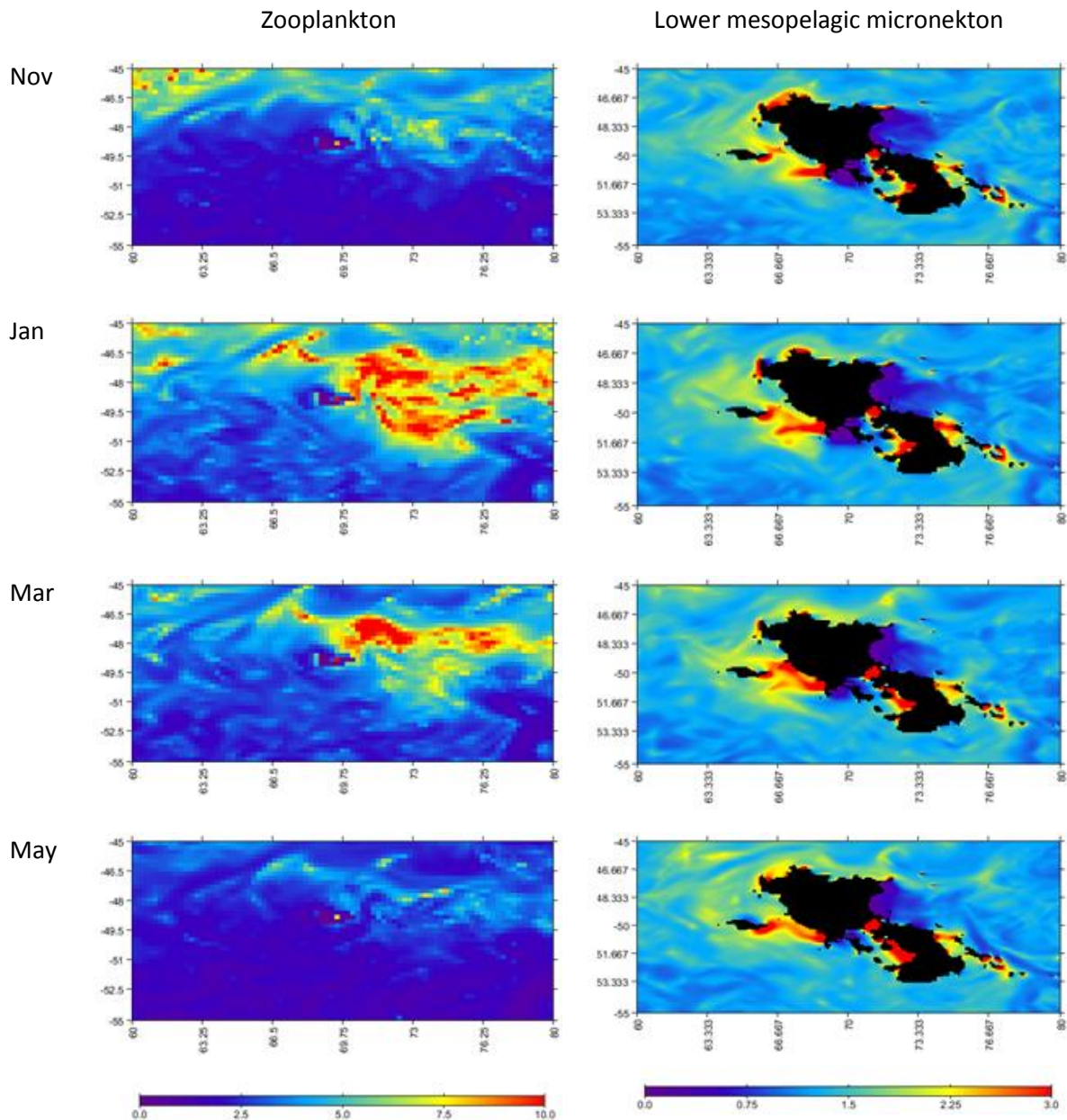
Figure 9: Predicted monthly biomass distribution (g of wet weight per m^2) of zooplankton and the lower mesopelagic micronekton group in the Kerguelen region from Model Seapodym (Lehodey, pers. comm).

2.3   Seabirds and marine mammals

The Kerguelen archipelago hosts one of the diverse and abundant marine birds and mammals populations of the Indian sector of the Southern Ocean. The Kerguelen Islands is the site of reproduction of 29 seabird with several of them classified as vulnerable or near threatened by IUCN. Some species are strictly endemic to the Kerguelen Islands. Three species of pinnipeds, the subantarctic fur seal and the Southern elephant seal reproduce at Kerguelen. The marine area of these islands is essential for all these species as it provides essential foraging areas especially during the reproductive period. However, some species forage all year long in the coastal zone (Kerguelen shag, gentoo penguin, kelp gull *Larus dominicanus judithae* and the Kerguelen tern *Sterna virgata*).

The seabird and pinnipeds community of Kerguelen constitutes, after South Georgia, the second consuming biomass of the Southern ocean in terms of prey caught per year. The waters off Kerguelen

are also the foraging habitat of different species of cetaceans (odontoceti : sperm whale, killer whale, long-finned pilot whale, Commerson dolphin, southern right whale dolphin, Hourglass dolphin and beaked whale) and mysticeti (humpback whale, fin whale, blue whale (pygmy), fin whale, southern right whale). Historically, the waters of Kerguelen were an important area of foraging of cetaceans which were exploited at the whaling station of Port Jeanne d'Arc in the Morbihan Bay and afterwards from whaling vessels until the middle of the 1970's. This has considerably reduced their number and these species were threatened of extinction in the area. Similarly, the king penguins and subantarctic fur seals populations were also heavily exploited during the 19th century and almost disappeared from the area, but the population have recovered since then.

Most of these species exploit a vast at-sea gradient of habitats from the coastal zone to the oceanic province, from the surface to the deep oceanic zones. The marine birds and mammals communities have various trophic niches characterized by crustaceans, mesopelagic and benthic fish and calmar (with various proportions of these different preys in their diet).

Information on the at-sea distribution of these species are from two sources. First, the telemetric tagging realised by CEBC-CNRS over the past 20 years, these data are accessible in the database of the UMS PELAGIS. The tracking allows the determination of the movements of different species between the colonies and the feeding zones, and thus to identify and characterize preferential foraging habitats (Figures 10 to 12). However, these data are biased as only individuals of some colonies are tracked and mostly during the breeding season. The second source of information is from at-sea observations from fishing vessels (database PêcheKer-MNHN) and from observations conducted from the R/V « Marion Dufresne » (at-sea survey database from CEBC-UMS-PELAGIS) (Figures 10 and 11). The third source of information is from the staff of the national natural reserve, especially in the Morbihan Bay. Observation data do not allow to know the origin of the birds and marine mammals that are observed but give a comprehensive synoptic vision of the distribution of these species for sectors that are regularly visited by vessels.
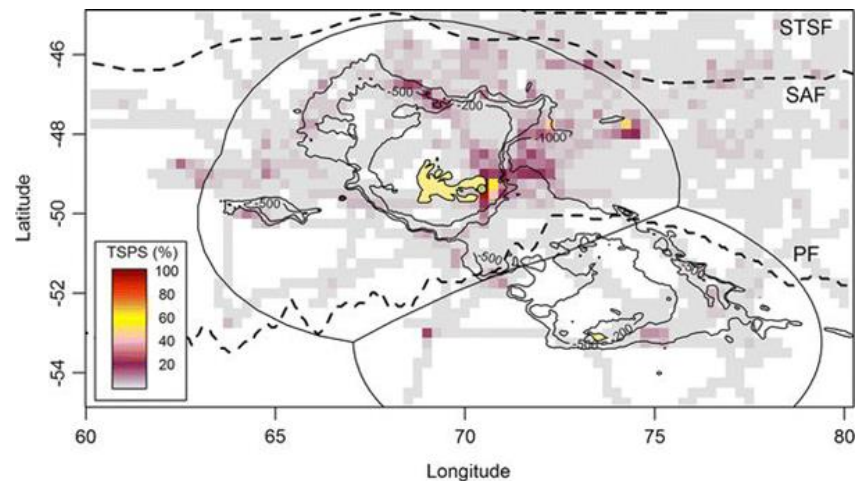
Figure 10: Standardised time spent per square from Wandering albatross *Diomedea exulans* tracking data. Contours of the Kerguelen/Heard Plateau, colony (green point), exclusive economic zones (solid lines) and fronts (PF Polar Front, SAF SubAntarctic Front, STSF southern Subtropical Front) (dashed lines) are represented (Thiers et al. 2016). Their at sea distribution shows that they are selecting the slopes of the Plateau and the PF meander.
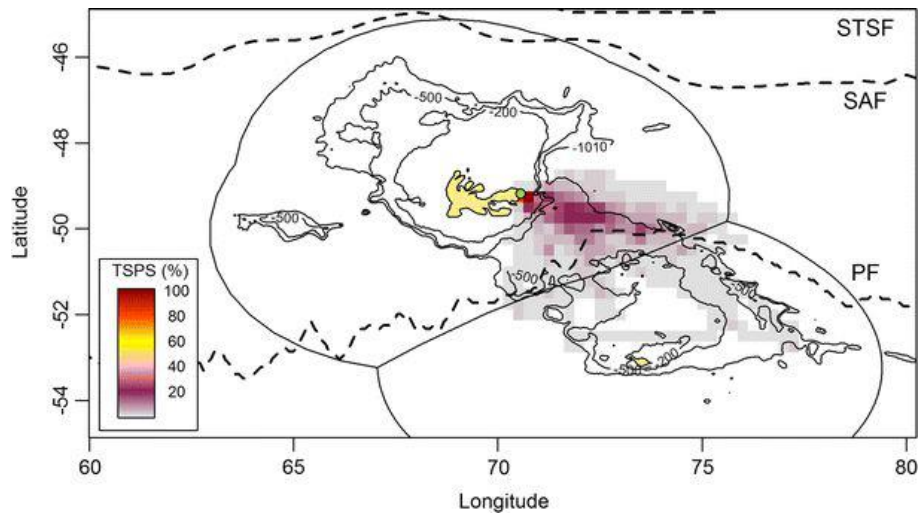
Figure 11: Standardized time spent per square for King penguins from the Ratmanoff colony in the eastern part of Kerguelen. Their at-sea distribution shows that they are selecting the PF meander and the cold water coming from the Fawn Trough (Thiers et al. 2016, Bost et al.2009).

Important at-sea habitat

The identification of important marine mammals habitats is either linked to one of these various types of information (at sea observations for cetaceans) or a combination of information of them (wandering albatross, black-browed albatross, white-chinned petrel) (Figures 12 to 14).
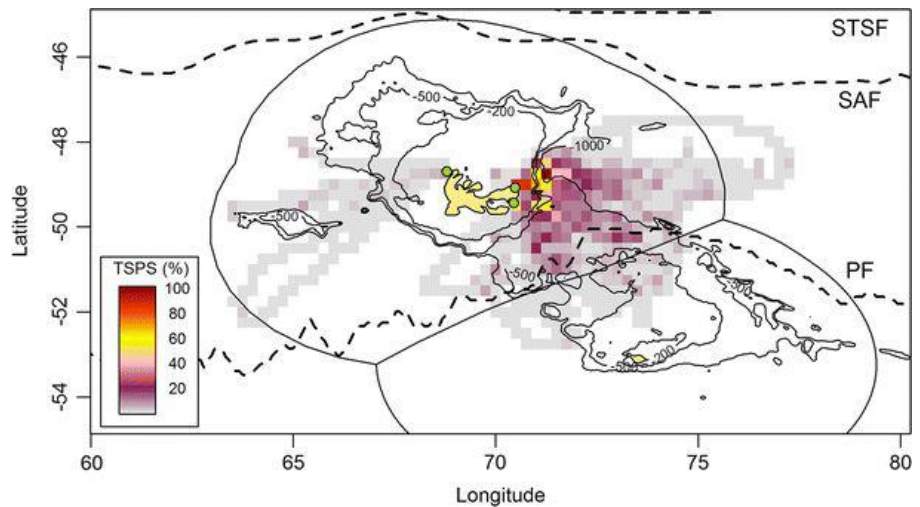
Figure 12: Standardised time spent per square from Antarctic fur seal *Arctocephalus gazella* tracking data. Contours of the Kerguelen/Heard Plateau, colonies (green dots), exclusive economic zones (solid lines) and fronts (PF Polar Front, SAF Subantarctic Front, STSF southern Subtropical Front) (dashed lines) are represented (Thiers et al. 2016). Their at -sea distribution shows that they are selecting the PF meander and the cold water coming from the Fawn Trough.
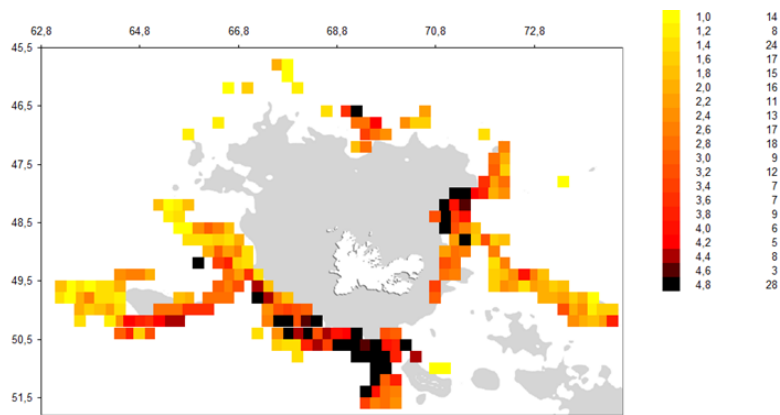
Figure 13: Mean number (on a 0.2° grid basis) of subantarctic fur seals by observation made by observer on board fishing vessels (PecheKer database).
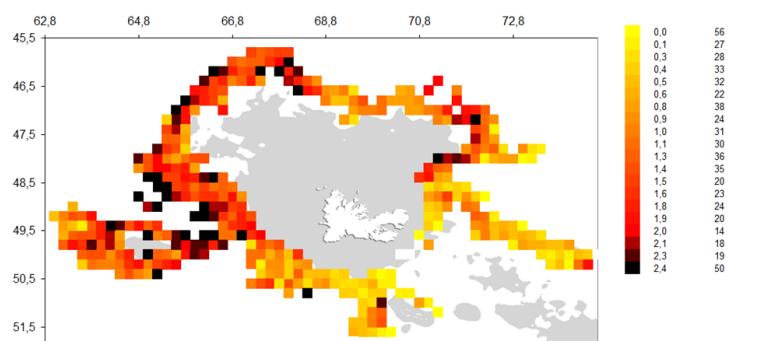
Figure 14: Mean number (on a 0.2° grid basis) of sperm whales by observation made by observer on board fishing vessels (PecheKer database).

This information allows identifying important habitats for a great number of species within the Kerguelen EEZ but also outside in the CCAMLR and in the subtropical areas (Figure 15) (Delord et al. 2013, 2014). Some species forage all year long in the Kerguelen EEZ, others forage only during part of the year (during the reproductive period) and some only partially.
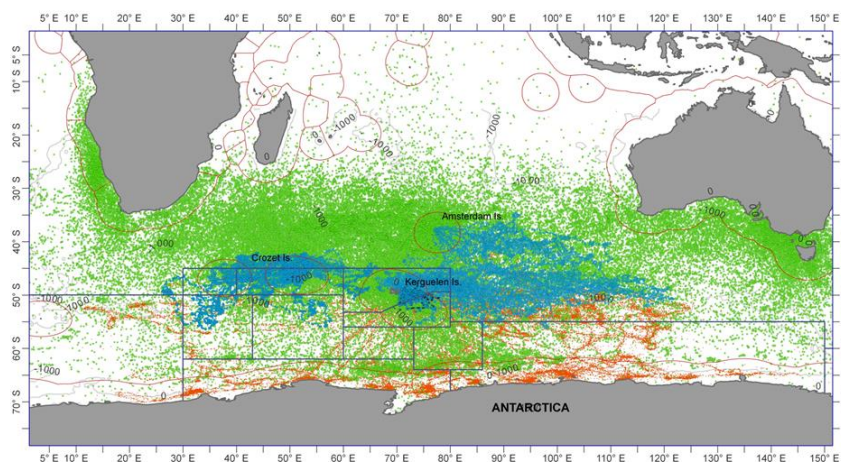
Figure 15: Map of locations in Indian Ocean of breeding and non-breeding seabirds (green: albatrosses and petrels, skuas; orange: seals; blue: penguins). The CCAMLR (Commission for the Conservation of Antarctic Marine Living Resources) statistical divisions (blue lines) and EEZs (red lines) are shown (Delord et al. 2013, CEBC-CNRS database).

The criteria for characterizing important habitats were also linked to other factors such as endemism (mainly the coastal and neritic zone), multispecific use of an area, the vulnerability of species and the diversity of ecological habitats that are used by marine birds and mammals.

2.4 Benthic realm

2.4.1 Littoral and nearshore areas

The coastal benthic zone is here considered between the supratidal domain and 100 m depth. It includes various patchy habitats and ecosystems, which are unique to the Kerguelen Islands in this part of the ocean (e.g. deep and blocking mussel-beds) but also globally (numerous fjords with entrance sills). Since 2011, the IPEV program n° 1044 PROTEKER, carried out thanks to a partnership with the TAF national natural reserve, aims at setting up a nearshore long-term sub-marine observatory for the inventory of the Kerguelen Islands coastal marine species and ecosystems and the monitoring of coastal biodiversity facing the impacts of environmental changes related to global warming. For this purpose, nine different stations were defined in contrasting areas, which are representative of the diversity of coastal habitats: kelp forest zones, habitats with sponges and fjords. These sites were also instrumented with temperature recorders and colonisation plates to study benthic assemblage dynamics.

2.4.2 Neritic zone and shelf break – VME indicators

The benthic Kerguelen populations can be characterized spatially following the distribution of indicator taxa of vulnerable marine ecosystems (VME) (Figure 16). These taxa were defined according to the CCAMLR VME's protocol with consideration of the patrimonial aspect, the role in structuring the habitat, if the taxon is a bioindicator of the existence of a remarkable benthic ecosystem or if the taxon is sensitive to human pressure.

Over the Kerguelen shelf, the geographic distribution of sampled VME indicator taxa by the POKER surveys were used for modelling potential habitats of these taxa by using ecological niche modelling based on catch data POKER campaigns. These distributions highlight contrasting and complementary patterns. The study area can thus be divided into sectors that can be attached specific conservation issues that will be described in chapter 3.
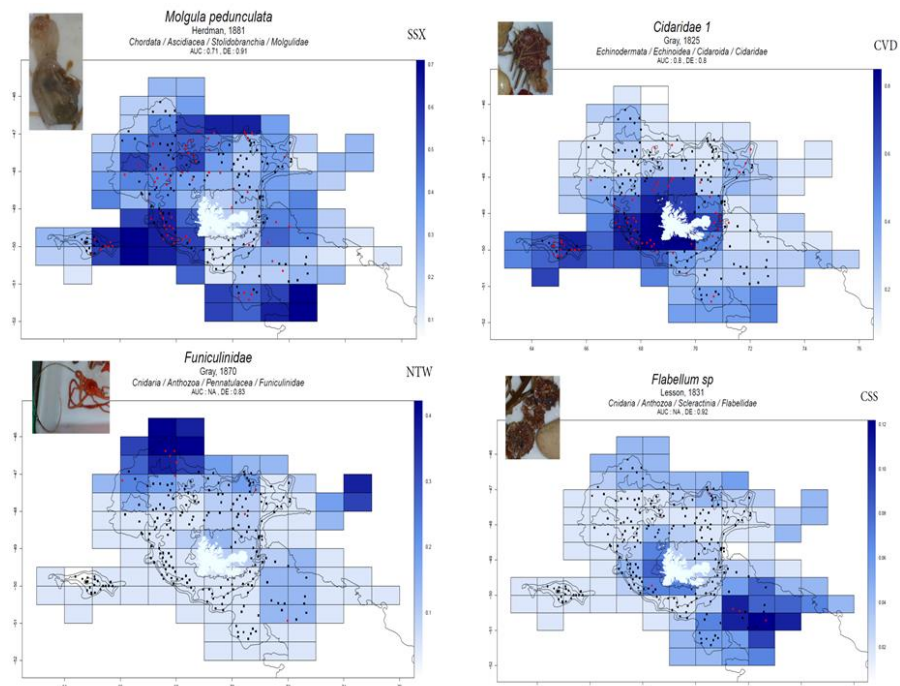
Figure 16: Some distributions of vulnerable marine ecosystems (VME) benthic taxa used for our analysis.

2.4.3 Demersal fish

Our knowledge on demersal fish of the Kerguelen Islands shelf and the surrounding deep areas is based on historic dataset among which:

- Oceanographic surveys on the R/V « Marion-Dufresne » MD03 and MD04 during the 70',
- Coastal surveys with "La Japonaise" and "La Curieuse" during the 80' and the 90',
- Fisheries surveys in the neritic zone (SKALP in 1987/1988, Poker 1 in 2006, POKER 2 in 2011, POKER 3 in 2013 and PIGE in 2015) restricted to the 100-1000 m bathymetric range,
- Our knowledge of the bathyal domain is mainly derived from fisheries monitoring (dataset PECHEKER).

Duhamel (1987), Koubbi (1992), Duhamel et al. (2005), Koubbi et al. (2000, 2001 and 2009) described the life cycles of the main fish species of the coastal and neritic zone. These studies identify functional areas such as position of spawning grounds, larval concentrations or nursery grounds which are important to consider for conservation. Life stages spatial segregations are observed for some species with ontogenic migrations from the spawning grounds to the nursery areas. The species trophic level needs to be particularly considered throughout the life stages of Fish underlining the strong zooplanktonic dependence of many neritic shelf species.

About 20 demersal species from the neritic to the deep zone are included in the ecoregionalisation process. It includes commercial species (Mackerel Icefish *Champsocephalus gunnari*, Grey Notothen *Lepidonotothen squamifrons*, Marbled Notothen *Notothenia rossii*, Patagonian Toothfish *Dissostichus eleginoides*, Bigeye Grenadier *Macrourus carinatus* and Skates *Bathyraja* spp.). Potential habitats of these species were calculated using Boosted Regression Trees (Duhamel et al., 2014).

3 Ecoregionalisation

3.1 Pelagic ecoregions
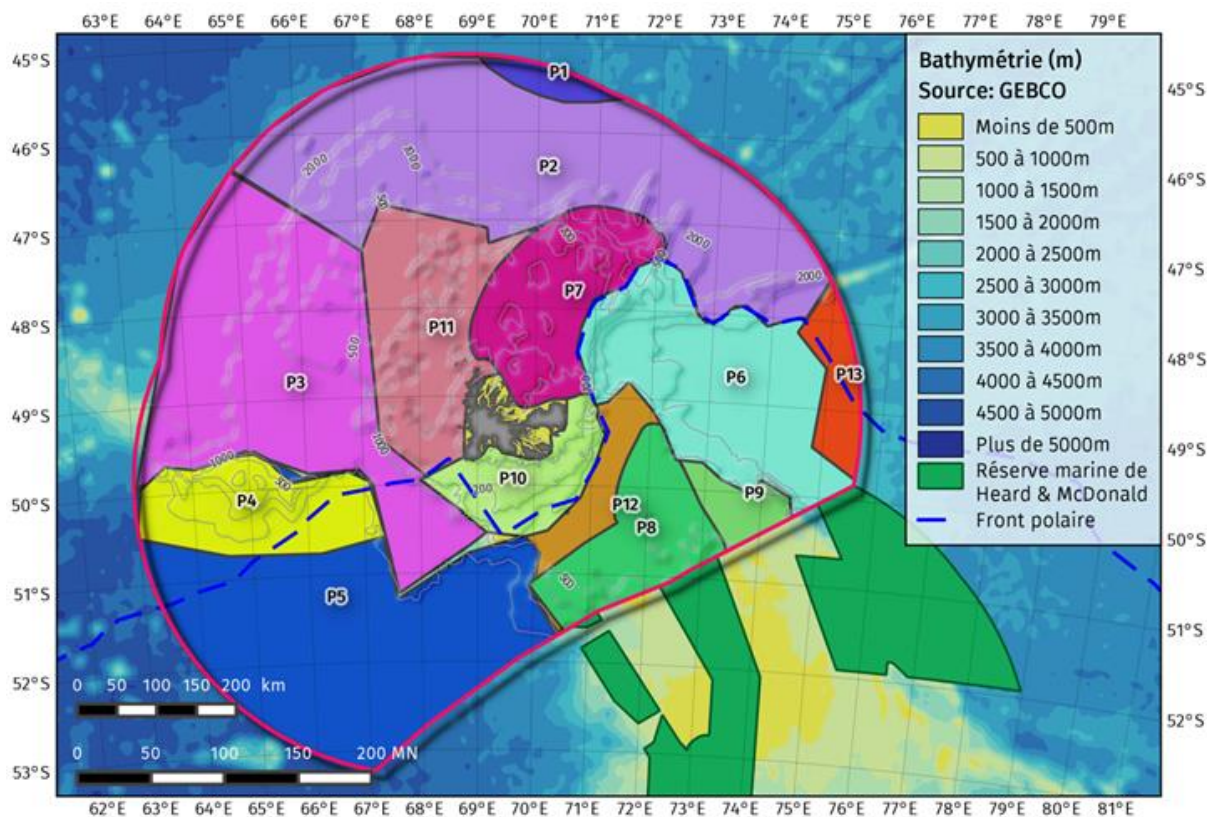
Figure 17: Map of the pelagic ecoregions.

The workshop determined 12 main pelagic ecoregions (P1 to P12) based on expert knowledge on oceanographic processes, pelagic assemblages and on keystone species distribution such as mesopelagic fish (Figure 17). The main conclusions are:

1. The Kerguelen EEZ lays south of the SAF.

    There is only a small area north of the Kerguelen EEZ that is subantarctic (P1). Even if it is unique, the subantarctic area will be more representative in the rest of the CCAMLR 58.5.1. rectangle. The SAF is known to be a biogeographic barrier for pelagic faunas and the subantarctic zone is where Antarctic, subantarctic and subtropical faunas (plankton and mesopelagic fish) can be found.

    However, the oceanic zone north of the island shelf break (P2) is important because it is characterised by the maximal intensity of the ACC which brings high energy in this area. The ACC also influence the northern shelf break.

    This northern area is low in silicates.

2. The Polar Front and its meander

    The main feature explaining the pelagic regionalisation of this zone is the PF. In the Kerguelen oceanic area, this front is constrained by the topography of the Kerguelen shelf. The PF seems more spatially stable in this area than in other sectors of the Southern Ocean. It is associated with a jet which transports water through a canyon located in the southwestern part of the deep passage between the islands shelves of Kerguelen and Heard (P12). After running along the southern Kerguelen shelf break, the PF is continuing along the eastern shelf break and meanders afterwards following the Gallieni Spur. The meander creates a retention of waters in subsurface which favours pelagic productivity and subsequently provides favourable foraging areas to marine birds and mammals (P6). One has to notice that the PF is not constrained by the topography in the southeastern part of the area meaning that it can fluctuates spatially according mesoscale activity and cannot be considered as a fixed boundary. For the ecoregionalisation process, the PF in the southwestern area is included in one region (P5) because of its possible variability and is the boundary between regions in the rest of the area where it is constrained by topography.

    In the ecoregionalisation process, the area (P6) where the PF meander is an area of average production. High concentrations of larvae and juveniles are observed (mesopelagic fish, Muraenolepididae, …). It is a unique zone of recirculation which has a key role for the life cycle of different fish. *K. anderssoni*, a myctophid has high young larvae concentrations indicating a possible spawning in this area. This area is also an Area of Ecological Significance because of the northernmost extent of cold waters.

3. Iron enrichment

    A west/east axis is observed. The waters coming from the southwest are limited in iron, they get enriched with arriving towards the Plateau and crossing the passage between the island shelves of Kerguelen and Heard (P12 and P8). It is the reason why the P8 area gets richer in iron which favours planktonic production and, ultimately, concentration of marine birds and mammals.

4. Areas of high biological productivity.

    The northeastern shelf off the Baleiniers Gulf (P7) is a possible retention zone for pelagic organisms and is one of the most regularly productive zone in the area. Different fish have their larval development in this area among which *C. gunnari* as this species spawns in the canyon of the Baleiniers Gulf or *L. squamifrons* for which this area is a nursery ground.

    The other highly productive area is the southern Plateau south of the Kerguelen Island shelf

(P8) with parts over the Heard islands shelf. It is one of the most productive area of the POOZ (Permanent Open Ocean Zone) of the Indian part of the Southern Ocean.

The third area (P9) is located just south of the meander where cold waters are brought towards the subsurface, structuring mid- to high trophic organisms and their interactions, i.e. favours the accessibility of mesopelagic fish for top predators such as the King penguins.

5.   South and western shelf areas

The southern shelf area is between the Pf and the coast (P10). P11 lies in the western part of the shelf.

6.   Skiff bank (P4)

There is a bank effect linked to the presence of this large seamount with the PF at its southern limit. Fish larvae are very abundant.

6.   HNLC and western oceanic zone

Most of the western oceanic zone beside the Skiff bank is influenced by Antarctic waters and are considered being HNLC (High Nutrient Low Chlorophyll) areas (P3). The biological production is slow because the waters are limited in iron.

3.2   Top predators ecoregionalisation
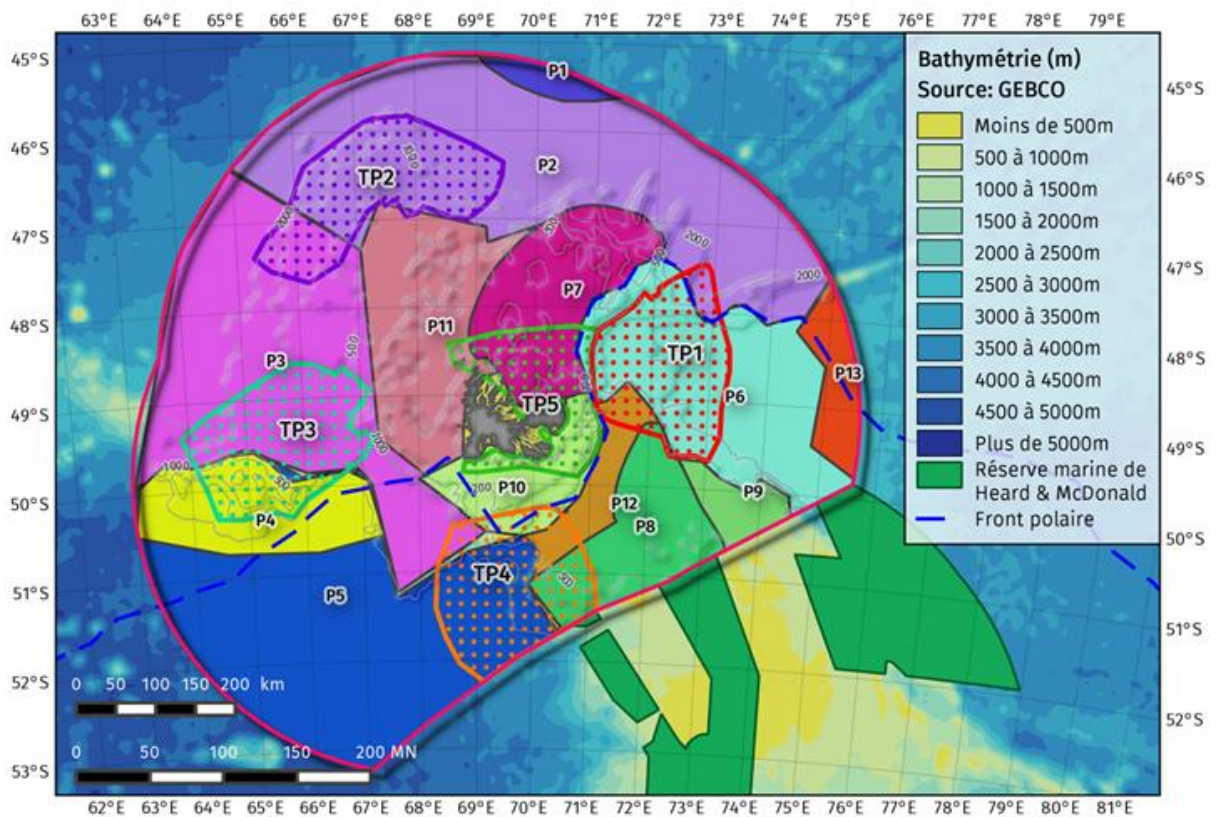
Figure 18: Important bird areas (in dotted lines) overlaid on the pelagic ecoregions.

Among the different species of top predators occurring in the oceanic zone of the Kerguelen Islands, not all of them have the same level of conservation (status of conservation, rarity, vulnerability …). One should consider the responsibility of the Kerguelen EEZ in maintaining these populations of marine birds and mammals.

Among all species, species requesting priorities are procellariiforms: wandering albatross, black-browed albatross, white-chinned petrel and grey petrel (vulnerability criteria and importance of the

Kerguelen population relatively to the world population). Then we find rockhopper and macaroni penguins because of their IUCN status of consideration. The Commerson dolphin is another example because it is endemic. Elephant seals appeared to be very important in terms of number of individuals compared to the world population.

The Important areas for top predators (TP 1 to 4, Figure 18) can be determined as following:

1. PF meander (TP1)

   This area has a horseshoe shape and is a highly important area for the foraging of various species. Penguins forage in this area because of the accessibility and abundance of preys and also because of predictable trophic resources. It is the case of the macaroni and rockhopper penguins, species with a high patrimonial value in Kerguelen but also the King penguin. The wandering albatross also have a high patrimonial value for Kerguelen; individuals for the Courbet colony in the eastern part of the islands are using this PF meander. The black-browed albatross is also observed.

   This area is also where there is a high concentration of sperm whales along the eastern part of the archipelago. Fur seals which reproduce in the Courbet peninsula also forage preferentially in this area. Historically, fur seals colonies were the most important in the NE sector of the Courbet Peninsula because of their proximity with this sector.

2. NW and north shelf break (TP2)

   This region gathers high concentrations of teutophageous species. The wandering albatross coming from Crozet occur in this area such as the black-browed albatross, sperm whales which also forage on Patagonian toothfish and pilot whale.

3. West shelf break and northern Skiff seamounts (TP3)

   This area, over the northern part, has the same ecological function as the NW and western part of the shelf; the same species are found. The southern edge of the area is influenced by the PF which attracts fur seals.

4. SW passage of the Plateau (TP4)

   This area is located between the island shelves of Kerguelen and Heard. High concentrations of fur seals are observed such as diving petrels and black-browed albatross along the external border of the shelf. An important concentration of males of elephant seals is observed. They forage on benthic preys. This area is probably important for the feeding of Macaroni penguins and white-chinned petrel which are two species with a high patrimonial value for Kerguelen.

5. Coastal zone (TP5)

   We observe an assemblage of species that are strictly dependant of the coastal zone. Most of them are ichthyophagous (Kerguelen shag, gentoo penguin, Commerson dolphin present all year long) but some are planctophagous like Prion sp. which occurs in the area only seasonally. Historically, this zone had high concentrations of whales (humpback and southern right whales).

3.3 Benthic and demersal fish ecoregionalisation
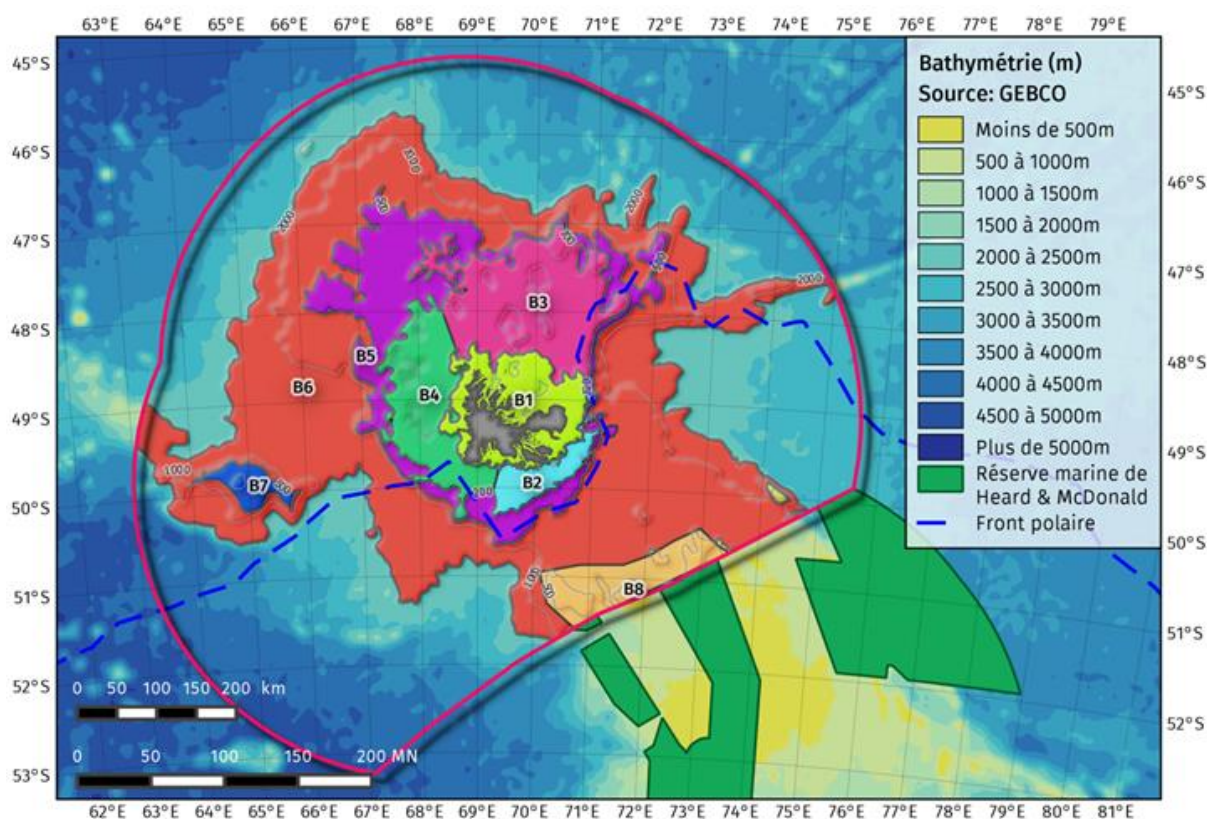
Figure 19: Map of the benthic ecoregions.

The ecoregionalisation of the benthic realm (Figure 19) is linked to depth and nature of substrate, which are the dominant factors controlling benthic biodiversity patterns. Benthic ecoregions (B1 to B8) were defined from the coast to the limit of the Kerguelen EEZ. Some of these areas were subdivided to represent main benthic and demersal fish assemblages.

1. The coastal zone (B1)

   It is located from the shoreline to 100 m depth and includes high water wracks made up of marine debris (mostly kelp), the intertidal zone, kelp forests (subdivided into the *Durvillea antarctica* sub-zone and the *Macrocystis pyrifera* sub-zone), fjords (occurrence of entrance sills towards the open sea), several open bays and an emblematic large basin with an entrance sill (the Morbihan Bay) (Arnaud 1974, Delépine 1976). The Kerguelen archipelago is characterized by numerous islands and islets of various sizes. For this report, there is no geographic subdivision of the area as a specific working group will meet soon. The identified coastal habitats are very patchy and diversified within the archipelago; they are differently exposed to the diverse influences of the open sea (swell, winds and storms) and of the land (water runoff from rivers and melting glaciers). The coastal zone hosts different species, some of them being endemic as for some benthic invertebrates and fish, and plays a major functional role in the life cycle of different species. One example is the critical ecological part the macroalgae *Macrocystis pyrifera* plays for numerous invertebrates, fish and mammals (e.g. Commerson's dolphin). Another emblematic example is provided by *L. squamifrons*, a fish which has one spawning ground in the northern fjord and possibly another one in one fjord of the Morbihan bay beside the ones observed in the southern shelf break or in the Kerguelen-Heard seamounts.

2. The shelf (100 to 200m)

It is divided into three zones: the northeastern shelf (B3), the southwestern shelf (B4) and the southern shelf (B2). The NE and SW shelves are very different in their topography and present specific benthic assemblages of VME taxa. The NE shelf presents high abundances of benthos and demersal fish. The abundances in the SW shelf seem less important but it gathers the highest diversity of VMEs (red corals and Euryalidae (ophiuroids). The southern shelf is less specific compared to the other ones.

3. The shelf break (200 to 500m) (B5)

There is less information on this area which is known to be important for commercial species as different spawning grounds are observed.

4. The deep zone (500 to 2000m) (B6)

There is an important change of fauna at 500 m, depth where deep fish were observed such as grenadier and antimora. There are very few information on this large area for benthos and cephalopods for which we assume high concentrations in the western part because of the importance of top predators feeding on them.

5. Abyssal zone

These areas are not known and need to be investigated.

6. Skiff Seamount (B7)

It is the only seamount disconnected from the shelf. It is very important biogeographically as it indicates potential connectivity between islands shelves like for the lithod *Paralomis aculeata*. Benthic abundances are lower than over the NE shelf but the species diversity is larger. Spawning grounds are observed for two fish, *C. gunnari* over the seamount and Patagonian toothfish in the deeper zone. However, there is no specific fish assemblage over this seamount.

7. Kerguelen-Heard seamounts (B8)

This area is less known. There is a spawning ground of *L. squamifrons*.

The shelf and the shelf break can be considered as important areas for different demersal fish species with high abundances over the NE shelf. They are spawning grounds for *Channichthys rhinoceratus, Zanchlorhynchus spinifer, C. gunnari* with one of its major spawning ground in the Baleiniers Gulf. *L. squamifrons* and *N. rossii* also have spawning grounds in the southern and eastern shelf break respectively. In the deeper zone, in the west of the shelf, we find the unique spawning ground of Patagonian toothfish of the Kerguelen Plateau. This one seems to be quite spread in depths ranging from 800 to 1100m and seems to surround the Skiff seamounts.

4 Synthesis and recommendations

Synthetic maps were produced by different experts of the workshop on the pelagic environment, the benthic environment including demersal fish and invertebrates and for the birds and marine mammals. These maps show several ecoregions identified by major characteristics and specificities compared to the rest of the Indian part of the Southern Ocean (Indian side).

The experts found relevant to combine the pelagic and benthic ecoregions to obtain a global ecoregional map (Figure 20) with 18 ecoregions (E1 to 18) based mainly on:

- Habitat characteristics (bathymetry, oceanography, primary production …),

- Types of species assemblages with consideration of endemicity and conservation status,

- Functionality (essential habitats such as spawning grounds, nursery grounds or foraging

habitats, areas of high primary and secondary production or, structure of the habitat by benthic species,…).
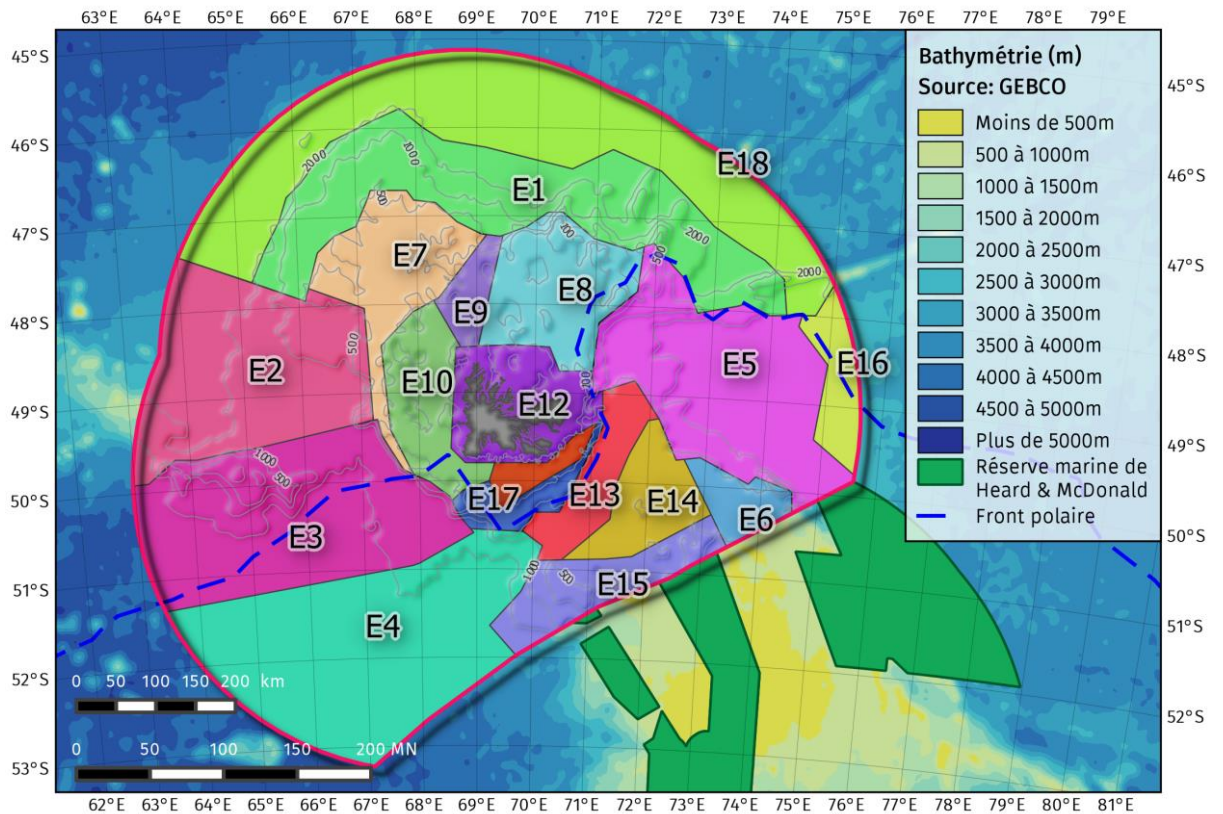
Figure 20: Ecoregional map combining the benthic, pelagic and top predators regionalisation.

In this process, the workshop verified the superposition of the ecoregional synthetic map (Figure 20) with specific habitats of species (birds and mammals distribution, essential fish habitats ...)(Figures 18 and 21). It corrected some of the boundaries of ecoregions with these ecological parameters so that some essential species habitats are mainly within one region. For example, the northern region was modified to better integrate top predators distribution and was mainly limited to the shelf break.
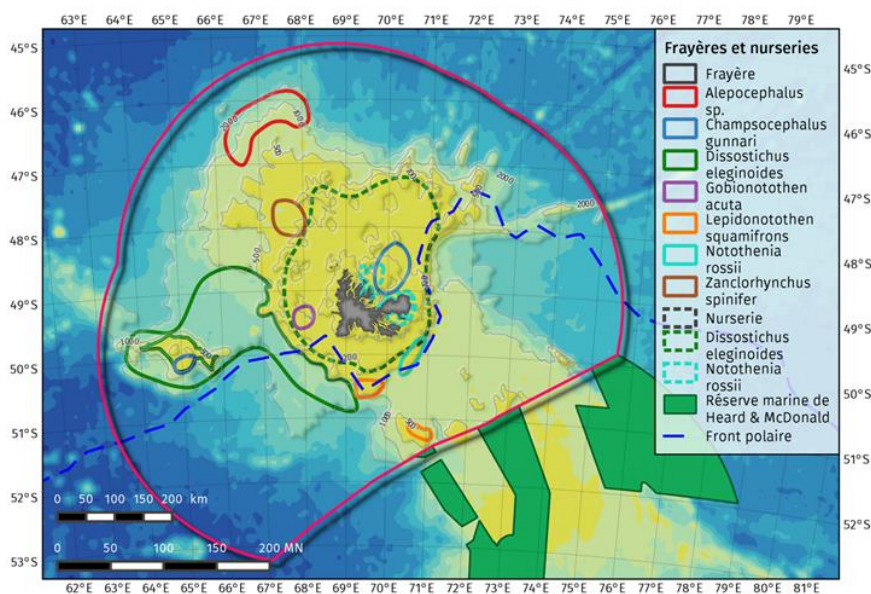
Figure 21: Essential Fish Habitats (spawning grounds and nursery areas) of the most dominant neritic species.

For the coastal zone, the workshop proposed to include the entire coastal area to the limit of the 100 m isobaths. Differentiation of coastal areas depending on kelp forest distribution, hydrology and geographic features (bays, inner shelf canyons and fjords) will complete this approach.

For each of the main final ecoregions, the workshop summarized the essential characteristics that support the creation of the ecoregion and estimated the ecological importance of it with a grade from 0 (non particular), 1 for low importance to 3 high ecological value (Figure 22).

The workshop consider that region 16 should be looked at a broader scale by combining the oceanography of the area which shows high numbers of eddies with top predator distribution such as elephant seals.

The process of extending the national natural reserve off the 12 nautical miles in the Kerguelen EEZ will now add to this approach the analysis of fisheries and other human activities.

The workshop indicated the need to continue research and monitoring over this vast area and to identify special research zones such as observatories to:

- Study the impacts of global change;

- Minimize knowledge gaps in ecology and environment;

- Consider natural variability;

- Study the resistance and resilience towards potential human impacts.
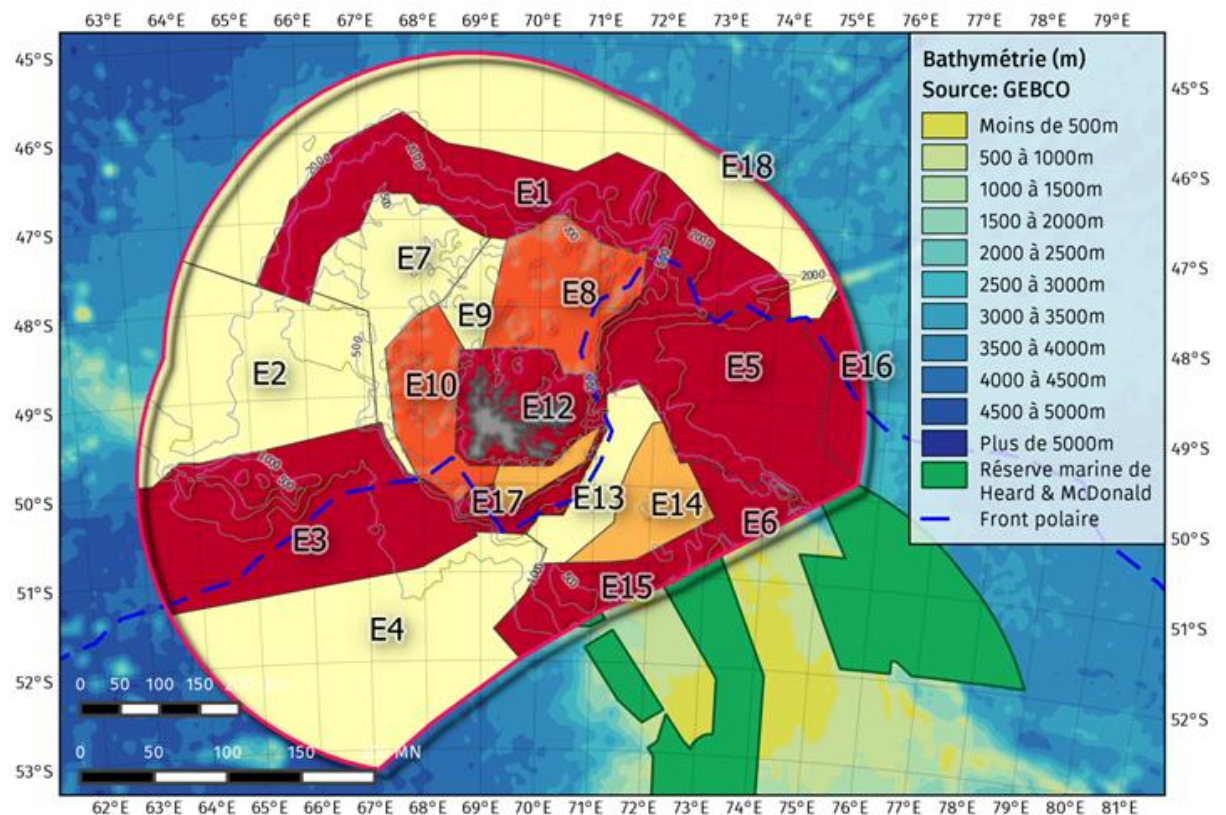
Figure 22: Priority areas based on ecological particularities. 0 (yellow): non particular, 1 (light orange): low, 2 (orange): medium and 3 (red): high ecological value.

Ecoregion	Essential characteristic of the ecoregion	Ecological Importance 0 non particular 1 low, 2 medium, 3 high ecological value
E1. Northern shelf-break	It is the northernmost area of the Indian part of the Southern Ocean and for CCAMLR. It is south of the SAF with high intensity of the ACC. A retention zone is observed in the central part of the ecoregion. The north western and south-eastern parts of the ecoregion are areas of high abundance and biodiversity for birds and marine mammals that rely on the available squids. It is also an area of high diversity and abundance of demersal fish including endemic species found over the shelf break. This area gathers species with high heritage issues.	3
E2. Western oceanic zone	This area is outside the island shelf over the Kerguelen Plateau.	0
E3. Skiff bank	This ecoregion includes the Skiff bank and the surrounding southern oceanic zone to gather the entire bathymetric gradient from the top of the bank to the deep areas. The Skiff bank is the largest bank in the area. The Skiff bank is an essential area for fish with a spawning ground for icefish. It is important for Patagonian toothfish. This ecoregion extends to include part of the PF in its southern part. There is a high diversity of indicator taxa that are specific to VMEs.	3
E4. South West oceanic zone	This area is very deep and outside the island shelf.	0
E5. Polar Front meander	It is the northernmost area of the PF in the Indian part of the Southern Ocean and also the northernmost distribution of species assemblages with Antarctic affinity. Iron fertilization is observed. It is the major region of foraging activity of marine birds and mammals consuming mesopelagic resources. The western part of the area is very stable from one year to another promoting foreseeable fishing habitat for top predators. Historic hunting of the pygmy blue whale occurred.	3

Ecoregion	Essential characteristic of the ecoregion	Ecological Importance 0 non particular 1 low, 2 medium, 3 high ecological value
E6. Cold water incursion	It is the northernmost distribution of Antarctic waters in subsurface, structuring the vertical distribution of micronekton and making mesopelagic preys more accessible to top predators. Historic hunting of the pygmy blue whale occurred.	3
E7. North western shelf and western shelf-break	Neritic zone with the particularity of the presence of a spawning ground for *Z. spinifer*.	1
E8. North Eastern Shelf Productive area	This area is characterised by the high phytoplanktonic biomass. There is a high biomass and diversity of VME indicators taxa. The Commerson's dolphins are present and macaroni penguins rely on this habitat in summer.	2
E9. North neritic zone	Neritic area.	0
E10. Western shelf	This ecoregion shows high taxa diversity of VME indicators. It is a spawning ground of *G. acuta.*	2
E11. Southern shelf	Neritic area.	1
E12. Coastal zone	The coastal environment is characterized by various habitats such as fjords, bays of various sizes and kelp forests. The coastal zone is highly influenced by freshwater runoff from rivers. Among these areas, the Morbihan Bay is one of the largest bay with numerous islands and islets. It is also the coastal marine area with the best scientific knowledge due to long term studies and also a key breeding and feeding area for many seabird The northern areas are characterized by the presence of fjords, bays and islands of various sizes. The bay of Baleiniers is a nursery ground for larval fish. Some fjords show spawning grounds for *L. squamifrons.*	3

Ecoregion	Essential characteristic of the ecoregion	Ecological Importance 0 non particular 1 low, 2 medium, 3 high ecological value
	All the coastal area is a spawning ground for coastal fish, some of them being endemic. They also are nurseries for neritic fish such as *N. rossii*. Commerson dolphin occurs; they are in high concentration in the Morbihan Bay. The coastal zone shows presence of VME taxa. Coastal zones are historic areas showing high concentration of humpback whales.	
E13. Kerguelen-Heard passage	Deep zone between the Kerguelen island shelf and Heard island shelf.	0
E14. Productive Southern area	This area between the Kerguelen and Heard island shelf show high phytoplankton production. It is a fishing area for fur seals and king-macaroni penguins.	1
E15. Kerguelen-Heard seamounts	This area gathers the Kerguelen-Heard seamounts and is at the border with the Australian EEZ. It is facing some of the HIMI MPA. These habitats are covered with mud. It also covers the prime foraging habitat of juvenile males of elephant seals. *L. squamifrons* has one of its spawning grounds over one of the seamount.	3
E16. Eastern oceanic zone	This area extent largely in 58.5.1. It is a highly dynamic productive area linked to the Kerguelen panache. It is an important zone for elephant seals, rockhopper penguins and petrels.	3
E17. Southern shelf break	It is a spawning of *L. squamifrons* and *N. rossii.*	3
E18. Northern oceanic zone	It is the oceanic area between the shelf break and the SAF.	0

References:

Arnaud, P., 1974. Contribution à la bionomie marine benthique des régions Antarctiques et Subantarctiques. Tethys 6, 467-653.

Améziane, N., Eléaume, M., Hemery, L.G., Monniot, F., Hemery, A., Hautecoeur, M., Dettai A., 2011b. Biodiversity of the benthos off Kerguelen Islands: overview and perspectives. *In*: The Kerguelen Plateau, Marine Ecosystem and Fisheries, Duhamel G. & Welsford D. (eds). Société Française d'Ichyologie pub., Paris, 157-167.

Améziane, N., Eléaume, M., Pruvost, P., Duhamel, G., Kerguelen group, 2011a. Estimating the biodiversity and distribution of the northern part of the Kerguelen Islands slope, shelf, and shelf-break for ecoregionalisation: benthos and demersal fish. CCAMLR Marine Protected Areas Worshop, WS-MPA-11/9, 19 p.

Bost, C.A., Cotté, C., Bailleul, F, Cherel, Y., Charrassin, J.B., Guinet, C., Ainley, D.G., Weimerskirch, H., 2009. Importance of Southern Ocean fronts for seabird and marine mammals. Journal of Marine Systems, 79, Special Issue on Processes at Oceanic Fronts (JMS-SIOF), 363-376.

Carlotti, F., Jouandet, M.P., Nowaczyk, A., Harmelin-Vivien, M., Lefèvre, D., Richard, P., Zhu, Y., Zhou, M., 2015. Mesozooplankton structure and functioning during the onset of the Kerguelen phytoplankton bloom during the KEOPS2 survey. Biogeosciences, 12, 4543-4563, doi:10.5194/bg-12-4543-2015.

Charriaud, E., Gamberoni, L., 1987. Observations hydrologiques et flux géostrophiques entre les Kerguelen et Amsterdam. Résultats de la campagne KERAMS 1 (16-20 février 1987). Rapport Intermédiaire du Laboratoire d'Océanographie Physique du Muséum National d'Histoire Naturelle de Paris.

De Broyer, C., Koubbi, P., Griffiths, H.J., Raymond, B., Udekem d'Acoz, C. d', Van de Putte, A.P., Danis, B., David, B., Grant, S., Gutt, J., Held, C., Hosie, G., Huettmann, F., Post, A., Ropert-Coudert, Y., 2014. Biogeographic Atlas of the Southern Ocean. Scientific Committee on Antarctic Research, Cambridge, XII+498 p.

Delépine, R., 1976. Note préliminaire sur la répartition des algues marines aux îles Kerguelen. CNFRA 39, 153-159.

Delord, K., Bost, C.A., Guinet, C., Weimerskirch, H., 2011. Estimating the biodiversity of the sub-Antarctic Indian part for the ecoregionalisation of CCAMLR areas 58.5.1 and 58.6: Part II. foraging habitats of top predators from French Antarctic Territories – areas of ecological significance in the Southern Ocean. WS-MPA-11/08.

Delord, K., Barbraud, C., Bost, C.A., Cherel, Y., Guinet, C., Weimerskirch, H., 2013. Atlas of top predators from French Southern Territories in the Southern Indian Ocean. CEBC-CNRS, 252 p. DOI: 10.15474/AtlasTopPredatorsOI_CEBC.CNRS_FrenchSouthernTerritories.

Delord, K., Barbraud, C., Bost, C.A., Deceuninck, B., Lefebvre, T., Lutz, R., Micol, T., Phillips, R.A., Trathan, P.N., Weimerskirch, H., 2014. Areas of importance for seabirds tracked from French southern territories, and recommendations for conservation. Marine Policy, 48,1–13.

d'Ovidio, F., De Monte, S., Della Penna, A., Cotté, C., Guinet, C., 2013. Ecological implications of eddy retention in the open ocean: a Lagrangian approach. J. Phys, A, 45.

d'Ovidio, F., Della Penna, A., Trull, T.W, Nencioli, F., Pujol, I., Rio, M.H., Park, Y.H., Cotté, C., Zhou, M., Blain, S., 2015. The biogeochemical structuring role of horizontal stirring: Lagrangian perspectives on iron delivery downstream of the Kerguelen plateau. Biogeosciences 12, 5567-5581.

Duhamel, G., 1987. Ichtyofaune des secteurs Indien occidental et Atlantique oriental de l'Océan Austral: biogéographie, cycles biologiques et dynamique des populations. Doct. Etat: Université Pierre et Marie

Curie, Paris.

Duhamel, G., Hulley, P.A., 1993. Ichtyofaune meso et bathypelagique. *In:* Duhamel, G. ed. Campagnes SKALP 1987 et 1988 aux îles Kerguelen à bord des navires "SKIF" et "KALPER". Publications de l'Institut Français pour la Recherche et la Technologie Polaires, 93-01, 285-295.

Duhamel G., 1998. The pelagic fish community of the polar frontal zone off the Kerguelen Islands. Milano - Italia, Springer-Verlag.

Duhamel, G., Gasco, N., Davaine, P., 2005. Poissons des îles Kerguelen et Crozet. Guide régional de l'océan Austral. Patrimoines Naturels, 63, 1-419.

Duhamel, G., Bertignac, M., Gasco, N., Hautecoeur, M., 2011. Major fishery events in Kerguelen Islands: *Notothenia rossii*, *Champsocephalus gunnari*, *Dissostichus eleginoides* – current distribution and status of stocks. WS-MPA-11/P04.

Duhamel, G., Welsford, D., 2011. The Kerguelen Plateau: Marine Ecosystem and Fisheries. Paris: Société Française d'Ichtyologie.

Duhamel, G., Hulley, P.A., Causse, R., Koubbi, P., Vacchi, M., Pruvost, P., Vigetta, S., Irisson, J.O., Mormède, S., Belchier, M., Dettai, A., Detrich, H.W., Gutt, J., Jones, C.D., Kock, K.H., Lopez Abellan, L.J., Van de Putte, A.P., 2014. Biogeographic patterns of fish. Biogeographic Atlas of the Southern Ocean, 7, 328-362.

Gambéroni, L., Geronimi, J., Jeannin, P.F., Murail, J.F., 1982. Study of frontal zones in the Crozet-Kerguelen region. Oceanol. Acta, 5, 3, 291-299.

Grant, S., Constable, A., Raymond, B., Doust, S., 2006. Bioregionalisation of the Southern Ocean: Report of Experts Workshop (Hobart, September 2006): ACE-CRC and WWF Australia, 45 p.

Hulley, P.A., 1990. Family Myctophidae. *In:* Fishes of the Southern Ocean (Gon, O., ed.), 146-178. Grahamstown: J.L.B. Smith Institute of Ichthyology.

Koubbi, P., Ibanez, F., Duhamel, G., 1991. Environmental influences on spatio-temporal oceanic distribution of ichthyoplankton around the Kerguelen Islands (Southern Ocean). Marine Ecology Progress Series, 72, 3, 225-238.

Koubbi, P., 1992. L'ichtyoplancton de la partie indienne de la province kerguelenienne (Bassin de Crozet et plateau de Kerguelen) : identification, distribution spatio-temporelle et stratégies de développement larvaire ». Thèse Univ. Paris VI en Océanologie Biologique.

Koubbi, P., 1993. Influence of the frontal zones on ichthyoplankton and mesopelagic fish assemblage in the Crozet Basin (Indian sector of the Southern Ocean). Polar Biology, 13: 557-564.

Koubbi, P., Duhamel, G., Hebert, C., 2000. Role of bay, fjord and seamount on the early life history of *Lepidonotothen squamifrons* from the Kerguelen islands. Polar Biology, 23, 7, 459-46.

Koubbi, P., Duhamel, G., Hebert, C., 2001. Seasonal relative abundance of fish larvae inshore at Iles Kerguelen, Southern ocean. Antarctic Science, 13,4, 385-392.

Koubbi, P., Duhamel, G., Harlay, X., Eastwood, P., Durand, I., Park, Y.H., 2003. Distribution of larval *Krefftichthys anderssoni* (Myctophidae, Pisces) at the Kerguelen archipelago (Southern Indian Ocean) modelled using GIS and habitat suitability: 215-223. In: Antarctic Biology in a global context (Huiskes et al., eds). Backhyus Publisher, Leiden, NL.

Koubbi, P., Duhamel., G., Hecq, J.H., Beans, C., Loots, C., Pruvost, P., Tavernier, E., Vacchi, M., Vallet, C., 2009. Ichthyoplankton in the neritic and coastal zone of Antarctica and Subantarctic islands. In: 38th International Liège Colloquium on Ocean Dynamics - Revisiting the role of zooplankton in pelagic ecosystems, Liège (Belgique). Journal of Marine System, 78, 4, 547-556.

Koubbi, P., Hulley, P.A., Raymond B., Penot, F., Gasparini, S., Labat, J.-P., Pruvost P., Mormède, S., Irisson, J.O., Duhamel, G., Mayzaud, P., 2011. Estimating the biodiversity of the sub-Antarctic Indian part for ecoregionalisation: Part I. Pelagic realm of CCAMLR areas 58.5.1 and 58.6. CCAMLR. WS-MPA-11/11, 1-39.

Koubbi, P., Crawford, R., Alloncle, N., Ameziane, N., Barbraud, C., Besson, D., Bost, C., Delord, K., Duhamel, G., Douglass, L., Guinet, C., Hosie, G., Hulley, P., Irisson, J.O., Kovacs, K., Lagabrielle, E., Leslie, R., Lombard, A.T., Makhado, A., Martinez, C., Mormède, S., Penot, F., Pistorius, P., Pruvost, P., Raymond, B., Reuillard, E., Ringelstein, J., Samaai, T., Tixier, P., Verheye, H.M., Vigetta, S., Von Quillfeldt, C., Weimerskirch, H., 2012. Estimating the biodiversity of Planning Domain 5 (Marion and Prince Edward Islands - Del Cano - Crozet) for ecoregionalisation. WG-EMM 12/33.

Koubbi, P., De Broyer, C., Griffiths, H.J., Raymond, B., Udekem d'Acoz, C. d', Van de Putte, A.P., Danis, B., David, B., Grant, S., Gutt, J., Held, C., Hosie, G., Huettmann, F., Post, A., Ropert-Coudert, Y., 2014. Conclusion. In: De Broyer C., Koubbi P., Griffiths H.J., Raymond B., Udekem d'Acoz C. d', et al. (eds.). Biogeographic Atlas of the Southern Ocean. Scientific Committee on Antarctic Research, Cambridge, 470-475.

Lasbleiz, M., Leblanc, K., Blain, S., Ras, J., Cornet-Barthaux, V., Hélias Nunige, S., Quéguiner, B., 2014. Pigments, elemental composition (C, N, P, and Si), and stoichiometry of particulate matter in the naturally iron fertilized region of Kerguelen in the Southern Ocean. Biogeosciences, 11, 5931-5955, doi:10.5194/bg-11-5931-2014.

Lehodey, P., Murtugudde, R., Senina, I., 2010. Bridging the gap from ocean models to population dynamics of large marine predators: a model of mid-trophic functional groups. Progress in Oceanography, 84, 69–84.

Lehodey, P., Conchon, A., Senina, I., Domokos, R., Calmettes, B., Jouanno, J., Hernandez, O., Kloser, R., 2015. Optimization of a micronekton model with acoustic data. – ICES Journal of Marine Science, 72, 5, 1399-1412.

Loots, C., Koubbi, P., Duhamel, G., 2007. Habitat modelling of *Electrona antarctica* (Myctophidae, Pisces) in Kerguelen by Generalized Additive Models and Geographic Information System. Polar Biology, 30, 8, 951-959.

Martin, A., Pruvost, P., 2007. Pecheker, relational database for analysis and management of fisheries and related biological data from the French southern ocean fisheries monitoring scientific programs, Muséum national d'Histoire naturelle.

Martin, J.H., Gordon, R.M., Fitzwater, S.E., 1990. Iron in Antarctic waters. Nature, 345, 156–158.

Mongin, M., Molina, E., Trull, T.W., 2008. Seasonality and scale of the Kerguelen plateau phytoplankton bloom: A remote sensing and modeling analysis of the influence of natural iron fertilization in the Southern Ocean. Deep-Sea Res. II, 55, 880–892, doi:10.1016/j.dsr2.2007.12.039.

Mosseri, J., Quéguiner, B., Armand, L., Cornet-Barthaux, V., 2008. Impact of iron on silicon utilization by diatoms in the Southern Ocean: A case study of Si/N cycle decoupling in a naturally iron-enriched area. Deep-Sea Res. Pt. II, 55, 801–819, doi:10.1016/j.dsr2.2007.12.003.

Orsi, A.H., Whitworth, T., Nowlin, W.D., 1995. On the meridional extent and fronts of the Antarctic Circumpolar Current. Deep-Sea Research I, 42, 641–673.

Park, Y.H., Gambéroni, L., Charriaud, E., 1991. Frontal structure and transport of the Antarctic Circumpolar current in the south Indian Ocean sector, 40-80°E. Marine Chemistry, 35, 45-62.

Park, Y.H., Charriaud, E., Gamberoni, L., Kartavtseff, A., 1993. Rapport de la campagne MD 68/SUZIL effectuee du 12/04 au 20/05/91. Volume 1 : Hydrologie. Rapport des campagnes à la mer, IFRTP. - 05/1993, 1, 214 p.

Park, Y.H., Charriaud, E., Fieux, M., 1998. Thermohaline structure of the Antarctic surface water/winter water in the Indian sector of the Southern Ocean. Journal of Marine Systems, 17, 5–23.

Park, Y.H., Fuda, J.L., Durand, I., Naveira Garabato, A.C., 2008. Internal tides and vertical mixing over the Kerguelen Plateau. Deep SeaRes., Part II, 55, 582–593.

Park, Y.H., Durand, I., Kestenare, E., Rougier, G., Zhou, M., d'Ovidio, F., Cotté, C., Lee, J.H., 2014. Polar Front around the Kerguelen Islands: An up-to-date determination and associated circulation of surface/subsurface waters, J. Geophys. Res.- Oceans, 119, 6575–6592, doi:10.1002/2014JC010061.

Pruvost, P., Martin, A., Denys, G., Causse, R., 2011. PECHEKER-SIMPA – A tool for fisheries management and ecosystem modelling.WS-MPA-11/P02.

Quéroué, F., Sarthou, G., Planquette, H.F., Bucciarelli, E., Chever, F., van der Merwe, P., Lannuzel, D., Townsend, A.T., Cheize, M., Blain, S., d'Ovidio, F., Bowie, A.R., 2015. High variability in dissolved iron concentrations in the vicinity of the Kerguelen Islands (Southern Ocean). Biogeosciences, 12, 3869-3883, doi:10.5194/bg-12-3869-2015.

Roquet, F., Park, H.Y., Guinet, C., Bailleul, F., Charrassin, J.B., 2009. Observations of the Fawn Trough Current over the Kerguelen Plateau from instrumented elephant seals. Journal of Marine Systems, 78, 377-393.

Tagliabue, A., Mtshali, T., Aumont, O., Bowie, A.R., Klunder, M.B., Roychoudhury, A.N., Swart, S., 2012. A global compilation dissolved iron measurements: focus on distributions and processes in the Southern Ocean. Biogeosciences, 9, 2333-2349, doi:10.5194/bg-9-2333-2012.

Thiers, L., Delord, K., Bost, C.A., Guinet, C., Weimerskirch, H., 2016. Important marine sectors for the top predator community around Kerguelen Archipelago. Polar Biology.

van der Merwe, P., Bowie, A.R., Quéroué, F., Armand, L., Blain, S., Chever, F., Davies, D., Dehairs, F., Planchon, F., Sarthou, G., Townsend, A.T., Trull, T.W., 2015. Sourcing the iron in the naturally fertilised bloom around the Kerguelen Plateau: particulate trace metal dynamics. Biogeosciences, 12, 739-755, doi:10.5194/bg-12-739-2015.

Vierros, M., Rice, J., Ardron, J., 2008. Global Open Oceans and Deep Seabed (GOODS) Biogeographic Classification. UNESCO, IOC 54.

Bibliography

[Abraham, 1998] Abraham, E.R., 1998. The generation of plankton patchiness by turbulent stirring. Nature, 391:577. doi:10.1038/35361.

[Abraham and Bowen, 2002] Abraham, E.R., Bowen, M.M., 2002. Chaotic stirring by a mesoscale surface-ocean flow. Chaos: An Interdisciplinary Journal of Nonlinear Science, 12:373–381. doi:https://doi.org/10.1063/1.1481615. PMID: 12779567.

[Abrahms et al., 2018] Abrahms, B., Scales, K.L., Hazen, E.L., Bograd, S.J., Schick, R.S., Robinson, P.W., Costa, D.P., 2018. Mesoscale activity facilitates energy gain in a top predator. Proc. R. Soc. B, 285:20181101. doi:10.1098/rspb.2018.1101.

[Addison et al., 2018] Addison, P.F.E., Collins, D.J., Trebilco, R., Howe, S., Bax, N., Hedge, P., Jones, G., Miloslavich, P., Roelfsema, C., Sams, M., Stuart-Smith, R.D., Scanes, P., von Baumgarten, P., McQuatters-Gollop, A., editor: Robert Blasiak, H., 2018. A new wave of marine evidence-based management: emerging challenges and solutions to transform monitoring, evaluating, and reporting. ICES Journal of Marine Science, 75:941–952. doi:10.1093/icesjms/fsx216.

[Agnew, 1997] Agnew, D.J., 1997. Review-[U+0080][U+0094]The CCAMLR Ecosystem Monitoring Programme. Antarctic Science, 9:235–242. doi:10.1017/S095410209700031X.

[Andrello et al., 2013] Andrello, M., Mouillot, D., Beuvier, J., Albouy, C., Thuiller, W., Manel, S., 2013. Low connectivity between mediterranean marine protected areas: A biophysical modeling approach for the dusky grouper epinephelus marginatus. PLOS ONE, 8:1–15. doi:10.1371/journal.pone.0068564.

[Ansell et al., 1996] Ansell, A., Gibson, R., Barnes, M., Press, U., 1996. Coastal fisheries in the Pacific Islands. Oceanography and Marine Biology: an annual review, 34:531.

[Ansong et al., 2017] Ansong, J., Gissi, E., Calado, H., 2017. An approach to ecosystem-based management in maritime spatial planning process. Ocean & Coastal Management, 141:65 – 81. doi:https://doi.org/10.1016/j.ocecoaman.2017.03.005.

[Antoine et al., 1996] Antoine, D., André, J.M., Morel, A., 1996. Oceanic primary production: 2. estimation at global scale from satellite (coastal zone color scanner) chlorophyll. Global Biogeochemical Cycles, 10:57–69. doi:10.1029/95GB02832.

[Appeltans et al., 2012] Appeltans, W., Ahyong, S., Anderson, G., Angel, M., Artois, T., Bailly, N., Bamber, R., Barber, A., Bartsch, I., Berta, A., Błażewicz-Paszkowycz, M., Bock, P., Boxshall, G., Boyko, C., Brandão, S., Bray, R., Bruce, N., Cairns, S., Chan, T.Y., Cheng, L., Collins, A., Cribb, T., Curini-Galletti, M., Dahdouh-Guebas, F., Davie, P., Dawson, M., De Clerck, O., Decock, W., De Grave, S., de Voogd, N., Domning, D., Emig, C., Erséus, C., Eschmeyer, W., Fauchald, K., Fautin, D., Feist, S., Fransen, C., Furuya, H., Garcia-Alvarez, O., Gerken, S., Gibson, D., Gittenberger, A., Gofas, S., Gómez-Daglio, L., Gordon, D., Guiry, M., Hernandez, F., Hoeksema, B., Hopcroft, R., Jaume, D., Kirk, P., Koedam, N., Koenemann, S., Kolb, J., Kristensen, R., Kroh, A., Lambert, G., Lazarus, D., Lemaitre, R., Longshaw, M., Lowry, J., Macpherson, E., Madin, L., Mah, C., Mapstone, G., McLaughlin, P., Mees, J., Meland, K., Messing, C., Mills, C., Molodtsova, T., Mooi, R., Neuhaus, B., Ng, P., Nielsen, C., Norenburg, J., Opresko, D., Osawa, M., Paulay, G., Perrin, W., Pilger, J., Poore, G., Pugh, P., Read, G., Reimer, J., Rius, M., Rocha, R., Saiz-Salinas, J., Scarabino, V., Schierwater, B., Schmidt-Rhaesa, A., Schnabel, K., Schotte, M., Schuchert, P., Schwabe, E., Segers, H., Self-Sullivan, C., Shenkar, N., Siegel, V., Sterrer, W., Stöhr, S., Swalla, B., Tasker, M., Thuesen, E., Timm, T., Todaro, M., Turon, X., Tyler, S., Uetz, P., van der Land, J., Vanhoorne, B., van Ofwegen, L., van Soest, R., Vanaverbeke, J., Walker-Smith, G., Walter, T., Warren, A., Williams, G., Wilson, S., Costello, M., 2012. The Magnitude of Global Marine Species Diversity. Current Biology, 22:2189 – 2202. doi:https://doi.org/10.1016/j.cub.2012.09.036.

[Ariza et al., 2015] Ariza, A., Garijo, J., Landeira, J., Bordes, F., Hernández-León, S., 2015. Migrant biomass and respiratory carbon flux by zooplankton and micronekton in the subtropical northeast Atlantic Ocean (Canary Islands). Progress in Oceanography, 134:330 – 342. doi:https://doi.org/10.1016/j.pocean.2015.03.003.

[Armand et al., 2008] Armand, L.K., Cornet-Barthaux, V., Mosseri, J., Quéguiner, B., 2008. Late summer diatom biomass and community structure on and around the naturally iron-fertilised Kerguelen Plateau in the Southern Ocean. Deep Sea Research Part II: Topical Studies in Oceanography, 55:653 – 676. doi:https://doi.org/10.1016/j.dsr2.2007.12.031. KEOPS: Kerguelen Ocean and Plateau compared Study.

[Atema, 1988] Atema, J., 1988. Distribution of chemical stimuli. Sensory biology of aquatic animals, 1:29–56.

[Backus, 1986] Backus, R.H., 1986. Biogeographic boundaries in the open ocean. Pelagic Biogeography.

[Bailleul et al., 2007] Bailleul, F., Charrassin, J.B., Ezraty, R., Girard-Ardhuin, F., McMahon, C.R., Field, I.C., Guinet, C., 2007. Southern elephant seals from kerguelen islands confronted by antarctic sea ice. changes in movements and in diving behaviour. Deep Sea Research Part II: Topical Studies in Oceanography, 54:343–355. doi:10.1016/j.dsr2.2006.11.005.

[Bailleul et al., 2010] Bailleul, F., Cotté, C., Guinet, C., 2010. Mesoscale eddies as foraging area of a deep-diving predator, the southern elephant seal. Marine Ecology Progress Series, 408:251–264. doi:10.3354/meps08560.

[Bainbridge, 1958] Bainbridge, R., 1958. The speed of swimming of fish as related to size and to the frequency and amplitude of the tail beat. Journal of experimental biology, 35:109–133.

[Bakun, 2006] Bakun, A., 2006. Fronts and eddies as key structures in the habitat of marine fish larvae: opportunity, adaptive response and competitive advantage. Scientia Marina, 70:105–122. doi:10.3989/scimar.2006.70s2105.

[Barboza et al., 2017] Barboza, C., Cabrini, T., Mattos, G., Skinner, V., Cardoso, R., 2017. Variability of macrofauna distribution along a dissipative log-spiral sandy beach in Rio de Janeiro, Southeastern Brazil. Scientia Marina, 81:111–120. doi: 10.3989/scimar.04467.03A.

[Barton et al., 2010] Barton, A.D., Dutkiewicz, S., Flierl, G., Bragg, J., Follows, M.J., 2010. Patterns of Diversity in Marine Phytoplankton. Science, 327:1509–1511. doi:10.1126/science.1184961.

[Barton et al., 2014] Barton, A.D., Ward, B.A., Williams, R.G., Follows, M.J., 2014. The impact of fine-scale turbulence on phytoplankton community structure. Limnology and Oceanography: Fluids and Environments, 4:34–49. doi:10.1215/ 21573689-2651533.

[Bauer et al., 2015] Bauer, R.K., Bonhommeau, S., Brisset, B., Fromentin, J.M., 2015. Aerial surveys to monitor bluefin tuna abundance and track efficiency of management measures. Marine Ecology Progress Series, 534:221–234. doi:10.3354/ meps11392.

[Beamish, 1978] Beamish, F., 1978. 2 - swimming capacity. In W. Hoar, D. Randall, editors, Locomotion, volume 7 of *Fish Physiology*, pages 101 – 187. Academic Press. doi:https://doi.org/10.1016/S1546-5098(08)60164-8.

[Beamish et al., 1999] Beamish, R., Leask, K., Ivanov, O., Balanov, A., Orlov, A., Sinclair, B., 1999. The ecology, distribution, and abundance of midwater fishes of the Subarctic Pacific gyres. Progress in Oceanography, 43:399 – 442. doi: https://doi.org/10.1016/S0079-6611(99)00017-8.

[Béhagle et al., 2016] Béhagle, N., Cotté, C., Ryan, T.E., Gauthier, O., Roudaut, G., Brehmer, P., Josse, E., Cherel, Y., 2016. Acoustic micronektonic distribution is structured by macroscale oceanographic processes across 20–50°S latitudes in the South-Western Indian Ocean. Deep Sea Research Part I: Oceanographic Research Papers, 110:20 – 32. doi:https://doi.org/10.1016/j.dsr.2015.12.007.

[Bell et al., 2018] Bell, J.D., Cisneros-Montemayor, A., Hanich, Q., Johnson, J.E., Lehodey, P., Moore, B.R., Pratchett, M.S., Reygondeau, G., Senina, I., Virdin, J., Wabnitz, C.C., 2018. Adaptations to maintain the contributions of small-scale fisheries to food security in the Pacific Islands. Marine Policy, 88:303 – 314. doi: https://doi.org/10.1016/j.marpol.2017.05.019.

[Bellingham and Willcox, 1996] Bellingham, J.G., Willcox, J.S., 1996. Optimizing AUV oceanographic surveys. Proceedings of Symposium on Autonomous Underwater Vehicle Technology, pages 391–398. doi:http://dx.doi.org/10.1109/AUV.1996.532439.

[Benoit Bird, 2006] Benoit Bird, K., 2006. Effects of scattering layer composition, animal size, and numerical density on the frequency dependence of volume backscatter. The Journal of the Acoustical Society of America, 120:3001–3001. doi:10.1121/1.4786994.

[Benoit-Bird, 2004] Benoit-Bird, K.J., 2004. Prey caloric value and predator energy needs: foraging predictions for wild spinner dolphins. Marine Biology, 145:435–444. doi:10.1007/s00227-004-1339-1.

[Benway et al., 2014] Benway, H.M., Hofmann, E., St. John, M., 2014. Building International Research Partnerships in the North Atlantic–Arctic Region. Eos, Transactions American Geophysical Union, 95:317–317. doi:10.1002/2014EO350007.

[Berline et al., 2014] Berline, L., Rammou, A.M., Doglioli, A., Molcard, A., Petrenko, A., 2014. A connectivity-based eco-regionalization method of the mediterranean sea. PLOS ONE, 9:1–9. doi:10.1371/journal.pone.0111978.

[Beron-Vera et al., 2008] Beron-Vera, F.J., Olascoaga, M.J., Goni, G.J., 2008. Oceanic mesoscale eddies as revealed by lagrangian coherent structures. Geophysical Research Letters, 35. doi:10.1029/2008GL033957.

[Bettencourt et al., 2012] Bettencourt, J.H., López, C., Hernández-García, E., 2012. Oceanic three-dimensional Lagrangian coherent structures: A study of a mesoscale eddy in the Benguela upwelling region. Ocean Modelling, 51:73 – 83. doi: https://doi.org/10.1016/j.ocemod.2012.04.004.

[Blain et al., 2007] Blain, S., Quéguiner, B., Armand, L., Belviso, S., Bombled, B., Bopp, L., Bowie, A., Brunet, C., Brussaard, C., Carlotti, F., et al., 2007. Effect of natural iron fertilization on carbon sequestration in the Southern Ocean. Nature, 446:1070. doi:doi.org/10.1038/nature05700.

[Blain et al., 2008a] Blain, S., Quéguiner, B., Trull, T., 2008a. The natural iron fertilization experiment KEOPS (KErguelen Ocean and Plateau compared Study): An overview. Deep Sea Research Part II: Topical Studies in Oceanography, 55:559–565. doi:10.1016/j.dsr2.2008.01.002.

[Blain et al., 2008b] Blain, S., Sarthou, G., Laan, P., 2008b. Distribution of dissolved iron during the natural iron-fertilization experiment KEOPS (Kerguelen Plateau, Southern Ocean). Deep Sea Research Part II: Topical Studies in Oceanography, 55:594–605. doi:10.1016/j.dsr2.2007.12.028.

[Blain et al., 2001] Blain, S., Tréguer, P., Belviso, S., Bucciarelli, E., Denis, M., Desabre, S., Fiala, M., Jézéquel, V.M., Fèvre, J.L., Mayzaud, P., Marty, J.C., Razouls, S., 2001. A biogeochemical study of the island mass effect in the context of the iron hypothesis: Kerguelen Islands, Southern Ocean. Deep Sea Research Part I: Oceanographic Research Papers, 48:163 – 187. doi:https://doi.org/10.1016/S0967-0637(00)00047-9.

[Block et al., 2011] Block, B.A., Jonsen, I.D., Jorgensen, S.J., Winship, A.J., Shaffer, S.A., Bograd, S.J., Hazen, E.L., Foley, D.G., Breed, G., Harrison, A.L., et al., 2011. Tracking apex marine predator movements in a dynamic ocean. Nature, 475:86–90.

[Bocher et al., 2001] Bocher, P., Cherel, Y., Labat, J.P., Mayzaud, P., Razouls, S., Jouventin, P., 2001. Amphipod-based food web: Themisto gaudichaudii caught in nets and by seabirds in Kerguelen waters, southern Indian Ocean. Marine Ecology Progress Series, 223:261–276. doi:doi:10.3354/meps223261.

[Boehlert et al., 2001] Boehlert, G.W., Costa, D.P., Crocker, D.E., Green, P., O'Brien, T., Levitus, S., Le Boeuf, B.J., 2001. Autonomous Pinniped Environmental Samplers: Using Instrumented Animals as Oceanographic Data Collectors. Journal of Atmospheric and Oceanic Technology, 18:1882–1893. doi:10.1175/1520-0426(2001) 018⟨1882:APESUI⟩2.0.CO;2.

[Boehme et al., 2008] Boehme, L., Thorpe, S., Biuw, M., Fedak, M., Meredith, M., 2008. Monitoring drake passage with elephant seals: Frontal structures and snapshots of transport. Limnology and Oceanography, 53:2350–2360.

[Boffetta et al., 2002] Boffetta, G., Celani, A., Musacchio, S., Vergassola, M., 2002. Intermittency in two-dimensional Ekman-Navier-Stokes turbulence. Phys. Rev. E, 66:026304. doi:10.1103/PhysRevE.66.026304.

[Boffetta and Ecke, 2012] Boffetta, G., Ecke, R.E., 2012. Two-Dimensional Turbulence. Annual Review of Fluid Mechanics, 44:427–451. doi:10.1146/annurev-fluid-120710-101240.

[Boffetta et al., 2001] Boffetta, G., Lacorata, G., Redaelli, G., Vulpiani, A., 2001. Detecting barriers to transport: a review of different techniques. Physica D: Nonlinear Phenomena, 159:58–70. doi:10.1016/S0167-2789(01)00330-X.

[Boffetta and Musacchio, 2010] Boffetta, G., Musacchio, S., 2010. Evidence for the double cascade scenario in two-dimensional turbulence. Phys. Rev. E, 82:016307. doi:10.1103/PhysRevE.82.016307.

[Bon et al., 2015] Bon, C., Della Penna, A., d'Ovidio, F., Y.P. Arnould, J., Poupart, T., Bost, C.A., 2015. Influence of oceanographic structures on foraging strategies: Macaroni penguins at Crozet Islands. Movement Ecology, 3:32. doi:10.1186/s40462-015-0057-2.

[Bost et al., 2009] Bost, C.A., Cotté, C., Bailleul, F., Cherel, Y., Charrassin, J.B., Guinet, C., Ainley, D.G., Weimerskirch, H., 2009. The importance of oceanographic fronts to marine birds and mammals of the southern oceans. Journal of Marine Systems, 78:363–376.

[Bost et al., 2015] Bost, C.A., Cotté, C., Terray, P., Barbraud, C., Bon, C., Delord, K., Gimenez, O., Handrich, Y., Naito, Y., Guinet, C., et al., 2015. Large-scale climatic anomalies affect marine predator foraging behaviour and demography. Nature communications, 6. doi:10.1038/ncomms9220.

[Bouffard et al., 2014] Bouffard, J., Nencioli, F., Escudier, R., Doglioli, A.M., Petrenko, A.A., Pascual, A., Poulain, P.M., Elhmaidi, D., 2014. Lagrangian analysis of satellite-derived currents: Application to the North Western Mediterranean coastal dynamics. Advances in Space Research, 53:788 – 801. doi:https://doi.org/10.1016/j.asr.2013.12.020.

[Boyd and Murray, 2001] Boyd, I.L., Murray, A.W.A., 2001. Monitoring a marine ecosystem using responses of upper trophic level predators. Journal of Animal Ecology, 70:747–760. doi:10.1046/j.0021-8790.2001.00534.x.

[Boyd et al., 2012] Boyd, P.W., Arrigo, K.R., Strzepek, R., Dijken, G.L., 2012. Mapping phytoplankton iron utilization: Insights into Southern Ocean supply mechanisms. Journal of Geophysical Research: Oceans, 117. doi:10.1029/2011JC007726.

[Boyd et al., 2007] Boyd, P.W., Jickells, T., Law, C.S., Blain, S., Boyle, E.A., Buesseler, K.O., Coale, K.H., Cullen, J.J., de Baar, H.J.W., Follows, M., Harvey, M., Lancelot, C., Levasseur, M., Owens, N.P.J., Pollard, R., Rivkin, R.B., Sarmiento, J., Schoemann, V., Smetacek, V., Takeda, S., Tsuda, A., Turner, S., Watson, A.J., 2007. Mesoscale Iron Enrichment Experiments 1993-2005: Synthesis and Future Directions. Science, 315:612–617. doi:10.1126/science.1131669.

[Bradbury et al., 2008] Bradbury, I.R., Laurel, B., Snelgrove, P.V., Bentzen, P., Campana, S.E., 2008. Global patterns in marine dispersal estimates: the influence of geography, taxonomic category and life history. Proceedings of the Royal Society of London B: Biological Sciences, 275:1803–1809. doi:10.1098/rspb.2008.0216.

[Bras et al., 2017] Bras, Y.L., Jouma'a, J., Guinet, C., 2017. Three-dimensional space use during the bottom phase of southern elephant seal dives. Movement Ecology, 5:18. doi:10.1186/s40462-017-0108-y.

[Bray et al., 2017] Bray, L., Kassis, D., Hall-Spencer, J., 2017. Assessing larval connectivity for marine spatial planning in the Adriatic. Marine Environmental Research, 125:73 – 81. doi:https://doi.org/10.1016/j.marenvres.2017.01.006.

[Breder, 1967] Breder, C., 1967. On the survival value of fish schools. Zoologica, 52:25–40.

[Brodeur and Yamamura, 2005] Brodeur, R., Yamamura, O., 2005. Micronekton of the North Pacific. PICES Scientific Report, 30:1–115.

[Brophy et al., 2009] Brophy, J., Murphy, S., Rogan, E., 2009. The diet and feeding ecology of the short-beaked common dolphin (Delphinus delphis) in the northeast Atlantic. International Whaling Commission Scientific Committee, 18.

[Bryce et al., 1999] Bryce, S.A., Omernik, J.M., Larsen, D.P., 1999. Environmental Review: Ecoregions: A Geographic Framework to Guide Risk Characterization and Ecosystem Management. Environmental Practice, 1:141–155. doi:10.1017/S1466046600000582.

[Béhagle et al., 2017] Béhagle, N., Cotté, C., Lebourges-Dhaussy, A., Roudaut, G., Duhamel, G., Brehmer, P., Josse, E., Cherel, Y., 2017. Acoustic distribution of discriminated micronektonic organisms from a bi-frequency processing: The case study of eastern Kerguelen oceanic waters. Progress in Oceanography, 156:276 – 289. doi:https://doi.org/10.1016/j.pocean.2017.06.004.

[Calil and Richards, 2010] Calil, P.H.R., Richards, K.J., 2010. Transient upwelling hot spots in the oligotrophic North Pacific. Journal of Geophysical Research: Oceans, 115. doi:10.1029/2009JC005360.

[Camphuysen, 2006] Camphuysen, C., 2006. Top predators in marine ecosystems: their role in monitoring and management, volume 12. Cambridge University Press.

[Capello et al., 2016] Capello, M., Deneubourg, J., Robert, M., Holland, K., Schaefer, K., Dagorn, L., 2016. Population assessment of tropical tuna based on their associative behavior around floating objects. Scientific reports, 6:36415. doi:10.1038/srep36415.

[Capet et al., 2008a] Capet, X., McWilliams, J.C., Molemaker, M.J., Shchepetkin, A.F., 2008a. Mesoscale to submesoscale transition in the california current system. part i: Flow structure, eddy flux, and observational tests. Journal of Physical Oceanography, 38:29–43. doi:10.1175/2007JPO3671.1.

[Capet et al., 2008b] Capet, X., McWilliams, J.C., Molemaker, M.J., Shchepetkin, A.F., 2008b. Mesoscale to Submesoscale Transition in the California Current System. Part II: Frontal Processes. Journal of Physical Oceanography, 38:44–64. doi:10.1175/2007JPO3672.1.

[Carlotti et al., 2015] Carlotti, F., Jouandet, M.P., Nowaczyk, A., Harmelin-Vivien, M., Lefèvre, D., Richard, P., Zhu, Y., Zhou, M., 2015. Mesozooplankton structure and functioning during the onset of the Kerguelen phytoplankton bloom during the KEOPS2 survey. Biogeosciences, 12:4543–4563. doi:10.5194/bg-12-4543-2015.

[Carlson et al., 2010] Carlson, D.F., Fredj, E., Gildor, H., Rom-Kedar, V., 2010. Deducing an upper bound to the horizontal eddy diffusivity using a stochastic Lagrangian model. Environmental Fluid Mechanics, 10:499–520. doi:10.1007/s10652-010-9181-0.

[Carreras et al., 2017] Carreras, C., Ordóñez, V., Zane, L., Kruschel, C., Nasto, I., Macpherson, E., Pascual, M., 2017. Population genomics of an endemic Mediterranean fish: differentiation by fine scale dispersal and adaptation. Scientific Reports, 7:43417. doi:10.1038/srep43417.

[Casaux et al., 1998] Casaux, R., Baroni, A., Carlini, A., 1998. The diet of the Antarctic fur seal Arctocephalus gazella at Harmony Point, Nelson Island, South Shetland Islands. Polar Biology, 20:424–428. doi:10.1007/s003000050324.

[Catul et al., 2011] Catul, V., Gauns, M., Karuppasamy, P.K., 2011. A review on mesopelagic fishes belonging to family Myctophidae. Reviews in Fish Biology and Fisheries, 21:339–354. doi:10.1007/s11160-010-9176-4.

[Ceriani et al., 2017] Ceriani, S.A., Weishampel, J.F., Ehrhart, L.M., Mansfield, K.L., Wunder, M.B., 2017. Foraging and recruitment hotspot dynamics for the largest atlantic loggerhead turtle rookery. Scientific reports, 7:16894. doi:10.1038/s41598-017-17206-3.

[Chambault et al., 2017] Chambault, P., Roquet, F., Benhamou, S., Baudena, A., Pauthenet, E., de Thoisy, B., Bonola, M., Reis, V.D., Crasson, R., Brucker, M., Maho, Y.L., Chevallier, D., 2017. The Gulf Stream frontal system: A key oceanographic feature in the habitat selection of the leatherback turtle? Deep Sea Research Part I: Oceanographic Research Papers, 123:35 – 47. doi:https://doi.org/10.1016/j.dsr.2017.03.003.

[Chelton et al., 2007] Chelton, D.B., Schlax, M.G., Samelson, R.M., de Szoeke, R.A., 2007. Global observations of large oceanic eddies. Geophysical Research Letters, 34. doi:10.1029/2007GL030812.

[Cherel et al., 2008] Cherel, Y., Ducatez, S., Fontaine, C., Richard, P., Guinet, C., 2008. Stable isotopes reveal the trophic position and mesopelagic fish diet of female southern elephant seals breeding on the kerguelen islands. Marine Ecology Progress Series, 370:239–247.

[Cherel et al., 2010] Cherel, Y., Fontaine, C., Richard, P., Labatc, J.P., 2010. Isotopic niches and trophic levels of myctophid fishes and their predators in the southern ocean. Limnology and oceanography, 55:324–332.

[Christaki et al., 2008] Christaki, U., Obernosterer, I., Van Wambeke, F., Veldhuis, M., Garcia, N., Catala, P., 2008. Microbial food web structure in a naturally iron-fertilized area in the Southern Ocean (Kerguelen Plateau). Deep Sea Research Part II: Topical Studies in Oceanography, 55:706–719. doi:10.1016/j.dsr2.2007.12.009.

[Christensen et al., 2003] Christensen, V., Guénette, S., Heymans, J.J., Walters, C.J., Watson, R., Zeller, D., Pauly, D., 2003. Hundred-year decline of North Atlantic predatory fishes. Fish and Fisheries, 4:1–24. doi:10.1046/j.1467-2979.2003.00103.x.

[Ciappa and Costabile, 2014] Ciappa, A., Costabile, S., 2014. Oil spill hazard assessment using a reverse trajectory method for the Egadi marine protected area (Central Mediterranean Sea). Marine Pollution Bulletin, 84:44 – 55. doi:https://doi.org/10.1016/j.marpolbul.2014.05.044.

[Coleman et al., 2004] Coleman, F.C., Figueira, W.F., Ueland, J.S., Crowder, L.B., 2004. The Impact of United States Recreational Fisheries on Marine Fish Populations. Science, 305:1958–1960. doi:10.1126/science.1100397.

[Collins et al., 2008] Collins, M.A., Xavier, J.C., Johnston, N.M., North, A.W., Enderlein, P., Tarling, G.A., Waluda, C.M., Hawker, E.J., Cunningham, N.J., 2008. Patterns in the distribution of myctophid fish in the northern Scotia Sea ecosystem. Polar Biology, 31:837–851. doi:10.1007/s00300-008-0423-2.

[Costa et al., 2017] Costa, A., Petrenko, A.A., Guizien, K., Doglioli, A.M., 2017. On the calculation of betweenness centrality in marine connectivity studies using transfer probabilities. PLOS ONE, 12:1–10. doi:10.1371/journal.pone.0189021.

[Costello et al., 2012] Costello, M.J., Wilson, S., Houlding, B., 2012. Predicting Total Global Species Richness Using Rates of Species Description and Estimates of Taxonomic Effort. Systematic Biology, 61:871. doi:10.1093/sysbio/syr080.

[Cotté et al., 2011a] Cotté, C., d'Ovidio, F., Chaigneau, A., Lévy, M., Taupier-Letage, I., Mate, B., Christophe, G., 2011a. Scale-dependent interactions of mediterranean whales with marine dynamics. Limnology Oceanography, 106:219–232. doi:10.4319/lo.2011.56.1.0219.

[Cotté et al., 2011b] Cotté, C., d'Ovidio, F., Chaigneau, A., Lévy, M., Taupier-Letage, I., Mate, B., Guinet, C., 2011b. Scale-dependent interactions of Mediterranean whales with marine dynamics. Limnology and Oceanography, 56:219–232.

[Cotté et al., 2015] Cotté, C., d'Ovidio, F., Dragon, A.C., Guinet, C., Lévy, M., 2015. Flexible preference of southern elephant seals for distinct mesoscale features within the antarctic circumpolar current. Progress in Oceanography, 131:46 – 58. doi: http://dx.doi.org/10.1016/j.pocean.2014.11.011.

[Cotté et al., 2007] Cotté, C., Park, Y.H., Guinet, C., Bost, C.A., 2007. Movements of foraging king penguins through marine mesoscale eddies. Proceedings of the Royal Society B: Biological Sciences, 274:2385–2391. doi:10.1098/rspb.2007.0775.

[Cowen et al., 2006] Cowen, R.K., Paris, C.B., Srinivasan, A., 2006. Scaling of Connectivity in Marine Populations. Science, 311:522–527. doi:10.1126/science.1122039.

[Coyle and Jr, 2000] Coyle, K.O., Jr, G.L.H., 2000. Seasonal differences in the distribution, density and scale of zooplankton patches in the upper mixed layer near the western Aleutian Islands. Plankton Biol. Ecol, 47:31–42.

[Crawford et al., 2007] Crawford, R.J.M., Underhill, L.G., Upfold, L., Dyer, B.M., 2007. An altered carrying capacity of the benguela upwelling ecosystem for african penguins (spheniscus demersus). ICES Journal of Marine Science, 64:570–576. doi: 10.1093/icesjms/fsm009.

[Cronin et al., 2014] Cronin, T.W., Johnsen, S., Marshall, N.J., Warrant, E.J., 2014. Visual ecology. Princeton University Press.

[Crowder and Norse, 2008] Crowder, L., Norse, E., 2008. Essential ecological insights for marine ecosystem-based management and marine spatial planning. Marine Policy, 32:772 – 778. doi:https://doi.org/10.1016/j.marpol.2008.03.012. The Role of Marine Spatial Planning in Implementing Ecosystem-based, Sea Use Management.

[Cury et al., 2000] Cury, P., Bakun, A., Crawford, R.J.M., Jarre, A., Quiñones, R.A., Shannon, L.J., Verheye, H.M., 2000. Small pelagics in upwelling systems: patterns of interaction and structural changes in "wasp-waist" ecosystems. ICES Journal of Marine Science, 57:603–618. doi:10.1006/jmsc.2000.0712.

[Cury et al., 2003] Cury, P., Shannon, L., Shin, Y.J., 2003. The functioning of marine ecosystems: a fisheries perspective. Responsible fisheries in the marine ecosystem, pages 103–123.

[Daneri and Carlini, 2002] Daneri, G., Carlini, A., 2002. Fish prey of southern elephant seals, Mirounga leonina, at King George Island. Polar Biology, 25:739–743. doi:10.1007/s00300-002-0408-5.

[Davis et al., 2014] Davis, M.P., Holcroft, N.I., Wiley, E.O., Sparks, J.S., Smith, W.L., 2014. Species-specific bioluminescence facilitates speciation in the deep sea. Marine biology, 161:1139–1148.

[Davoren, 2013] Davoren, G.K., 2013. Distribution of marine predator hotspots explained by persistent areas of prey. Marine Biology, 160:3043–3058. doi:10.1007/s00227-013-2294-5.

[De Baar et al., 1995] De Baar, H.J., De Jong, J.T., Bakker, D.C., Löscher, B.M., Veth, C., Bathmann, U., Smetacek, V., 1995. Importance of iron for plankton blooms and carbon dioxide drawdown in the Southern Ocean. Nature, 373:412. doi:doi.org/10.1038/373412a0.

[de Baar et al., 2005] de Baar, H.J.W., Boyd, P.W., Coale, K.H., Landry, M.R., Tsuda, A., Assmy, P., Bakker, D.C.E., Bozec, Y., Barber, R.T., Brzezinski, M.A., Buesseler, K.O., Boyé, M., Croot, P.L., Gervais, F., Gorbunov, M.Y., Harrison, P.J., Hiscock, W.T., Laan, P., Lancelot, C., Law, C.S., Levasseur, M., Marchetti, A., Millero, F.J., Nishioka, J., Nojiri, Y., van Oijen, T., Riebesell, U., Rijkenberg, M.J.A., Saito, H., Takeda, S., Timmermans, K.R., Veldhuis, M.J.W., Waite, A.M., Wong, C.S., 2005. Synthesis of iron fertilization experiments: From the Iron Age in the Age of Enlightenment. Journal of Geophysical Research: Oceans, 110. doi:10.1029/2004JC002601.

[De Broyer et al., 2014] De Broyer, C., Koubbi, P., Griffiths, H., Grant, S.A., 2014. Biogeographic atlas of the Southern Ocean. Scientific Committee on Antarctic Research Cambridge.

[De Busserolles et al., 2014] De Busserolles, F., Fitzpatrick, J.L., Marshall, N.J., Collin, S.P., 2014. The influence of photoreceptor size and distribution on optical sensitivity in the eyes of lanternfishes (myctophidae). PloS one, 9:e99957.

[de Busserolles and Marshall, 2017] de Busserolles, F., Marshall, N.J., 2017. Seeing in the deep-sea: visual adaptations in lanternfishes. Phil. Trans. R. Soc. B, 372:20160070.

[de Jonge et al., 2006] de Jonge, V., Elliott, M., Brauer, V., 2006. Marine monitoring: Its shortcomings and mismatch with the EU Water Framework Directive's objectives. Marine Pollution Bulletin, 53:5 – 19. doi:https://doi.org/10.1016/j. marpolbul.2005.11.026. Recent Developments in Estuarine Ecology and Management.

[De Monte et al., 2012] De Monte, S., Cotté, C., d'Ovidio, F., Lévy, M., Le Corre, M., Weimerskirch, H., 2012. Frigatebird behaviour at the ocean–atmosphere interface: integrating animal behaviour with multi-satellite data. Journal of The Royal Society Interface, 9:3351–3358. doi:10.1098/rsif.2012.0509.

[De Monte et al., 2013] De Monte, S., Soccodato, A., Alvain, S., d'Ovidio, F., 2013. Can we detect oceanic biodiversity hotspots from space? The ISME journal, 7:2054. doi:10.1038/ismej.2013.72.

[Deagle et al., 2007] Deagle, B.E., Gales, N.J., Evans, K., Jarman, S.N., Robinson, S., Trebilco, R., Hindell, M.A., 2007. Studying Seabird Diet through Genetic Analysis of Faeces: A Case Study on Macaroni Penguins (Eudyptes chrysolophus). PLOS ONE, 2:1–10. doi:10.1371/journal.pone.0000831.

[Della Penna et al., 2015] Della Penna, A., De Monte, S., Kestenare, E., Guinet, C., d'Ovidio, F., 2015. Quasi-planktonic behavior of foraging top marine predators. Scientific reports, 5. doi:10.1038/srep18063.

[Delpeche-Ellmann and Soomere, 2013a] Delpeche-Ellmann, N.C., Soomere, T., 2013a. Investigating the Marine Protected Areas most at risk of current-driven pollution in the Gulf of Finland, the Baltic Sea, using a Lagrangian transport model. Marine Pollution Bulletin, 67:121 – 129. doi:https://doi.org/10.1016/j.marpolbul.2012.11. 025.

[Delpeche-Ellmann and Soomere, 2013b] Delpeche-Ellmann, N.C., Soomere, T., 2013b. Using Lagrangian models to assist in maritime management of Coastal and Marine

Protected Areas. Journal of Coastal Research, pages 36–41. doi:10.2112/SI65-007. 1.

[Denman and Abbott, 1988] Denman, K.L., Abbott, M.R., 1988. Time evolution of surface chlorophyll patterns from cross-spectrum analysis of satellite color images. Journal of Geophysical Research: Oceans, 93:6789–6798. doi:10.1029/ JC093iC06p06789.

[Domenici, 2001] Domenici, P., 2001. The scaling of locomotor performance in predator–prey encounters: from fish to killer whales. Comparative Biochemistry and Physiology Part A: Molecular & Integrative Physiology, 131:169 – 182. doi: https://doi.org/10.1016/S1095-6433(01)00465-2.

[Domingues et al., 2008] Domingues, C.M., Church, J.A., White, N.J., Gleckler, P.J., Wijffels, S.E., Barker, P.M., Dunn, J.R., 2008. Improved estimates of upper-ocean warming and multi-decadal sea-level rise. Nature, 453:1090. doi:10.1038/ nature07080.

[Douvere, 2008] Douvere, F., 2008. The importance of marine spatial planning in advancing ecosystem-based sea use management. Marine Policy, 32:762 – 771. doi: https://doi.org/10.1016/j.marpol.2008.03.021. The Role of Marine Spatial Planning in Implementing Ecosystem-based, Sea Use Management.

[d'Ovidio et al., 2013] d'Ovidio, F., De Monte, S., Della Penna, A., Cotté, C., Guinet, C., 2013. Ecological implications of eddy retention in the open ocean: a Lagrangian approach. Journal of Physics A: Mathematical and Theoretical, 46:254023. doi: 10.1088/1751-8113/46/25/254023.

[d'Ovidio et al., 2015] d'Ovidio, F., Della Penna, A., Trull, T.W., Nencioli, F., Pujol, M.I., Rio, M.H., Park, Y.H., Cotté, C., Zhou, M., Blain, S., 2015. The biogeochemical structuring role of horizontal stirring: Lagrangian perspectives on iron delivery downstream of the Kerguelen plateau. Biogeosciences, 12:5567–5581. doi: 10.5194/bg-12-5567-2015.

[d'Ovidio et al., 2004] d'Ovidio, F., Fernández, V., Hernández-García, E., López, C., 2004. Mixing structures in the Mediterranean Sea from finite-size Lyapunov exponents. Geophysical Research Letters, 31. doi:10.1029/2004GL020328.

[d'Ovidio et al., 2010] d'Ovidio, F., Monte, S.D., Alvain, S., Dandonneau, Y., Lévy, M., 2010. Fluid dynamical niches of phytoplankton types. Proceedings of the National Academy of Sciences, 107:18366–18370. doi:10.1073/pnas.1004620107.

[Døving, 1986] Døving, K., 1986. Functional properties of the fish olfactory system. In Progress in Sensory Physiology 6, pages 39–104. Springer.

[Døving, 1989] Døving, K.B., 1989. Molecular cues in salmonid migration. In Molecules in physics, chemistry, and biology, pages 299–329. Springer.

[Dragon et al., 2010] Dragon, A.C., Monestiez, P., Bar-Hen, A., Guinet, C., 2010. Linking foraging behaviour to physical oceanographic structures: Southern elephant seals and mesoscale eddies east of kerguelen islands. Progress In Oceanography, 87:61–71. doi:10.1016/j.pocean.2010.09.025.

[Drucker, 1996] Drucker, E.G., 1996. The Use of Gait Transition Speed in Comparative Studies of Fish Locomotion 1. American Zoologist, 36:555–566. doi:10.1093/icb/36.6.555.

[Dubois et al., 2016] Dubois, M., Rossi, V., Ser-Giacomi, E., Arnaud-Haond, S., López, C., Hernández-García, E., 2016. Linking basin-scale connectivity, oceanography and population dynamics for the conservation and management of marine ecosystems. Global Ecology and Biogeography, 25:503–515. doi:https://doi.org/10.1111/geb.12431.

[Ducklow et al., 2001] Ducklow, H.W., Steinberg, D.K., Buesseler, K.O., 2001. Upper ocean carbon export and the biological pump. OCEANOGRAPHY-WASHINGTON DC-OCEANOGRAPHY SOCIETY-, 14:50–58.

[Duhamel, 1998] Duhamel, G., 1998. The Pelagic Fish Community of the Polar Frontal Zone off the Kerguelen Islands", bookTitle="Fishes of Antarctica: A biological overview, pages 63–74. Springer Milan, Milano. doi:10.1007/978-88-470-2157-0_5.

[Duhamel et al., 2005] Duhamel, G., Gasco, N., Davaine, P., 2005. Poissons des îles Kerguelen et Crozet(guide régional de l'océan Austral). Patrimoines naturels.

[Dunstan et al., 2018] Dunstan, P.K., Moore, B.R., Bell, J.D., Holbrook, N.J., Oliver, E.C., Risbey, J., Foster, S.D., Hanich, Q., Hobday, A.J., Bennett, N.J., 2018. How can climate predictions improve sustainability of coastal fisheries in pacific small-island developing states? Marine Policy, 88:295 – 302. doi:https://doi.org/10.1016/j.marpol.2017.09.033.

[Dutkiewicz et al., 2009] Dutkiewicz, S., Follows, M.J., Bragg, J.G., 2009. Modeling the coupling of ocean ecology and biogeochemistry. Global Biogeochemical Cycles, 23. doi:10.1029/2008GB003405.

[Eckart, 1948] Eckart, C., 1948. An analysis of the stirring and mixing processes in incompressible fluids. Journal of Marine Research, 7:265–275.

[Eckert et al., 2006] Eckert, S.A., Bagley, D., Kubis, S., Ehrhart, L., Johnson, C., Stewart, K., DeFreese, D., 2006. Internesting and postnesting movements and foraging

habitats of leatherback sea turtles (Dermochelys coriacea) nesting in Florida. Chelonian Conservation and Biology, 5:239–248. doi:10.2744/1071-8443(2006)5[239:IAPMAF]2.0.CO;2.

[Edwards and Richardson, 2004] Edwards, M., Richardson, A.J., 2004. Impact of climate change on marine pelagic phenology and trophic mismatch. Nature, 430:881. doi:10.1038/nature02808.

[Ehler, 2017] Ehler, C., 2017. A Guide to Evaluating Marine Spatial Plans. doi:10.17605/OSF.IO/HY9RS.

[Ehler, 2018] Ehler, C.N.N., 2018. Marine spatial planning. Offshore Energy and Marine Spatial Planning, pages 6–17.

[Elliott, 2011] Elliott, M., 2011. Marine science and management means tackling exogenic unmanaged pressures and endogenic managed pressures – A numbered guide. Marine Pollution Bulletin, 62:651 – 655. doi:https://doi.org/10.1016/j.marpolbul.2010.11.033.

[Elliott and Jonge, 1996] Elliott, M., Jonge, V.N.D., 1996. The need for monitoring the monitors and their monitoring. Marine Pollution Bulletin, 32:248 – 249. doi:https://doi.org/10.1016/0025-326X(96)00009-4.

[Estes et al., 2011] Estes, J.A., Terborgh, J., Brashares, J.S., Power, M.E., Berger, J., Bond, W.J., Carpenter, S.R., Essington, T.E., Holt, R.D., Jackson, J.B.C., Marquis, R.J., Oksanen, L., Oksanen, T., Paine, R.T., Pikitch, E.K., Ripple, W.J., Sandin, S.A., Scheffer, M., Schoener, T.W., Shurin, J.B., Sinclair, A.R.E., Soulé, M.E., Virtanen, R., Wardle, D.A., 2011. Trophic Downgrading of Planet Earth. Science, 333:301–306. doi:10.1126/science.1205106.

[Ewing et al., 2014] Ewing, G., Lyle, J., Mapleston, A., 2014. Developing a low-cost monitoring regime to assess relative abundance and population characteristics of Sand Flathead. Institute for Marine and Antarctic Studies Report.

[Fach et al., 2002] Fach, B.A., Hofmann, E.E., Murphy, E.J., 2002. Modeling studies of Antarctic krill Euphausia superba survival during transport across the Scotia Sea. Marine Ecology Progress Series, 231:187–203. doi:10.3354/meps231187.

[Fach and Klinck, 2006] Fach, B.A., Klinck, J.M., 2006. Transport of Antarctic krill (Euphausia superba) across the Scotia Sea. Part I: Circulation and particle tracking simulations. Deep Sea Research Part I: Oceanographic Research Papers, 53:987 – 1010. doi:https://doi.org/10.1016/j.dsr.2006.03.006.

[Faunce et al., 2015] Faunce, C.H., Cahalan, J., Bonney, J., Swanson, R., 2015. Can observer sampling validate industry catch reports from trawl fisheries? Fisheries Research, 172:34 – 43. doi:https://doi.org/10.1016/j.fishres.2015.06.007.

[Ferrari and Wunsch, 2009] Ferrari, R., Wunsch, C., 2009. Ocean Circulation Kinetic Energy: Reservoirs, Sources, and Sinks. Annual Review of Fluid Mechanics, 41:253–282. doi:10.1146/annurev.fluid.40.111406.102139.

[Figueroa and Moffat, 2000] Figueroa, D., Moffat, C., 2000. On the influence of topography in the induction of coastal upwelling along the Chilean Coast. Geophysical Research Letters, 27:3905–3908. doi:10.1029/1999GL011302.

[Fiúza, 1983] Fiúza, A.F.G., 1983. Upwelling Patterns off Portugal, pages 85–98. Springer US, Boston, MA. doi:10.1007/978-1-4615-6651-9_5.

[Flores et al., 2008] Flores, H., Van de Putte, A.P., Siegel, V., Pakhomov, E.A., Van Franeker, J.A., Meesters, E.H., Volckaert, F.A., 2008. Distribution, abundance and ecological relevance of pelagic fishes in the Lazarev Sea, Southern Ocean. Marine Ecology Progress Series, 367:271–282. doi:doi.org/10.3354/meps07530.

[Flynn and Paxton, 2013] Flynn, A.J., Paxton, J.R., 2013. Spawning aggregation of the lanternfish Diaphus danae (family Myctophidae) in the north-western Coral Sea and associations with tuna aggregations. Marine and Freshwater Research, 63:1255–1271. doi:10.1071/MF12185.

[Follows et al., 2007] Follows, M.J., Dutkiewicz, S., Grant, S., Chisholm, S.W., 2007. Emergent Biogeography of Microbial Communities in a Model Ocean. Science, 315:1843–1846. doi:10.1126/science.1138544.

[Fossette et al., 2008] Fossette, S., Kelle, L., Girondot, M., Goverse, E., Hilterman, M.L., Verhage, B., de Thoisy, B., Georges, J.Y., 2008. The world's largest leatherback rookeries: A review of conservation-oriented research in French Guiana/Suriname and Gabon. Journal of Experimental Marine Biology and Ecology, 356:69 – 82. doi:https://doi.org/10.1016/j.jembe.2007.12.024. Sea turtles: physiological, molecular and behavioural ecology and conservation biology.

[Frederiksen et al., 2005] Frederiksen, M., Wright, P.J., Harris, M.P., Mavor, R.A., Heubeck, M., Wanless, S., 2005. Regional patterns of kittiwake Rissa tridactyla breeding success are related to variability in sandeel recruitment. Marine Ecology Progress Series, 300:201–211.

[Fromentin et al., 2003] Fromentin, J.M., Farrugio, H., Deflorio, M., De Metrio, G., 2003. Preliminary results of aerial surveys of bluefin tuna in the western Mediterranean Sea. Collective Volume of Scientific Papers, 55:1019–1027.

[Froyland et al., 2007] Froyland, G., Padberg, K., England, M.H., Treguier, A.M., 2007. Detection of Coherent Oceanic Structures via Transfer Operators. Phys. Rev. Lett., 98:224503. doi:10.1103/PhysRevLett.98.224503.

[Froyland et al., 2014] Froyland, G., Stuart, R.M., van Sebille, E., 2014. How well-connected is the surface of the global ocean? Chaos: An Interdisciplinary Journal of Nonlinear Science, 24:033126. doi:10.1063/1.4892530.

[Fujiwara et al., 2017] Fujiwara, N., Kirchen, K., Donges, J.F., Donner, R.V., 2017. A perturbation-theoretic approach to Lagrangian flow networks. Chaos, 27:035813. doi:10.1063/1.4978549.

[Gaines et al., 2010] Gaines, S.D., White, C., Carr, M.H., Palumbi, S.R., 2010. Designing marine reserve networks for both conservation and fisheries management. Proceedings of the National Academy of Sciences. doi:10.1073/pnas.0906473107.

[Garrett, 1983] Garrett, C., 1983. On the initial streakness of a dispersing tracer in two-and three-dimensional turbulence. Dynamics of Atmospheres and Oceans, 7:265–277. doi:10.1016/0377-0265(83)90008-8.

[Gasol et al., 2003] Gasol, J.M., del Giorgio, P.A., Duarte, C.M., 2003. Biomass distribution in marine planktonic communities. Limnology and Oceanography, 42:1353–1363. doi:10.4319/lo.1997.42.6.1353.

[Gauthier et al., 2014] Gauthier, S., Oeffner, J., O'Driscoll, R.L., 2014. Species composition and acoustic signatures of mesopelagic organisms in a subtropical convergence zone, the New Zealand Chatham Rise. Marine Ecology Progress Series, 503:23–40. doi:doi.org/10.3354/meps10731.

[Genin et al., 2005] Genin, A., Jaffe, J.S., Reef, R., Richter, C., Franks, P.J.S., 2005. Swimming Against the Flow: A Mechanism of Zooplankton Aggregation. Science, 308:860–862. doi:10.1126/science.1107834.

[Gjøsaeter and Kawaguchi, 1980] Gjøsaeter, J., Kawaguchi, K., 1980. A review of the world resources of mesopelagic fish. 193. Food & Agriculture Org.

[Goetze and Ohman, 2010] Goetze, E., Ohman, M.D., 2010. Integrated molecular and morphological biogeography of the calanoid copepod family Eucalanidae. Deep Sea Research Part II: Topical Studies in Oceanography, 57:2110 – 2129. doi:https://doi.org/10.1016/j.dsr2.2010.09.014. Species Diversity of Marine Zooplankton.

[Gopalakrishnan Meena et al., 2018] Gopalakrishnan Meena, M., Nair, A.G., Taira, K., 2018. Network community-based model reduction for vortical flows. Phys. Rev. E, 97:063103. doi:10.1103/PhysRevE.97.063103.

[Gordon et al., 1985] Gordon, J.D.M., Nishida, S., Nemoto, T., 1985. The diet of mesopelagic fish from the Pacific coast of Hokkaido, Japan. Journal of the Oceanographical Society of Japan, 41:89–97. doi:10.1007/BF02109178.

[Gower et al., 1980] Gower, J., Denman, K., Holyer, R., 1980. Phytoplankton patchiness indicates the fluctuation spectrum of mesoscale oceanic structure. Nature, 288:157. doi:10.1038/288157a0.

[Greely et al., 1999] Greely, T.M., Gartner Jr, J.V., Torres, J.J., 1999. Age and growth of Electrona antarctica (Pisces: Myctophidae), the dominant mesopelagic fish of the Southern Ocean. Marine Biology, 133:145–158. doi:10.1007/s002270050453.

[Griffa et al., 2013] Griffa, A., Haza, A., Özgökmen, T.M., Molcard, A., Taillandier, V., Schroeder, K., Chang, Y., Poulain, P.M., 2013. Investigating transport pathways in the ocean. Deep Sea Research Part II: Topical Studies in Oceanography, 85:81 – 95. doi:https://doi.org/10.1016/j.dsr2.2012.07.031. Modern Physical Oceanography and Professor H.T. Rossby.

[Grimm, 1960] Grimm, R.J., 1960. Feeding behavior and electrical stimulation of the brain of carassius auratus. Science, 131:162–163.

[Grünbaum, 1998] Grünbaum, D., 1998. Schooling as a strategy for taxis in a noisy environment. Evolutionary Ecology, 12:503–522. doi:10.1023/A:1006574607845.

[Gui et al., 2014] Gui, F., Wang, P., Wu, C., 2014. Evaluation approaches of fish swimming performance. Agricultural Sciences, 5:106. doi:10.4236/as.2014.52014.

[Guidi et al., 2012] Guidi, L., Calil, P.H.R., Duhamel, S., Björkman, K.M., Doney, S.C., Jackson, G.A., Li, B., Church, M.J., Tozzi, S., Kolber, Z.S., Richards, K.J., Fong, A.A., Letelier, R.M., Gorsky, G., Stemmann, L., Karl, D.M., 2012. Does eddy-eddy interaction control surface phytoplankton distribution and carbon export in the North Pacific Subtropical Gyre? Journal of Geophysical Research: Biogeosciences, 117. doi:10.1029/2012JG001984.

[Guinet et al., 2014] Guinet, C., Vacquié-Garcia, J., Picard, B., Bessigneul, G., Lebras, Y., Dragon, A.C., Viviant, M., Arnould, J.P., Bailleul, F., 2014. Southern elephant seal foraging success in relation to temperature and light conditions: insight into prey distribution. Marine Ecology Progress Series, 499:285–301. doi:doi.org/10.3354/meps10660.

[Haddock et al., 2010] Haddock, S.H., Moline, M.A., Case, J.F., 2010. Bioluminescence in the Sea. Annual Review of Marine Science, 2:443–493. doi:10.1146/annurev-marine-120308-081028. PMID: 21141672.

[Hadjighasem et al., 2016] Hadjighasem, A., Karrasch, D., Teramoto, H., Haller, G., 2016. Spectral-clustering approach to Lagrangian vortex detection. Physical Review E, 93:063107. doi:10.1103/PhysRevE.93.063107.

[Hairer and Mattingly, 2006] Hairer, M., Mattingly, J.C., 2006. Ergodicity of the 2D Navier-Stokes Equations with Degenerate Stochastic Forcing. Annals of Mathematics, 164:993–1032.

[Hall, 1924] Hall, F.G., 1924. The functions of the swimbladder of fishes. The Biological Bulletin, 47:79–126.

[Haller, 2001] Haller, G., 2001. Lagrangian structures and the rate of strain in a partition of two-dimensional turbulence. Physics of Fluids, 13:3365–3385. doi:doi:10.1063/1.1403336.

[Haller, 2015] Haller, G., 2015. Lagrangian coherent structures. Annual Review of Fluid Mechanics, 47:137–162. doi:10.1146/annurev-fluid-010313-141322.

[Haller and Yuan, 2000] Haller, G., Yuan, G., 2000. Lagrangian coherent structures and mixing in two-dimensional turbulence. Phys. D, 147:352–370. doi:10.1016/S0167-2789(00)00142-1.

[Halpern et al., 2007] Halpern, B.S., Selkoe, K.A., Micheli, F., Kappel, C.V., 2007. Evaluating and Ranking the Vulnerability of Global Marine Ecosystems to Anthropogenic Threats. Conservation Biology, 21:1301–1315. doi:10.1111/j.1523-1739.2007.00752.x.

[Halpern et al., 2008] Halpern, B.S., Walbridge, S., Selkoe, K.A., Kappel, C.V., Micheli, F., D'Agrosa, C., Bruno, J.F., Casey, K.S., Ebert, C., Fox, H.E., Fujita, R., Heinemann, D., Lenihan, H.S., Madin, E.M.P., Perry, M.T., Selig, E.R., Spalding, M., Steneck, R., Watson, R., 2008. A Global Map of Human Impact on Marine Ecosystems. Science, 319:948–952. doi:10.1126/science.1149345.

[Hamdani et al., 2001] Hamdani, E.H., Kasumyan, A., Døving, K.B., 2001. Is feeding behaviour in crucian carp mediated by the lateral olfactory tract? Chemical senses, 26:1133–1138.

[Handegard et al., 2012] Handegard, N.O., Buisson, L.d., Brehmer, P., Chalmers, S.J., Robertis, A., Huse, G., Kloser, R., Macaulay, G., Maury, O., Ressler, P.H., Stenseth, N.C., Godø, O.R., 2012. Towards an acoustic-based coupled observation and modelling system for monitoring and predicting ecosystem dynamics of the open ocean. Fish and Fisheries, 14:605–615. doi:10.1111/j.1467-2979.2012.00480.x.

[Hara, 1975] Hara, T.J., 1975. Olfaction in fish. Progress in neurobiology, 5:271–335.

[Harriague and Albertelli, 2007] Harriague, A.C., Albertelli, G., 2007. Environmental factors controlling macrofaunal assemblages on six microtidal beaches of the Ligurian Sea (NW Mediterranean). Estuarine, Coastal and Shelf Science, 73:8 – 16. doi:https://doi.org/10.1016/j.ecss.2006.12.007.

[Hays, 2003] Hays, G.C., 2003. A review of the adaptive significance and ecosystem consequences of zooplankton diel vertical migrations. In M.B. Jones, A. Ingólfsson, E. Ólafsson, G.V. Helgason, K. Gunnarsson, J. Svavarsson, editors, Migrations and Dispersal of Marine Organisms, pages 163–170. Springer Netherlands, Dordrecht.

[Hays et al., 2005] Hays, G.C., Richardson, A.J., Robinson, C., 2005. Climate change and marine plankton. Trends in Ecology & Evolution, 20:337 – 344. doi: https://doi.org/10.1016/j.tree.2005.03.004. SPECIAL ISSUE: BUMPER BOOK REVIEW.

[Haza et al., 2012] Haza, A.C., Özgökmen, T.M., Griffa, A., Garraffo, Z.D., Piterbarg, L., 2012. Parameterization of particle transport at submesoscales in the Gulf Stream region using Lagrangian subgridscale models. Ocean Modelling, 42:31 – 49. doi:https://doi.org/10.1016/j.ocemod.2011.11.005.

[Heithaus et al., 2008] Heithaus, M.R., Frid, A., Wirsing, A.J., Worm, B., 2008. Predicting ecological consequences of marine top predator declines. Trends in ecology & evolution, 23:202–210. doi:doi.org/10.1016/j.tree.2008.01.003.

[Herskin and Steffensen, 1998] Herskin, J., Steffensen, J., 1998. Energy savings in sea bass swimming in a school: measurements of tail beat frequency and oxygen consumption at different swimming speeds. Journal of Fish Biology, 53:366–376.

[Hidaka et al., 2001a] Hidaka, K., Kawaguchi, K., Murakami, M., Takahashi, M., 2001a. Downward transport of organic carbon by diel migratory micronekton in the western equatorial Pacific:: its quantitative and qualitative importance. Deep Sea Research Part I: Oceanographic Research Papers, 48:1923 – 1939. doi: https://doi.org/10.1016/S0967-0637(01)00003-6.

[Hidaka et al., 2001b] Hidaka, K., Kawaguchi, K., Murakami, M., Takahashi, M., 2001b. Downward transport of organic carbon by diel migratory micronekton in the western equatorial Pacific:: its quantitative and qualitative importance. Deep Sea Research Part I: Oceanographic Research Papers, 48:1923 – 1939. doi: https://doi.org/10.1016/S0967-0637(01)00003-6.

[Higgs and Attrill, 2015] Higgs, N., Attrill, M., 2015. Biases in biodiversity: wide-ranging species are discovered first in the deep sea. Frontiers in Marine Science, 2:61. doi:10.3389/fmars.2015.00061.

[Hindell et al., 2011] Hindell, M.A., Lea, M.A., Bost, C.A., Charrassin, J.B., Gales, N., Goldsworthy, S., Page, B., Robertson, G., Wienecke, B., O'Toole, M., et al., 2011. Foraging habitats of top predators, and areas of ecological significance, on the kerguelen plateau. The Kerguelen Plateau: marine ecosystem and fisheries. Société Française d'Ichtyologie, Paris, pages 203–215.

[Hobday and Pecl, 2014] Hobday, A.J., Pecl, G.T., 2014. Identification of global marine hotspots: sentinels for change and vanguards for adaptation action. Reviews in Fish Biology and Fisheries, 24:415–425. doi:10.1007/s11160-013-9326-6.

[Hoegh-Guldberg and Bruno, 2010] Hoegh-Guldberg, O., Bruno, J.F., 2010. The Impact of Climate Change on the World's Marine Ecosystems. Science, 328:1523–1528. doi:10.1126/science.1189930.

[Holling, 1959] Holling, C.S., 1959. The Components of Predation as Revealed by a Study of Small-Mammal Predation of the European Pine Sawfly. The Canadian Entomologist, 91:293–320. doi:10.4039/Ent91293-5.

[Holloway and Kristmannsson, 1984] Holloway, G., Kristmannsson, S.S., 1984. Stirring and transport of tracer fields by geostrophic turbulence. Journal of Fluid Mechanics, 141:27–[U+0080][U+0093]50. doi:10.1017/S0022112084000720.

[Hopkins et al., 1993] Hopkins, T.L., Ainley, D.G., Torres, J.J., Lancraft, T.M., 1993. Trophic structure in open waters of the marginal ice zone in the Scotia-Weddell confluence region during spring (1983). Polar Biology, 13:389–397. doi:10.1007/BF01681980.

[Hopkins et al., 1996] Hopkins, T.L., Sutton, T.T., Lancraft, T.M., 1996. The trophic structure and predation impact of a low latitude midwater fish assemblage. Progress in Oceanography, 38:205 – 239. doi:https://doi.org/10.1016/S0079-6611(97)00003-7.

[Hudson et al., 2014] Hudson, J.M., Steinberg, D.K., Sutton, T.T., Graves, J.E., Latour, R.J., 2014. Myctophid feeding ecology and carbon transport along the northern Mid-Atlantic Ridge. Deep Sea Research Part I: Oceanographic Research Papers, 93:104 – 116. doi:https://doi.org/10.1016/j.dsr.2014.07.002.

[Huhn et al., 2012] Huhn, F., Kameke, A., Pérez-Muñuzuri, V., Olascoaga, M.J., Beron-Vera, F.J., 2012. The impact of advective transport by the South Indian Ocean Countercurrent on the Madagascar plankton bloom. Geophysical Research Letters, 39. doi:10.1029/2012GL051246.

[Hulley et al., 2011] Hulley, P.A., Duhamel, G., Duhamel, G., 2011. Aspects of lantern-fish distribution in the Kerguelen Plateau region. The Kerguelen Plateau: marine ecosystems and fisheies. G. Duhamel and DC Welsford, Editors, pages 183–195.

[Huyer, 1983] Huyer, A., 1983. Coastal upwelling in the California current system. Progress in Oceanography, 12:259 – 284. doi:https://doi.org/10.1016/0079-6611(83)90010-1.

[Iacobello et al., 2018] Iacobello, G., Scarsoglio, S., Ridolfi, L., 2018. Visibility graph analysis of wall turbulence time-series. Physics Letters A, 382:1 – 11. doi:https://doi.org/10.1016/j.physleta.2017.10.027.

[Irigoien et al., 2014] Irigoien, X., Klevjer, T.A., Røstad, A., Martinez, U., Boyra, G., Acuña, J., Bode, A., Echevarria, F., Gonzalez-Gordillo, J., Hernandez-Leon, S., et al., 2014. Large mesopelagic fishes biomass and trophic efficiency in the open ocean. Nature communications, 5. doi:dx.doi.org/10.1038/ncomms4271.

[Iudicone et al., 2002] Iudicone, D., Lacorata, G., Rupolo, V., Santoleri, R., Vulpiani, A., 2002. Sensitivity of numerical tracer trajectories to uncertainties in OGCM velocity fields. Ocean Modelling, 4:313 – 325. doi:https://doi.org/10.1016/S1463-5003(02)00006-9.

[Iudicone et al., 2016] Iudicone, D., Rodgers, K.B., Plancherel, Y., Aumont, O., Ito, T., Key, R.M., Madec, G., Ishii, M., 2016. The formation of the ocean's anthropogenic carbon reservoir. Scientific reports, 6:35473. doi:10.1038/srep35473.

[Jahncke et al., 2004] Jahncke, J., Checkley, D.M., Hunt, G.L., 2004. Trends in carbon flux to seabirds in the peruvian upwelling system: effects of wind and fisheries on population regulation. Fisheries Oceanography, 13:208–223. doi:10.1111/j.1365-2419.2004.00283.x.

[Jansen et al., 1998] Jansen, J.K., Boveng, P.L., Bengtson, J.L., 1998. Foraging modes of chinstrap penguins: contrasts between day and night. Marine Ecology Progress Series, 165:161–172. doi:doi:10.3354/meps165161.

[Jeandel et al., 1998] Jeandel, C., Ruiz-Pino, D., Gjata, E., Poisson, A., Brunet, C., Charriaud, E., Dehairs, F., Delille, D., Fiala, M., Fravalo, C., Miquel, J.C., Park, Y.H., Pondaven, P., Quéguiner, B., Razouls, S., Shauer, B., Tréguer, P., 1998. KERFIX, a time-series station in the Southern Ocean: a presentation. Journal of Marine Systems, 17:555 – 569. doi:https://doi.org/10.1016/S0924-7963(98)00064-5.

[Johansson et al., 1993] Johansson, S., Hansson, S., Araya-Nuñez, O., 1993. Temporal and spatial variation of coastal zooplankton in the Baltic Sea. Ecography, 16:167–173. doi:10.1111/j.1600-0587.1993.tb00068.x.

[Kaartvedt et al., 2012] Kaartvedt, S., Staby, A., Aksnes, D.L., 2012. Efficient trawl avoidance by mesopelagic fishes causes large underestimation of their biomass. Marine Ecology Progress Series, 456:1–6. doi:doi.org/10.3354/meps09785.

[Kai et al., 2009] Kai, E.T., Rossi, V., Sudre, J., Weimerskirch, H., Lopez, C., Hernandez-Garcia, E., Marsac, F., Garcon, V., 2009. Top marine predators track lagrangian coherent structures. Proceedings of the National Academy of Sciences of the United States of America, 106:8245–8250. doi:10.1073/pnas.0811034106.

[Kasumyan, 2004] Kasumyan, A., 2004. The olfactory system in fish: structure, function, and role in behavior. Journal of Ichthyology, 44:S180.

[Kasumyan and Marusov, 2003] Kasumyan, A., Marusov, E., 2003. Behavioral responses of intact and chronically anosmiated minnows phoxinus phoxinus (cyprinidae) to free amino acids. Journal of Ichthyology, 43:528–538.

[Kasumyan and Döving, 2003] Kasumyan, A.O., Döving, K.B., 2003. Taste preferences in fishes. Fish and fisheries, 4:289–347.

[Kern and Coyle, 2000] Kern, J.W., Coyle, K.O., 2000. Global block kriging to estimate biomass from acoustic surveys for zooplankton in the western Aleutian Islands. Canadian Journal of Fisheries and Aquatic Sciences, 57:2112–2121. doi:10.1139/f00-152.

[Kinzer et al., 1993] Kinzer, J., Böttger-Schnack, R., Schulz, K., 1993. Aspects of horizontal distribution and diet of myctophid fish in the Arabian Sea with reference to the deep water oxygen deficiency. Deep Sea Research Part II: Topical Studies in Oceanography, 40:783 – 800. doi:https://doi.org/10.1016/0967-0645(93)90058-U.

[Kleerekoper, 1969] Kleerekoper, H., 1969. Olfaction in fishes. Indiana University Press.

[Klein et al., 2005] Klein, P., Hua, B.L., Le Gentil, S., Sasaki, H., 2005. The vertical pump organized by the mesoscale oceanic eddies. Annual Report of the Earth Simulator Center, pages 331–334.

[Klein et al., 1998] Klein, P., Treguier, A.M., Hua, B.L., 1998. Three-dimensional stirring of thermohaline fronts. Journal of Marine Research, 56:589–612. doi:doi:10.1357/002224098765213595.

[Kloser et al., 2009] Kloser, R.J., Ryan, T.E., Young, J.W., Lewis, M.E., 2009. Acoustic observations of micronekton fish on the scale of an ocean basin: potential and challenges. ICES Journal of Marine Science, 66:998–1006. doi:10.1093/icesjms/fsp077.

[Koizumi et al., 2014] Koizumi, K., Hiratsuka, S., Saito, H., 2014. Lipid and fatty acids of three edible myctophids, Diaphus watasei, Diaphus suborbitalis, and Benthosema pterotum: high levels of icosapentaenoic and docosahexaenoic acids. Journal of oleo science, 63:461–470. doi:doi.org/10.5650/jos.ess13224.

[Koltai and Renger, 2018] Koltai, P., Renger, D.R.M., 2018. From Large Deviations to Semidistances of Transport and Mixing: Coherence Analysis for Finite Lagrangian Data. Journal of Nonlinear Science. doi:10.1007/s00332-018-9471-0.

[Kooyman et al., 1992] Kooyman, G.L., Cherel, Y., Maho, Y.L., Croxall, J.P., Thorson, P.H., Ridoux, V., Kooyman, C.A., 1992. Diving Behavior and Energetics During Foraging Cycles in King Penguins. Ecological Monographs, 62:143–163. doi:10.2307/2937173.

[Koslow et al., 2011] Koslow, J.A., Goericke, R., Lara-Lopez, A., Watson, W., 2011. Impact of declining intermediate-water oxygen on deepwater fishes in the California Current. Marine Ecology Progress Series, 436:207–218. doi:doi.org/10.3354/meps09270.

[Koubbi, 1993] Koubbi, P., 1993. Influence of the frontal zones on ichthyoplankton and mesopelagic fish assemblages in the Crozet Basin (Indian sector of the Southern Ocean). Polar Biology, 13:557–564. doi:10.1007/BF00236398.

[Koubbi et al., 2016a] Koubbi, P., Guinet, C., Alloncle, N., Ameziane, N., Azam, C., Baudena, A., Weimerskirch, H., 2016a. Ecoregionalisation of the Kerguelen and Crozet islands oceanic zone. Part I: Introduction and Kerguelen oceanic zone. CCAMLR Document WG-EMM-16/43.

[Koubbi et al., 2011a] Koubbi, P., Hulley, P., Raymond, B., Penot, F., Gasparini, S., Labat, J., Pruvost, P., Mormède, S., Irisson, J., Duhamel, G., et al., 2011a. Estimating the biodiversity of the sub-Antarctic Indian part for ecoregionalisation: Part I. Pelagic realm of CCAMLR areas 58.5. 1 and 58.6. CCAMLR. WS-MPA-11, 11.

[Koubbi et al., 1991] Koubbi, P., Ibanez, F., Duhamel, G., 1991. Environmental influences on spatio-temporal oceanic distribution of ichthyoplankton around the Kerguelen Islands (Southern Ocean). Marine Ecology Progress Series, 72:225–238.

[Koubbi et al., 2016b] Koubbi, P., Mignard, C., Causse, R., Da Silva, O., Baudena, A., Bost, C., Cotte, C., d'Ovidio, F., Della Penna, A., Delord, K., et al., 2016b. Ecoregionalisation of the Kerguelen and Crozet islands oceanic zone. Part II: The Crozet oceanic zone. CCAMLR Document WG-EMM-16/43.

[Koubbi et al., 2011b] Koubbi, P., Moteki, M., Duhamel, G., Goarant, A., Hulley, P.A., O'Driscoll, R., Ishimaru, T., Pruvost, P., Tavernier, E., Hosie, G., 2011b. Ecoregionalization of myctophid fish in the Indian sector of the Southern Ocean: Results from generalized dissimilarity models. Deep Sea Research Part II: Topical Studies in Oceanography, 58:170 – 180. doi:https://doi.org/10.1016/j.dsr2.2010.09.007. Census of Antarctic Marine Life: Diversity and Change in the Southern Ocean Ecosystems.

[Koz, 1995] Koz, A., 1995. A review of the trophic role of mesopelagic fish of the family Myctophidae in the Southern Ocean ecosystem. CCAMLR Science, 2:71–77.

[Kozlov, 1995] Kozlov, A., 1995. A review of the trophic role of mesopelagic fish of the family Myctophidae in the Southern Ocean ecosystem. CCAMLR Science, 2:71–77.

[Kraichnan and Montgomery, 1980] Kraichnan, R.H., Montgomery, D., 1980. Two-dimensional turbulence. Reports on Progress in Physics, 43:547.

[Kris-Etherton et al., 2002] Kris-Etherton, P.M., Harris, W.S., Appel, L.J., 2002. Fish consumption, fish oil, omega-3 fatty acids, and cardiovascular disease. Circulation.

[Kuhn et al., 1963] Kuhn, W., Ramel, A., Kuhn, H., Marti, E., 1963. The filling mechanism of the swimbladder. Experientia, 19:497–511.

[Kwon et al., 2009] Kwon, E.Y., Primeau, F., Sarmiento, J.L., 2009. The impact of remineralization depth on the air–sea carbon balance. Nature Geoscience, 2:630.

[Lacour et al., 2017] Lacour, L., Ardyna, M., Stec, K., Claustre, H., Prieur, L., Poteau, A., D'Alcala, M.R., Iudicone, D., 2017. Unexpected winter phytoplankton blooms in the North Atlantic subpolar gyre. Nature Geoscience, 10:836. doi:10.1038/ngeo3035.

[Lam and Bishop, 2008] Lam, P.J., Bishop, J.K., 2008. The continental margin is a key source of iron to the HNLC North Pacific Ocean. Geophysical Research Letters, 35. doi:10.1029/2008GL033294.

[Lapeyre and Klein, 2006] Lapeyre, G., Klein, P., 2006. Impact of the small-scale elongated filaments on the oceanic vertical pump. Journal of Marine Research, 64:835–851. doi:doi:10.1357/002224006779698369.

[Lara-Lopez et al., 2012] Lara-Lopez, A.L., Davison, P., Koslow, J.A., 2012. Abundance and community composition of micronekton across a front off Southern California. Journal of Plankton Research, 34:828–848. doi:10.1093/plankt/fbs016.

[Lavoie et al., 2000] Lavoie, D., Simard, Y., Saucier, F.J., 2000. Aggregation and dispersion of krill at channel heads and shelf edges: the dynamics in the saguenay - st. lawrence marine park. Canadian Journal of Fisheries and Aquatic Sciences, 57:1853–1869. doi:10.1139/f00-138.

[Lawry, 1973] Lawry, J.V., 1973. The olfactory epithelium of the lantern fish, tarletonbeania crenularis (myctophidae). Cell and Tissue Research, 138:31–39.

[Lea et al., 2006] Lea, M.A., Guinet, C., Cherel, Y., Duhamel, G., Dubroca, L., Pruvost, P., Hindell, M., 2006. Impacts of climatic anomalies on provisioning strategies of a Southern Ocean predator. Marine Ecology Progress Series, 310:77–94. doi: doi:10.3354/meps310077.

[Lea et al., 2008] Lea, M.A., Guinet, C., Cherel, Y., Hindell, M., Dubroca, L., Thalmann, S., 2008. Colony-based foraging segregation by Antarctic fur seals at the Kerguelen Archipelago. Marine Ecology Progress Series, 358:273–287. doi: doi.org/10.3354/meps07305.

[Lea et al., 2002] Lea, M.A., Nichols, P.D., Wilson, G., 2002. Fatty acid composition of lipid-rich myctophids and mackerel icefish (champsocephalus gunnari) – southern ocean food-web implications. Polar Biology, 25:843–854. doi:10.1007/s00300-002-0428-1.

[Lee et al., 2012] Lee, C.R., Choi, K.H., Kang, H.K., Yang, E.J., Noh, J.H., Choi, D.H., 2012. Biomass and trophic structure of the plankton community in subtropical and temperate waters of the northwestern Pacific Ocean. Journal of Oceanography, 68:473–482. doi:10.1007/s10872-012-0111-2.

[Lehahn et al., 2017] Lehahn, Y., d'Ovidio, F., Koren, I., 2017. Satellite-Based Lagrangian View on Phytoplankton Dynamics. Annual Review of Marine Science, 10.

[Lehahn et al., 2018] Lehahn, Y., d'Ovidio, F., Koren, I., 2018. A satellite-based lagrangian view on phytoplankton dynamics. Annual Review of Marine Science, 10:99–119. doi:10.1146/annurev-marine-121916-063204. PMID: 28961072.

[Lehahn et al., 2007] Lehahn, Y., d'Ovidio, F., Lévy, M., Heifetz, E., 2007. Stirring of the northeast Atlantic spring bloom: A Lagrangian analysis based on multisatellite data. Journal of Geophysical Research, 112:C08005. doi:10.1029/2006JC003927.

[Lehahn et al., 2011] Lehahn, Y., d'Ovidio, F., Lévy, M., Amitai, Y., Heifetz, E., 2011. Long range transport of a quasi isolated chlorophyll patch by an Agulhas ring. Geophysical Research Letters, 38. doi:10.1029/2011GL048588.

[Lehodey et al., 2002] Lehodey, P., Andre, J.M., Bertigna, M., Hampton, J., Stoens, A., Menkes, C., Memery, L., Grima, N., 2002. Predicting skipjack tuna forage distributions in the equatorial Pacific using a coupled dynamical bio-geochemical model. Fisheries Oceanography, 7:317–325. doi:10.1046/j.1365-2419.1998.00063.x.

[Lévy et al., 2012] Lévy, M., Ferrari, R., Franks, P.J., Martin, A.P., Rivière, P., 2012. Bringing physics to life at the submesoscale. Geophysical Research Letters, 39.

[Lévy et al., 2015] Lévy, M., Jahn, O., Dutkiewicz, S., Follows, M.J., d'Ovidio, F., 2015. The dynamical landscape of marine phytoplankton diversity. Journal of The Royal Society Interface, 12. doi:10.1098/rsif.2015.0481.

[Lévy and Klein, 2004] Lévy, M., Klein, P., 2004. Does the low frequency variability of mesoscale dynamics explain a part of the phytoplankton and zooplankton spectral variability? Proceedings of the Royal Society of London A: Mathematical, Physical and Engineering Sciences, 460:1673–1687. doi:10.1098/rspa.2003.1219.

[Lindner and Donner, 2017] Lindner, M., Donner, R.V., 2017. Spatio-temporal organization of dynamics in a two-dimensional periodically driven vortex flow: A Lagrangian flow network perspective. Chaos: An Interdisciplinary Journal of Nonlinear Science, 27:035806. doi:10.1063/1.4975126.

[Logerwell and Wilson, 2004] Logerwell, E.A., Wilson, C.D., 2004. Species discrimination of fish using frequency-dependent acoustic backscatter. ICES Journal of Marine Science, 61:1004–1013. doi:10.1016/j.icesjms.2004.04.004.

[Loots et al., 2007] Loots, C., Koubbi, P., Duhamel, G., 2007. Habitat modelling of Electrona antarctica (Myctophidae, Pisces) in Kerguelen by generalized additive models and geographic information systems. Polar Biology, 30:951–959. doi:10.1007/s00300-007-0253-7.

[Lourie and Vincent, 2004] Lourie, S.A., Vincent, A.C.J., 2004. Using Biogeography to Help Set Priorities in Marine Conservation. Conservation Biology, 18:1004–1020. doi:10.1111/j.1523-1739.2004.00137.x.

[MacArthur and Pianka, 1966] MacArthur, R.H., Pianka, E.R., 1966. On Optimal Use of a Patchy Environment. The American Naturalist, 100:603–609. doi:10.1086/282454.

[Mackas and Boyd, 1979] Mackas, D.L., Boyd, C.M., 1979. Spectral Analysis of Zooplankton Spatial Heterogeneity. Science, 204:62–64. doi:10.1126/science.204.4388.62.

[Magris et al., 2014] Magris, R.A., Pressey, R.L., Weeks, R., Ban, N.C., 2014. Integrating connectivity and climate change into marine conservation planning. Biological Conservation, 170:207 – 221. doi:https://doi.org/10.1016/j.biocon.2013.12.032.

[Mahadevan, 2016] Mahadevan, A., 2016. The impact of submesoscale physics on primary productivity of plankton. Annual review of marine science, 8:161–184.

[Mahadevan and Campbell, 2002] Mahadevan, A., Campbell, J.W., 2002. Biogeochemical patchiness at the sea surface. Geophysical Research Letters, 29:32–1–32–4. doi:10.1029/2001GL014116.

[Mahadevan et al., 2012] Mahadevan, A., D'Asaro, E., Lee, C., Perry, M.J., 2012. Eddy-driven stratification initiates north atlantic spring phytoplankton blooms. Science, 337:54–58. doi:10.1126/science.1218740.

[Malyukina et al., 1969] Malyukina, G., Dmitrieva, N., Marusov, E., Yurkevich, G., 1969. Olfaction and its role in fish behavior. Itogi Nauki, Ser. Biol. Zool, pages 32–78.

[Malyukina et al., 1980] Malyukina, G., Kasumyan, A., Marusov, E., 1980. The role of olfaction in fish behavior. Sensory Systems, pages 30–44.

[Mancho et al., 2004] Mancho, A., Small, D., Wiggins, S., 2004. Computation of hyperbolic trajectories and their stable and unstable manifolds for oceanographic flows represented as data sets. Nonlinear Processes in Geophysics, 11:17–33.

[Mancho et al., 2006] Mancho, A.M., Small, D., Wiggins, S., 2006. A tutorial on dynamical systems concepts applied to lagrangian transport in oceanic flows defined as finite time data sets: Theoretical and computational issues. Physics Reports, 437:55–124. doi:10.1016/j.physrep.2006.09.005.

[Mann and Lazier, 2013] Mann, K.H., Lazier, J.R., 2013. Dynamics of marine ecosystems: biological-physical interactions in the oceans. John Wiley & Sons.

[Mariani et al., 2010] Mariani, P., MacKenzie, B.R., Iudicone, D., Bozec, A., 2010. Modelling retention and dispersion mechanisms of bluefin tuna eggs and larvae in the northwest Mediterranean Sea. Progress in Oceanography, 86:45 – 58. doi: https://doi.org/10.1016/j.pocean.2010.04.027. CLimate Impacts on Oceanic TOp Predators (CLIOTOP).

[Mariano et al., 2016] Mariano, A.J., Ryan, E.H., Huntley, H.S., Laurindo, L., Coelho, E., Griffa, A., Özgökmen, T.M., Berta, M., Bogucki, D., Chen, S.S., Curcic, M., Drouin, K., Gough, M., Haus, B.K., Haza, A.C., Hogan, P., Iskandarani, M., Jacobs, G., Kirwan, A.D., Laxague, N., Lipphardt, B., Magaldi, M.G., Novelli, G., Reniers, A., Restrepo, J.M., Smith, C., Valle-Levinson, A., Wei, M., 2016. Statistical properties of the surface velocity field in the northern Gulf of Mexico sampled by GLAD drifters. Journal of Geophysical Research: Oceans, 121:5193–5216. doi:10.1002/2015JC011569.

[Martin, 2003] Martin, A., 2003. Phytoplankton patchiness: the role of lateral stirring and mixing. Progress in Oceanography, 57:125 – 174. doi:https://doi.org/10.1016/S0079-6611(03)00085-5.

[Martin, 1990] Martin, J.H., 1990. Glacial-interglacial CO2 change: The Iron Hypothesis. Paleoceanography, 5:1–13. doi:10.1029/PA005i001p00001.

[Martin et al., 2013] Martin, P., Loeff, M.R., Cassar, N., Vandromme, P., d'Ovidio, F., Stemmann, L., Rengarajan, R., Soares, M., González, H.E., Ebersbach, F., Lampitt, R.S., Sanders, R., Barnett, B.A., Smetacek, V., Naqvi, S.W.A., 2013. Iron fertilization enhanced net community production but not downward particle flux during the Southern Ocean iron fertilization experiment LOHAFEX. Global Biogeochemical Cycles, 27:871–881. doi:10.1002/gbc.20077.

[McAdam and van Sebille, 2018] McAdam, R., van Sebille, E., 2018. Surface Connectivity and Inter-ocean Exchanges From Drifter-Based Transition Matrices. Journal of Geophysical Research: Oceans, pages n/a–n/a. doi:10.1002/2017JC013363.

[McGillicuddy Jr, 2016] McGillicuddy Jr, D.J., 2016. Mechanisms of physical-biological-biogeochemical interaction at the oceanic mesoscale. Annual Review of Marine Science, 8:125–159.

[McGillicuddy Jr et al., 1998] McGillicuddy Jr, D.J., Robinson, A., Siegel, D., Jannasch, H., Johnson, R., Dickey, T., McNeil, J., Michaels, A., Knap, A., 1998. Influence of mesoscale eddies on new production in the Sargasso Sea. Nature, 394:263. doi:10.1038/28367.

[McGowan, 1974] McGowan, J.A., 1974. The nature of oceanic ecosystems. Biology of the Ocean Pacific.

[McLachlan, 1996] McLachlan, A., 1996. Physical factors in benthic ecology: effects of changing sand particle size on beach fauna. Marine Ecology Progress Series, 131:205–217. doi:10.3354/meps131205.

[McManus and Woodson, 2012] McManus, M.A., Woodson, C.B., 2012. Plankton distribution and ocean dispersal. Journal of Experimental Biology, 215:1008–1016. doi:10.1242/jeb.059014.

[Melià et al., 2016] Melià, P., Schiavina, M., Rossetto, M., Gatto, M., Fraschetti, S., Casagrandi, R., 2016. Looking for hotspots of marine metacommunity connectivity: a methodological framework. Scientific Reports, 6:23705.

[Mengerink et al., 2014] Mengerink, K.J., Van Dover, C.L., Ardron, J., Baker, M., Escobar-Briones, E., Gjerde, K., Koslow, J.A., Ramirez-Llodra, E., Lara-Lopez, A., Squires, D., Sutton, T., Sweetman, A.K., Levin, L.A., 2014. A Call for Deep-Ocean Stewardship. Science, 344:696–698. doi:10.1126/science.1251458.

[Miron et al., 2017] Miron, P., Beron-Vera, F.J., Olascoaga, M.J., Sheinbaum, J., Pérez-Brunius, P., Froyland, G., 2017. Lagrangian dynamical geography of the Gulf of Mexico. Scientific reports, 7:7021.

[Molkenthin et al., 2017] Molkenthin, N., Kutza, H., Tupikina, L., Marwan, N., Donges, J.F., Feudel, U., Kurths, J., Donner, R.V., 2017. Edge anisotropy and the geometric perspective on flow networks. Chaos: An Interdisciplinary Journal of Nonlinear Science, 27:035802. doi:10.1063/1.4971785.

[Mongin et al., 2008] Mongin, M., Molina, E., Trull, T.W., 2008. Seasonality and scale of the kerguelen plateau phytoplankton bloom: A remote sensing and modeling analysis of the influence of natural iron fertilization in the southern ocean. Deep Sea Research Part II: Topical Studies in Oceanography, 55:880 – 892. doi:https://doi.org/10.1016/j.dsr2.2007.12.039. KEOPS: Kerguelen Ocean and Plateau compared Study.

[Monroy et al., 2017] Monroy, P., Rossi, V., Ser-Giacomi, E., López, C., Hernández-García, E., 2017. Sensitivity and robustness of larval connectivity diagnostics obtained from Lagrangian Flow Networks. ICES Journal of Marine Science, 74:1763–1779. doi:10.1093/icesjms/fsw235.

[Mooers et al., 2005] Mooers, C., Meinen, C., Baringer, M., Bang, I., Rhodes, R., Barron, C.N., Bub, F., 2005. Cross validating ocean prediction and monitoring systems. Eos, Transactions American Geophysical Union, 86:269–273. doi:10.1029/2005EO290002.

[Mora et al., 2011] Mora, C., Tittensor, D.P., Adl, S., Simpson, A.G.B., Worm, B., 2011. How Many Species Are There on Earth and in the Ocean? PLOS Biology, 9:1–8. doi:10.1371/journal.pbio.1001127.

[Moreno et al., 2016] Moreno, G., Dagorn, L., Capello, M., Lopez, J., Filmalter, J., Forget, F., Sancristobal, I., Holland, K., 2016. Fish aggregating devices (fads) as scientific platforms. Fisheries Research, 178:122 – 129. doi:https://doi.org/10.1016/j.fishres.2015.09.021. The use of fishing vessels as scientific platforms.

[Muñoz et al., 2015] Muñoz, M., Reul, A., Plaza, F., Gómez-Moreno, M.L., Vargas-Yañez, M., Rodríguez, V., Rodríguez, J., 2015. Implication of regionalization and connectivity analysis for marine spatial planning and coastal management in the Gulf of Cadiz and Alboran Sea. Ocean & Coastal Management, 118:60 – 74. doi:https://doi.org/10.1016/j.ocecoaman.2015.04.011. Coastal systems under change.

[Neighbors and Nafpaktitis, 1982] Neighbors, M.A., Nafpaktitis, B.G., 1982. Lipid compositions, water contents, swimbladder morphologies and buoyancies of nineteen species of midwater fishes (18 myctophids and 1 neoscopelid). Marine Biology, 66:207–215. doi:10.1007/BF00397024.

[Nencioli et al., 2011] Nencioli, F., d'Ovidio, F., Doglioli, A., Petrenko, A., 2011. Surface coastal circulation patterns by in situ detection of Lagrangian coherent structures. Geophysical Research Letters, 38. doi:10.1029/2011GL048815.

[Nencioli et al., 2013] Nencioli, F., d'Ovidio, F., Doglioli, A.M., Petrenko, A.A., 2013. In situ estimates of submesoscale horizontal eddy diffusivity across an ocean front. Journal of Geophysical Research: Oceans, 118:7066–7080. doi:10.1002/2013JC009252.

[Neuheimer et al., 2011] Neuheimer, A., Thresher, R., Lyle, J., Semmens, J., 2011. Tolerance limit for fish growth exceeded by warming waters. Nature Climate Change, 1:110. doi:10.1038/nclimate1084.

[Nordstrom et al., 2013] Nordstrom, C.A., Battaile, B.C., Cotte, C., Trites, A.W., 2013. Foraging habitats of lactating northern fur seals are structured by thermocline depths and submesoscale fronts in the eastern bering sea. Deep Sea Research Part II: Topical Studies in Oceanography, 88:78–96.

[Noss, 1990] Noss, R.F., 1990. Indicators for Monitoring Biodiversity: A Hierarchical Approach. Conservation Biology, 4:355–364. doi:10.1111/j.1523-1739.1990.tb00309.x.

[O'Brien, 1979] O'Brien, W.J., 1979. The predator-prey interaction of planktivorous fish and zooplankton: Recent research with planktivorous fish and their zooplankton prey shows the evolutionary thrust and parry of the predator-prey relationship. American Scientist, 67:572–581.

[Ogren et al., 2004] Ogren, P., Fiorelli, E., Leonard, N.E., 2004. Cooperative control of mobile sensor networks: Adaptive gradient climbing in a distributed environment. IEEE Transactions on Automatic control, 49:1292–1302.

[Okubo, 1978] Okubo, A., 1978. Horizontal Dispersion and Critical Scales for Phytoplankton Patches. Spatial pattern in plankton communities, 3:21–42. doi: 10.1007/978-1-4899-2195-6_2.

[Okubo, 1986] Okubo, A., 1986. Dynamical aspects of animal grouping: swarms, schools, flocks, and herds. Advances in biophysics, 22:1–94.

[Olascoaga et al., 2008] Olascoaga, M., Beron-Vera, F., Brand, L., Kocak, H., 2008. Tracing the early development of harmful algal blooms on the West Florida Shelf with the aid of Lagrangian coherent structures. Journal of Geophysical Research: Oceans, 113.

[Olascoaga et al., 2013] Olascoaga, M.J., Beron-Vera, F.J., Haller, G., Trinanes, J., Iskandarani, M., Coelho, E., Haus, B.K., Huntley, H., Jacobs, G., Kirwan, A., et al., 2013. Drifter motion in the gulf of mexico constrained by altimetric lagrangian coherent structures. Geophysical Research Letters, 40:6171–6175.

[Olivar et al., 2017] Olivar, M.P., Hulley, P.A., Castellón, A., Emelianov, M., López, C., Tuset, V.M., Contreras, T., Molí, B., 2017. Mesopelagic fishes across the tropical and equatorial Atlantic: Biogeographical and vertical patterns. Progress in Oceanography, 151:116 – 137. doi:https://doi.org/10.1016/j.pocean.2016.12.001.

[Omernik and Bailey, 1997] Omernik, J.M., Bailey, R.G., 1997. Distinguishing between watersheds and ecoregions. JAWRA Journal of the American Water Resources Association, 33:935–949. doi:10.1111/j.1752-1688.1997.tb04115.x.

[Orr et al., 2005] Orr, J.C., Fabry, V.J., Aumont, O., Bopp, L., Doney, S.C., Feely, R.A., Gnanadesikan, A., Gruber, N., Ishida, A., Joos, F., et al., 2005. Anthropogenic ocean acidification over the twenty-first century and its impact on calcifying organisms. Nature, 437:681. doi:10.1038/nature04095.

[Ottino, 1989] Ottino, J.M., 1989. The kinematics of mixing: stretching, chaos, and transport, volume 3 of Cambridge Texts in Applied Mathematics. Cambridge University Press.

[Padberg-Gehle and Schneide, 2017] Padberg-Gehle, K., Schneide, C., 2017. Network-based study of Lagrangian transport and mixing. Nonlinear Processes in Geophysics, 24:661–671.

[Pakhomov et al., 1994] Pakhomov, E., Perissinotto, R., McQuaid, C., 1994. Comparative structure of the macrozooplankton/micronekton communities of the Subtropical and Antarctic Polar Fronts. Marine ecology progress series. Oldendorf, 111:155–169. doi:10.3354/meps111155.

[Pakhomov et al., 1996] Pakhomov, E., Perissinotto, R., McQuaid, C., 1996. Prey composition and daily rations of myctophid fishes in the southern ocean. Marine Ecology Progress Series, pages 1–14.

[Pakhomov and Yamamura, 2010a] Pakhomov, E., Yamamura, O., 2010a. Advisory Panel on Micronekton Sampling Inter-calibration Experiment, North Pacific Marine Science Organization. Report of the Advisory Panel on Micronekton Sampling Inter-calibration Experiment.

[Pakhomov and Yamamura, 2010b] Pakhomov, E., Yamamura, O., 2010b. Report of the advisory panel on micronekton sampling inter-calibration experiment.

[Palomares and Pauly, 2011] Palomares, M., Pauly, D., 2011. A brief history of fishing in the Kerguelen Islands, France. Harper S and Zeller D (eds.), Fisheries catch reconstructions: Islands, Part II. Fisheries Centre Research Reports, 19:15–20.

[Parekh et al., 2006] Parekh, P., Dutkiewicz, S., Follows, M.J., Ito, T., 2006. Atmospheric carbon dioxide in a less dusty world. Geophysical Research Letters, 33. doi:10.1029/2005GL025098.

[Park et al., 2014] Park, Y.H., Durand, I., Kestenare, E., Rougier, G., Zhou, M., d'Ovidio, F., Cotté, C., Lee, J.H., 2014. Polar Front around the Kerguelen Islands: An up-to-date determination and associated circulation of surface/subsurface waters. Journal of Geophysical Research: Oceans, 119:6575–6592. doi:10.1002/2014JC010061.

[Parrish and Hamner, 1997] Parrish, J.K., Hamner, W.M., 1997. Animal groups in three dimensions: how species aggregate. Cambridge University Press.

[Pauly et al., 1998] Pauly, D., Christensen, V., Dalsgaard, J., Froese, R., Torres, F., 1998. Fishing Down Marine Food Webs. Science, 279:860–863. doi:10.1126/science.279.5352.860.

[Pavlov and Kasumyan, 2000] Pavlov, D., Kasumyan, A., 2000. Patterns and mechanisms of schooling behavior in fish: a review. Journal of Ichthyology, 40:S163.

[Pearcy, 1983] Pearcy, W.G., 1983. Quantitative Assessment of the Vertical Distributions of Micronektonic Fishes with Opening/Closing Midwater Trawls. Biological Oceanography, 2:289–310. doi:10.1080/01965581.1983.10749463.

[Penna et al., 2017] Penna, A.D., Koubbi, P., Cotté, C., Bon, C., Bost, C.A., d'Ovidio, F., 2017. Lagrangian analysis of multi-satellite data in support of open ocean Marine Protected Area design. Deep Sea Research Part II: Topical Studies in Oceanography, 140:212 – 221. doi:https://doi.org/10.1016/j.dsr2.2016.12.014. Future of oceanic animals in a changing ocean.

[Pereira et al., 2011] Pereira, J., Neves, V., Prieto, R., Silva, M., Cascão, I., Oliveira, C., Cruz, M., Medeiros, J., Barreiros, J., Porteiro, F., Clarke, D., 2011. Diet of mid-Atlantic Sowerby's beaked whales Mesoplondon bidens. Deep Sea Research Part I: Oceanographic Research Papers, 58:1084 – 1090. doi:https://doi.org/10.1016/j.dsr.2011.08.004.

[Phillips et al., 2015] Phillips, J.D., Schwanghart, W., Heckmann, T., 2015. Graph theory in the geosciences. Earth-Science Reviews, 143:147 – 160. doi:https://doi.org/10.1016/j.earscirev.2015.02.002.

[Piontkovski et al., 1997] Piontkovski, S., Williams, R., Peterson, W., Yunev, O., Minkina, N., Vladimirov, V., Blinko, A., 1997. Spatial heterogeneity of the planktonic fields in the upper mixed layer of the open ocean. Marine Ecology Progress Series, 148:145–154. doi:10.3354/meps148145.

[Pitcher, 1986] Pitcher, T.J., 1986. Functions of shoaling behaviour in teleosts. In The behaviour of teleost fishes, pages 294–337. Springer.

[Planes et al., 2009] Planes, S., Jones, G.P., Thorrold, S.R., 2009. Larval dispersal connects fish populations in a network of marine protected areas. Proceedings of the National Academy of Sciences, 106:5693–5697. doi:10.1073/pnas.0808007106.

[Platt and Denman, 1975] Platt, T., Denman, K.L., 1975. Spectral Analysis in Ecology. Annual Review of Ecology and Systematics, 6:189–210. doi:10.1146/annurev.es.06.110175.001201.

[Poje et al., 2014] Poje, A.C., Özgökmen, T.M., Lipphardt, B.L., Haus, B.K., Ryan, E.H., Haza, A.C., Jacobs, G.A., Reniers, A.J.H.M., Olascoaga, M.J., Novelli, G., Griffa, A., Beron-Vera, F.J., Chen, S.S., Coelho, E., Hogan, P.J., Kirwan, A.D., Huntley, H.S., Mariano, A.J., 2014. Submesoscale dispersion in the vicinity of the Deepwater Horizon spill. Proceedings of the National Academy of Sciences, 111:12693–12698. doi:10.1073/pnas.1402452111.

[Poje et al., 2002] Poje, A.C., Toner, M., Kirwan, A.D., Jones, C.K.R.T., 2002. Drifter Launch Strategies Based on Lagrangian Templates. Journal of Physical Oceanography, 32:1855–1869. doi:10.1175/1520-0485(2002)032⟨1855:DLSBOL⟩2.0.CO;2.

[Polovina et al., 2006] Polovina, J., Uchida, I., Balazs, G., Howell, E.A., Parker, D., Dutton, P., 2006. The kuroshio extension bifurcation region: A pelagic hotspot for juvenile loggerhead sea turtles. Deep Sea Research Part II: Topical Studies in Oceanography, 53:326–339. doi:10.1016/j.dsr2.2006.01.006.

[Polovina, 1996] Polovina, J.J., 1996. Decadal variation in the trans-Pacific migration of northern bluefin tuna (Thunnus thynnus) coherent with climate-induced change in prey abundance. Fisheries Oceanography, 5:114–119. doi:10.1111/j.1365-2419. 1996.tb00110.x.

[Potier et al., 2007] Potier, M., Marsac, F., Cherel, Y., Lucas, V., Sabatié, R., Maury, O., Ménard, F., 2007. Forage fauna in the diet of three large pelagic fishes (lancetfish, swordfish and yellowfin tuna) in the western equatorial Indian Ocean. Fisheries Research, 83:60 – 72. doi:https://doi.org/10.1016/j.fishres.2006.08.020.

[Prants, 2013] Prants, S., 2013. Dynamical systems theory methods to study mixing and transport in the ocean. Physica Scripta, 87:038115.

[Prants et al., 2014a] Prants, S., Budyansky, M., Uleysky, M.Y., 2014a. Identifying Lagrangian fronts with favourable fishery conditions. Deep Sea Research Part I: Oceanographic Research Papers, 90:27–35. doi:10.1016/j.dsr.2014.04.012.

[Prants et al., 2014b] Prants, S., Budyansky, M., Uleysky, M.Y., 2014b. Lagrangian fronts in the ocean. Izvestiya, Atmospheric and Oceanic Physics, 50:284–291. doi:10.1134/S0001433814030116.

[Prants et al., 2017] Prants, S.V., Uleysky, M.Y., Budyansky, M.V., 2017. Lagrangian oceanography: large-scale transport and mixing in the ocean. Springer.

[Press et al., 1988] Press, W.H., Teukolsky, S.A., Vetterling, W.T., Flannery, B.P., 1988. Numerical recipes in C. Cambridge University Press, 1:3.

[Pujol et al., 2016] Pujol, M.I., Faugère, Y., Taburet, G., Dupuy, S., Pelloquin, C., Ablain, M., Picot, N., 2016. DUACS DT2014: the new multi-mission altimeter data set reprocessed over 20 years. Ocean Science, 12:1067–1090. doi:https://doi. org/10.5194/os-12-1067-2016.

[Pusch et al., 2004] Pusch, C., Hulley, P., Kock, K.H., 2004. Community structure and feeding ecology of mesopelagic fishes in the slope waters of King George Island (South Shetland Islands, Antarctica). Deep Sea Research Part I: Oceanographic Research Papers, 51:1685 – 1708. doi:https://doi.org/10.1016/j.dsr.2004.06.008.

[Pusineri et al., 2008] Pusineri, C., Chancollon, O., Ringelstein, J., Ridoux, V., 2008. Feeding niche segregation among the Northeast Atlantic community of oceanic

top predators. Marine Ecology Progress Series, 361:21–34. doi:doi.org/10.3354/meps07318.

[Pyke, 1984] Pyke, G.H., 1984. Optimal Foraging Theory: A Critical Review). Annual Review of Ecology and Systematics, 15:523–575. doi:10.1146/annurev.es.15.110184.002515.

[Qiu and Jones, 2013] Qiu, W., Jones, P.J., 2013. The emerging policy landscape for marine spatial planning in Europe. Marine Policy, 39:182 – 190. doi:https://doi.org/10.1016/j.marpol.2012.10.010.

[Radakov, 1972] Radakov, D., 1972. Schooling of fish as an ecological phenomenon. Nauka, Moscow.

[Radakov, 1973] Radakov, D.V., 1973. Schooling in the ecology of fish.

[Ramanathan, 1981] Ramanathan, V., 1981. The Role of Ocean-Atmosphere Interactions in the CO2 Climate Problem. Journal of the Atmospheric Sciences, 38:918–930. doi:10.1175/1520-0469(1981)038⟨0918:TROOAI⟩2.0.CO;2.

[Ramirez-Llodra et al., 2011] Ramirez-Llodra, E., Tyler, P.A., Baker, M.C., Bergstad, O.A., Clark, M.R., Escobar, E., Levin, L.A., Menot, L., Rowden, A.A., Smith, C.R., Van Dover, C.L., 2011. Man and the Last Great Wilderness: Human Impact on the Deep Sea. PLOS ONE, 6:1–25. doi:10.1371/journal.pone.0022588.

[Reese et al., 2005] Reese, D., Miller, T., Brodeur, R., 2005. Community structure of near-surface zooplankton in the northern california current in relation to oceanographic conditions. Deep Sea Research Part II: Topical Studies in Oceanography, 52:29 – 50. doi:https://doi.org/10.1016/j.dsr2.2004.09.027. U.S. GLOBEC Biological and Physical Studies of Plankton, Fish and Higher Trophic Level Production, Distribution, and Variability in the Northeast Pacific.

[Rengstorf et al., 2013] Rengstorf, A.M., Yesson, C., Brown, C., Grehan, A.J., 2013. High-resolution habitat suitability modelling can improve conservation of vulnerable marine ecosystems in the deep sea. Journal of Biogeography, 40:1702–1714. doi:10.1111/jbi.12123.

[Resplandy et al., 2009] Resplandy, L., Lévy, M., d'Ovidio, F., Merlivat, L., 2009. Impact of submesoscale variability in estimating the air-sea CO2 exchange: Results from a model study of the POMME experiment. Global Biogeochemical Cycles, 23. doi:10.1029/2008GB003239.

[Reynolds et al., 2005] Reynolds, J.D., Dulvy, N.K., Goodwin, N.B., Hutchings, J.A., 2005. Biology of extinction risk in marine fishes. Proceedings of the Royal Society of London B: Biological Sciences, 272:2337–2344. doi:10.1098/rspb.2005.3281.

[Robison, 2009] Robison, B.H., 2009. Conservation of Deep Pelagic Biodiversity. Conservation Biology, 23:847–858. doi:10.1111/j.1523-1739.2009.01219.x.

[Rodríguez-Méndez et al., 2017] Rodríguez-Méndez, V., Ser-Giacomi, E., Hernández-García, E., 2017. Clustering coefficient and periodic orbits in flow networks. Chaos: An Interdisciplinary Journal of Nonlinear Science, 27:035803. doi: 10.1063/1.4971787.

[Ropert-Coudert and Wilson, 2005] Ropert-Coudert, Y., Wilson, R.P., 2005. Trends and perspectives in animal-attached remote sensing. Frontiers in Ecology and the Environment, 3:437–444. doi:10.1890/1540-9295(2005)003[0437:TAPIAR]2.0.CO; 2.

[Rossi et al., 2008] Rossi, V., López, C., Sudre, J., Hernández-García, E., Garçon, V., 2008. Comparative study of mixing and biological activity of the Benguela and Canary upwelling systems. Geophysical Research Letters, 35. doi:10.1029/ 2008GL033610.

[Rossi et al., 2014] Rossi, V., Ser-Giacomi, E., López, C., Hernández-García, E., 2014. Hydrodynamic provinces and oceanic connectivity from a transport network help designing marine reserves. Geophysical Research Letters, 41:2883–2891.

[Rosso et al., 2014] Rosso, I., Hogg, A.M., Strutton, P.G., Kiss, A.E., Matear, R., Klocker, A., van Sebille, E., 2014. Vertical transport in the ocean due to submesoscale structures: Impacts in the Kerguelen region. Ocean Modelling, 80:10 – 23. doi:https://doi.org/10.1016/j.ocemod.2014.05.001.

[Royce, 2013] Royce, W.F., 2013. Introduction to the fishery sciences. Academic Press.

[Rypina and Pratt, 2017] Rypina, I.I., Pratt, L.J., 2017. Trajectory encounter volume as a diagnostic of mixing potential in fluid flows. Nonlinear Processes in Geophysics, 24:189. doi:10.5194/npg-24-189-2017.

[Sabarros et al., 2009] Sabarros, P.S., Mnard, F., Lvnez, J., TewKai, E., Ternon, J., 2009. Mesoscale eddies influence distribution and aggregation patterns of micronekton in the mozambique channel. Marine Ecology Progress Series, 395:101– 107. doi:10.3354/meps08087.

[Sabourenkov, 1991] Sabourenkov, E., 1991. Myctophids in the diet of antarctic predators. Selected scientific papers, pages 335–368.

[Sakshaug et al., 1994] Sakshaug, E., Bjørge, A., Gulliksen, B., Loeng, H., Mehlum, F., 1994. Structure, biomass distribution, and energetics of the pelagic ecosystem in the Barents Sea: A synopsis. Polar Biology, 14:405–411. doi:10.1007/BF00240261.

[Sala, 2006] Sala, E., 2006. Top predators provide insurance against climate change. Trends in ecology & evolution, 21:479–480. doi:doi.org/10.1016/j.tree.2006.07.006.

[Sandulescu et al., 2006] Sandulescu, M., Hernández-Garcìa, E., López, C., Feudel, U., 2006. Kinematic studies of transport across an island wake, with application to the Canary islands. Tellus A: Dynamic Meteorology and Oceanography, 58:605–615. doi:10.1111/j.1600-0870.2006.00199.x.

[Sankaran et al., 2005] Sankaran, M., Hanan, N.P., Scholes, R.J., Ratnam, J., Augustine, D.J., Cade, B.S., Gignoux, J., Higgins, S.I., Le Roux, X., Ludwig, F., et al., 2005. Determinants of woody cover in African savannas. Nature, 438:846. doi:10.1038/nature04070.

[Sarmiento et al., 2004] Sarmiento, J.L., Slater, R., Barber, R., Bopp, L., Doney, S.C., Hirst, A.C., Kleypas, J., Matear, R., Mikolajewicz, U., Monfray, P., Soldatov, V., Spall, S.A., Stouffer, R., 2004. Response of ocean ecosystems to climate warming. Global Biogeochemical Cycles, 18. doi:10.1029/2003GB002134.

[Saunders et al., 2013] Saunders, R.A., Fielding, S., Thorpe, S.E., Tarling, G.A., 2013. School characteristics of mesopelagic fish at south georgia. Deep Sea Research Part I: Oceanographic Research Papers, 81:62–77.

[Scales et al., 2018] Scales, K.L., Hazen, E.L., Jacox, M.G., Castruccio, F., Maxwell, S.M., Lewison, R.L., Bograd, S.J., 2018. Fisheries bycatch risk to marine megafauna is intensified in Lagrangian coherent structures. Proceedings of the National Academy of Sciences of the United States of America. doi:10.1073/pnas.1801270115.

[Scales et al., 2014a] Scales, K.L., Miller, P.I., Embling, C.B., Ingram, S.N., Pirotta, E., Votier, S.C., 2014a. Mesoscale fronts as foraging habitats: composite front mapping reveals oceanographic drivers of habitat use for a pelagic seabird. Journal of The Royal Society Interface, 11. doi:10.1098/rsif.2014.0679.

[Scales et al., 2014b] Scales, K.L., Miller, P.I., Hawkes, L.A., Ingram, S.N., Sims, D.W., Votier, S.C., 2014b. On the Front Line: frontal zones as priority at-sea conservation areas for mobile marine vertebrates. Journal of Applied Ecology, 51:1575–1583. doi:10.1111/1365-2664.12330.

[Schoener, 1971] Schoener, T.W., 1971. Theory of Feeding Strategies. Annual Review of Ecology and Systematics, 2:369–404. doi:10.1146/annurev.es.02.110171.002101.

[Schroeder et al., 2012] Schroeder, K., Chiggiato, J., Haza, A.C., Griffa, A., Özgökmen, T.M., Zanasca, P., Molcard, A., Borghini, M., Poulain, P.M., Gerin, R., Zambianchi, E., Falco, P., Trees, C., 2012. Targeted Lagrangian sampling of submesoscale dispersion at a coastal frontal zone. Geophysical Research Letters, 39. doi:10.1029/2012GL051879.

[Ser-Giacomi et al., 2017] Ser-Giacomi, E., Rodríguez-Méndez, V., López, C., Hernández-García, E., 2017. Lagrangian Flow Network approach to an open flow model. The European Physical Journal Special Topics, 226:2057–2068. doi: https://doi.org/10.1140/epjst/e2017-70044-2.

[Ser-Giacomi et al., 2015a] Ser-Giacomi, E., Rossi, V., López, C., Hernández-García, E., 2015a. Flow networks: A characterization of geophysical fluid transport. Chaos: An Interdisciplinary Journal of Nonlinear Science, 25:036404. doi: 10.1063/1.4908231.

[Ser-Giacomi et al., 2015b] Ser-Giacomi, E., Vasile, R., Hernández-García, E., López, C., 2015b. Most probable paths in temporal weighted networks: An application to ocean transport. Physical Review E, 92:012818. doi:10.1103/PhysRevE.92.012818.

[Ser-Giacomi et al., 2015c] Ser-Giacomi, E., Vasile, R., Recuerda, I., Hernández-García, E., López, C., 2015c. Dominant transport pathways in an atmospheric blocking event. Chaos: An Interdisciplinary Journal of Nonlinear Science, 25:087413. doi: 10.1063/1.4928704.

[Sfakiotakis et al., 1999] Sfakiotakis, M., Lane, D.M., Davies, J.B.C., 1999. Review of fish swimming modes for aquatic locomotion. Oceanic Engineering, IEEE Journal of, 24:237–252.

[Shadden et al., 2005] Shadden, S.C., Lekien, F., Marsden, J.E., 2005. Definition and properties of lagrangian coherent structures from finite-time lyapunov exponents in two-dimensional aperiodic flows. Physica D: Nonlinear Phenomena, 212:271–304. doi:10.1016/j.physd.2005.10.007.

[Shanks, 2009] Shanks, A.L., 2009. Pelagic Larval Duration and Dispersal Distance Revisited. The Biological Bulletin, 216:373–385. doi:10.1086/BBLv216n3p373. PMID: 19556601.

[Shannon et al., 2000] Shannon, L.J., Cury, P.M., Jarre, A., 2000. Modelling effects of fishing in the Southern Benguela ecosystem. ICES Journal of Marine Science, 57:720–722. doi:10.1006/jmsc.2000.0716.

[Shaw and Sachs, 1967] Shaw, E., Sachs, B.D., 1967. Development of the optomotor response in the schooling fish, menidia menidia. Journal of comparative and physiological psychology, 63:385.

[Shephard et al., 2012] Shephard, S., Fung, T., Houle, J.E., Farnsworth, K.D., Reid, D.G., Rossberg, A.G., 2012. Size-selective fishing drives species composition in the Celtic Sea. ICES Journal of Marine Science, 69:223–234. doi:10.1093/icesjms/fsr200.

[Shraiman and Siggia, 2000] Shraiman, B.I., Siggia, E.D., 2000. Scalar turbulence. Nature, 405:639. doi:10.1038/35015000.

[Shreeve et al., 2009] Shreeve, R.S., Collins, M.A., Tarling, G.A., Main, C.E., Ward, P., Johnston, N.M., 2009. Feeding ecology of myctophid fishes in the northern Scotia Sea. Marine Ecology Progress Series, 386:221–236.

[Sibert et al., 1999] Sibert, J.R., Hampton, J., Fournier, D.A., Bills, P.J., 1999. An advection–diffusion–reaction model for the estimation of fish movement parameters from tagging data, with application to skipjack tuna (Katsuwonus pelamis). Canadian Journal of Fisheries and Aquatic Sciences, 56:925–938. doi:10.1139/f99-017.

[Siegel et al., 2008] Siegel, D.A., Mitarai, S., Costello, C.J., Gaines, S.D., Kendall, B.E., Warner, R.R., Winters, K.B., 2008. The stochastic nature of larval connectivity among nearshore marine populations. Proceedings of the National Academy of Sciences. doi:10.1073/pnas.0802544105.

[Simard and Lavoie, 1999] Simard, Y., Lavoie, D., 1999. The rich krill aggregation of the Saguenay - St. Lawrence Marine Park: hydroacoustic and geostatistical biomass estimates, structure, variability, and significance for whales. Canadian Journal of Fisheries and Aquatic Sciences, 56:1182–1197. doi:10.1139/f99-063.

[Smetacek et al., 2004] Smetacek, V., Assmy, P., Henjes, J., 2004. The role of grazing in structuring Southern Ocean pelagic ecosystems and biogeochemical cycles. Antarctic Science, 16:541â[U+0080][U+0093]558. doi:10.1017/S0954102004002317.

[Smith et al., 2011] Smith, A.D.M., Brown, C.J., Bulman, C.M., Fulton, E.A., Johnson, P., Kaplan, I.C., Lozano-Montes, H., Mackinson, S., Marzloff, M., Shannon, L.J., Shin, Y.J., Tam, J., 2011. Impacts of Fishing Low–Trophic Level Species on Marine Ecosystems. Science, 333:1147–1150.

[Smith and Ferrari, 2009] Smith, K.S., Ferrari, R., 2009. The Production and Dissipation of Compensated Thermohaline Variance by Mesoscale Stirring. Journal of Physical Oceanography, 39:2477–2501. doi:10.1175/2009JPO4103.1.

[Soccodato et al., 2016] Soccodato, A., d'Ovidio, F., Lévy, M., Jahn, O., Follows, M.J., Monte, S.D., 2016. Estimating planktonic diversity through spatial dominance patterns in a model ocean. Marine Genomics, 29:9 – 17. doi:https://doi.org/10.1016/j.margen.2016.04.015.

[Soomere et al., 2015] Soomere, T., Delpeche-Ellmann, N., Torsvik, T., Viikmäe, B., 2015. Towards a New Generation of Techniques for the Environmental Management of Maritime Activities. In Environmental Security of the European Cross-Border Energy Supply Infrastructure, pages 103–132. Springer. doi:10.1007/978-94-017-9538-8_8.

[Spalding et al., 2007] Spalding, M.D., Fox, H.E., Allen, G.R., Davidson, N., FerdaÃ±a, Z.A., Finlayson, M., Halpern, B.S., Jorge, M.A., Lombana, A., Lourie, S.A., Martin, K.D., McManus, E., Molnar, J., Recchia, C.A., Robertson, J., 2007. Marine Ecoregions of the World: A Bioregionalization of Coastal and Shelf Areas. BioScience, 57:573–583. doi:10.1641/B570707.

[St. John et al., 2016] St. John, M.A., Borja, A., Chust, G., Heath, M., Grigorov, I., Mariani, P., Martin, A.P., Santos, R.S., 2016. A Dark Hole in Our Understanding of Marine Ecosystems and Their Services: Perspectives from the Mesopelagic Community. Frontiers in Marine Science, 3:31. doi:10.3389/fmars.2016.00031.

[Stobutzki and Bellwood, 1994] Stobutzki, I.C., Bellwood, D.R., 1994. An analysis of the sustained swimming abilities of pre- and post-settlement coral reef fishes. Journal of Experimental Marine Biology and Ecology, 175:275 – 286. doi:https://doi.org/10.1016/0022-0981(94)90031-0.

[Su and Pohlmann, 2009] Su, J., Pohlmann, T., 2009. Wind and topography influence on an upwelling system at the eastern Hainan coast. Journal of Geophysical Research: Oceans, 114. doi:10.1029/2008JC005018.

[Sullivan et al., 1993] Sullivan, C.W., Arrigo, K.R., McClain, C.R., Comiso, J.C., Firestone, J., 1993. Distributions of Phytoplankton Blooms in the Southern Ocean. Science, 262:1832–1837. doi:10.1126/science.262.5141.1832.

[Sulman et al., 2013] Sulman, M.H., Huntley, H.S., Lipphardt, B., Kirwan, A., 2013. Leaving flatland: Diagnostics for Lagrangian coherent structures in three-dimensional flows. Physica D: Nonlinear Phenomena, 258:77 – 92. doi:https://doi.org/10.1016/j.physd.2013.05.005.

[Sundermeyer and Price, 1998] Sundermeyer, M.A., Price, J.F., 1998. Lateral mixing and the North Atlantic Tracer Release Experiment: Observations and numerical

simulations of Lagrangian particles and a passive tracer. Journal of Geophysical Research: Oceans, 103:21481–21497. doi:10.1029/98JC01999.

[Suneel et al., 2016] Suneel, V., Ciappa, A., Vethamony, P., 2016. Backtrack modeling to locate the origin of tar balls depositing along the west coast of India. Science of The Total Environment, 569-570:31 – 39. doi:https://doi.org/10.1016/j.scitotenv.2016.06.101.

[Sutton et al., 2017] Sutton, T.T., Clark, M.R., Dunn, D.C., Halpin, P.N., Rogers, A.D., Guinotte, J., Bograd, S.J., Angel, M.V., Perez, J.A.A., Wishner, K., Haedrich, R.L., Lindsay, D.J., Drazen, J.C., Vereshchaka, A., Piatkowski, U., Morato, T., Błachowiak-Samołyk, K., Robison, B.H., Gjerde, K.M., Pierrot-Bults, A., Bernal, P., Reygondeau, G., Heino, M., 2017. A global biogeographic classification of the mesopelagic zone. Deep Sea Research Part I: Oceanographic Research Papers, 126:85 – 102. doi:https://doi.org/10.1016/j.dsr.2017.05.006.

[Tabeling, 2002] Tabeling, P., 2002. Two-dimensional turbulence: a physicist approach. Physics Reports, 362:1 – 62. doi:https://doi.org/10.1016/S0370-1573(01)00064-3.

[Teichmann, 1959] Teichmann, H., 1959. Über die leistung des geruchssinnes beim aal [angüilla anguilla (l.)]. Zeitschrift für vergleichende Physiologie, 42:206–254.

[Tittensor et al., 2010] Tittensor, D.P., Mora, C., Jetz, W., Lotze, H.K., Ricard, D., Berghe, E.V., Worm, B., 2010. Global patterns and predictors of marine biodiversity across taxa. Nature, 466:1098. doi:10.1038/nature09329.

[Toner et al., 2003] Toner, M., Kirwan, A.D., Poje, A.C., Kantha, L.H., Müller-Karger, F.E., Jones, C.K.R.T., 2003. Chlorophyll dispersal by eddy-eddy interactions in the Gulf of Mexico. Journal of Geophysical Research: Oceans, 108. doi:10.1029/2002JC001499.

[Tracey et al., 2016] Tracey, S.R., Hartmann, K., Leef, M., McAllister, J., 2016. Capture-induced physiological stress and postrelease mortality for Southern bluefin tuna (Thunnus maccoyii) from a recreational fishery. Canadian Journal of Fisheries and Aquatic Sciences, 73:1547–1556. doi:10.1139/cjfas-2015-0516.

[Tsuji and Haneda, 1971] Tsuji, F.I., Haneda, Y., 1971. Luminescent system in a myctophid fish, Diaphus elucens Brauer. Nature, 233:623. doi:doi.org/10.1038/233623a0.

[Turner, 1989] Turner, M.G., 1989. Landscape ecology: the effect of pattern on process. Annual review of ecology and systematics, 20:171–197.

[Tyler et al., 2011] Tyler, E.H.M., Somerfield, P.J., Berghe, E.V., Bremner, J., Jackson, E., Langmead, O., Palomares, M.L.D., Webb, T.J., 2011. Extensive gaps and biases in our knowledge of a well-known fauna: implications for integrating biological traits into macroecology. Global Ecology and Biogeography, 21:922–934. doi:10.1111/j.1466-8238.2011.00726.x.

[Valinassab et al., 2007] Valinassab, T., Pierce, G.J., Johannesson, K., 2007. Lantern fish (Benthosema pterotum) resources as a target for commercial exploitation in the Oman Sea. Journal of Applied Ichthyology, 23:573–577. doi:10.1111/j. 1439-0426.2007.01034.x.

[van Haren and Compton, 2013] van Haren, H., Compton, T.J., 2013. Diel Vertical Migration in Deep Sea Plankton Is Finely Tuned to Latitudinal and Seasonal Day Length. PLOS ONE, 8:1–8. doi:10.1371/journal.pone.0064435.

[van Sebille et al., 2018] van Sebille, E., Griffies, S.M., Abernathey, R., Adams, T.P., Berloff, P., Biastoch, A., Blanke, B., Chassignet, E.P., Cheng, Y., Cotter, C.J., Deleersnijder, E., Döös, K., Drake, H.F., Drijfhout, S., Gary, S.F., Heemink, A.W., Kjellsson, J., Koszalka, I.M., Lange, M., Lique, C., MacGilchrist, G.A., Marsh, R., Adame, C.G.M., McAdam, R., Nencioli, F., Paris, C.B., Piggott, M.D., Polton, J.A., Rühs, S., Shah, S.H., Thomas, M.D., Wang, J., Wolfram, P.J., Zanna, L., Zika, J.D., 2018. Lagrangian ocean analysis: Fundamentals and practices. Ocean Modelling, 121:49 – 75. doi:https://doi.org/10.1016/j.ocemod.2017.11.008.

[Vicsek and Zafeiris, 2012] Vicsek, T., Zafeiris, A., 2012. Collective motion. Physics Reports, 517:71–140.

[Viikmäe et al., 2011] Viikmäe, B., Soomere, T., Parnell, K., Delpeche, N., 2011. Spatial planning of shipping and offshore activities in the Baltic Sea using Lagrangian trajectories. Journal of Coastal Research, page 956.

[Vrana et al., 2005] Vrana, B., Allan, I.J., Greenwood, R., Mills, G.A., Dominiak, E., Svensson, K., Knutsson, J., Morrison, G., 2005. Passive sampling techniques for monitoring pollutants in water. TrAC Trends in Analytical Chemistry, 24:845–868. doi:10.1016/j.trac.2005.06.006.

[Waluda et al., 2001] Waluda, C.M., Rodhouse, P.G., Trathan, P.N., Pierce, G.J., 2001. Remotely sensed mesoscale oceanography and the distribution of illex argentinus in the south atlantic. Fisheries Oceanography, 10:207–216. doi:10.1046/j.1365-2419. 2001.00165.x.

[Washburn et al., 1998] Washburn, L., Emery, B.M., Jones, B.H., Ondercin, D.G., 1998. Eddy stirring and phytoplankton patchiness in the subarctic North Atlantic in late

summer. Deep Sea Research Part I: Oceanographic Research Papers, 45:1411 – 1439. doi:https://doi.org/10.1016/S0967-0637(98)00023-5.

[Watkins, 1996] Watkins, T.B., 1996. Predator-Mediated Selection on Burst Swimming Performance in Tadpoles of the Pacific Tree Frog, Pseudacris regilla. Physiological Zoology, 69:154–167. doi:10.1086/physzool.69.1.30164205.

[Watson et al., 2018] Watson, J.R., Fuller, E.C., Castruccio, F.S., Samhouri, J.F., 2018. Fishermen Follow Fine-Scale Physical Ocean Features for Finance. Frontiers in Marine Science, 5. doi:10.3389/fmars.2018.00046.

[Webb et al., 2010] Webb, T.J., Vanden Berghe, E., O'Dor, R., 2010. Biodiversity's Big Wet Secret: The Global Distribution of Marine Biological Records Reveals Chronic Under-Exploration of the Deep Pelagic Ocean. PLOS ONE, 5:1–6. doi:10.1371/journal.pone.0010223.

[Wells et al., 2004] Wells, R.S., Rhinehart, H.L., Hansen, L.J., Sweeney, J.C., Townsend, F.I., Stone, R., Casper, D.R., Scott, M.D., Hohn, A.A., Rowles, T.K., 2004. Bottlenose Dolphins as Marine Ecosystem Sentinels: Developing a Health Monitoring System. EcoHealth, 1:246–254. doi:10.1007/s10393-004-0094-6.

[Wiebe, 1971] Wiebe, P.H., 1971. A computer model study of zooplankton patchiness and its effects on sampling errors. Limnology and Oceanography, 16:29–38. doi:10.4319/lo.1971.16.1.0029.

[Wiggins, 2005] Wiggins, S., 2005. The dynamical systems approach to Lagrangian transport in oceanic flows. Annual Review of Fluid Mechanics, 37:295–328. doi:10.1146/annurev.fluid.37.061903.175815.

[Woodson and Litvin, 2015] Woodson, C.B., Litvin, S.Y., 2015. Ocean fronts drive marine fishery production and biogeochemical cycling. Proceedings of the National Academy of Sciences, 112:1710–1715. doi:10.1073/pnas.1417143112.

[Worm et al., 2003] Worm, B., Lotze, H.K., Myers, R.A., 2003. Predator diversity hotspots in the blue ocean. Proceedings of the National Academy of Sciences, 100:9884–9888. doi:10.1073/pnas.1333941100.

[Yoder et al., 1994] Yoder, J.A., Ackleson, S.G., Barber, R.T., Flament, P., Balch, W.M., 1994. A line in the sea. Nature, 371:689. doi:10.1038/371689a0.

[Young et al., 1982] Young, W.R., Rhines, P.B., Garrett, C.J.R., 1982. Shear-Flow Dispersion, Internal Waves and Horizontal Mixing in the Ocean. Journal of Physical Oceanography, 12:515–527. doi:10.1175/1520-0485(1982)012⟨0515:SFDIWA⟩2.0.CO;2.

[Zeller and Pauly, 2018] Zeller, D., Pauly, D., 2018. The 'presentist bias' in time-series data: Implications for fisheries science and policy. Marine Policy, 90:14 – 19. doi:https://doi.org/10.1016/j.marpol.2018.01.015.